THE UNIVERSITY
of EDINBURGH

Iron and Titanium Amino-Phenolate Complexes in Controlled Alkene Polymerisation

Daniel L. Coward

A thesis submitted at the University of Edinburgh for the Degree of Doctor of Philosophy

2019

Abstract

Transition metals have long been used as both catalysts and mediators in the polymerisation of many monomers. This thesis explores the use of iron and titanium amino-phenolate complexes as mediators in the polymerisation of alkene monomers.

Initial work focused on understanding the fundamental mechanisms behind the organometallic-mediated radical polymerisation (OMRP) of styrene, methyl methacrylate (MMA) and vinyl acetate using a novel and fully characterised *tert*-butyl substituted amine-bis(phenolate) iron(II) complex. A range of temperatures and conditions were explored to elucidate the equilibrium between propagation and termination reactions in the polymerisation. It was found that in the polymerisation of MMA, propagation was favoured at low conversion with good control and reasonable dispersities. Mechanistic studies suggest that propagation proceeds through a reversible-termination OMRP mechanism. At higher conversions, irreversible termination reactions become dominant. The polymerisation temperature significantly affects the nature of termination, dictating whether termination is either bimolecular or via catalytic chain transfer (CCT). The polymerisation of styrene shows well-controlled behaviour with dispersities as low as 1.27, which is the first time this has been achieved for iron-mediated OMRP. The use of alternative initiation methods, such as macroinitiators and photoinitiators, is also discussed.

A family of titanium(III) amino-phenolate complexes were used as mediators in the polymerisation of methacrylates. Well-controlled polymerisations were achieved, with linear first-order kinetics and dispersities as low as 1.09. The nature of the substituents on the ligand greatly affects the tacticity of the resultant polymer, with large bulky groups having a more significant effect in promoting isotactic polymer. Detailed experimental and computational studies suggest that the polymerisation mechanism is not radical or ionic, but instead proceeds through a coordinating-type mechanism. This mechanism is suggested to be bimetallic, involving a titanium(IV)-enolate complex and an MMA-coordinated titanium(III) species, with polymerisation propagating *via* a group transfer mechanism, which is rarely exhibited in transition metals. This also likely represents the first example of the initiation of a coordination polymerisation with a conventional azo initiator, without the need for pyrophoric or expensive activators.

Lay Summary

Transition metals have long been used as both catalysts and mediators in the polymerisation of many monomers. This thesis explores the use of iron and titanium complexes, which are more environmentally friendly than current alternatives, as mediators to synthesise well-controlled polymers. This work has particularly focussed on the synthesis of poly(styrene) and poly(methyl methacrylate) so that polymers with a specific molecular weight can be produced, which is crucial for effective use in a range of speciality applications.

Iron and titanium complexes, based on a ligand framework called amino-phenolate, were used as polymerisation mediators, and a range of temperatures and conditions were explored to understand how different mechanisms interplay with one another. The iron complex showed moderate control over the polymerisation of styrene and methyl methacrylate, under certain specific conditions, but termination quickly became dominant, typically resulting in the loss of control. However, the titanium complexes showed excellent control over the polymerisation of methacrylates. The titanium-mediated polymerisation mechanism was studied in depth both experimentally and computationally.

Declaration

The work described in this thesis is of my own, unless I have acknowledged help from a named person or referenced a published source. This thesis has not been submitted, in whole or in part, for any other degree.

Signature: D. L. Coward

Date: 29/04/2019

Acknowledgements

This thesis is the culmination of years of hard work and the generous support and encouragement from a great number of people. Firstly, I would like to thank my supervisor Professor Michael Shaver for giving me the opportunity to join the group. I am grateful for your guidance, ideas, motivation and knowledge of all things craft beer. Thank you to the School of Chemistry at the University of Edinburgh for providing the environment in which to work and learn.

I would also like to thank the Soft Matter and Functional Interfaces (SOFI) CDT and all the people involved, for the funding of my PhD and providing ongoing training and networking opportunities. I would not be in the career I am today without SOFI.

Thank you to all the past and present members of the Green Materials Laboratory for being there for me every single day, through the good times and the bad. Thank you to Ben for providing me with considerable help on a challenging PhD project and for putting up with my frequent questions. Thank you to Emily for teaching me about the Schlenk line and all I know about air-sensitive chemistry. Thank you to Fern, Stefan, Meng and Jarret for support at the start, and to Yasmeen, Gerry, Eszter and Vishal for support at the end.

I would like to thank Professor Rinaldo Poli, my supervisor during my research placement in Toulouse, and the members of Equipe G. It was a wonderful and unforgettable experience.

Thank you to all my family and friends for their support and motivation throughout the PhD. Thank you to my colleagues at TL Brand & Co for giving me the final push towards the finish line.

Thank you to Mum, Dad and Matthew. You believed in me when I didn't believe in myself.

Finally, thank you to Stephanie. I met you at the start, and I'm with you at the end. I cannot possibly thank you enough for everything you have done for me. You are the most thoughtful, kind and considerate person that I have ever met, and I am so lucky to have had you by my side throughout it all. I can't wait to spend the rest of my life with you. I love you, forever and always.

Table of Contents

List of Abbreviations

°C	degree Celsius
µL	microliters
^{i}Bu	isobutyl (2-methylpropyl)
^{n}Bu	butyl
^{t}Bu	tertiary-butyl (1,1-dimethylethyl)
AIBN	2,2'-azobisisobutyronitrile
ATRP	atom transfer radical polymerisation
CCT	catalytic chain transfer
CI	coordination-insertion
CMRP	cobalt-mediated radical polymerisation
CRP	controlled radical polymerisation
CRT	catalysed radical termination
Đ	dispersity (molecular weight distribution)
Da	daltons
dn/dc	differential index of refraction
DCM	dichloromethane
DFT	density functional theory
DT	degenerative transfer
g	grams
GPC	gel permeation chromatography
GTP	group transfer polymerisation
hr	hour
IP	isoprene
Lig	ligand
M	metal
M_n	number average molecular weight
$M_{n,th}$	theoretical molecular weight
M_w	weight average molecular weight
Me	methyl

MeCN	acetonitrile
min	minutes
MMA	methyl methacrylate
mL	millilitre
mol	mole
mol%	mole percent
OMRP	organometallic-mediated radical polymerisation
PMMA	poly(methyl methacrylate)
P_n	polymer chain with degree of polymerisation “n”
PSty	poly(styrene)
PVAc	poly(vinyl acetate)
ROP	ring-opening polymerisation
RT	reversible termination
Sty	styrene
THF	tetrahydrofuran
Tol	toluene
V-70	2,2'-azobis(4-methoxy-2,4-dimethylvaleronitrile)
VAc	vinyl acetate

Ligands

The following ligands have been used in this thesis.

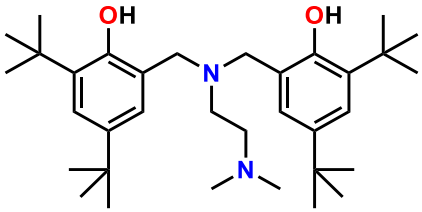

Lig1H_2

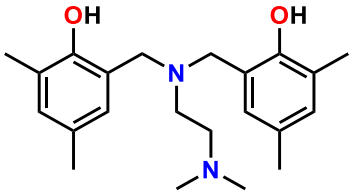

Lig2H_2

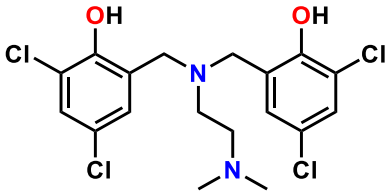

Lig3H_2

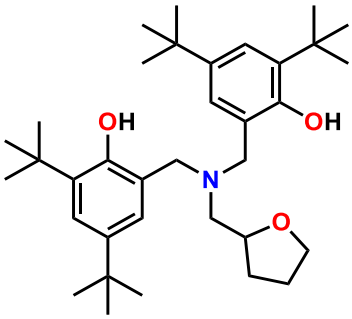

Lig4H_2

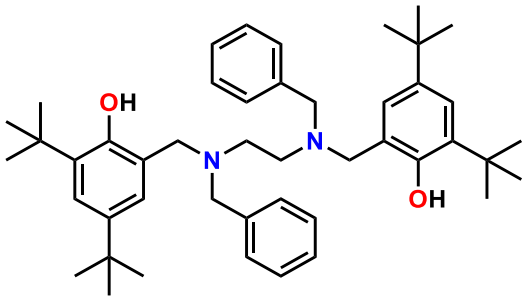

Lig5H_2

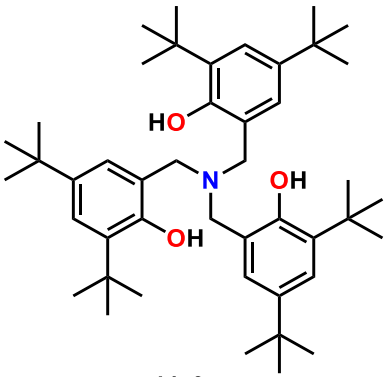

Lig6H_3

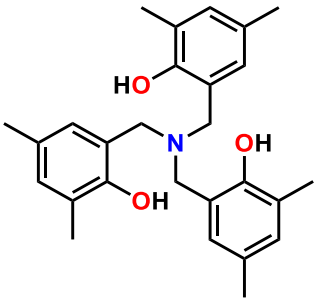

Lig7H_3

Complexes

The following complexes have been used in this thesis.

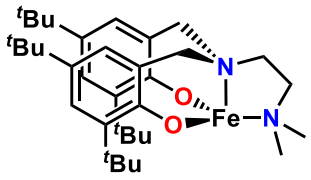

Fe1

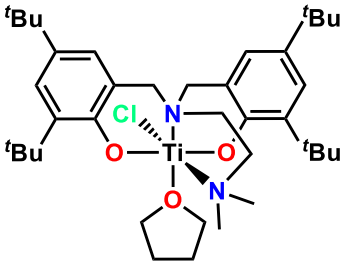

Ti1

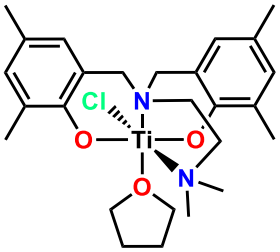

Ti2

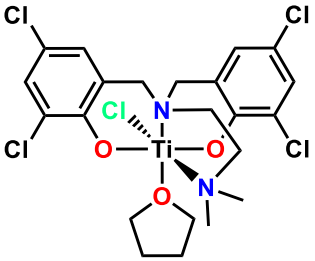

Ti3

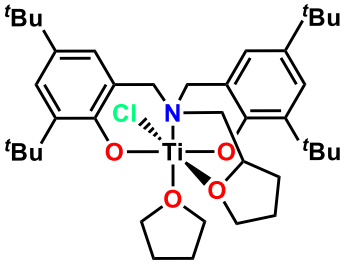

Ti4

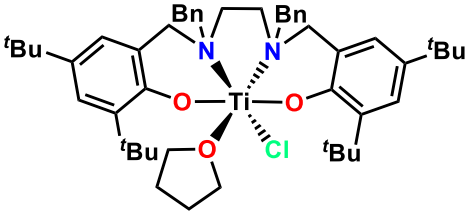

Ti5

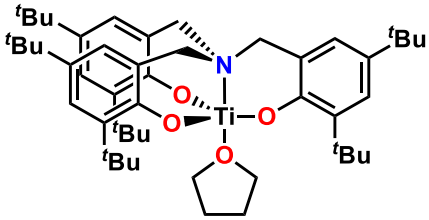

Ti6

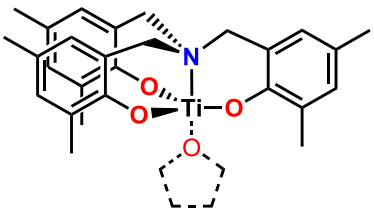

Ti7

Publications

D. L. Coward, B. R. M. Lake, R. Poli and M. P. Shaver, Radically Initiated Group Transfer Polymerization of Methacrylates by Titanium Amino-Phenolate Complexes. *Macromolecules*, 2019, **52**, 3252-3256.

D. L. Coward, B. R. M. Lake and M. P. Shaver, Understanding Organometallic-Mediated Radical Polymerization with an Iron(II) Amine-Bis(phenolate). *Organometallics*, 2017, **36**, 3322-3328.

D. L. Coward, B. R. M. Lake and M. P. Shaver, Organometallic-Mediated Radical Polymerization in *Metal-Catalyzed Polymerization: Fundamentals to Applications*. 2017, CRC Press, 179-202.

“Wear sunscreen. If I could offer you only one tip for the future, sunscreen would be it. The long-term benefits of sunscreen have been proved by scientists, whereas the rest of my advice has no basis more reliable than my own meandering experience. I will dispense this advice now.”

Mary Schmich & Baz Luhrmann

1 Introduction

1.1 Controlled Radical Polymerisation

Controlled radical polymerisation (CRP) has revolutionised the way we approach radical polymerisations. Until the mid-1990s, the ability to maintain functional group tolerance of radical polymerisations whilst achieving excellent control over molecular weight and dispersity was challenging, due to the inherent diffusion-controlled irreversible termination reactions.[1] However the development of methodologies such as atom transfer radical polymerisation (ATRP)[2–4] and reversible addition-fragmentation chain transfer (RAFT),[5] which have been able to offer such control, has led to the design and synthesis of a variety of molecular architectures and new materials.

Radical polymerisation (RP) has, for many years, been an important synthetic route for several industrially important polymers, with approximately 50% of all commercial polymeric material being synthesised through RP.[1] This is due to its functional group tolerance, facile process conditions and the ability to develop a wide range of (co)polymers from a variety of vinyl monomers (-CH=CH_2).[1] Therefore, the ability to exert a degree of control over the process would have great industrial implications, especially for speciality applications where precise properties are fundamental to the final product. Several different methods have been developed which use different mechanisms to achieve this control. These include nitroxide-mediated polymerisation (NMP), atom transfer radical polymerisation and reversible addition-fragmentation chain transfer polymerisation.[6]

All these methods work by establishing a dynamic equilibrium between active radical species (the propagating chains) and dormant chains, in which the equilibrium lies heavily towards the dormant species. This is due to the concentration of active radicals having a greater contribution to the rate of irreversible termination (r_t) than to the rate of propagation (r_p), as shown in Equations 1.1 and 1.2. The result is that irreversible termination is suppressed but not eliminated. Couple this with a fast initiation process, and well-controlled polymers can be synthesised.

$$r_p = k_p[M][P\cdot] \qquad r_t = 2k_t[M\cdot]^2$$

Equations 1.1 & 1.2 - Kinetics of a radical polymerisation.

Whilst there has been some debate as to what defines a controlled radical polymerisation, the following are generally considered to be the key characteristics:[6,7]

1) The molecular weight is determined by the monomer conversion and the ratio of the concentration of monomer to controlling species.
2) The lifetime of a propagating chain is increased from seconds (for a conventional radical polymerisation) to several minutes or hours.
3) Rapid consumption of the initiating species (ATRP, NMP) or chain transfer agent (RAFT).
4) Low dispersity (Đ) of the resultant polymer.
5) High end group fidelity that allows for further chain extensions.
6) There is a constant concentration of growing chains throughout the polymerisation. However, this is not unique to CRP processes alone and is also associated with conventional free radical polymerisations.
7) The rate of termination and chain transfer reactions are strongly reduced (in the case of ATRP and NMP), while they are outcompeted by reversible chain transfer in RAFT.
8) Radicals are predominantly in a dormant state in the case of ATRP and NMP, while they are constantly reshuffled in the RAFT process, yet the overall radical concentration is not reduced.

The usefulness of CRP extends beyond the synthesis of linear homopolymers. A myriad of molecular architectures have been made, including gradient and block copolymers, functional polymers and grafted polymers.[2,8] Even more complex structures such as brush-shaped molecules, star (co)polymers and dendrimers can be made using multifunctional initiators.[6] This has led to the development of new materials with improved mechanical properties.

Whilst CRP research to date has been predominantly academic, the potential for industrial applications is clear and significant progress has been made.[9] It was predicted in 2000 that CRP products would account for a market value in excess of $20 billion a year.[10] Whilst, with hindsight, this was a rather optimistic prediction (CRP will never entirely supersede free radical polymerisation) it does demonstrate the belief that industry has in CRP. CRP is most

likely to make inroads into the speciality polymer market with applications in, for example, coatings, adhesives, surfactants, drug delivery systems and surface modifiers.[1] DuPont Performance Coatings was one of the first adopters of the technology and used CRP, in particular the products of catalytic chain transfer reactions, to synthesise various components of paints and coatings.

1.1.1 Methods of Control

Controlled radical polymerisation, also known as reversible-deactivation radical polymerisation (RDRP), can be allocated to one of two categories depending on the mechanism used to control the polymerisation.[11] The two categories vary in the exchange equilibria between the reactive radical and the dormant species. Those methods based on dissociation (Scheme 1.1a) are termed "reversible termination" (RT), and operate through a rapid and dynamic equilibrium between propagating radical and dormant species, lowering the radical concentration and thus suppressing irreversible bimolecular termination. Polymerisations are slower than the equivalent free radical polymerisation.

On the other hand, those methods based on associative exchange (Scheme 1.1b) are called "degenerative transfer" (DT). DT operates through a rapid degenerative exchange and, along with a chain-length dependent termination rate, gives well-controlled growth. However, DT requires a constant influx of new radicals from the initiation source.

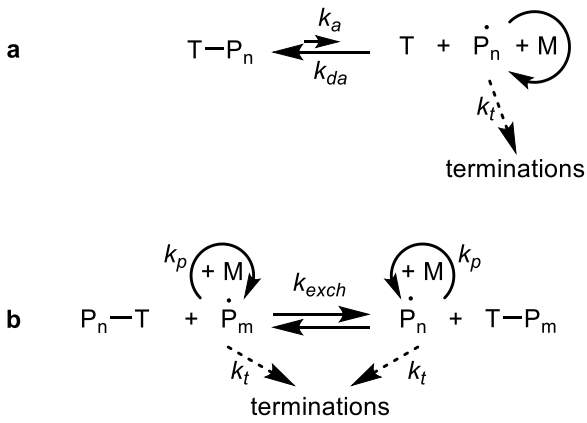

Scheme 1.1 - Mechanism of a) dissociative and b) associative exchange equilibria. M = monomer, T = trapping species.[12]

One such RT technique is nitroxide-mediated polymerisation (NMP), where the trapping species T is a stable nitroxide radical. One example of an NMP mediator is (2,2,6,6-tetramethylpiperidin-1-yl)oxyl, also called TEMPO (Figure 1.1).

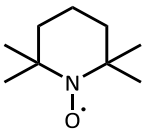

Figure 1.1 - (2,2,6,6-Tetramethylpiperidin-1-yl)oxyl (TEMPO).

An example of a commonly used DT technique is reversible addition-fragmentation chain transfer (RAFT) polymerisation, where T is a thiocarbonyl fragment (Scheme 1.2).

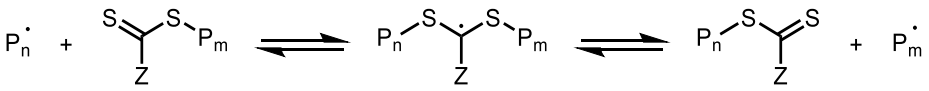

Scheme 1.2 - RAFT mechanism.

In addition to NMP and RAFT, metal-mediated methods have also been the subject of significant research and arguably dominate the field of CRP.[13] This is due to the ease of use, the monomer scope and the ability to tune the metal framework for the desired application.

Metal complexes can mediate a radical polymerisation in two ways. Firstly, the metal complex itself can behave as the trapping species and form a dormant species through a metal-carbon bond. This is called Organometallic-Mediated Radical Polymerisation (OMRP).[14] Secondly, the trapping species can be an oxidised metal halide, X-M^{x+1}, where X is a halogen atom that is transferred from the metal to the active radical to form a halogen-capped dormant species and a reduced metal complex. This is called Atom Transfer Radical Polymerisation (ATRP).

1.1.2 ATRP

ATRP was developed in 1995 by two research groups concurrently. Matyjaszewski reported the polymerisation of styrene using a Cu(I)/Cu(II) system,[15] requiring as little as 1 mol% of catalyst, whereas Sawamoto used a Ru(II)/Ru(III) system to control the polymerisation of methyl methacrylate (MMA).[16] The excellent polymerisation control, in both cases, arises from the fast initiation and catalysed intermittent activation of a dormant species to form

propagation radicals. Since then, copper has proven to be the most successful metal for ATRP mediators, and a wide range of copper based systems have been developed to control the polymerisation of many different vinyl monomers.[17]

A typical metal-mediated polymerisation proceeds in much the same way as other CRP methods, with initiation, propagation and both reversible and (suppressed) irreversible termination. The ATRP initiator is usually a simple alkyl halide such as PECl (phenyl ethylchloride, Figure 1.2a) or EBrP (ethyl 2-bromopropionate, Figure 1.2b), and requires the metal to initially be in the lower oxidation state. In the case of R-ATRP (Reverse Atom Transfer Radical Polymerisation, where the metal is initially in the higher, and often more stable, oxidation state), a conventional radical initiator such as AIBN (azobisisobutyronitrile, Figure 1.2c) can be used. Fast initiation is required for good polymerisation control and low dispersities.

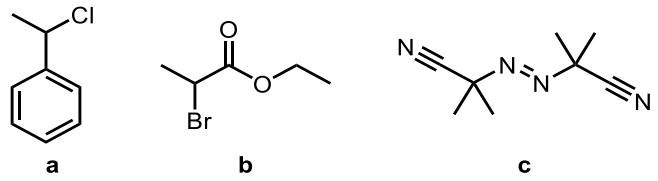

Figure 1.2 - a) PECl (phenyl ethylchloride), b) EBrP (ethyl 2-bromopropionate), c) AIBN (azobisisobutyronitrile).

Propagation then proceeds as normal for a radical polymerisation. The dynamic equilibrium between active and dormant species is rapidly formed. This reversible deactivation is formed by cleaving the carbon-halogen bond in $X\text{-}M^{x+1}$ and subsequently capping the active radical, yielding a dormant species and the metal M^x in the lower oxidation state.

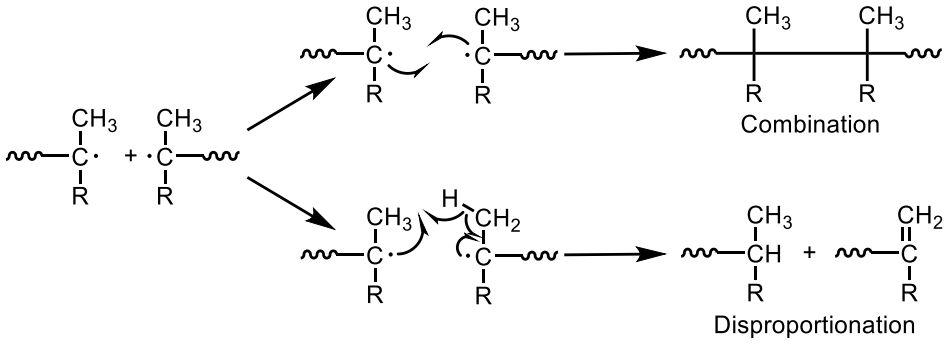

Figure 1.3 - Mechanisms of bimolecular termination.[18]

Irreversible termination is unavoidable with a radical polymerisation, and bimolecular termination occurs through either disproportionation or combination (Figure 1.3). In a disproportionation termination step, one radical transfers a hydrogen atom to the other to form two stable molecules, one of which has an alkene terminus. In a combination termination step, two growing chain radicals form a covalent bond in a single stable molecule with doubled molecular weight. The relative extent of these reactions is highly dependent on the nature of the radicals.[19] It is suggested that styrenes primarily undergo coupling,[20,21] whereas methacrylates undergo both disproportionation and combination.[21,22]

The polymerisation rate in ATRP is dependent on the rate constant of propagation and on the concentration of monomer and growing radicals, where this concentration of growing radicals is itself dependent on the equilibrium constant between the dormant species and active radicals.[23] All these rate constants are influenced by the nature of the metal complex and the ligand framework, the chosen monomer, and the reaction conditions (e.g. solvent, temperature and pressure).

ATRP is now very much established as an excellent technique with which precisely defined polymeric materials may be produced. The mechanisms of control are well-understood, numerous metal complexes have proven to be excellent mediators, and several review papers discuss the field in great depth.[23–25]

Research into copper-based ATRP systems has mainly focused on the development of new initiation systems. Initial work involved the use of large quantities of air-sensitive Cu(I) complexes, whereas more recent systems can use less than 50 ppm of catalyst. These systems involve the slow and continuous regeneration of the Cu(I) activator using an external radical source.[26]

Most recently, work has focussed on using ATRP in dispersed media such as within microemulsions, miniemulsions and emulsions.[27–30] In particular, ATRP in aqueous and supercritical CO_2 dispersed systems would reduce the environmental impact and the cost of the process, due to the use of these environmentally and chemically benign solvents.[31,32] However, ATRP within dispersed media has proved to be challenging, not least because the polymerisation must be controlled whilst maintaining colloid stability. Work has also focussed on the development of oxygen-tolerant ATRP. Radical polymerisations are inherently sensitive to being quenched by oxygen to form inactive peroxy radicals. In many

cases, the metal complexes themselves are also air-sensitive, losing their reactivity upon reaction with oxygen and/or water. Therefore, it is usual for great care to be taken to ensure the polymerisation environment is entirely dry and deoxygenated. However, it has been found that ATRP techniques with regeneration of the catalyst can tolerate a small amount of oxygen. This can be achieved in many ways, including the use of an excess of reducing agent such as Cu^0,[33] amines in the presence of light,[34] ascorbic acid,[35] or by simple elimination of the reaction vessel's headspace.[36] Matyjaszewski and co-workers have also conducted an ATRP in the open air, by converting oxygen to carbon dioxide using glucose oxidase enzyme.[37]

It is predicted that future work regarding ATRP will focus on developing more active catalysts, with the aim of polymerising less active monomers such as vinyl acetate or *N*-vinylamides, and gaining a deeper mechanistic understanding of the polymerisation to facilitate the scale up of polymerisation processes.[24]

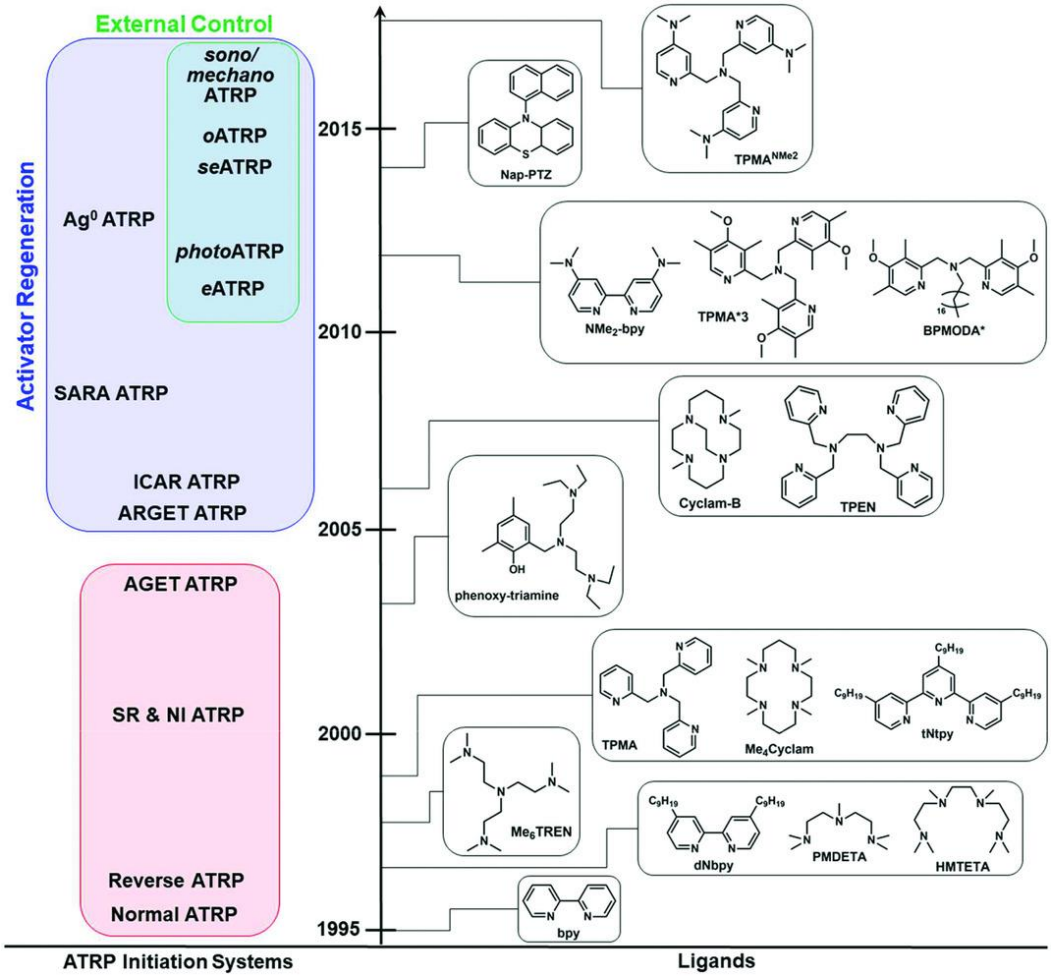

Figure 1.4 - Timeline of the development of copper-based ATRP.[24]

1.1.3 OMRP

Similar to ATRP, though mechanistically distinct, OMRP is a method of controlling a polymerisation that involves the reversible homolytic cleavage of a metal-carbon bond. This bond is formed between a metal complex, acting as a mediator, and the propagating polymer chain. The control is highly dependent on the strength of this metal-carbon bond, and therefore fine tuning of the electronic and steric properties of the ligand and metal centre is required.

There are two mechanisms through which an OMRP may proceed. This can be by either reversible termination (RT-OMRP) or degenerative transfer (DT-OMRP). In any given polymerisation, the prevalent mechanism depends on the metal, ligand and reaction conditions. RT-OMRP uses the metal centre as a spin trap, and reversibly deactivates a propagating polymer chain. In this dormant state the polymer is unable to propagate and add further monomer units or react with another propagating chain. This dormant species can then reactivate, releasing the active propagating polymer chain and leaving behind the chemically-unmodified metal complex (Scheme 1.3). The nature of the deactivated metal-polymer species is dependent on the monomer, and is either bound to the metal as a single σ-bonded ligand or a chelate *via* an additional metal-heteroatom dative bond. A RT-OMRP is initiated either by using a conventional radical initiator (such as AIBN) and a reduced metal complex M^x, or by using an oxidised metal complex with a preformed metal-carbon bond (R-M^{x+1}), with the former method the most commonly used. For a low dispersity polymer the rate of initiation (k_i) must be very fast, with the rate of deactivation (k_d) much faster than the rate of propagation (k_p) to maintain a low concentration of active radicals.

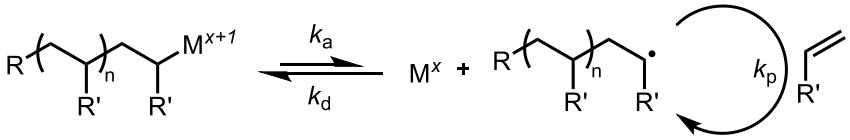

Scheme 1.3 - Reversible termination OMRP (RT-OMRP).

DT-OMRP is mechanistically similar to a RAFT polymerisation, and usually has a very low rate of polymerisation at the start because the radicals generated from initiation immediately react with the metal complex and form the DT-OMRP dormant species (P_n-M^{x+1}). Polymerisation only occurs once the total concentration of radicals generated exceeds the

concentration of metal mediator, because additional radicals produced then either react with monomer or displace the metal-bound radical (associative exchange), which then reacts with a monomer (Scheme 1.4).

Control using a DT-OMRP mechanism relies on the rate of termination (k_t) being strongly dependent on the polymer chain length, with shorter chains terminating much more rapidly than longer chains. Since radicals are released from the initiator continuously throughout the polymerisation, the associative exchange mechanism allows for rapid and reversible release of the longer chain radicals, which terminate slowly. Therefore, for a well-controlled polymerisation, the rate of associative exchange (k_{ex}) must be considerably higher than the rate of propagation (k_p).

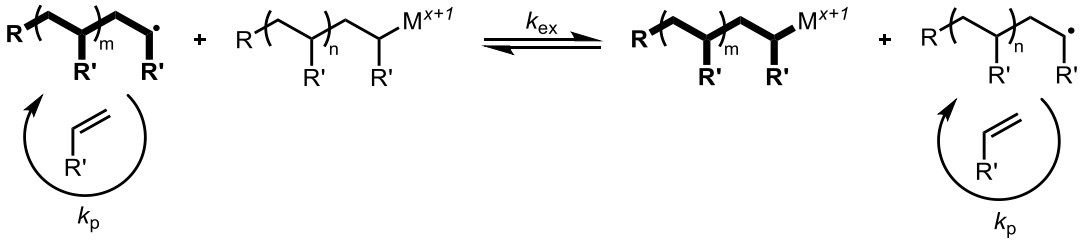

Scheme 1.4 - Degenerative transfer OMRP (DT-OMRP).

In addition to RT-OMRP and DT-OMRP, where the polymer chains propagate and grow, there are two important side-reactions to consider which impact the progress of the polymerisation, namely; catalytic chain transfer (CCT) and catalysed radical termination (CRT).

CCT (Scheme 1.5) is due to H-atom transfer from the radical terminus of the propagating polymer, which results in an alkene-terminated dead polymer chain, and a metal hydride complex (H-M^{x+1}). This transfer may occur either through direct H-abstraction from the radical chain end by the metal complex (M^x), or *via* β-H elimination from an OMRP dormant species (P_n-M^{x+1}). This requires a vacant coordination site *cis* to the coordinated polymer chain. The resultant metal hydride (H-M^{x+1}) is then able to initiate the growth of a new chain through reaction with the monomer used. Polymers synthesised through CCT characteristically have short chain lengths, an alkene terminus (often observable by ^{1}H NMR) and molecular weights independent of monomer conversion.[11]

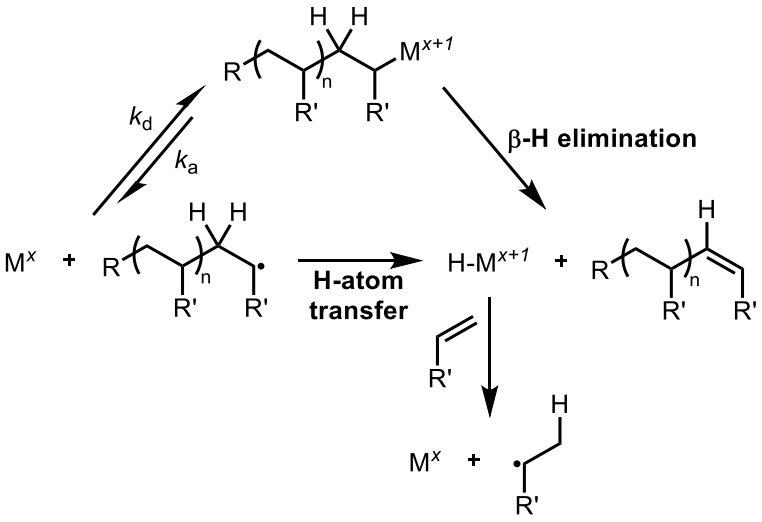

Scheme 1.5 - Catalytic chain transfer (CCT).

In some cases, as suggested above, CCT is an undesirable side-reaction of a controlled polymerisation. However, there are many cases in the literature where it is of benefit to synthesise polymers through CCT.[38] For example, polymers with short chain lengths may have industrial applicability in areas where long-chain polymers would be problematic, such as in melt-processing and coatings. Another advantage of CCT is the presence of the alkene terminus of the polymer which provides the opportunity for post-polymerisation functionalisation. Thiol-ene click chemistry is one such method of exploiting these alkene groups and introducing functionality to the polymer. Haddleton and co-workers have extensively studied the combination of CCT polymerisation and thiol-ene chemistry to understand the most effective catalysts for this process,[39] and to synthesise polymers with a range of architectures.[40]

One would expect that CCT would have no effect on the overall number of radicals present in a controlled reaction polymerisation; for each radical that is lost, a new radical is generated. However, CRT (Scheme 1.6) results in a significant loss of radicals from the reaction, with the potential to quench and terminate the entire polymerisation. Instead of the reaction of the metal hydride (H-M^{x+1}) with an equivalent of monomer or β-H elimination from an OMRP dormant chain (P_n-M^{x+1}), either of these species may undergo a reaction with an additional radical chain ($^{\bullet}P_m$). This leads to a dead chain with a saturated terminus (H-P_m) or to a coupled chain (P_n-P_m). The reduced metal complex is regenerated, and therefore allowed to re-enter the catalytic cycle.

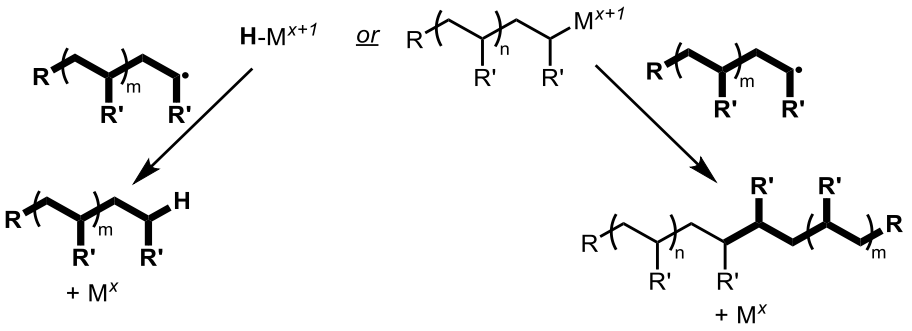

Scheme 1.6 - Catalysed radical termination (CRT).

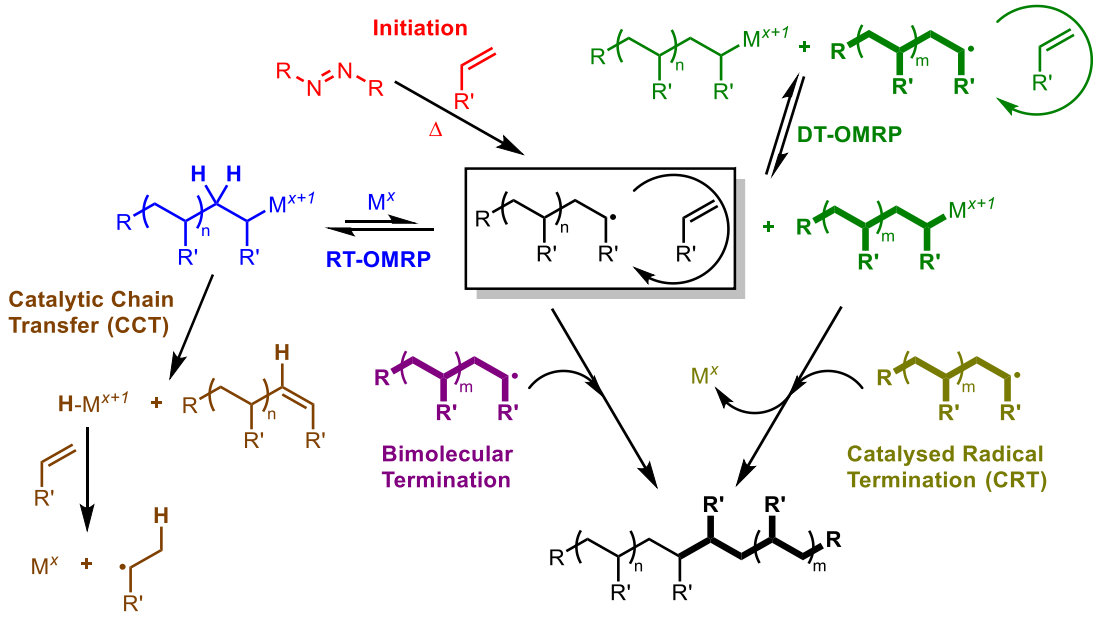

Scheme 1.7 - Overview of mechanisms involved in OMRP.

The possible interplay between the aforementioned OMRP-based mechanisms (and ATRP) became apparent soon after the first reports on ATRP. Poli and co-workers described a family of half-sandwich molybdenum-based complexes which were able to control the polymerisation of styrene by simultaneous RT-OMRP and ATRP mechanisms when the reactions are performed under (R-)ATRP conditions.[41–43] The complexes may also mediate CCT under slightly different reaction conditions. Whilst possible mechanistic interplay has been exhibited in titanium-[44] and osmium-mediated[45] systems, iron-based systems are currently the most common and well-understood systems displaying interplay. This includes α-diimine,[46–51] amine bis(phenolate),[52–56] and β-ketiminate-ligated[57] iron complexes.

Interplay between ATRP and OMRP (and CCT/CRT) is possible since the equilibrium in an ATRP reaction is heavily weighted towards the reduced metal complex (M^x) and the halogen-

capped dormant polymer (Scheme 1.8). The resulting high concentration of reduced metal complex (M^x) enables the complex to act as a spin-trap for propagating radicals, reversibly forming metal-carbon bonds and thus allowing an OMRP equilibrium to establish, potentially imparting significant control over a reaction performed under (R-)ATRP conditions. However, since the formation of the OMRP dormant species (P_n-M^{x+1}, as discussed above) may also be a prerequisite for the occurrence of CCT and CRT reactions, the existence of an OMRP equilibrium during an ATRP reaction does not necessarily result in an increase in control over dispersity and molecular weight. Additionally, given the high concentration of the reduced metal complex (M^x) in an ATRP reaction, CCT *via* direct H-atom transfer is possible, even in the absence of a simultaneous OMRP equilibrium. This would lead to short-chained oligomers with alkene end-groups.

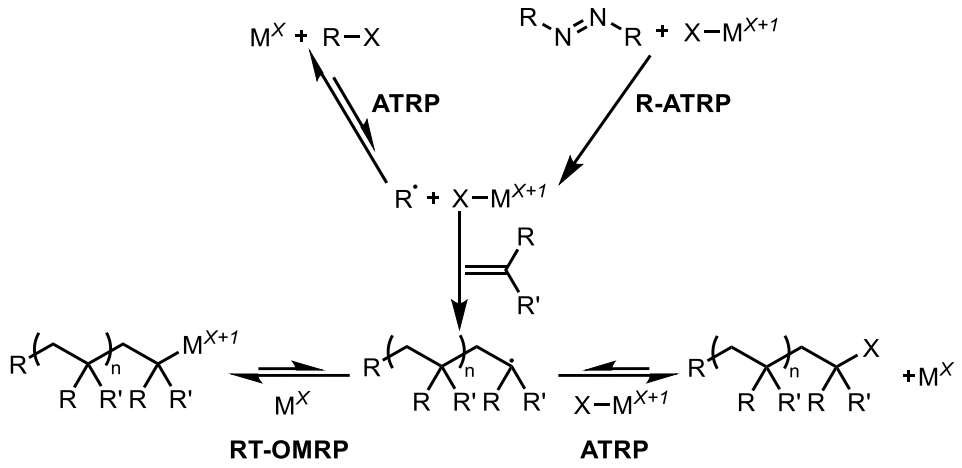

Scheme 1.8 - Interplay between ATRP and OMRP.

1.1.3.1 Metals Used in OMRP

Aside from iron and titanium, which will be discussed in more detail below, a variety of metals have previously been used as mediators of OMRP.

The first example of OMRP was described by Wayland and co-workers in 1992, with rhodium(II) tetramesitylporphyrinato **1** complexes and their derivatives used as initiator and mediator of the polymerisation of acrylic acid, methyl acrylate and ethyl acrylate. The trapping species was also able to reinitiate polymerisation, which resulted in broad dispersities of 1.75-2.75 and a relatively uncontrolled polymerisation.

Cobalt is by far the most widely used metal for OMRP, with a significant body of work exploring a range of complexes and monomers.[58] Early work by Wayland and co-workers used cobalt porphyrin complexes to polymerise acrylates.[59] Derivatives of cobalt tetramesitylporphyrin (TMP) **2** were used to both initiate and control the polymerisation of methyl acrylate. The polymerisation was living and controlled, with dispersities between 1.1 and 1.3.

Vinyl acetate has been a monomer of particular interest for those working with cobalt-mediated radical polymerisations (CMRP),[60–69] due to the difficulty of achieving control through ATRP, with the first example of an efficient OMRP appearing in 2005.[70] Jérôme and co-workers used $Co(acac)_2$ **3** as mediator and V-70 as initiator to polymerise vinyl acetate in the absence of solvent at 30 °C. An induction period of 12 hours was required to oxidise the Co(II) species to a Co(III) organometallic complex. After this, a well-controlled polymerisation was observed with molecular weights that increased linearly with conversion, and dispersities between 1.1 and 1.2. This long induction period is highly indicative of a DT-OMRP mechanism. Using AIBN instead of V-70, and higher reaction temperatures, gave an uncontrolled polymerisation and polymers with much broader dispersities (Đ = 2.0-3.5), suggesting the presence of irreversible chain termination reactions. The same protocol has been used to polymerise vinyl acetate in both aqueous suspension[60] and miniemulsion,[71] with both achieving high conversions. Work has also been done to control the polymerisation of vinyl acetate in supercritical carbon dioxide.[72] Aside from vinyl acetate, CMRP has been particularly effective at controlling the polymerisation of other notoriously difficult monomers. These include acrylonitrile,[73] butyl acrylate,[74] and a variety of N-vinyl amides.[75]

Furthermore, it is possible to switch the polymerisation from a DT-OMRP mechanism to an RT-OMRP mechanism through the use of an additional ligand, such as pyridine or triethylamine.[76,77] This removes the requirement for an induction period before the polymerisation starts.

There has been significant work to understand why cobalt is so effective as a mediator of OMRP and, in particular, why **3** does not suffer the same problem of sequence errors as other OMRP systems.[78] This is especially true for controlled vinyl acetate polymerisations. A polymer with no sequence errors would typically have head-to-tail (HT) monomer addition throughout the entire polymer chain. However, occasionally a head-to-head (HH) monomer

addition will occur, and often in OMRP-based systems the dormant species which follows a HH addition is difficult to reactivate. This results in irreversible termination and a broader dispersity. It was postulated that, in the case of **3**, either the number of HH additions is reduced, or the dormant Co-PVAc **4** species is easy to reactivate, irrespective of HT or HH addition. Experimental evidence showed that neither of these two assumptions were correct. DFT calculations were used to investigate the difference in bond-dissociation energy (BDE) between the 5-membered dormant species **4a** (formed by HH addition) and the 6-membered dormant species **4b** (formed by HT addition), and illustrated in Figure 1.5. It was found that this difference in BDE was virtually zero. Chelation of the carbonyl group has a prominent effect in the 5-membered ring, but this is cancelled out by the higher reactivity of the 6-membered ring. This lack of difference is responsible for suppressing the impact of sequence errors.

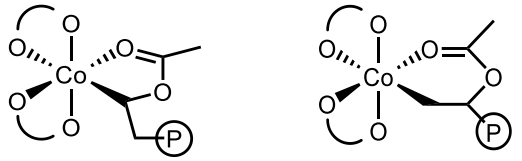

4a **4b**

Figure 1.5 - 5-membered and 6-membered Co-PVAc **4** dormant species.

More recent work investigated using cobalt to mediate the copolymerisation of ethylene with polar monomers such as vinyl acetate, acrylonitrile and *N*-methyl vinyl acetamide (NMVA).[79] A **3**-PVAc macroinitiator was used with a reaction temperature of 40°C. Ethylene-vinyl acetate copolymers were synthesised at a range of ethylene pressures from 10 bar to 50 bar. In all cases the dispersity of the resultant polymer was lower than 1.2 except at very high conversion. ^{1}H NMR spectroscopy showed that the composition of the polymer, and as a result the thermal properties, was dependent on the ethylene pressure. As the pressure was increased from 10 to 50 bar the ethylene content in the polymer increased from 13 to 54 mol%. NMR spectroscopy also suggested that the copolymer had a random sequence structure with negligible branching. This was due to the relatively low reaction temperature which suppressed side reactions. The composition of the ethylene-NMVA copolymer was also dependent on the ethylene pressure used. However, this was not true for the ethylene-acrylonitrile copolymer, which contained fewer ethylene units. This was due to the reactivity ratio of ethylene-acrylonitrile supporting preferential acrylonitrile addition, whereas the reactivity ratios for ethylene-vinyl acetate and ethylene-NMVA are roughly the same.

A study by Detrembleur and co-workers explored using **3** to trap halomethyl radicals ($XCH_2^{\bullet}$), which was then able to act as an initiating species.[80] This also has the added benefit of chain-end functionality, termed a telechelic polymer. The alkylcobalt(III) initiator, **3**-CH_2X, was synthesised using V-70 or AIBN, tris(trimethylsilyl)silane (TTMSS) and an excess of CH_2X_2 (X = Cl or Br). TTMSS is proposed to behave as a radical reducing agent which, in combination with V-70/AIBN, yields tris(trimethylsilyl) radicals ($(Me_3Si)_3Si^{\bullet}$) which in turn abstract a halogen atom from CH_2X_2 giving $XCH_2^{\bullet}$. This species is then trapped by **3**. The presence of TTMSS is crucial for the synthesis, and no product is attained in its absence. **3**-CH_2Br was used to initiate and control the polymerisation of vinyl acetate at 40°C. No induction period was observed, and molecular weights increased with conversion. Dispersities were low (Đ < 1.2) at low conversion but increased as molecular weights reached 100000 Da.

Furthermore, various chromium and vanadium complexes have been used as OMRP mediators. Chromium was first used in the 1970s by Minoura and co-workers, where $Cr(acac)_2$ **5** and benzoyl peroxide were used to initiate and control the radical polymerisation of a range of vinyl monomers.[81–84] Further advances came in 2008, when Poli, Smith and co-workers used chromium β-diketiminate **6** complexes (Figure 1.6) to control the polymerisation of vinyl acetate.[85] It was found that the strength of the chromium-vinyl acetate bond in the dormant species is highly dependent on the steric nature of the aryl substituents, and therefore allows for fine tuning of the ligand framework to provide optimum control.

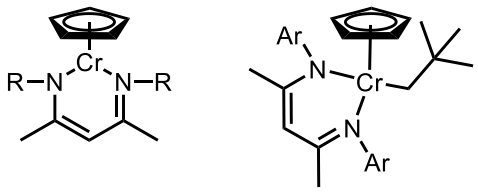

6 **7**

Figure 1.6 - Chromium β-diketiminate complex **6** and $CpCrL(CH_2CMe_3)$ **7**, where L = 2,6-dimethylphenyl β-diketiminato.

Attempts were also made to synthesise a chromium(III) alkyl complex for use as a single-component OMRP reagent.[86] This would be of particular benefit since the complex would behave as both the initiator and mediator of the polymerisation, and thus simplify the polymerisation set-up. The complex $CpCrL(CH_2CMe_3)$ **7** (Figure 1.6) was synthesised and used in the room temperature polymerisation of vinyl acetate. Whilst the polymerisation was very

slow (taking in excess of 400 hours) and reached only low conversions (14%), molecular weight increased linearly with conversion. However, the rate constant of the polymerisation decreased over time, which suggests that the growing chains were partially deactivating.

Vanadium complexes were first used in OMRP in 2010, when Shaver and co-workers used vanadium bis(imino)pyridine **8** (Figure 1.7) in the OMRP of vinyl acetate.[87] AIBN was used as the initiator with a reaction temperature of 120 °C, promoting RT-OMRP conditions. Dispersities as low as 1.3 were achieved and molecular weights increased linearly with conversion. Lower reaction temperatures gave broader dispersities, likely due to inferior initiation and chain exchange. The resultant polymer lacked halogen end groups, suggesting that the OMRP equilibrium dominated over the ATRP equilibrium.

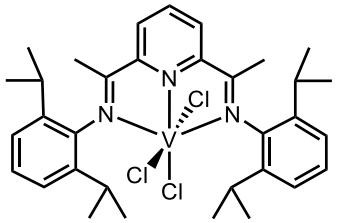

8

Figure 1.7 - [BIMPY]VCl_3, where [BIMPY] = 2,6-(ArN=CMe)$_2C_5H_3N$ and Ar = 2,6-(^{i}Pr)$_2C_6H_3$.

1.2 Iron and Titanium

Research in the field of controlled radical polymerisation has been dominated by ATRP and copper, which offers control over a wide range of homopolymers, block copolymers and macromolecular architectures.[88] However there are still concerns over residual toxic copper which also discolours the isolated polymer. There has been some work to reduce the catalyst used in the polymerisation,[24,25] such as through the development of Activator ReGenerated by Electron Transfer (ARGET) ATRP. This involves using non-radical-forming soluble reducing agents which are able to regenerate the Cu(I) metal without reacting with the propagating radicals. In addition, Initiators for Continuous Activator Regeneration (ICAR) ATRP uses conventional radical initiators to regenerate the activator which drastically lowers the required copper concentration. However, reducing the concentration of metal negatively affects the dispersity of the polymer.

Even more preferable would be to use a metal with a toxicity lower than that of copper, so that any residual metal would be less of an issue whilst also giving a colourless polymer product. A vast array of transition and main group metals have shown some usefulness in reversible deactivation radical polymerisation.[13] Of these, iron and titanium are perhaps the most exciting and promising. They are highly Earth abundant (Figure 1.8) and relatively inexpensive with a low toxicity, and so are more industrially promising than copper.[12] In particular, there has been very little research to investigate titanium complexes within CRP.

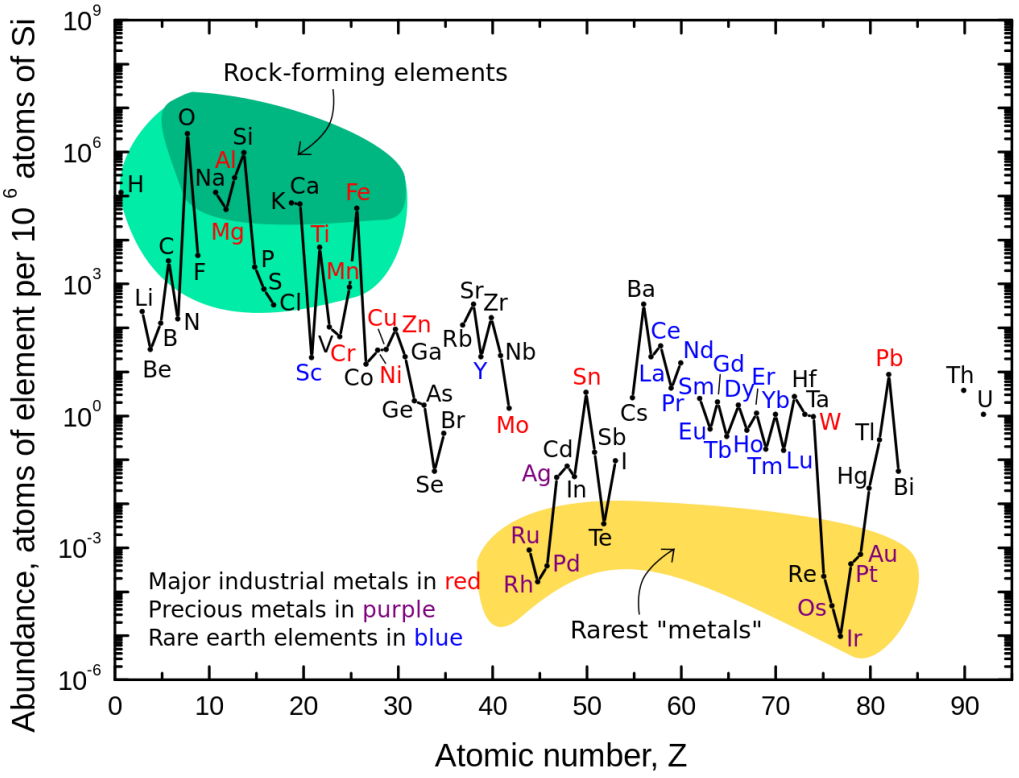

Figure 1.8 - Abundance of the chemical elements in Earth's upper continental crust as a function of atomic number.[89]

1.2.1 Use in Catalysis

The use of iron compounds as catalysts in organic synthesis is attractive for several reasons.[90,91] As stated above, iron is in plentiful supply (as the most abundant metal in the Earth's crust after aluminium) and is therefore much cheaper than precious metals which are often used in catalysis. The increase in price of transition and rare earth metals over recent years has prompted further research into these cheaper alternatives. Some iron compounds

are also incorporated into biological systems and therefore have a relatively low toxicity. This is especially important for many applications, including pharmaceuticals, food and cosmetics. Whilst iron is still lagging behind palladium as the most versatile catalytic metal for use in organic synthesis, this gap is decreasing by the year. Iron is able to adopt oxidation states from 0 to +5, and can therefore behave as an iron-centred nucleophile, catalysing reactions such as nucleophilic substitutions, hydrogenation, cycloisomerisation, and the hydrofunctionalisation of alkenes and alkynes.[92] Iron has also been extensively used as a catalyst in C-H activation,[93,94] water oxidation,[95–97] epoxidation,[98] and olefin-carbonyl metathesis.[99,100]

Most of the examples of iron-based chemistry concern iron(II) (ferrous) or iron(III) (ferric) complexes.[101] A coordination number of 6 with an octahedral ligand sphere is preferred for the iron(II) complex ($[Ar]3d^6 4s^0$), and the iron(II) complex is readily oxidised in air to its iron(III) analogue ($[Ar]3d^5 4s^0$), which often exhibits an octahedral coordination structure. This one-electron difference between two accessible and stable oxidation states means that iron is a good candidate to act as a mediator in CRP. In addition, iron in low oxidation states shows the most potential for iron-catalysed reactions because it can form more reactive complexes, but iron(III) has the advantage that, unlike iron(II), it is not susceptible to oxidation.

There are numerous examples of iron complexes being used in one-electron radical reactions.[102,103] By way of a select few examples, Nakamura and co-workers reported a coupling reaction between alkynes and aromatic sulfonyl chlorides to give (*E*)-β-chlorovinylsulfones with 100% regio- and stereoselectivities.[104] This reaction was promoted by iron(II) acetylacetonate, $Fe(acac)_2$ **9**, (10 mol%) in the presence of a $(p\text{-Tol})_3P$ ligand (10 mol%) in toluene at 110 °C. Several functional groups, such as chloride, bromide, iodide, nitro, ketone, and aldehyde, were tolerated under the reaction conditions. The reaction mechanism involved initial electron transfer from the iron(II) catalyst to the aromatic sulfonyl chloride to generate a sulfonyl radical that adds to the alkyne. The vinyl radical then abstracts $Cl^{\bullet}$ from the previously formed iron(III) chloride, thereby regenerating the iron(II) catalyst and yielding the final product. Baran and co-workers reported the use of **9** or $Fe(dibm)_3$ (**10**, dibm = diisobutyrylmethane), alongside $PhSiH_3$ under ambient conditions, to react heteroatom-substituted olefins with electron-deficient olefins (Figure 1.9).[105]

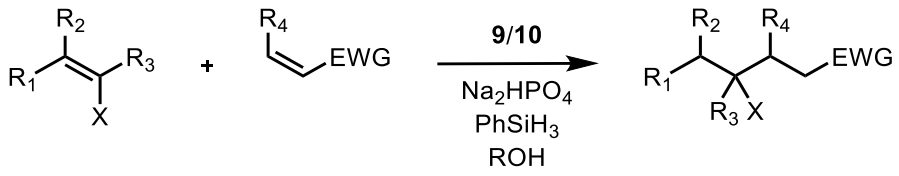

Figure 1.9 - Reaction of a heteroatom-substituted olefin with an electron-deficient olefin.[105] X = heteroatom (O, N, S, B, Si, F, Cl, Br, I).

The advantages of using titanium as a metal in catalysis are very similar to those of iron. Titanium is also extremely abundant and therefore cheap to buy. Stable oxidation states of +2, +3 and +4 exist, with +4 being the most stable. One particularly useful titanium complex is titanium trichloride **11** ($TiCl_3$), frequently used in the stereospecific polymerisation of propylene and various reductive coupling reactions.[106] Titanium is also well known as titanium dioxide **12** (TiO_2), a pure white powder commonly used as a pigment in paints. Furthermore, titanocene monochloride **13**, Cp_2TiCl (Cp = cyclopentadienyl), is a reagent widely used in radical and organometallic chemistry and demonstrates many of the fundamental principles of "Green Chemistry" such as waste minimisation, catalytic behaviour, toxicity and energy efficiency.[107]

It is clear that developing iron and titanium complexes for use in controlled radical polymerisations is of interest, both academically and industrially, because these complexes would have the benefit of being considerably greener and more environmentally friendly than current alternatives.

1.2.2 Use in Controlling Polymerisations

1.2.2.1 Iron

A wide range of iron complexes have been synthesised and screened for their use in CRP over the last 25 years, with the first reports coming from the same research groups that initially developed ATRP mediators. In 1997 Sawamoto and co-workers polymerised MMA using the iron(II) complex $FeCl_2(PPh_3)_2$ **14** with organic halides, such as $CH_3CBr(CO_2Et)_2$, as initiators.[108] Dispersities achieved were reasonably narrow (Đ = 1.1-1.3). In the same year Matyjaszewski and co-workers used $FeBr_2$ **15** in the ATRP of styrene and MMA.[109] Coordinating ligand frameworks used include phosphine and bipyridine derivatives, and dispersities as low as 1.1

were achieved. The degree of control was strongly influenced by the structure of the ligand and the chosen monomer, with electron-rich frameworks giving fast conversions and lower dispersities.

Iron(II)-mediated ATRP has proved to be particularly successful as a method of CRP because of its facile experimental setup, use of inexpensive catalysts and simple initiators.[101] The iron complex typically comprises an iron(II) halide and a ligand. The ligand framework is able to control both the solubility and the reactivity of the redox reaction. However, iron(III)-mediated R-ATRP may have greater industrial significance, owing to iron(III) complexes being oxidatively stable and thus avoiding the air-sensitive properties of iron(II) complexes.

The first example of an R-ATRP mediated by iron was published in 1998, when Teyssié reported the R-ATRP of MMA using $FeCl_3$ **16** and AIBN in the presence of triphenylphosphine ligands. Dispersities were low (Đ < 1.3) although molecular weights did not increase linearly with conversion.[110]

Following these early examples of iron-mediated controlled radical polymerisation, numerous papers have been published describing the use of many different iron complexes, and review papers have been produced which thoroughly cover the literature in this field.[12,101] Some select examples will be discussed, with a particular focus on those used within OMRP.

Phosphines are a frequently used family of ligands for iron-mediated CRP, most of which use iron(II) or iron(III) chloride/bromide as the metal.[12] Polymerisations have predominantly focussed on styrene and MMA, with reported dispersities anywhere between 1.15 and 1.8.[12] It has been shown that phosphines which contain electron donating groups give higher polymerisation rates,[111] and therefore may be preferable for certain monomers, such as simple acrylates.

Iron α-diimine **17** complexes (Figure 1.10) have also been studied in detail as mediators for both ATRP[46–48,112] and OMRP.[49] Investigations have centred on the relationship between the metal spin state of the oxidised iron species and the tendency to undergo ATRP over CCT. It was found that high spin Fe(III) complexes were effective for ATRP, whereas low spin Fe(III) complexes preferred organometallic pathways.

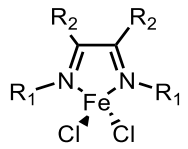

17

Figure 1.10 - Iron α-diimine complexes.

The OMRP of styrene using iron α-diimine **17** was particularly successful, with dispersities as low as 1.4 and molecular weights in reasonable agreement with theoretical values. However, conversions were limited and required a considerable excess of metal complex (8 equivalents), due to the instability of the Fe(III)-styrene dormant species at the high reaction temperature used (120 °C). Lower catalyst loadings (2 equivalents) gave better results, with dispersities nearer to 1.3. More elaborate ligand frameworks, such as iminopyridine- and aminopyridine-based ligands, have also been used in iron-ATRP.[113,114]

Gibson and co-workers used a series of tridentate iron(II) salicylaldiminato **18** complexes in the ATRP of styrene in the presence of 1-phenylethyl bromide as initiator.[115] The complexes were found to be highly active, with the molecular weights linearly increasing with conversion and in agreement with theoretical values. Dispersities were low (approximately Đ = 1.1) and decreased with monomer conversion. Polymerisation control was poor when the analogous iron(III) complexes were used in the R-ATRP of styrene and MMA.

$Fe(acac)_2$ **9** has been shown to be a good mediator of the polymerisation of vinyl acetate, using V-70 as initiator at 30 °C.[116] Dispersities as low as 1.29 were achieved, although molecular weights were considerably higher than theoretical values. The higher oxidation state derivative, $Fe(acac)_3$ **19**, is also able to control the polymerisation, with a reducing agent used *in situ* to generate the required iron(II) species for OMRP control.[117]

A series of iron(II) β-ketiminate **20** complexes were synthesised and used as mediators in the CRP of styrene and MMA.[57] The complexes were poor ATRP mediators, but dispersities as low as 1.58 for styrene and 1.23 for MMA were achieved under OMRP conditions, with the better performance with MMA likely to be due to the formation of a stronger metal-carbon bond in the dormant species. With the MMA polymerisation, molecular weights "top out" at higher conversions, after which molecular weights become independent of conversion. This suggests that CCT becomes kinetically competitive with propagation, which is consistent with results from the iron α-diimine **17** systems.

A series of monometallic pentacoordinate iron(III) chloride **21** complexes (Figure 1.11) were synthesised and used as mediators in the reverse-ATRP of styrene and MMA.[118] Reasonable control was exhibited, with dispersities as low as 1.1 for both monomers. Kinetic studies showed controlled behaviour, with evidence again for the presence of CCT as a competing mechanism.

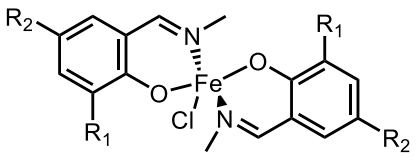

21

Figure 1.11 - Bis-chelated iron(III) half salen complexes.

Qiu and co-workers used an iron(III) dithiocarbamate **22** complex in the R-ATRP of styrene and MMA.[119] No additional ligands such as nitrogen-based or phosphine-based compounds were used. The resultant polymers had low dispersities (Đ = 1.1-1.3) and were functionalised with a dithiocarbamate group as the polymer end-group. Various chain-extension reactions under UV light or thermal treatments were used to show the chain-end fidelity of the polymer.

Grubbs and co-workers used a series of highly active iron(II) complexes bearing imidazolylidene ligands (NHC, Figure 1.12) in the ATRP of styrene and MMA.[120] The molecular weights of the polystyrene obtained from using [NHC]$FeCl_2$ **23** increased linearly with conversion and were in agreement with theoretical values. Dispersities decreased with conversion and were less than 1.2 at conversions greater than 80%. The polymerisation mediated by [NHC]$FeBr_2$ **24** had a higher rate constant than with **23**. The use of imidazolylidene ligands was considered to be particularly attractive because they are easy to prepare and handle, and less toxic than phosphines and amines.

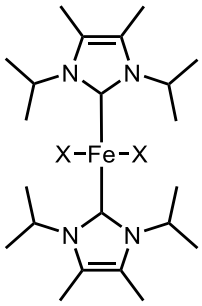

23, X = Cl
24, X = Br

Figure 1.12 - Iron(II) imidazolylidene complexes.

Nagashima and co-workers have reported the use of reusable and environmentally friendly ionic trinuclear iron catalysts bearing nitrogen substituents of triazacyclononane (tacn) ligands in the ATRP of styrene and MMA.[121] The iron complex $[(Me_3tacn)_2Fe_2Cl_3]^+[(Me_3tacn)FeCl_3]^-$ **25**, which is soluble in methanol, was found to be an excellent catalyst for the ATRP of styrene, with dispersities as low as 1.2. Molecular weights in excess of 100000 Da were achieved but were also significantly greater than the theoretical values. The iron species could be recovered from the polymer purification process and could be reused in a further ATRP reaction. After three repetitions there was still no evidence of catalyst deactivation.

In addition to their use in CRP, iron complexes have been used in the ring-opening polymerisation (ROP) of cyclic esters.[122–130] Byers and co-workers used bis(imino)pyridine iron bis(alkoxide) **26** complexes in the polymerisation of *rac*-lactide.[128,130] It was shown that the activity of the catalyst was sensitive to the nature of the initiating alkoxide, and to the oxidation state and electron density of the iron complex. Pang and co-workers used a series of air-stable iron(III) chloride complexes based upon the Schiff base ligand framework in the polymerisation of lactide and ε-caprolactone, in the presence of propylene oxide.[131]

Iron complexes have also been used in the synthesis of polyolefins, such as polyethylene and polypropylene,[132–137] with a detailed review paper comprehensively covering the field.[138] Brookhart and co-workers used tridentate iron(II) pyridine bis-imine **27** complexes in the polymerisation of ethylene to linear, high-density polyethylene.[132] The complexes were activated with methylaluminoxane (MAO) and found to be robust and extremely active.

Work by Gibson and co-workers investigated the use of iron halide **28** complexes, bearing chelating 2,6-bis(imino)pyridyl ligands, in the polymerisation of ethylene.[133] The complexes were also activated with MAO yielding highly active catalysts, with productivities in the range 3750-20600 g $mmol^{-1}$ h^{-1} bar^{-1}. Molecular weights were found to be in the range 14000-611000 Da. In some cases, a bimodal molecular weight distribution was observed, with lower molecular weights attributed to chain transfer to the aluminium in MAO and with higher molecular weights attributed to predominantly β-H transfer. More recently, Guan, Huang and co-workers used iron phosphine-iminoquinoline **29** complexes in the polymerisation of ethylene and 1-octene.[135] MAO was used as activator to yield catalysts with activities up to 10^8 g mol^{-1} h^{-1}. Dispersities were generally broad, with values between 1.5 and 18.8.

1.2.2.2 Titanium

The earliest example of the use of titanium in radical polymerisations appeared in 2003.[139] Titanocene dichloride **30**, Cp_2TiCl_2, was used as a chain growth mediator in the polymerisation of MMA, initiated by AIBN. Dispersities were broad (Đ = 1.9-2.9) implying only a small degree of control. Further studies showed that the method of control was due to reduction of **30** to the Ti(III) analogue.[44]

Virtually all work on titanium-mediated radical polymerisation has focussed on **30** and its derivatives, and has been predominantly carried out by Asandei and co-workers. The first report, in 2004, showed that a system involving **30**, zinc and an epoxide was able to initiate and control the polymerisation of styrene.[140] The system showed the typical characteristics of a controlled polymerisation, with a linear dependence of molecular weight on monomer conversion and narrow dispersities (Đ = 1.1-1.3). The mechanism of control was suggested to occur in a number of stages (Scheme 1.9):

1) *In situ* formation of the Ti(III) analogue **13** from **30** through reduction using zinc metal.
2) Radical ring-opening (RRO) of the epoxide, yielding a Ti-alkoxide radical species **31**.
3) Radical initiation of the polymerisation, using **31**.
4) Reversible trapping of the propagating radical species using a second equivalent of **13**, through both reversible-deactivation and degenerative chain transfer.

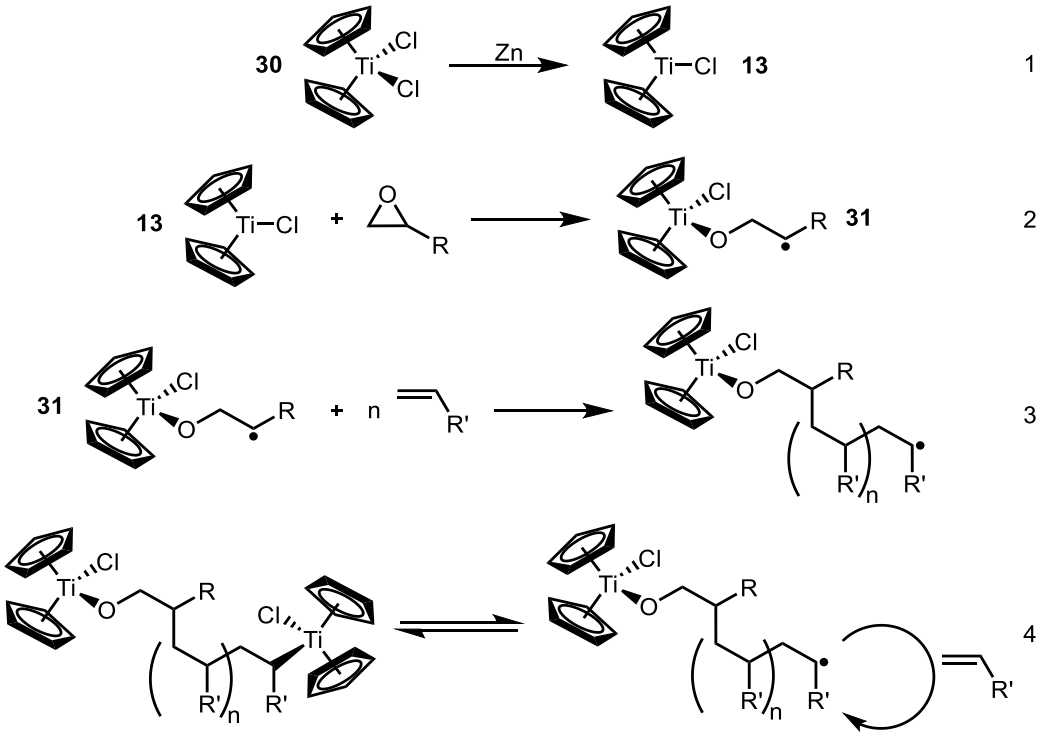

Scheme 1.9 - Mechanism of polymerisation of styrene using **30**.[140]

The best initiator was found to be the monosubstituted, oxygen-rich diepoxide 1,4-butanediol diglycidyl ether (BDGE). In addition to styrene, para-substituted styrenes were also polymerised and copolymerised with reasonable control.

The group has studied this system extensively, investigating the wide array of parameters available to optimise the polymerisation. Work exploring the ligand effects shows that the titanocene framework was a better mediator than complexes based on alkoxides, bisketonates, scorpionates or half-sandwiches. Bisketonates were shown to be ineffective mediators of styrene polymerisations,[141] as were scorpionates.[142] However alkoxides were shown to exert some control over the polymerisation, using (^{i}PrO)$_3$TiCl **32** as the mediator, albeit with dispersities between 1.4 and 1.5.[141] Half-sandwich complexes, such as CpTiCl$_3$ **33** and Cp*TiCl$_3$ **34**, also demonstrated poorer performance than **30**.[142] Cp* (pentamethylcyclopentadiene) is more electron donating than Cp and thus gives a stronger metal-carbon bond. The consequence is that temperatures in excess of 110 °C are required for “living” behaviour.

In addition to the above, a range of substituted metallocenes were synthesised to investigate the effect of increased steric bulk on the Cp ring.[143] The work concluded that there is only a

weak dependence of the polymerisation on the nature of the substituent. This was attributed to a constant balance between the electronic and steric effects, as the size of the substituent increased. The effect of the halide was more pronounced, with **30** shown to be a better mediator than Cp_2TiBr_2 **35**.

Other parameters were also investigated, including the effect of reducing agents, temperature, and reagent ratios.[144] Many metals, such as Cu, Ni and Cr, were shown to be unable to reduce **30**. Whereas metals such as Al and Fe give free-radical or poorly controlled polymerisations (Đ > 1.5). Zinc alloy, powder or preferably nanoparticles were shown to be the best at reducing **30** to give a well-controlled polymerisation, with an optimum ratio of Cp_2TiCl_2:Zn = 1:2 and optimum temperature of 70-90 °C. The effect of solvents and additives were also explored.[145] With respect to solubility of **13** and dispersity of the resulting polymer, dioxane was shown to be the best solvent, just ahead of THF. Finally the nature of the initiator was explored, with a range of peroxide initiators tested.[146] Two equivalents of Ti(III) were still required per equivalent of peroxide - one used in the redox initiation and one used in the reversible termination process. In addition, similar rates of polymerisation to epoxide initiation show that initiation of the peroxide occurs through the redox reaction, rather than thermal decomposition. Benzoyl peroxide was shown to be the superior initiator of those tested.

Whilst there are few examples of titanium complexes being used in CRP, the utilisation of titanium(IV) complexes in the coordination-insertion polymerisation of alkenes is near-ubiquitous.[147–154] In particular, metallocenes have proved to be exceptionally versatile and effective catalysts for the stereoselective polymerisation of olefins. They can polymerise 1-alkenes *via* a migratory insertion mechanism, as in the Ziegler-Natta polymerisation.[155]

There are several examples of the use of titanium complexes in the polymerisation of MMA.[156–164] However, the majority of these have an ionic-based polymerisation mechanism and typically require a co-catalyst. For example, Holmes and co-workers investigated the anionic polymerisation of MMA using a tris(isopropoxy)titanium ester enolate **36** and an analogous 'ate' complex **37**, with the latter shown to produce poly(methyl methacrylate) (PMMA) at -30 °C in a high yield with a low dispersity (Đ < 1.4).[156]

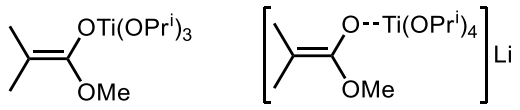

36 **37**

Figure 1.13 - Tris(isopropoxy)titanium ester enolate **36** and the analogous 'ate' complex **37**.

Chen and co-workers reported the homopolymerisation and block copolymerisation of methacrylates by the cationic titanium methyl complex, CGCTiMe$^+$MeB$(C_6F_5)_3^-$ (**38**, CGC = $Me_2Si(Me_4C_5)(t\text{-BuN})$).[157] The polymerisation was able to proceed at room temperature and produced highly syndiotactic PMMA.

Shiono and co-workers synthesised a norbornene-propylene-methyl methacrylate block terpolymer using a fluorenylamide-ligated titanium **39** complex.[159] The polymerisation of the MMA block required an additional aluminium compound, behaving as a Lewis acid, to activate the MMA. The syndiotactic ratio of the MMA block was found to be 78%, which was said to be almost the same as the stereoregularity of anionic MMA polymerisation by $^i Bu_2Al(BHT)$ and lithium initiators (BHT = butylated hydroxytoluene). Shiono, Grubbs and co-workers subsequently synthesised ethylene-propylene-methyl methacrylate and ethylene-hexene-methyl methacrylate block copolymers using **39**.[164] The complex was activated by modified MAO and 2,6-di-*tert*-butyl-4-methylphenol. After the olefin copolymerisation had finished, MMA is added and activated by the aluminium-based Lewis acid to promote anionic polymerisation. The resultant block copolymer was found to have a high molecular weight (> 100000 Da).

Okuda and co-workers used a neutral alkyl titanium ester enolate **40** complex supported by a tetradentate bis(phenoxy)sulfur-donor [O$^-$,S,S,O$^-$]-type ligand in the polymerisation of MMA.[160] The complex was readily activated to the corresponding cationic ester enolate complex, and a mixture of the two gave a highly active polymerisation system producing PMMA with a low dispersity (Đ < 1.1). The neutral complex was also able to polymerise MMA alone, if first activated with $Al(C_6F_5)_3$.

There are some examples of titanium complexes being used in the ROP of cyclic esters. Bounor-Legaré and co-workers reported the ROP of ε-caprolactone initiated by titanium *n*-propoxide Ti(O-*n*-Pr)$_4$ **41**.[165] The polymerisation was performed at 100 °C in the absence of solvent, and was confirmed to proceed *via* a coordination-insertion mechanism. Dispersities

were broad and generally greater than approximately 1.9. Gibson, Long and co-workers synthesised a family of titanium(IV) bis(iso-propoxide) **42** complexes supported by tetradentate Schiff base (salen) ligands and investigated their suitability for initiating the ring-opening polymerisation of *rac*-lactide.[166] It was shown that polymerisation activities correlated with the electronic properties of the ligand substituents, with electron-withdrawing substituents on the ligand having a detrimental effect on the polymerisation. On the other hand, the use of an electron-donating alkoxy-functionalised ligand resulted in a very high polymerisation activity. The polymerisation was well-controlled with dispersities lower than 1.2. Similar results were obtained by Chen and co-workers, who used hydrazine-bridging Schiff base ligands in the titanium-mediated ROP of L-lactide.[167] It was found that the dinuclear titanium complexes exhibited higher catalytic activity than the mononuclear complex.

1.3 Project Aims

There is a strong desire for green and environmentally friendly complexes which are effective mediators of controlled radical polymerisations. Furthermore, there is a distinct lack of mechanistic understanding of OMRP and its associated propagation and termination reactions. This is particularly true in the case of iron and titanium.

The overall aim of this research is to develop and use iron and titanium complexes in the controlled polymerisation of alkenes. In particular, this work will build on the extensive knowledge and experience of the amino-phenolate ligand framework. This research aims to delve deeper into the mechanisms behind these polymerisations to address the gaps in the mechanistic understanding of OMRP.

Chapter 2 explores the use of iron amine-bis(phenolate) complexes in the OMRP of a variety of monomers, with a focus on styrene, MMA and vinyl acetate. Iron amine-bis(phenolate) complexes have previously been shown to be excellent ATRP mediators,[52,53] and the interplay between ATRP and OMRP has been demonstrated.[55,168] However, this work aims to develop a greater understanding of the system, and to investigate how the mechanisms of OMRP compete with one another. Particular attention will be paid to the balance between

competing propagation and termination reactions, in order to develop a protocol in which the polymerisation is controlled.

The use of titanium complexes in CRP has received little attention. Whilst there are some previous examples of using titanium-based mediators in radical polymerisations of styrenes and (meth)acrylates, these methods either had unproved mechanisms or required expensive or pyrophoric activators. Chapter 3 aims to address this by using a family of titanium(III) amino-phenolate complexes in the controlled polymerisation of methacrylates. The work aims to investigate how and why the complexes can control the polymerisation so effectively, understand the polymerisation mechanism in detail, and to develop a set of optimum conditions for best control.

Figure 1.14 illustrates the monomers which are used within this work.

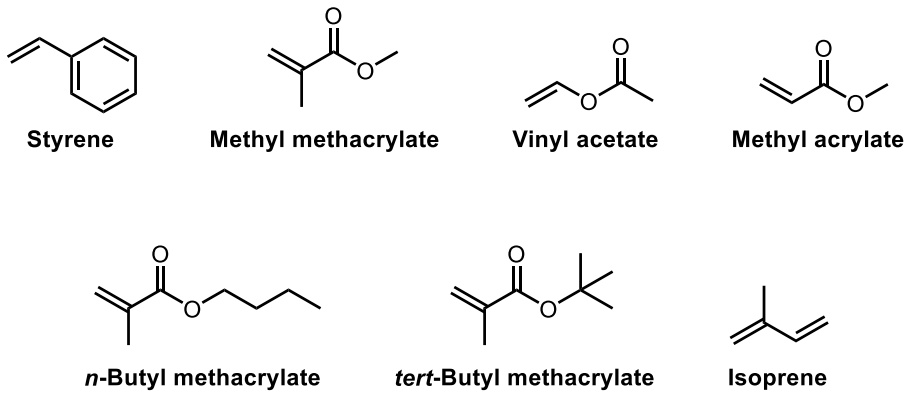

Figure 1.14 - Monomers used within this work.

1.4 References

1 K. Matyjaszewski and J. Spanswick, *Mater. Today*, 2005, **8**, 26–33.

2 K. Matyjaszewski and J. Xia, *Chem. Rev.*, 2001, **101**, 2921–2990.

3 M. Kamigaito, T. Ando and M. Sawamoto, *Chem. Rev.*, 2001, 101, 3689–3745.

4 M. Ouchi and M. Sawamoto, *Macromolecules*, 2017, **50**, 2603–2614.

5 S. Perrier, *Macromolecules*, 2017, **50**, 7433–7447.

6 W. A. Braunecker and K. Matyjaszewski, *Prog. Polym. Sci.*, 2007, **32**, 93–146.

7 M. H. Stenzel and C. Barner-Kowollik, *Mater. Horizons*, 2016, **3**, 471–477.

8 E. Blasco, M. B. Sims, A. S. Goldmann, B. S. Sumerlin and C. Barner-Kowollik, *Macromolecules*, 2017, **50**, 5215–5252.

9 M. Destarac, *Polym. Chem.*, 2018, **9**, 4947–4967.

10 R. R. Matheson, *Knowl. Found. Cambridge, MA, USA*, 2000.

11 L. E. N. Allan, M. R. Perry and M. P. Shaver, *Prog. Polym. Sci.*, 2012, **37**, 127–156.

12 R. Poli, L. E. N. Allan and M. P. Shaver, *Prog. Polym. Sci.*, 2014, **39**, 1827–1845.

13 F. di Lena and K. Matyjaszewski, *Prog. Polym. Sci.*, 2010, **35**, 959–1021.

14 M. Hurtgen, C. Detrembleur, C. Jérôme and A. Debuigne, *Polym. Rev.*, 2011, **51**, 188–213.

15 J. S. Wang and K. Matyjaszewski, *J. Am. Chem. Soc.*, 1995, **117**, 5614–5615.

16 M. Kato, M. Kamigaito, M. Sawamoto and T. Higashimura, *Macromolecules*, 1995, **28**, 1721–1723.

17 R. Whitfield, A. Anastasaki, V. Nikolaou, G. R. Jones, N. G. Engelis, E. H. Discekici, C. Fleischmann, J. Willenbacher, C. J. Hawker and D. M. Haddleton, *J. Am. Chem. Soc.*, 2017, **139**, 1003–1010.

18 K. Matyjaszewski and T. P. Davis, *Handbook of Radical Polymerization*, John Wiley & Sons, 2003.

19 T. G. Ribelli, K. F. Augustine, M. Fantin, P. Krys, R. Poli and K. Matyjaszewski, *Macromolecules*, 2017, **50**, 7920–7929.

20 C. H. Bamford and A. D. Jenkins, *Nature*, 1955, **176**, 78–78.

21 Y. Nakamura, T. Ogihara and S. Yamago, *ACS Macro Lett.*, 2016, **5**, 248–252.

22 M. Buback, F. Günzler, G. T. Russell and P. Vana, *Macromolecules*, 2009, **42**, 652–662.

23 K. Matyjaszewski, *Macromolecules*, 2012, **45**, 4015–4039.

24 T. G. Ribelli, F. Lorandi, M. Fantin and K. Matyjaszewski, *Macromol. Rapid Commun.*, 2019, **40**, 1800616.

25 C. Boyer, N. A. Corrigan, K. Jung, D. Nguyen, T. K. Nguyen, N. N. M. Adnan, S. Oliver, S. Shanmugam and J. Yeow, *Chem. Rev.*, 2016, **116**, 1803–1949.

26 K. Matyjaszewski, W. Jakubowski, K. Min, W. Tang, J. Huang, W. A. Braunecker and N. V. Tsarevsky, *Proc. Natl. Acad. Sci.*, 2006, **103**, 15309–15314.

27 K. Min and K. Matyjaszewski, *Macromolecules*, 2005, **38**, 8131–8134.

28 M. Fantin, P. Chmielarz, Y. Wang, F. Lorandi, A. A. Isse, A. Gennaro and K. Matyjaszewski, *Macromolecules*, 2017, **50**, 3726–3732.

29 K. Min, S. Yu, H. Lee, L. Mueller, S. S. Sheiko and K. Matyjaszewski, *Macromolecules*, 2007, **40**, 6557–6563.

30 J. Qiu, S. G. Gaynor and K. Matyjaszewski, *Macromolecules*, 1999, **32**, 2872–2875.

31 P. B. Zetterlund, Y. Kagawa and M. Okubo, *Chem. Rev.*, 2008, **108**, 3747–3794.

32 M. F. Cunningham, *Prog. Polym. Sci.*, 2008, **33**, 365–398.

33 K. Matyjaszewski, S. Coca, S. G. Gaynor, M. Wei and B. E. Woodworth, *Macromolecules*, 1998, **31**, 5967–5969.

34 J. Mosnáček, A. Eckstein-Andicsová and K. Borská, *Polym. Chem.*, 2015, **6**, 2523–2530.

35 A. Simakova, S. E. Averick, D. Konkolewicz and K. Matyjaszewski, *Macromolecules*, 2012, **45**, 6371–6379.

36 E. Liarou, R. Whitfield, A. Anastasaki, N. G. Engelis, G. R. Jones, K. Velonia and D. M. Haddleton, *Angew. Chemie - Int. Ed.*, 2018, **57**, 8998–9002.

37 A. E. Enciso, L. Fu, A. J. Russell and K. Matyjaszewski, *Angew. Chemie Int. Ed.*, 2018, **57**, 933–936.

38 A. A. Gridnev and S. D. Ittel, *Chem. Rev.*, 2001, **101**, 3611–3659.

39 G. Z. Li, R. K. Randev, A. H. Soeriyadi, G. Rees, C. Boyer, Z. Tong, T. P. Davis, C. R. Becer and D. M. Haddleton, *Polym. Chem.*, 2010, **1**, 1196–1204.

40 K. A. McEwan and D. M. Haddleton, *Polym. Chem.*, 2011, **2**, 1992–1999.

41 E. Le Grognec, J. Claverie and R. Poli, *J. Am. Chem. Soc.*, 2001, **123**, 9513–9524.

42 F. Stoffelbach, R. Poli and P. Richard, *J. Organomet. Chem.*, 2002, **663**, 269–276.

43 F. Stoffelbach, R. Poli, S. Maria and P. Richard, *J. Organomet. Chem.*, 2007, **692**, 3133–3143.

44 D. F. Grishin, S. K. Ignatov, A. A. Shchepalov and A. G. Razuvaev, *Appl. Organomet. Chem.*, 2004, **18**, 271–276.

45 W. A. Braunecker, W. C. Brown, B. C. Morelli, W. Tang, R. Poli and K. Matyjaszewski, *Macromolecules*, 2007, **40**, 8576–8585.

46 V. C. Gibson, R. K. O'Reilly, W. Reed, D. F. Wass, A. J. P. White and D. J. Williams, *Chem. Commun.*, 2002, **2**, 1850–1851.

47 M. P. Shaver, L. E. N. Allan, H. S. Rzepa and V. C. Gibson, *Angew. Chemie - Int. Ed.*, 2006, **45**, 1241–1244.

48 L. E. N. Allan, M. P. Shaver, A. J. P. White and V. C. Gibson, *Inorg. Chem.*, 2007, **46**, 8963–8970.

49 M. P. Shaver, L. E. N. Allan and V. C. Gibson, *Organometallics*, 2007, **26**, 4725–4730.

50 M. P. Johansson and M. Swart, *Dalt. Trans.*, 2011, **40**, 8419–8428.

51 R. Poli and M. P. Shaver, *Chem. - A Eur. J.*, 2014, **20**, 17530–17540.

52 L. E. N. Allan, J. P. MacDonald, A. M. Reckling, C. M. Kozak and M. P. Shaver, *Macromol. Rapid Commun.*, 2012, **33**, 414–418.

53 L. E. N. Allan, J. P. MacDonald, G. S. Nichol and M. P. Shaver, *Macromolecules*, 2014, **47**, 1249–1257.

54 R. Poli and M. P. Shaver, *Inorg. Chem.*, 2014, **53**, 7580–7590.

55 H. Schroeder, B. R. M. Lake, S. Demeshko, M. P. Shaver and M. Buback, *Macromolecules*, 2015, **48**, 4329–4338.

56 M. Buback, H. Schroeder and H. Kattner, *Macromolecules*, 2016, **49**, 3193–3213.

57 B. R. M. Lake and M. P. Shaver, *Dalt. Trans.*, 2016, **45**, 15840–15849.

58 A. Debuigne, R. Poli, C. Jérôme, R. Jérôme and C. Detrembleur, *Prog. Polym. Sci.*, 2009, **34**, 211–239.

59 B. B. Wayland, G. Poszmik, S. L. Mukerjee and M. Fryd, *J. Am. Chem. Soc.*, 1994, **116**, 7943–7944.

60 A. Debuigne, J.-R. Caille, C. Detrembleur and R. Jérôme, *Angew. Chemie - Int. Ed.*, 2005, **44**, 3439–3442.

61 R. Bryaskova, C. Detrembleur, A. Debuigne and R. Jérôme, *Macromolecules*, 2006, **39**, 8263–8268.

62 A. Debuigne, N. Willet, R. Jérôme and C. Detrembleur, *Macromolecules*, 2007, **40**, 7111–7118.

63 R. Bryaskova, N. Willet, P. Degée, P. Dubois, R. Jérôme and C. Detrembleur, *J. Polym. Sci. Part A Polym. Chem.*, 2007, **45**, 2532–2542.

64 R. Bryaskova, N. Willet, A. Debuigne, R. Jérôme and C. Detrembleur, *J. Polym. Sci. Part A Polym. Chem.*, 2007, **45**, 81–89.

65 A. Debuigne, J. Warnant, R. Jérôme, I. Voets, A. de Keizer, M. A. Cohen Stuart and C. Detrembleur, *Macromolecules*, 2008, **41**, 2353–2360.

66 Y. Piette, A. Debuigne, C. Jérôme, V. Bodart, R. Poli and C. Detrembleur, *Polym. Chem.*, 2012, **3**, 2880–2891.

67 C. Detrembleur, D.-L. Versace, Y. Piette, M. Hurtgen, C. Jérôme, J. Lalevée and A. Debuigne, *Polym. Chem.*, 2012, **3**, 1856–1866.

68 Y. Piette, A. Debuigne, V. Bodart, N. Willet, A.-S. Duwez, C. Jérôme and C. Detrembleur, *Polym. Chem.*, 2013, **4**, 1685–1693.

69 A. Kermagoret, C. Jérôme, C. Detrembleur and A. Debuigne, *Eur. Polym. J.*, 2015, **62**, 312–321.

70 A. Debuigne, J.-R. Caille and R. Jérôme, *Angew. Chemie - Int. Ed.*, 2005, **44**, 1101–1104.

71 C. Detrembleur, A. Debuigne, R. Bryaskova, B. Charleux and R. Jérôme, *Macromol.*

Rapid Commun., 2006, **27**, 37–41.

72 A. Kermagoret, N. D. Q. Chau, B. Grignard, D. Cordella, A. Debuigne, C. Jérôme and C. Detrembleur, *Macromol. Rapid Commun.*, 2016, **37**, 539–544.

73 A. Debuigne, C. Michaux, C. Jérôme, R. Jérôme, R. Poli and C. Detrembleur, *Chem. - A Eur. J.*, 2008, **14**, 7623–7637.

74 M. Hurtgen, A. Debuigne, C. Jérôme and C. Detrembleur, *Macromolecules*, 2010, **43**, 886–894.

75 A. Debuigne, A. N. Morin, A. Kermagoret, Y. Piette, C. Detrembleur, C. Jérôme and R. Poli, *Chem. - A Eur. J.*, 2012, **18**, 12834–12844.

76 S. Maria, H. Kaneyoshi, K. Matyjaszewski and R. Poli, *Chem. - A Eur. J.*, 2007, **13**, 2480–2492.

77 A. Debuigne, Y. Champouret, R. Jérôme, R. Poli and C. Detrembleur, *Chem. - A Eur. J.*, 2008, **14**, 4046–4059.

78 A. N. Morin, C. Detrembleur, C. Jérôme, P. De Tullio, R. Poli and A. Debuigne, *Macromolecules*, 2013, **46**, 4303–4312.

79 A. Kermagoret, A. Debuigne, C. Jérôme and C. Detrembleur, *Nat. Chem.*, 2014, **6**, 179–187.

80 J. Demarteau, A. Kermagoret, I. German, D. Cordella, K. Robeyns, J. De Winter, P. Gerbaux, C. Jérôme, A. Debuigne and C. Detrembleur, *Chem. Commun.*, 2015, **51**, 14334–14337.

81 M. Lee and Y. Minoura, *J. Chem. Soc. Faraday Trans. 1 Phys. Chem. Condens. Phases*, 1978, **74**, 1726–1737.

82 M. Lee, T. Morigami and Y. Minoura, *J. Chem. Soc. Faraday Trans. 1 Phys. Chem. Condens. Phases*, 1978, **74**, 1738–1749.

83 M. Lee, K. Utsumi and Y. Minoura, *J. Chem. Soc. Trans. i*, 1979, **75**, 1821–1829.

84 M. Lee, Y. Ishida and Y. Minoura, *J. Polym. Sci. Part A Polym. Chem.*, 1982, **20**, 457–465.

85 Y. Champouret, U. Baisch, R. Poli, L. Tang, J. L. Conway and K. M. Smith, *Angew. Chemie - Int. Ed.*, 2008, **47**, 6069–6072.

86 Y. Champouret, K. C. Macleod, U. Baisch, B. O. Patrick, K. M. Smith and R. Poli, *Organometallics*, 2010, **29**, 167–176.

87 M. P. Shaver, M. E. Hanhan and M. R. Jones, *Chem. Commun.*, 2010, **46**, 2127–2129.

88 K. Matyjaszewski and N. V. Tsarevsky, *Nat. Chem.*, 2009, **1**, 276–88.

89 Rare Earth Elements - Critical Resources for High Technology | U.S. Geological Survey Fact Sheet 087-02, https://pubs.usgs.gov/fs/2002/fs087-02/, (accessed 26 January 2019).

90 I. Bauer and H.-J. Knölker, *Chem. Rev.*, 2015, **115**, 3170–3387.

91 C. Bolm, J. Legros, J. Le Paih and L. Zani, *Chem. Rev.*, 2004, **104**, 6217–6254.

92 M. D. Greenhalgh, A. S. Jones and S. P. Thomas, *Iron-Catalysed Hydrofunctionalisation of Alkenes and Alkynes*, 2015, vol. 7.

93 C. Sun, B. Li and Z. Shi, *Chem. Rev.*, 2011, **111**, 1293–1314.

94 R. Shang, L. Ilies and E. Nakamura, *Chem. Rev.*, 2017, **117**, 9086–9139.

95 M. M. Najafpour, R. Safdari, F. Ebrahimi, P. Rafighi and R. Bagheri, *Dalt. Trans.*, 2016, **45**, 2618–2623.

96 J. L. Fillol, Z. Codolà, I. Garcia-Bosch, L. Gàmez, J. J. Pla and M. Costas, *Nat. Chem.*, 2011, **3**, 807–813.

97 Z. Codolà, L. Gómez, S. T. Kleespies, L. Que Jr, M. Costas and J. Lloret-Fillol, *Nat. Commun.*, 2015, **6**, 5865.

98 O. Cussó, M. Cianfanelli, X. Ribas, R. J. M. Klein Gebbink and M. Costas, *J. Am. Chem. Soc.*, 2016, **138**, 2732–2738.

99 J. R. Ludwig, P. M. Zimmerman, J. B. Gianino and C. S. Schindler, *Nature*, 2016, **533**, 374–379.

100 J. R. Ludwig, S. Phan, C. C. McAtee, P. M. Zimmerman, J. J. Devery and C. S. Schindler,

J. Am. Chem. Soc., 2017, **139**, 10832–10842.

101 Z. Xue, D. He and X. Xie, *Polym. Chem.*, 2015, **6**, 1660–1687.

102 A. Gualandi, L. Mengozzi and P. G. Cozzi, *Asian J. Org. Chem.*, 2017, **6**, 1160–1179.

103 A. Deepthi, V. Sathi and V. Nair, *Tetrahedron Lett.*, 2018, **59**, 2767–2777.

104 X. Zeng, L. Ilies and E. Nakamura, *Org. Lett.*, 2012, **14**, 954–956.

105 J. C. Lo, J. Gui, Y. Yabe, C. Pan and P. S. Baran, *Nature*, 2014, **516**, 343–348.

106 B. Rossi, S. Prosperini, N. Pastori, A. Clerici and C. Punta, *Molecules*, 2012, **17**, 14700–14732.

107 M. Castro Rodríguez, I. Rodríguez García, R. N. Rodríguez Maecker, L. Pozo Morales, J. E. Oltra and A. Rosales Martínez, *Org. Process Res. Dev.*, 2017, **21**, 911–923.

108 T. Ando, M. Kamigaito and M. Sawamoto, *Macromolecules*, 1997, **30**, 4507–4510.

109 K. Matyjaszewski, M. Wei, J. Xia and N. E. Mcdermott, *Macromolecules*, 1997, **30**, 8161–8164.

110 G. Moineau, P. Dubois, R. Jérôme, T. Senninger and P. Teyssié, *Macromolecules*, 1998, **31**, 545–547.

111 Y. Wang, Y. Kwak and K. Matyjaszewski, *Macromolecules*, 2012, **45**, 5911–5915.

112 V. C. Gibson, R. K. O'Reilly, D. F. Wass, A. J. P. White and D. J. Williams, *Macromolecules*, 2003, **36**, 2591–2593.

113 B. Göbelt and K. Matyjaszewski, *Macromol. Chem. Phys.*, 2000, **201**, 1619–1624.

114 R. K. O'Reilly, V. C. Gibson, A. J. P. White and D. J. Williams, *Polyhedron*, 2004, **23**, 2921–2928.

115 R. K. O'Reilly, V. C. Gibson, A. J. P. White and D. J. Williams, *J. Am. Chem. Soc.*, 2003, **125**, 8450–8451.

116 Z. Xue and R. Poli, *J. Polym. Sci. Part A Polym. Chem.*, 2013, **51**, 3494–3504.

117 J. Wang, J. Zhou, H. S. E. M. Sharif, D. He, Y. S. Ye, Z. Xue and X. Xie, *RSC Adv.*, 2015, **5**,

96345–96352.

118 E. Fazekas, G. S. Nichol, J. A. Garden and M. P. Shaver, *ACS Omega*, 2018, **3**, 16945–16953.

119 D.-Q. Qin, S.-H. Qin and K.-Y. Qiu, *J. Polym. Sci. Part A Polym. Chem.*, 2001, **39**, 3464–3473.

120 J. Louie and R. H. Grubbs, *Chem. Commun.*, 2000, **1363**, 1479–1480.

121 S. Niibayashi, H. Hayakawa, R.-H. Jin and H. Nagashima, *Chem. Commun.*, 2007, 1855.

122 B. J. O'Keefe, S. M. Monnier, M. A. Hillmyer and W. B. Tolman, *J. Am. Chem. Soc.*, 2001, **123**, 339–340.

123 B. J. O'Keefe, L. E. Breyfogle, M. A. Hillmyer and W. B. Tolman, *J. Am. Chem. Soc.*, 2002, **124**, 4384–4393.

124 V. C. Gibson, E. L. Marshall, D. Navarro-Llobet, A. J. P. White and D. J. Williams, *Dalt. Trans.*, 2002, **0**, 4321–4322.

125 X. Wang, K. Liao, D. Quan and Q. Wu, *Macromolecules*, 2005, **38**, 4611–4617.

126 H. R. Kricheldorf and D. O. Damrau, *Macromol. Chem. Phys.*, 1997, **198**, 1767–1774.

127 M. Stolt and A. Södergård, *Macromolecules*, 1999, **32**, 6412–6417.

128 A. B. Biernesser, B. Li and J. A. Byers, *J. Am. Chem. Soc.*, 2013, **135**, 16553–16560.

129 A. B. Biernesser, K. R. Delle Chiaie, J. B. Curley and J. A. Byers, *Angew. Chemie - Int. Ed.*, 2016, **55**, 5251–5254.

130 K. R. Delle Chiaie, A. B. Biernesser, M. A. Ortuño, B. Dereli, D. A. Iovan, M. J. T. Wilding, B. Li, C. J. Cramer and J. A. Byers, *Dalt. Trans.*, 2017, **46**, 12971–12980.

131 R. Duan, C. Hu, X. Li, X. Pang, Z. Sun, X. Chen and X. Wang, *Macromolecules*, 2017, **50**, 9188–9195.

132 B. L. Small, M. Brookhart and A. M. A. Bennett, *J. Am. Chem. Soc.*, 1998, **120**, 4049–4050.

133 G. J. P. Britovsek, M. Bruce, V. C. Gibson, B. S. Kimberley, P. J. Maddox, S. Mastroianni,

S. J. McTavish, C. Redshaw, G. A. Solan, S. Strömberg, A. J. P. White and D. J. Williams, *J. Am. Chem. Soc.*, 1999, **121**, 8728–8740.

134 G. J. P. Britovsek, V. C. Gibson, O. D. Hoarau, S. K. Spitzmesser, A. J. P. White and D. J. Williams, *Inorg. Chem.*, 2003, **42**, 3454–3465.

135 D. Zhang, Y. Zhang, W. Hou, Z. Guan and Z. Huang, *Organometallics*, 2017, **36**, 3758–3764.

136 I. S. Paulino and U. Schuchardt, *J. Mol. Catal. A Chem.*, 2004, **211**, 55–58.

137 Z. Ma, W. H. Sun, Z. L. Li, C. X. Shao, Y. L. Hu and X. H. Li, *Polym. Int.*, 2002, **51**, 994–997.

138 W. Zhang, W. H. Sun and C. Redshaw, *Dalt. Trans.*, 2013, **42**, 8988–8997.

139 D. F. Grishin, L. L. Semyonycheva, E. V. Telegina, A. S. Smirnov and V. I. Nevodchikov, *Russ. Chem. Bull.*, 2003, **52**, 505–507.

140 A. D. Asandei and I. W. Moran, *J. Am. Chem. Soc.*, 2004, **126**, 15932–15933.

141 A. D. Asandei and I. W. Moran, *J. Polym. Sci. Part A Polym. Chem.*, 2005, **43**, 6028–6038.

142 A. D. Asandei and I. W. Moran, *J. Polym. Sci. Part A Polym. Chem.*, 2005, **43**, 6039–6047.

143 A. D. Asandei and I. W. Moran, *J. Polym. Sci. Part A Polym. Chem.*, 2006, **44**, 1060–1070.

144 A. D. Asandei, I. W. Moran, G. Saha and Y. Chen, *J. Polym. Sci. Part A Polym. Chem.*, 2006, **44**, 2156–2165.

145 A. D. Asandei, I. W. Moran, G. Saha and Y. Chen, *J. Polym. Sci. Part A Polym. Chem.*, 2006, **44**, 2015–2026.

146 A. D. Asandei and G. Saha, *J. Polym. Sci. Part A Polym. Chem.*, 2006, **44**, 1106–1116.

147 M. Bochmann, *J. Chem. Soc. Dalt. Trans.*, 1996, 255–270.

148 H. H. Brintzinger, D. Fischer, R. Mülhaupt, B. Rieger and R. M. Waymouth, *Angew.*

Chemie Int. Ed. English, 1995, **34**, 1143–1170.

149 E. Y. X. Chen and T. J. Marks, *Chem. Rev.*, 2000, **100**, 1391–1434.

150 G. W. Coates, *Chem. Rev.*, 2000, **100**, 1223–1252.

151 H. G. Alt and A. Köppl, *Chem. Rev.*, 2000, **100**, 1205–1221.

152 G. J. Domski, J. M. Rose, G. W. Coates, A. D. Bolig and M. Brookhart, *Prog. Polym. Sci.*, 2007, **32**, 30–92.

153 H. Makio, H. Terao, A. Iwashita and T. Fujita, *Chem. Rev.*, 2011, **111**, 2363–2449.

154 D. Takeuchi, *Dalt. Trans.*, 2010, **39**, 311–328.

155 L. Resconi, L. Cavallo, A. Fait and F. Piemontesi, *Chem. Rev.*, 2000, **100**, 1253–1346.

156 T.-M. Yong, A. B. Holmes, P. L. Taylor, J. N. Robinson and J. A. Segal, *Chem. Commun.*, 1996, 863–864.

157 A. Rodriguez-Delgado, W. R. Mariott and E. Y. X. Chen, *Macromolecules*, 2004, **37**, 3092–3100.

158 J. Jin and E. Y. X. Chen, *Organometallics*, 2002, **21**, 13–15.

159 R. Tanaka, Y. Nakayama and T. Shiono, *Polym. Chem.*, 2013, **4**, 3974–3980.

160 B. Lian, T. P. Spaniol and J. Okuda, *Organometallics*, 2007, **26**, 6653–6660.

161 B. Lian, C. M. Thomas, C. Navarro and J. F. Carpentier, *Organometallics*, 2007, **26**, 187–195.

162 B. Lian, C. M. Thomas, C. Navarro and J.-F. Carpentier, *Macromolecules*, 2007, **40**, 2293–2294.

163 L. Postigo, A. B. Vázquez, J. Sánchez-Nieves, P. Royo and E. Herdtweck, *Organometallics*, 2008, **27**, 5588–5597.

164 X. Song, Q. Ma, Z. Cai, R. Tanaka, T. Shiono and R. B. Grubbs, *Macromol. Rapid Commun.*, 2016, **37**, 227–231.

165 J. Cayuela, V. Bounor-Legaré, P. Cassagnau and A. Michel, *Macromolecules*, 2006, **39**,

1338–1346.

166 C. K. A. Gregson, I. J. Blackmore, V. C. Gibson, N. J. Long, E. L. Marshall and A. J. P. White, *Dalt. Trans.*, 2006, 3134–3140.

167 H.-C. Tseng, H.-Y. Chen, Y.-T. Huang, W.-Y. Lu, Y.-L. Chang, M. Y. Chiang, Y.-C. Lai and H.-Y. Chen, *Inorg. Chem.*, 2016, **55**, 1642–1650.

168 B. R. M. Lake and M. P. Shaver, in *Controlled Radical Polymerization: Mechanisms*, American Chemical Society, 2015, pp. 311–326.

2 Iron

2.1 Iron Amino-Phenolate Complexes

Amine-bis(phenolate) (ABP) complexes have been extensively researched, primarily because the ligand framework is able to stabilise high oxidation state metals due to its strong σ- and π-donating character.[1] In particular, iron(III) ABP complexes (Figure 2.1) have been widely used, especially in cross-coupling reactions between aryl Grignard regents and alkyl halides, and in hydrofunctionalisation reactions.[2–5] Shaver and co-workers took inspiration from this work and studied iron(II) and iron(III) ABP complexes as polymerisation mediators.

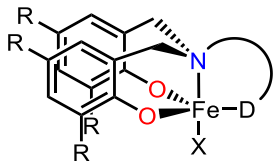

Figure 2.1 - Iron(III) amine-bis(phenolate). R = alkyl, halogen; D = donor atom (e.g. O, N); X = Cl, Br.

The seminal work involved screening a variety of iron(III) ABP complexes (Figure 2.2) in the R-ATRP of styrene and MMA.[6] AIBN was used as the radical initiator with 100 equivalents of monomer relative to the iron complex, and polymerisations were conducted at 120 °C for 1 hour. Various substituents on the phenolate ring and different donor arms were used. Polymerisations were well-controlled with dispersities as low as 1.11, and molecular weights of the resultant polymer were in good agreement with theoretical values. It was found that the electron-withdrawing chloro-substituted complexes were much more effective at controlling the polymerisation than the electron-releasing alkyl-substituted complexes. In the polymerisation of styrene, those reactions using iron chloride complexes had greater polymerisation rates than those using iron bromide complexes, whereas iron bromide complexes resulted in polymers with better dispersities.

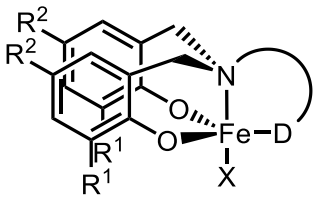

Furf = tetrahydro-2-furanyl
Py = 2-pyridinyl

	R_1	R_2	D	X
1	^{t}Bu	Me	CH_2Furf	Cl
2	^{t}Bu	Me	CH_2Furf	Br
3	^{t}Bu	^{t}Bu	CH_2Furf	Br
4	^{t}Bu	^{t}Bu	$(CH_2)_2OMe$	Br
5	Cl	Cl	$(CH_2)_2NMe_2$	Cl
6	Cl	Cl	$(CH_2)_2NMe_2$	Br
7	Cl	Cl	CH_2Furf	Cl
8	Cl	Cl	CH_2Py	Cl
9	Cl	Cl	CH_2Py	Br
10	Cl	Cl	$(CH_2)_2OMe$	Br

Figure 2.2 - Amine-bis(phenolate) iron(III) complexes used as polymerisation mediators.[6]

The subsequent study further investigated the polymerisation mechanism.[7] Comparing the steric and electronic effects revealed that the electronic properties of the ligand dominate the degree of control over the polymerisation. This was achieved through the screening of chloro- and methyl-substituted complexes, which are of a similar size but have significantly different electronic properties. The study also showed that the donor arm had little effect on how well the polymerisation is controlled. The effect of changing the concentration of AIBN initiator was also explored. In the polymerisation of styrene, a higher concentration resulted in greater reaction rates and higher conversions, but control over the polymerisation was lost. In MMA polymerisation, a high concentration of initiator also saw an increase in reaction rates and also slightly improved control. This suggests that OMRP is more dominant in MMA polymerisation than in styrene polymerisation, because an increased concentration of initiator typically promotes DT-OMRP, since this mechanism requires a constant influx of radicals throughout the polymerisation.

Figure 2.3 - Interplay between ATRP and OMRP in a controlled polymerisation. L = ligand framework.

Using $[Fe(N(SiMe_3)_2)_2]$ as a precursor, the analogous iron(II) ABP complexes can be synthesised.[8] The advantage of using these complexes is that OMRP can be isolated from ATRP, and thus the mechanistic interplay between ATRP and OMRP (Figure 2.3) in controlling styrene and MMA polymerisation can be explored. Using an iron(II) complex and an azo

initiator means that the polymerisation lacks a free halide atom, and so ATRP control is impossible. The polymerisation of styrene and MMA, mediated by the chloro-substituted iron(II) ABP complex, was studied using a combination of Mössbauer, EPR, NMR, and online Vis/NIR spectroscopy. The study showed that the polymerisation of styrene was predominately controlled through ATRP, with no evidence of RT-OMRP *via* an organometallic iron(III) species under the polymerisation conditions adopted. This was clearly demonstrated in the polymerisation data, where the ATRP of styrene was very well-controlled, with molecular weights close to theoretical values and dispersities lower than 1.16 with a range of halide initiators. The OMRP of styrene was considerably worse, with high molecular weights and very broad dispersities.

In contrast, the polymerisation of MMA showed a dual control mechanism, in which both ATRP and OMRP were active. This was also the case even when using an excess of ATRP initiator, R-Cl. Under ATRP conditions, dispersities as low as 1.2 were achieved with good conversion. Under OMRP conditions, control was significantly better than with styrene, as dispersities around 1.3 were achieved, albeit with high molecular weights.

Iron ABPs have also been used in the ATRP of styrene under high pressure of up to 6000 bar.[9] Using the chloro-substituted iron(III) ABP complex, the equilibrium constant and the propagation rate coefficient were enhanced through this increase in pressure. Control over the polymerisation was maintained, with dispersities less than 1.3 even at the highest pressure. Using this increased pressure also enabled high molecular weight poly(styrene) to be synthesised, with a molecular weight of 103000 Da and a dispersity of 1.4 achieved using a pressure of 5000 bar.

DFT calculations were used to further the understanding of the radical polymerisation of styrene mediated by the chloro- and methyl-substituted iron(II) ABP complexes.[10] It was found that there is a greater energy cost for the ATRP activation process involving the chloro-substituted system relative to the methyl-substituted system. On the other hand, the OMRP process provides slightly greater stabilisation for the chloro-substituted system than for the methyl-substituted system. As a result, both ATRP and OMRP trapping processes provide greater stabilisation for the chloro-substituted system, which is in agreement with the superior control observed experimentally. This effect is attributed to the inductive electron withdrawing effect of the chloro substituents on the phenolate ring.

While the interplay between ATRP and OMRP is now well-understood, there has been little work to fully understand the polymerisation under OMRP-only conditions. This chapter aims to investigate the OMRP of MMA, styrene, and vinyl acetate, using an iron(II) ABP complex. The aim is to develop a deeper understanding of this system, with a focus on the balance between competing propagation and termination reactions. A set of optimal experimental conditions are targeted, under which the polymerisation of the aforementioned monomers is controlled.

2.2 Complex Synthesis

The following work in this section was completed by Dr Benjamin R. M. Lake: Growing of crystals for x-ray crystallographic analysis, collection and computational analysis of x-ray crystallographic data.

The previous work investigating OMRP using iron(II) ABPs used a chloro-substituted complex.[8] However, previous experience has shown that the solubility of this complex is poor in common polymerisation solvents such as toluene and THF. Therefore, for this study, a new iron(II) complex was developed, with the ligand precursor chosen to have 2,4-*tert*-butyl substituents on the phenyl rings. This was due to the predicted increased solubility afforded by the sterically large alkyl groups. The ligand **Lig1**H_2 was synthesised through a simple Mannich reaction, starting from 2,4-di-*tert*-butylphenol. The iron(II) complex **Fe1** was synthesised by reacting equimolar amounts of the ligand **Lig1**H_2 with [Fe(N(SiMe$_3$)$_2$)$_2$THF] (Fe(HMDS)$_2$THF) at ambient temperature in toluene (Figure 2.4).

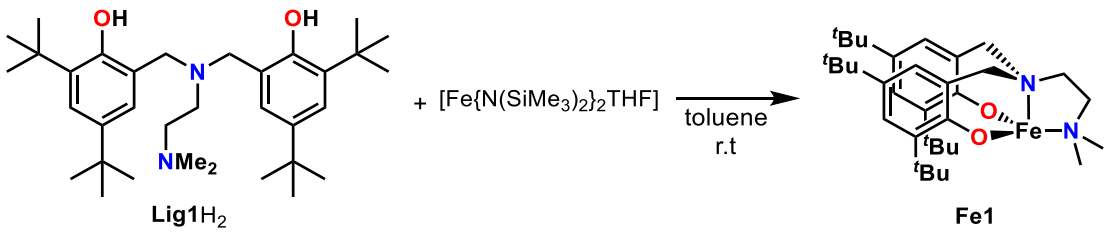

Figure 2.4 - Synthesis of the iron(II) amine–bis(phenolate) complex **Fe1**.

The complex was isolated in good yield as a pale-green amorphous solid, which was highly air- and moisture-sensitive. The ^{1}H NMR spectrum of the paramagnetic d^6 complex (Figure 2.5) exhibited many broad resonances between approximately 90 and −5 ppm, which

perhaps suggests desymmetrisation of the ligand by the formation of a $(\mu\text{-OAr})_2$-bridged dimer.[8] The solution magnetic moment of **Fe1** was found to be 4.8 μ_B, which suggests a high-spin complex.

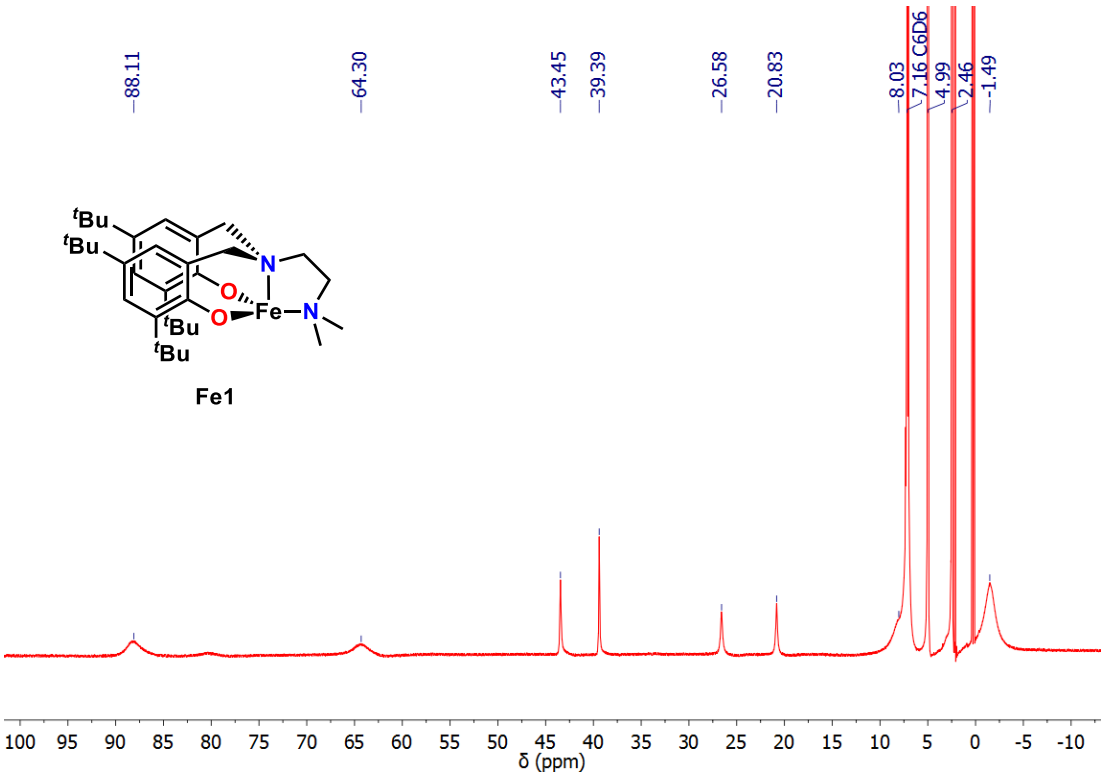

Figure 2.5 - ^{1}H NMR spectrum of complex **Fe1** (500 MHz, C_6D_6).

Attempts to obtain crystals of **Fe1** for single-crystal x-ray diffraction analysis were unsuccessful, which was likely to have been an unfortunate consequence of the improved solubility of the complex. However, reacting an equimolar amount of 4-dimethylaminopyridine (DMAP) with **Fe1** resulted in the formation of **Fe1·DMAP**. Pale-yellow crystals of **Fe1·DMAP** were formed through recrystallisation from MeCN which were suitable for single-crystal x-ray diffraction analysis (Figure 2.6). The structure of the complex was shown to be five-coordinate, with an N_3O_2-coordination sphere. The iron(II) metal centre is coordinated by one molecule of DMAP and the tetradentate ABP ligand. The metal-ligand bond lengths are comparable with similar complexes previously reported.[8,11]

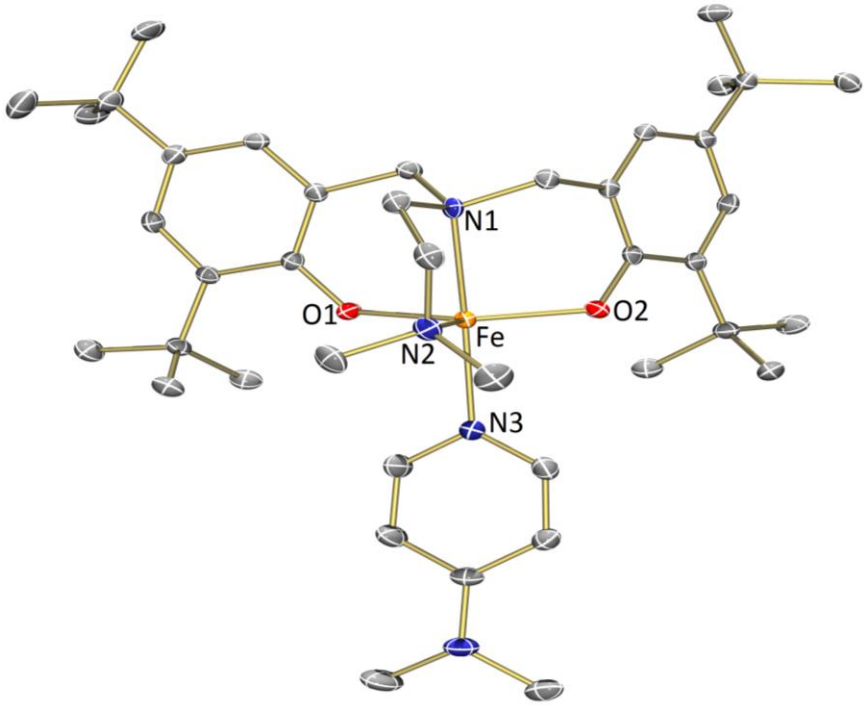

Figure 2.6 - Molecular structure of **Fe1·DMAP** with ellipsoids set at the 50% probability level. Hydrogen atoms and co-crystallised MeCN have been omitted for clarity. Selected bond lengths (Å) and angles (°): Fe-O1 1.9505(16), Fe-O2 1.9662(16), Fe-N1 2.2189(19), Fe-N2 2.243(2), Fe-N3 2.1814(19), N1-Fe-N3 173.82(7), O1-Fe-O2 142.06(7), N2-Fe-O1 104.58(7), N2-Fe-O2 112.51(7).

2.3 Methyl Methacrylate Polymerisation

The strength of the iron-carbon bond used to moderate an OMRP process is a vital factor if good control over the polymerisation is to be achieved. The bond must be sufficiently weak for productive propagation to occur. If the bond is too strong then an irreversible organometallic species would form, which would terminate the polymerisation and prevent further propagation. However, if the bond is too weak then the dormant species is unstable and the OMRP equilibrium lies towards the active species, resulting in an uncontrolled polymerisation.

Previous studies have suggested that at high temperatures (greater than 110°C, which is required for fast initiation of AIBN) formation of the iron-carbon bond is disfavoured.[8] Using a radical initiator with a lower half life temperature, such as V-70, allows the polymerisation to proceed at lower temperatures. AIBN has a 10 hour half life temperature of 65 °C, whereas V-70 has a 10 hour half life temperature of 30 °C. This means that by using V-70 in the

polymerisation a comparatively lower reaction temperature can be used whilst maintaining fast initiation. For example, instead of using reaction temperatures of 110-120 °C for fast initiation (as is necessary with AIBN), reaction temperatures of 75-80 °C may be used. Using V-70 and a lower reaction temperature may promote improved OMRP control.[7]

As discussed in chapter 1.1.3, using a polymerisation temperature which gives fast initiation (*i.e.* less than a few minutes for all the initiator to decompose) promotes control through RT-OMRP, whereas using a lower polymerisation temperature and an excess of initiator results in radicals forming over a prolonged period of time, and typically promotes DT-OMRP control. Both conditions will be investigated in the polymerisation of MMA mediated by **Fe1**.

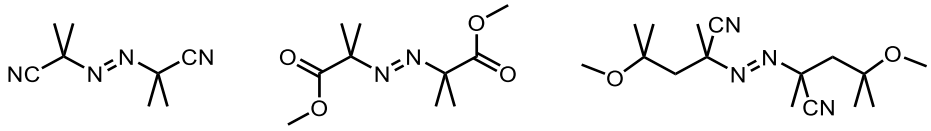

AIBN 10 hr $t_{1/2}$ = 65 °C

V-601 10 hr $t_{1/2}$ = 66 °C

V-70 10 hr $t_{1/2}$ = 30 °C

Figure 2.7 - AIBN, V-70 and V-601, which are the azo initiators used in this work.

2.3.1 High Temperature

For high temperature experiments, where very fast initiation is desired, a reaction temperature of 75 °C was chosen. At this temperature the half life of the initiator is 2 minutes (compared to 138 minutes for AIBN at 75 °C), and no further radicals will be introduced into the system after approximately 10 minutes, therefore promoting RT-OMRP control. Initial kinetics studies were performed to investigate the OMRP of MMA mediated by **Fe1** and initiated by V-70. A monomer to toluene volume ratio of 1:2 was chosen to ensure that the initiator was fully dissolved. The solubility of V-70 at ambient temperature in toluene is 3.0 g/100 g solvent, whereas the solubility of AIBN is 7.0 g/100 g solvent.[12]

The results (Table 2.1 and Figure 2.8) show that **Fe1** had control over the polymerisation for a short period of time. This is illustrated by an initial linear increase in conversion with respect to time, and molecular weights increasing with conversion. However, above moderate conversions (>25%) the polymerisation swiftly deviated from first-order kinetics and slowed considerably. This is most likely to be due to the onset of irreversible radical termination. This

is evident in the chromatography data, where there is the evolution of a high molecular weight shoulder at shorter retention time (Figure 2.9). This termination is also evident in the polymerisation data, where there is a sharp increase in dispersity after an initial decrease during the controlled polymerisation phase. Molecular weights were significantly higher than theoretical values which is not uncommon in the OMRP of MMA.[8,13]

Table 2.1 - Polymerisation of MMA at high temperature.

#	Time (min)	Conversion (%)	$M_{n,th}$ (Da)	M_n (Da)	Đ
2.1	7	17	1700	(a)	(a)
2.2	15	25	2500	11600	1.72
2.3	30	34	3400	14800	1.56
2.4	45	39	3900	18600	1.52
2.5	60	41	4100	18900	1.63

Conditions: [MMA]:[**Fe1**]:[V-70] = 100:1.00:1.00, MMA:toluene = 1:2 (v/v), 75 °C. Conversion determined by ^{1}H NMR spectroscopy. $M_{n,th}$ = $[MMA]_0/[\mathbf{Fe1}]_0$ × M(MMA) × conversion. (a) too little purified polymer obtained for GPC analysis.

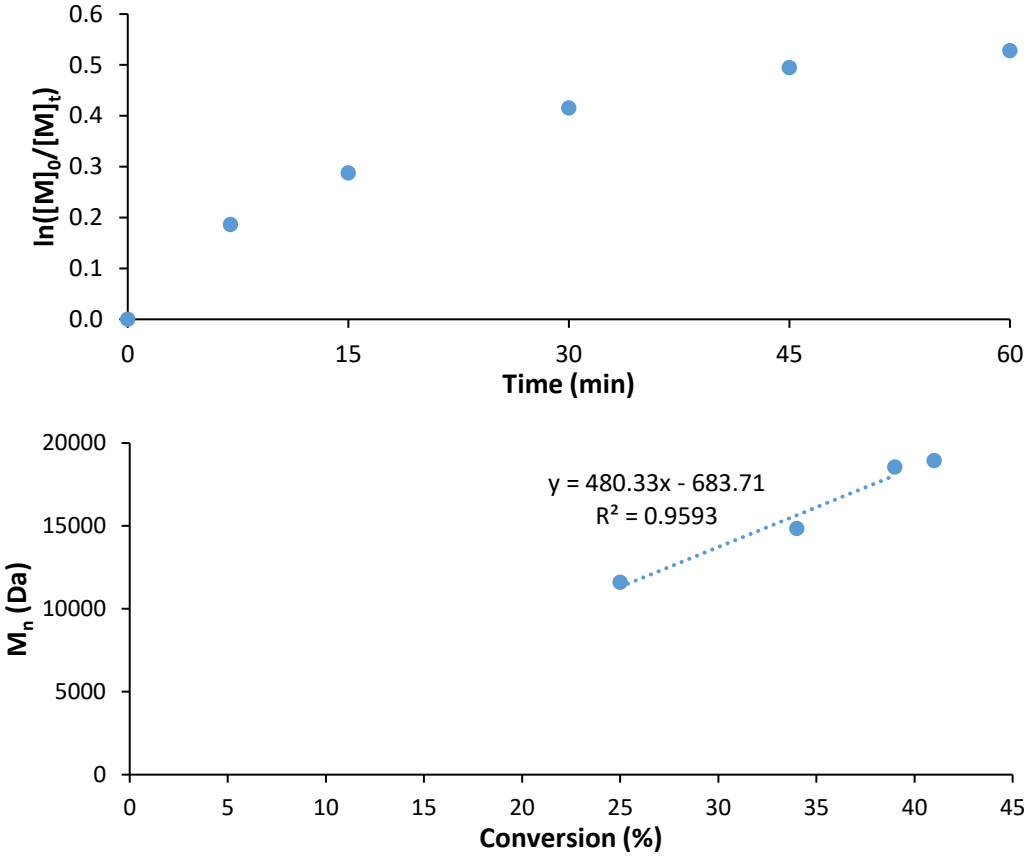

Figure 2.8 - Kinetics of polymerisation of MMA at high temperature (75 °C). [MMA]:[**Fe1**]:[V-70] = 100:1.00:1.00, MMA:toluene = 1:2 (v/v).

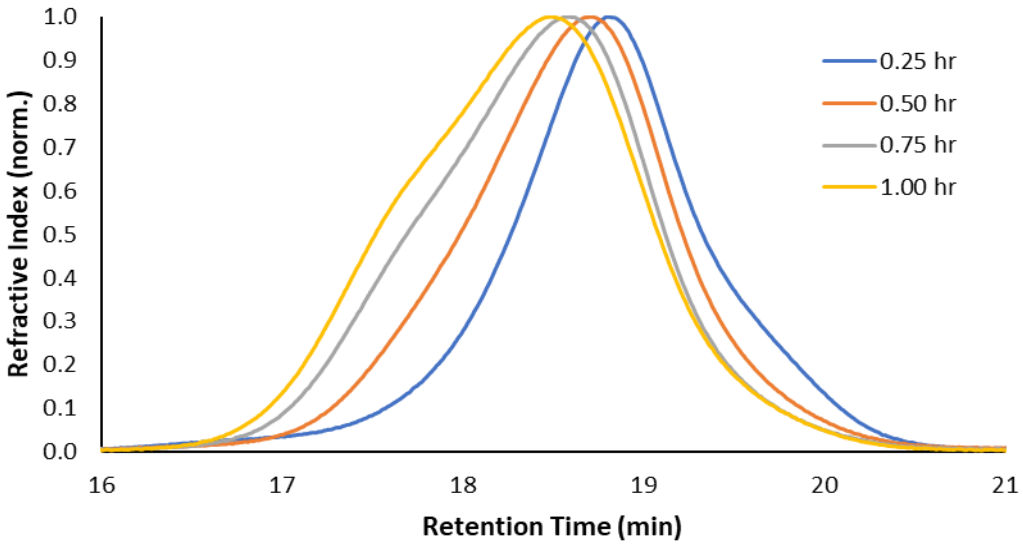

Figure 2.9 - Size exclusion chromatography data of polymer samples in Figure 2.8 showing the onset of irreversible radical termination, possibly by bimolecular termination, observed through the evolution of a high molecular weight shoulder. The molecular weight of the peak of the shoulder is approximately double the molecular weight of the main peak, suggesting the presence of some termination by combination.

To further understand the OMRP of MMA, a variety of reaction conditions and parameters were explored to investigate their effect on the control of the polymerisation (Table 2.2). Polymerisations **2.6**-**2.8** show that increasing the concentration of iron mediator had little effect on the polymerisation. Conversion, molecular weight and dispersity were all virtually unchanged as the concentration of mediator increased. Typically, it would be expected that increasing the concentration of iron complex allows for more initiating radicals and propagating chains to be trapped and reversibly deactivated. This would result in an increase in polymerisation rates and a decrease in molecular weights. However, these results tend to suggest that the iron ABP complex has minimal influence over the efficiency of the initiation process.

On the other hand, increasing the concentration of initiator (polymerisations **2.6**, **2.9**-**2.13**) had more of an effect on the polymerisation. As the concentration of initiator increased, conversion marginally improved whilst lowering molecular weights nearer to theoretical values. There was no apparent loss of control, as dispersity remained unchanged. These results, alongside the previous work investigating iron complexes in OMRP,[8,13] point towards an inherent poor initiation efficiency of azo initiators, including AIBN and V-70, when used with MMA and iron complexes. This results in molecular weights being considerably higher than theoretical values.

Table 2.2 - Effect of mediator concentration, initiator concentration, and solvent on MMA polymerisation at high temperature.

#	Equiv. Fe1	Equiv. V-70	Conv. (%)	$M_{n,th}$ (Da)	M_n (Da)	Đ
2.6	1	1.0	34	3400	14800	1.56
2.7	2	1.0	33	3300	15000	1.53
2.8	3	1.0	32	3200	15300	1.58
2.9	1	0.6	30	3000	18100	1.54
2.10	1	0.8	32	3200	15900	1.54
2.11	1	2.0	38	3800	12300	1.56
2.12	1	3.0	41	4100	10900	1.46
2.13	1	5.0	47	4700	9200	1.50
2.14[a]	1	1.0	38	3800	15800	1.58

Conditions: [MMA]:[**Fe1**]:[V-70] = 100:x:y, MMA:toluene = 1:2 (v/v), 75 °C, 30 min. Conversion determined by ^{1}H NMR spectroscopy. $M_{n,th}$ = $[MMA]_0/[\mathbf{Fe1}]_0$ × M(MMA) × conversion. [a]Performed in THF.

It is also interesting to consider the effect of solvent choice on the polymerisation (polymerisations **2.6** and **2.14**). The solvent had negligible effect on the polymerisation, with little change in conversion, molecular weight and dispersity when using THF, a more coordinating solvent, instead of toluene. This result suggests that the polymerisation is proceeding through a radical mechanism as opposed to a coordination-insertion (CI) mechanism, since a coordinating solvent would be likely to block the vacant coordination site on the iron complex, which is required for a CI polymerisation. On the other hand, the various species involved in OMRP would be no less soluble in a more coordinating solvent, and therefore no significant change in the polymerisation would be expected.

To further understand the polymerisation mechanism, the tacticity of the resultant polymer was considered. PMMA exists in three different isomeric forms, namely, isotactic, syndiotactic, and heterotactic (Figure 2.10). PMMA is often used in optical applications, for example fibre optics, and important properties such as glass transition temperature greatly depend on the microstructure content of the polymer.[14] Therefore, understanding the microstructure content is of importance in determining the suitability of a polymer for its intended application. In addition, understanding the tacticity also helps to provide useful mechanistic insight, because it is possible to compare the tacticity of the resultant PMMA with the tacticity typically expected from various polymerisation mechanisms.

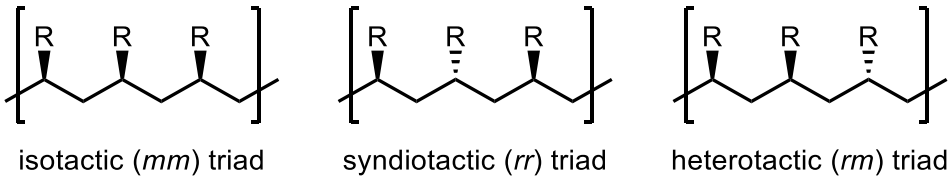

Figure 2.10 - Possible triads in a polymer - isotactic, syndiotactic and heterotactic.

^{1}H NMR spectroscopic analysis of the purified PMMA can be used to determine the relative ratio of mm:rm:rr triads in the polymer (Figure 2.11).[15] The peaks at 1.21 ppm, 1.01 ppm and 0.83 pm correspond with the mm, rm and rr triads respectively. In a typical free radical polymerisation of MMA, the tacticity is approximately 3:33:64.[16] In the OMRP of MMA mediated by **Fe1**, under these experimental reaction conditions, the tacticity was found to be 4:35:61. This further suggests that the polymerisation proceeds *via* a radical mechanism, as a change in tacticity would be expected with a coordination-insertion polymerisation, due to influence from the metal centre and the relatively bulky ABP ligand framework.

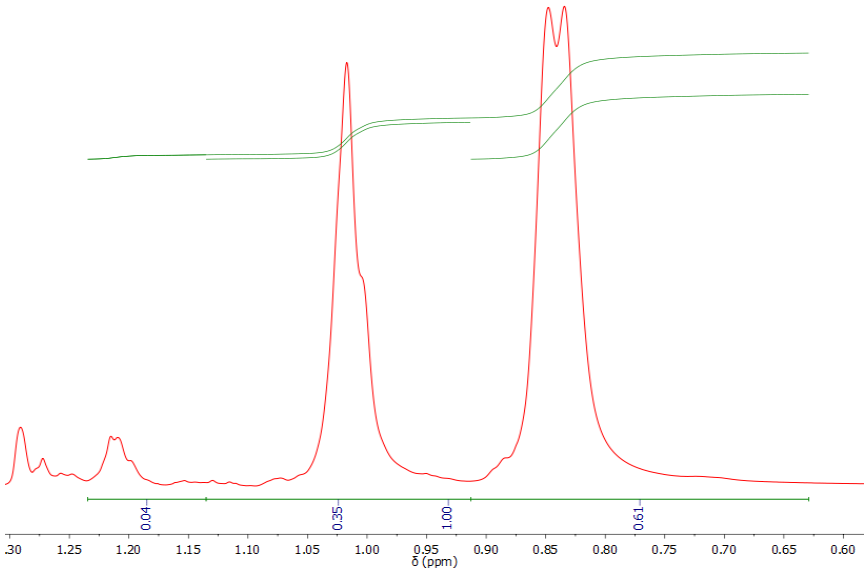

Figure 2.11 - ^{1}H NMR spectrum of purified PMMA, showing integration of the mm:rm:rr triads (500 MHz, $CDCl_3$).

More detailed kinetic studies on the polymerisation were also conducted. Different concentrations of monomer were used to investigate the effect on the polymerisation. The concentration of **Fe1** and initiator was kept constant by ensuring that the combined volume of monomer and solvent was unchanged. 100, 200 and 300 equivalents of MMA, with respect to **Fe1**, were used (Table 2.3). Figure 2.12 clearly shows that as the monomer concentration increased, the rate of propagation significantly increased. Irreversible radical termination is

again evident in the polymerisations with 100 and 200 equivalents of MMA, with the number of growing chains reducing over time and thus slowing the polymerisation. This results in the deviation from linear first-order kinetics.

Table 2.3 - Polymerisation kinetics of MMA at 75 °C, with varying monomer equivalents.

#	Equiv. MMA	Time (min)	Conv. (%)	$M_{n,th}$ (Da)	M_n (Da)	Đ
2.15	100	7	23	2300	(a)	(a)
2.16	100	14	33	3300	(a)	(a)
2.17	100	30	48	4800	9800	1.50
2.18	100	60	60	6000	10500	1.55
2.19	100	90	65	6500	11500	1.52
2.20	200	7	35	7000	10200	2.11
2.21	200	14	49	9800	12100	1.75
2.22	200	20	57	11400	13100	1.58
2.23	200	40	70	14000	14300	1.61
2.24	200	60	74	14800	14900	1.68
2.25	300	2	14	4200	25400	1.99
2.26	300	3	22	6600	20900	2.04
2.27	300	4	29	8700	14300	2.30
2.28	300	7	44	13200	14500	1.78
2.29	300	9	56	16800	15000	1.72

Conditions: [MMA]:[**Fe1**]:[V-70] = x:1.00:5.00, constant volume of MMA + toluene, 75 °C. Conversion determined by ^{1}H NMR spectroscopy. $M_{n,th}$ = $[MMA]_0/[\mathbf{Fe1}]_0$ × M(MMA) × conversion. (a) too little purified polymer obtained for GPC analysis.

It was possible to prevent this irreversible radical termination by using a high concentration of monomer. In the case of 300 equivalents of MMA (polymerisations **2.25**-**2.29**), where the polymerisation was conducted in the absence of any additional solvent, there is a linear increase in conversion with respect to time. After 9 minutes the polymerisation mixture solidified, preventing any further propagation or termination reactions. In this polymerisation, this solidification occurred before termination was able to become prevalent, and therefore a linear increase in conversion was observed throughout the polymerisation.

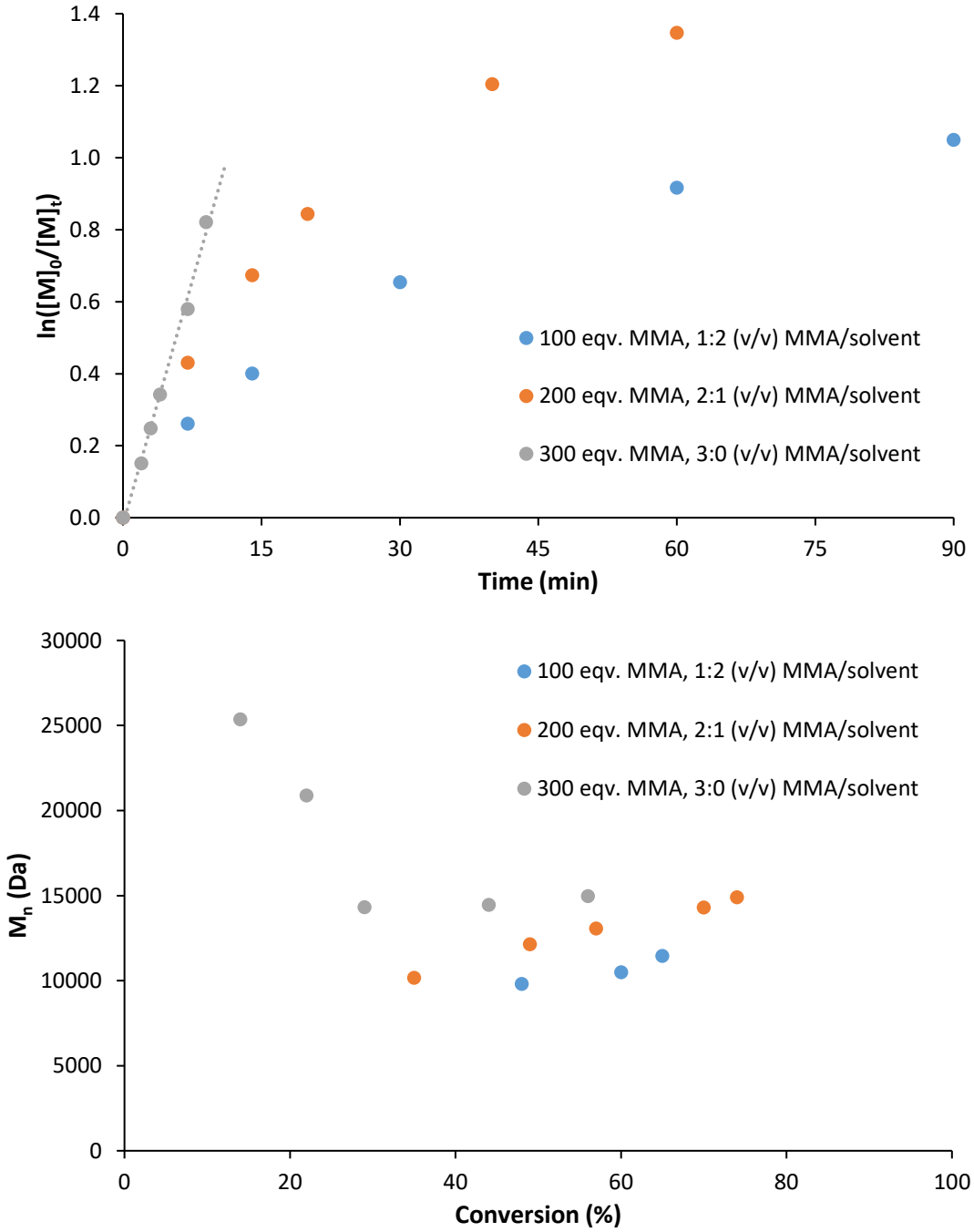

Figure 2.12 - Polymerisation kinetics of MMA at 75 °C, with varying monomer equivalents. [MMA]:[**Fe1**]:[V-70] = x:1.00:5.00. Constant volume of MMA + toluene.

Whilst the 300 equivalents of MMA polymerisation (in the absence of solvent) shows a linear increase in conversion with respect to time, molecular weight data (Table 2.3 and Figure 2.12) suggests that the polymerisation is not well-controlled, with inconsistent molecular weights and broad dispersities. This is due to using a large concentration of initiator, which is required to lower molecular weights to nearer theoretical values, and poor solubility of the V-70

initiator in the monomer. To address this issue, the concentration of V-70 was reduced from 5 equivalents to 1 equivalent (Table 2.4). Though molecular weights increase, some control can be regained.

Table 2.4 - Effect of initiator concentration on MMA polymerisation in the absence of solvent.

#	Equiv. V-70	Conversion (%)	$M_{n,th}$ (Da)	M_n (Da)	Đ
2.30	5	44	13200	14500	1.78
2.31	1	26	7800	19600	1.47

Conditions: [MMA]:[**Fe1**]:[V-70] = 300:1.00:x, bulk, 75 °C, 7 min. Conversion determined by ^{1}H NMR spectroscopy. $M_{n,th}$ = $[MMA]_0/[\mathbf{Fe1}]_0 \times M(MMA) \times$ conversion.

It is interesting to examine in closer detail an early time point in the MMA polymerisation, and to see how the conversion changes as the monomer concentration changes (Table 2.5). A graph of conversion after 7 minutes, versus the number of equivalents of MMA, shows a linear relationship (Figure 2.13). This is due to an increase in concentration of propagating radicals when a higher monomer concentration is used. A higher monomer concentration allows for better radical trapping by the iron complex, resulting in an overall improvement in initiator efficiency. After decomposition of the initiator and polymerisation for 7 minutes, there is no apparent significant termination. It is therefore possible, to a degree, to control the molecular weight by altering the monomer concentration and polymerising for 7 minutes. As a result, a polymer can be made to a desired molecular weight and with minimal termination. It is worth noting that the chromatography data for these polymerisations does show a small high molecular weight shoulder, suggesting a minimum amount of early irreversible radical termination, before the OMRP equilibrium is reached.

Table 2.5 - Effect of monomer concentration on MMA polymerisation.

#	Equiv. MMA	Conversion (%)	$M_{n,th}$ (Da)	M_n (Da)	Đ
2.32	100	23	2300	(a)	(a)
2.33	150	29	4400	(a)	(a)
2.34	200	35	7000	10200	2.11
2.35	250	40	10000	12700	1.59
2.36	300	44	13200	14500	1.78

Conditions: [MMA]:[**Fe1**]:[V-70] = x:1.00:5.00, Constant volume of MMA + toluene, 75 °C, 7 min. Conversion determined by ^{1}H NMR spectroscopy. $M_{n,th}$ = $[MMA]_0/[\mathbf{Fe1}]_0 \times M(MMA) \times$ conversion. (a) too little purified polymer obtained for GPC analysis.

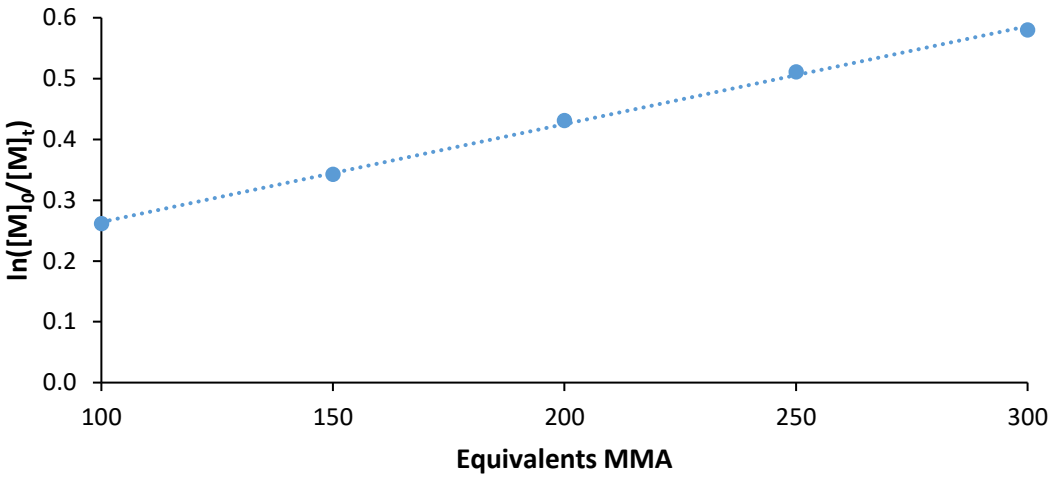

Figure 2.13 - Graph of conversion versus the number of equivalents of MMA, to demonstrate the effect of monomer concentration on MMA polymerisation.

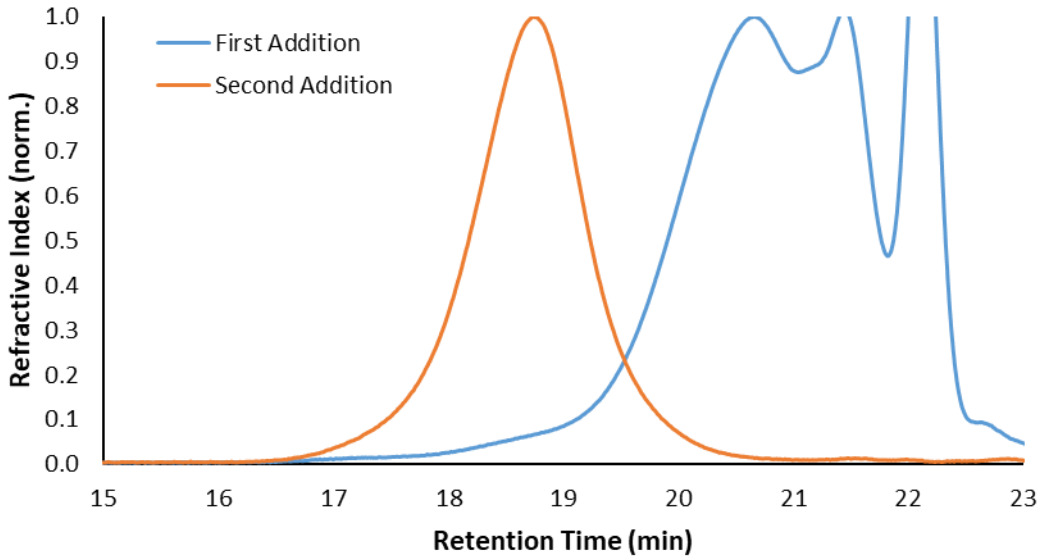

Figure 2.14 - Size exclusion chromatography data of the chain extension experiment. First addition: [MMA]:[**Fe1**]:[V-70] = 100:1.00:5.00, MMA:toluene = 1:2 (v/v), 75 °C, 7 min (polymerisation **2.37**). Second addition: 100 equiv. [MMA], 75 °C, 7 min (polymerisation **2.38**).

A key requirement of a well-controlled polymerisation is good chain-end fidelity, which is a measure of the number of chains which have their end-group still attached and are thus able to undergo further polymerisation. This is typically demonstrated through chain extensions, by methods such as sequential monomer addition or the synthesis of (multi)block copolymers.[17,18] To demonstrate the chain-end fidelity of one of these "7 minute" polymers, a chain extension experiment was performed (Figure 2.14). An initial 100 equivalents of MMA were first polymerised for 7 minutes, before a second 100 equivalents of MMA were added and polymerised for a further 7 minutes. The resultant polymer (polymerisation **2.38**) had a

conversion of 26%, a molecular weight of 13100 Da and a dispersity of 1.43. The increase in the molecular weight, from the first addition to the second addition of monomer, and the low resultant dispersity shows some evidence of reasonable chain-end fidelity. However, the dispersity is still relatively broad, suggesting that a number of chains have undergone radical termination, both before and after the second monomer addition. Consequently, it is difficult to draw conclusions from this experiment, especially with regard to the precise number of chains which have their end-group still attached. The extra peaks at long retention time in the chromatography data of polymer from the first addition of monomer (blue line) are due to the presence of residual catalyst and monomer in the crude sample.

2.3.2 Low Temperature

In addition to exploring the MMA polymerisation at a reaction temperature which provides fast initiation, the polymerisation was also investigated at lower temperatures (Table 2.6 and Figure 2.15). These conditions give rise to a slow release of initiator radicals and, consequently, may promote polymerisation control by DT-OMRP. This mechanism is particularly prevalent in the OMRP of less active monomers, such as vinyl acetate, mediated by $Co(acac)_2$.[19,20] As was to be expected, using a lower polymerisation temperature (30 °C instead of 75 °C) results in increased reaction times and lower propagation rates. Reaction times were extended from several minutes to several days. At 30 °C the half life of V-70 is approximately 10 hours, so there is a slow constant release of new initiator radicals throughout the polymerisation.

However, when compared to the MMA polymerisation at high temperature, considerably higher conversions were achieved. Despite the observed increase in conversion with respect to time, there was no change in molecular weight. The molecular weight of the synthesised PMMA remained at approximately 23000 Da throughout the polymerisation. This behaviour is characteristic of catalytic chain transfer as the method of termination,[13] and not bimolecular termination or catalysed radical termination. This is also confirmed in that there was no change in polymer dispersity as the conversion increases. The dispersity was found to be approximately 1.47, which represents moderate control over the polymerisation.

Table 2.6 - Polymerisation of MMA at low temperature.

#	Time (hr)	Conversion (%)	$M_{n,th}$ (Da)	M_n (Da)	Đ
2.39	6	31	3100	25900	1.44
2.40	18	60	6000	23000	1.44
2.41	24	70	7000	22800	1.47
2.42	42	80	8000	21500	1.50
2.43	48	83	8300	22600	1.44
2.44	72	88	8800	20800	1.50
2.45	94	92	9200	23800	1.40

Conditions: [MMA]:[**Fe1**]:[V-70] = 100:1.00:1.00, MMA:toluene = 1:2 (v/v), 30 °C. Conversion determined by ^{1}H NMR spectroscopy. $M_{n,th} = [MMA]_0/[\mathbf{Fe1}]_0 \times M(MMA) \times$ conversion.

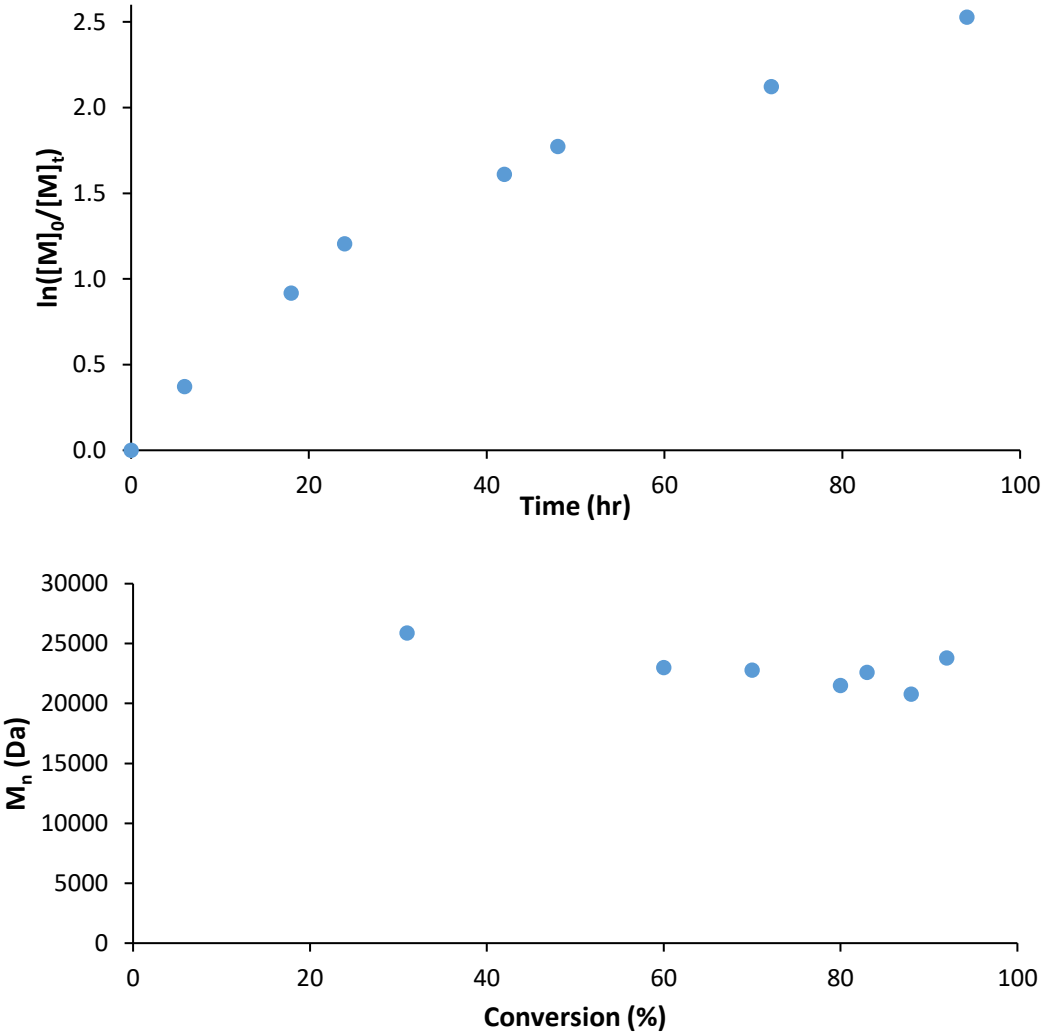

Figure 2.15 - Kinetics of polymerisation of MMA at low temperature (30 °C). [MMA]:[**Fe1**]:[V-70] = 100:1.00:1.00, MMA:toluene = 1:2 (v/v).

As discussed in chapter 1.1.3, CCT results in an alkene-terminated dead polymer chain, and a metal hydride complex (H-M^{x+1}). This metal hydride is then able to initiate the growth of a new chain through reaction with the MMA monomer. This accounts for the high conversions, as new polymer chains are constantly being formed. The number of radicals present at any one time within the system does not decrease, but instead remains approximately constant.

CCT in the iron-mediated polymerisation of MMA has previously been reported for both β-ketiminate[13] and α-diimine[21] iron complexes. The presence of CCT is further evidenced by the ^{1}H NMR spectrum of the purified PMMA (Figure 2.16), which contains resonances at 6.19 ppm and 5.46 ppm corresponding to olefinic protons on the alkene terminus at the chain end of the polymer. However, the percent incorporation of alkene into the polymer is only a fraction of that which would be expected if all chains contained an alkene terminus (approximately 15%), suggesting the presence of other termination mechanisms.

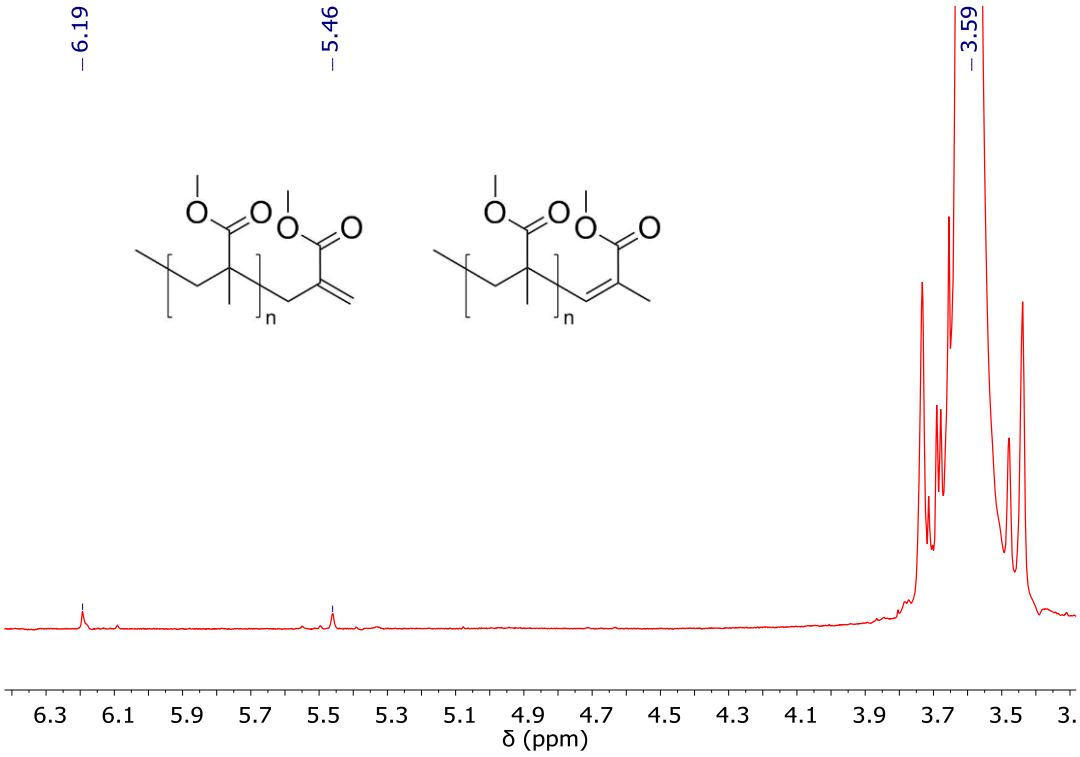

Figure 2.16 - ^{1}H NMR spectrum of purified PMMA, showing the presence of olefin protons (500 MHz, $CDCl_3$).

As with the high temperature MMA polymerisation, the tacticity of the synthesised polymer was calculated. The ratio of mm:rm:rr triads was found to be 3:31:66, again suggesting a radical polymerisation mechanism as opposed to a coordination-insertion mechanism.

2.4 Styrene Polymerisation

OMRP has been successful in controlling the polymerisation of acrylates, methacrylates, and less active monomers (LAMs) such as vinyl acetate.[22,23] However, styrene has proven to be particularly difficult to control with organometallic-only mechanisms, and ATRP is still the preferred metal-mediated method.[24] As discussed in chapter 1.2.2.2, a system based on Cp_2TiCl_2/Zn has demonstrated good control over the polymerisation of styrene.[25–29] Asandei and co-workers proposed a radical polymerisation mechanism, after the *in situ* reduction of Ti(IV) to Ti(III) and the radical ring opening of an epoxide to initiate the polymerisation.

Previous work suggested that using iron ABPs in the OMRP of styrene was unlikely to be productive, due to the poor metal-alkyl bond strength in the dormant species and thus the inability to mediate the polymerisation.[10] However, this has not been thoroughly explored experimentally and certainly not at a range of reaction temperatures. Firstly, complex **Fe1** was used as mediator in the polymerisation of styrene at 75 °C for 18 hours with V-70 as initiator (polymerisation **2.46**). The polymerisation was essentially uncontrolled, with a high molecular weight and very broad dispersity. This is consistent with the previous work using iron(II) ABP complexes in the polymerisation of styrene under RT-OMRP conditions.[8]

Table 2.7 - Effect of temperature, initiator concentration, and solvent on styrene polymerisation.

#	Temp. (°C)	Equiv. V-70	Conversion (%)	$M_{n,th}$ (Da)	M_n (Da)	Đ
2.46	75	1	50	5200	13200	2.67
2.47	50	1	45	4700	7700	2.04
2.48	30	1	30	3100	7200	1.54
2.49	30[a]	3.5	39	4100	3500	1.30
2.50	30[a,b]	3.5	38	4000	4000	1.32

Conditions: [Sty]:[**Fe1**]:[V-70] = 100:1.00:x, Sty:THF = 1:1 (v/v), 18 hr. Conversion determined by ^{1}H NMR spectroscopy. $M_{n,th}$ = $[Sty]_0/[\mathbf{Fe1}]_0$ × M(Sty) × conversion. [a]Sty:THF = 1:3 (v/v). [b]performed in toluene.

Interestingly lowering the temperature, and thereby slowing the rate of initiation, propagation and termination, had a significant effect on the polymerisation. Incrementally reducing the temperature from 75 °C to 30 °C (polymerisations **2.46**-**2.48**) slowed the polymerisation, as the conversion decreased from 50% to 30%. However, molecular weights were reduced closer to theoretical values. Control over the polymerisation was also

considerably improved, with the dispersity reducing from 2.67 to 1.54. It was possible to further lower the dispersity by increasing the amount of V-70 initiator from 1.0 to 3.5 equivalents and decreasing the overall concentration through the use of additional solvent (polymerisation **2.49**). Under these conditions a dispersity as low as 1.30 was achieved. Furthermore, the molecular weight was in close agreement with the theoretical value. This excellent control has not been seen before in the iron-OMRP of styrene. There was no significant difference when performing the polymerisation in THF or toluene (polymerisations **2.49** and **2.50**). As previously discussed, this suggests the presence of a radical polymerisation mechanism instead of a coordination-insertion polymerisation mechanism.

Kinetic studies were performed on the most well-controlled system to further understand the mechanism and the extent to which the polymerisation is controlled (Table 2.8 and Figure 2.17). Conversion very rapidly increased at the start of the polymerisation, before slowing considerably. After the initial rapid polymerisation, conversion increased linearly with time. However, this linearity persists only for a short time, before the polymerisation rate begins to slow. Molecular weights increased linearly with conversion and dispersities remained relatively low at all conversions. These results together form some evidence of a controlled polymerisation. Whilst iron-ATRP procedures are well-established and offer excellent control over styrene polymerisation,[30] this is the first time such control has been afforded through an iron-OMRP mechanism. It is also worth noting that molecular weights in the polymerisation of styrene are, in general, lower and much closer to theoretical values than in the polymerisation of MMA. This suggests that the initiator efficiency with iron/V-70/styrene is superior to that with MMA, and so fewer initiator radicals are required to attain lower molecular weights.

The rate of increase in molecular weight, with respect to conversion, is approximately half of that which would be expected if all iron centres present in the system were partaking in OMRP. This, along with the initial fast conversion, suggests a period of uncontrolled radical polymerisation and loss of radicals before a controlled OMRP equilibrium is established. This results in a number of small dead chains formed during initiation. The consequence of this is that it makes it difficult to fully deconvolute the chromatography data, and so dispersities towards the end of polymerisation are overestimated.

Table 2.8 - Kinetics of styrene polymerisation at low temperature.

#	Time (hr)	Conversion (%)	$M_{n,th}$ (Da)	M_n (Da)	Đ
2.51	2	27	2800	(a)	(a)
2.52	4	30	3100	(a)	(a)
2.53	6	33	3400	(a)	(a)
2.54	18	44	4600	3500	1.31
2.55	48	53	5500	3900	1.27
2.56	72	57	5900	4200	1.30
2.57	115	62	6500	4400	1.42

Conditions: [Sty]:[**Fe1**]:[V-70] = 100:1.00:3.50, Sty:THF = 1:3 (v/v), 30 °C. Conversion determined by ^{1}H NMR spectroscopy. $M_{n,th}$ = $[Sty]_0/[\mathbf{Fe1}]_0$ × M(Sty) × conversion. (a) too little purified polymer obtained for GPC analysis.

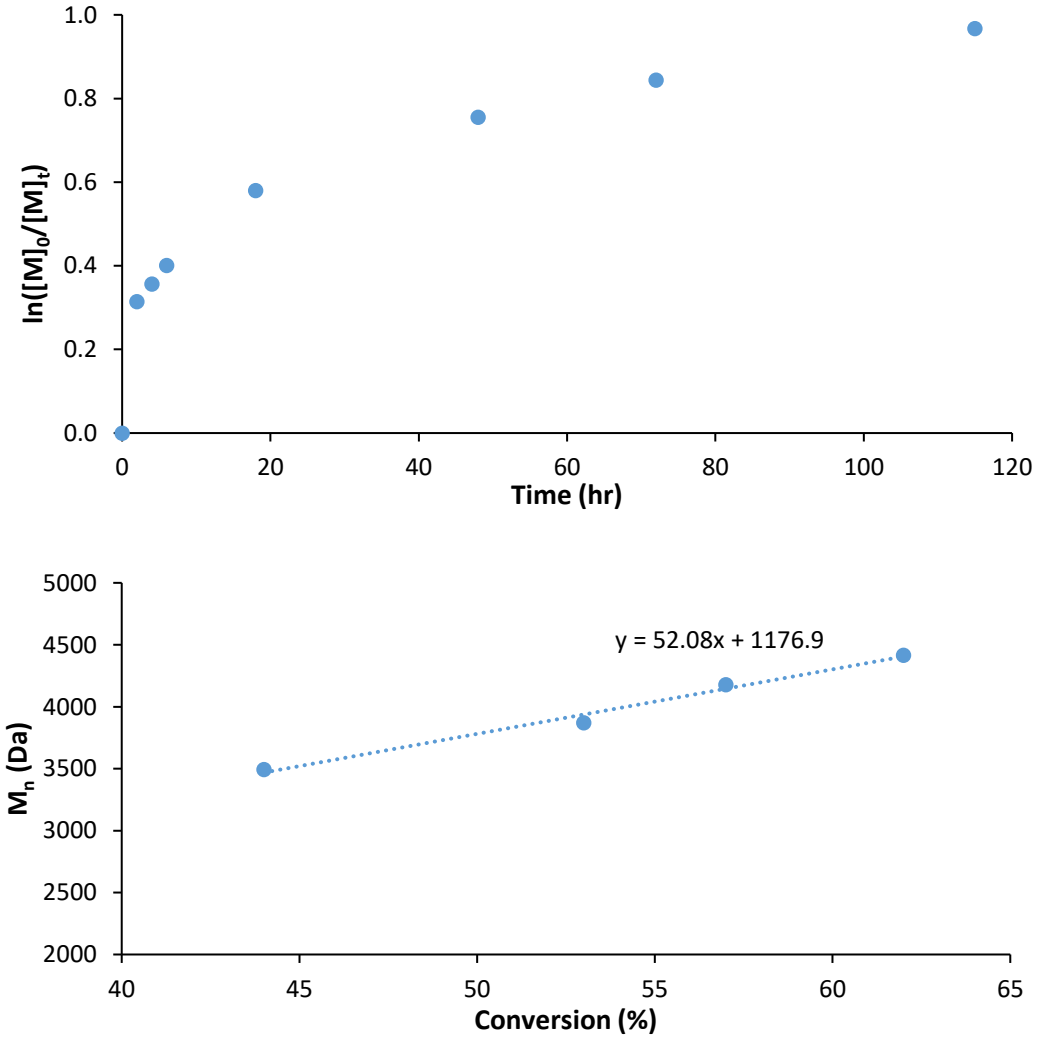

Figure 2.17 - Kinetics of styrene polymerisation at low temperature (30 °C). [Sty]:[**Fe1**]:[V-70] = 100:1.00:3.50, Sty:THF = 1:3 (v/v).

2.5 Vinyl Acetate Polymerisation

The true success story of OMRP has been the ability to control the polymerisation of vinyl acetate and other LAMs. LAMs have proven to be very difficult to polymerise by ATRP, although recent work now suggests this might be possible using copper.[31] However, many complexes, especially those based on cobalt[20,23,32] and iron,[33–35] have successfully controlled the polymerisation of vinyl acetate *via* OMRP. Complex **Fe1** was screened as mediator in the OMRP of vinyl acetate (Table 2.9). However, negligible poly(vinyl acetate) was obtained, even under the forcing conditions of 120 °C for 24 hours (polymerisation **2.60**). There was a distinct colour change in the polymerisation mixture, suggesting that initiation had taken place and that a purple iron(III) species had formed. It is thought that a highly stable deactive species forms upon reaction of a vinyl acetate radical with the iron(II) complex. From this point, no further polymerisation can occur. It is also not possible to insert other monomers into the iron(III)-vinyl acetate species, such as ε-caprolactone. The deactive species is likely to be either a five- or six-membered chelate stabilised by carbonyl donation from the monomer to the metal (Figure 2.18). No attempt was made to isolate and characterise this species.

Table 2.9 - OMRP of vinyl acetate at various temperatures.

#	Temperature (°C)	Time (hr)	Conversion (%)	$M_{n,th}$ (Da)	M_n (Da)	Đ
2.58	60	24	1	660	(a)	(a)
2.59	75	24	1	660	(a)	(a)
2.60	120	24	2	750	(a)	(a)

Conditions: [VAc]:[**Fe1**]:[V-70] = 100:1.00:1.00, VAc:toluene = 1:1 (v/v). Conversion determined gravimetrically. $M_{n,th}$ = $[VAc]_0/[\mathbf{Fe1}]_0$ × M(VAc) × conversion + M(**Fe1**). (a) too low conversion for GPC analysis.

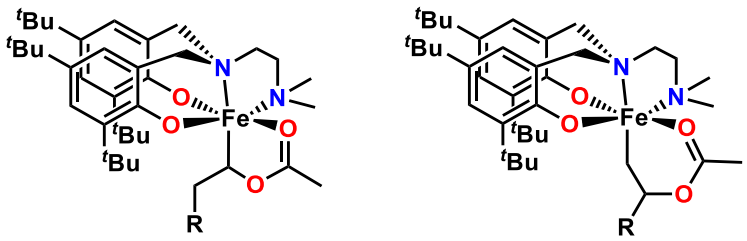

Figure 2.18 - Putative iron(III)-vinyl acetate species, stabilised by a five-membered ring (left) or a six-membered ring (right).

2.6 Alternative Initiation Methods

All the work described in this chapter has used V-70 as the radical initiator of the polymerisation. As discussed in chapter 2.3, the advantage of using V-70 over AIBN is that a comparatively lower reaction temperature can be used whilst maintaining fast initiation. However, because of the low half life temperature, there are some disadvantages associated with its use. V-70 is relatively expensive (compared to AIBN) and difficult to transport, because the initiator must always be kept below 0 °C to prevent decomposition. There is therefore a desire to explore the use of alternative initiators that are easier to transport and store. Furthermore, it would be advantageous to improve the initiator efficiency, so that a smaller quantity of initiator is required to obtain low molecular weights.

The use of photoinitiators in radical polymerisations is commonplace,[36,37] and the use of light as an external control to regulate controlled radical polymerisations (photo-CRP) has been thoroughly researched.[38,39] Examples of photo-CRP with iron complexes have also been reported.[40,41] It was therefore thought that the V-70 initiator could be replaced with a photoinitiator, whilst still performing the polymerisation at a similar reaction temperature. Haddleton and co-workers have previously used a simple UV nail gel curing lamp (λ_{max} = 360 nm) equipped with four 9W bulbs as the UV source in a photo-CRP reaction,[42,43] and the same experimental set-up was used here.

A range of commonly-available photoinitiators (Figure 2.19) were used in the **Fe1**-mediated polymerisation of MMA (Table 2.10). In all cases, the airtight vial containing the polymerisation mixture was irradiated under the UV lamp for 3 minutes, removed from the lamp and subsequently heated in an oil bath at the desired temperature for a period of time.

As well as serving as a thermal initiator, AIBN also behaves as a photoinitiator and was tested under photoinitiation conditions. However, as demonstrated by polymerisations **2.61**-**2.63**, AIBN has a very poor photoinitiation efficiency, and would require significantly more than 3 minutes under the UV lamp for full decomposition of the initiator. Continued thermal initiation throughout the polymerisation results in a high conversion but broad dispersities. At 30 °C (polymerisation **2.63**) the polymerisation is essentially an entirely uncontrolled free radical polymerisation.

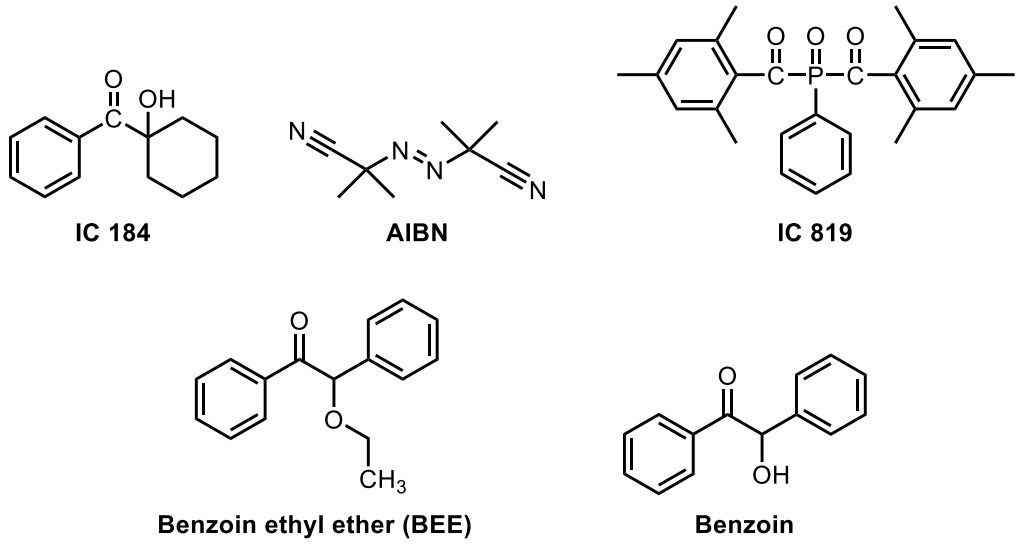

Figure 2.19 - Photoinitiators used in this work.

Table 2.10 - Polymerisation of MMA using various photoinitiators.

#	Initiator	Equiv. Init.	Time (hr)	Temp (°C)	Conv. (%)	M_n (Da)	Đ
2.61[a]	AIBN	1	1	120	60	12000	1.51
2.62	AIBN	1	3	70	79	35000	1.91
2.63	AIBN	1	18	30	15	60700	2.96
2.64	IC 184	1	24	30	0	-	-
2.65	IC 184	1	18	50	0	-	-
2.66	IC 184	1	18	70	0	-	-
2.67	IC 184	1	18	90	0	-	-
2.68	IC 819	0.5	3	70	20	23700	2.78
2.69	BEE	1	18	70	23	40400	2.34
2.70	Benzoin	1	16	70	0	-	-
2.71	Benzoin	0.5	16	70	0	-	-

Conditions: [MMA]:[**Fe1**]:[Initiator] = 100:1.00:x, MMA:toluene = 1:1 (v/v). Conversion determined by ^{1}H NMR spectroscopy. Irradiate under UV for 3 minutes, then heat in an oil bath at a desired temperature. [a]0 minutes under UV.

It was not possible to achieve any polymerisation whatsoever using IRGACURE® 184 (IC184) as photoinitiator (polymerisations **2.64**-**2.67**). This could be due to several reasons, such as poor absorption at 360 nm, or the initiator forming a strong and stable iron-alkyl bond that is unable to be broken, or the initiator reacting with the iron metal in some other undesirable way, perhaps by the hydroxyl group, to deactivate the complex. Similarly, no conversion was

achieved using benzoin as photoinitiator (polymerisations **2.70**-**2.71**). Polymerisation was able to occur using either IRGACURE® 819 (IC819, polymerisation **2.68**) or benzoin ethyl ether (BEE, polymerisation **2.69**) as photoinitiator, however conversions were low with very broad dispersities, which again suggests an uncontrolled free radical polymerisation.

It can be concluded that in this experimental set-up, 3 minutes of UV irradiation is too short a duration for full decomposition of the initiator. This is most likely to be due to poor absorption at 360 nm, which is the wavelength of light from the UV lamp. As a result, the incomplete initiation leads to radicals forming throughout the polymerisation, which gives the observed broad dispersities. It is estimated that approximately 1.5-2.0 hours of UV irradiation time would be required for full decomposition of the photoinitiator.

Based on this information, an alternative initiation method was tried. It was perhaps thought possible to first UV irradiate a mixture of **Fe1**, photoinitiator and solvent for a period of time such that the photoinitiator had fully decomposed, with the aim of forming a stable iron-alkyl species from the photoinitiator. After this time, MMA could be added and the mixture then heated to start a controlled polymerisation. This method was attempted using IC 819 as photoinitiator (Table 2.11).

Table 2.11 - Polymerisation of MMA, starting with a period of UV initiation in the absence of monomer.

#	UV Time (hr)	Heating Time (hr)	Conv. (%)	$M_{n,th}$ (Da)	M_n (Da)	Đ
2.72	1.0	3.0	36	3600	78700	1.85
2.73	1.5	2.0	30	3000	83900	1.69
2.74	1.5	3.0	38	3800	91100	1.57
2.75	1.5	4.5	47	4700	88900	1.60
2.76[a]	2.0	3.0	31	780	30500	1.46

Conditions: [MMA]:[**Fe1**]:[IC819] = 100:1.00:1.00, MMA:toluene = 1:1 (v/v), 30 °C. Conversion determined by ^{1}H NMR spectroscopy. $M_{n,th}$ = $[MMA]_0/[\mathbf{Fe1}]_0$ × M(MMA) × conversion. [a][MMA]:[**Fe1**]:[IC819] = 25:1.00:1.00.

In general, the polymerisation was controlled to a greater extent than in the previous photoinitiator experiments in Table 2.10. Using this new method, conversions were higher and dispersities were narrower. However, molecular weights were significantly higher than theoretical values, suggesting that approximately only 3-5% of the iron centres had a polymer chain growing from them. This is due to the metal-alkyl bond, formed between the iron and the photoinitiator radical, being relatively weak and easily broken. After this bond is broken,

perhaps promoted by the UV radiation, the radical which is released irreversibly terminates which results in an overall loss of radicals. Therefore, by the time the MMA is introduced, only a few radicals remain in the system to undergo a CRP. This results in the very high molecular weights.

The same method may be applied thermally by using an azo initiator (Table 2.12). V-601 was used, which has a similar half life to that of AIBN. The major difference between V-601 and AIBN is the absence of any cyano groups. Just as in the previous method, a mixture of **Fe1**, V-601 and solvent was heated at 95 °C for a period of time such that the V-601 had fully decomposed, with the aim of forming a stable iron-alkyl species from the initiator. After this time, MMA was added and the mixture then heated at a lower temperature (80 °C) to start a controlled polymerisation.

The results are broadly similar to those with the photoinitiator, but with some noticeable improvement. Conversions were higher, and molecular weights slightly closer to theoretical values, with either 9% (polymerisation **2.77**) or 17% (polymerisation **2.78**) of the iron centres having a polymer chain growing from them.

Table 2.12 - Polymerisation of MMA, starting with a period of thermal initiation in the absence of monomer.

#	Equiv. V-601	Initiation Time (hr)	Propagation Time (hr)	Conv. (%)	$M_{n,th}$ (Da)	M_n (Da)	Đ
2.77	1	1	2.0	61	6100	72500	1.63
2.78	5	1	1.5	69	6900	40000	1.65

Conditions: [MMA]:[**Fe1**]:[V-601] = 100:1.00:x, MMA:toluene = 1:1 (v/v). Initiation temperature of 95 °C. Propagation temperature of 80 °C. Conversion determined by ^{1}H NMR spectroscopy. $M_{n,th}$ = $[MMA]_0/[\mathbf{Fe1}]_0 \times M(MMA) \times$ conversion.

In order to explore how well-controlled the polymerisation was, kinetic experiments were performed (Table 2.13 and Figure 2.20). A mixture of **Fe1**, V-601 and solvent was heated at 100 °C for 30 minutes, which is sufficient to fully decompose V-601. After this time, MMA was added and the mixture then heated at 60 °C. Using an initiation temperature of 100 °C instead of 95 °C resulted in a significant loss of radicals, with approximately only 2% of the iron centres having a polymer chain growing from them. As a result, molecular weights were roughly 50 times greater than theoretical values. However, those polymer chains grew in a

controlled way, with conversion increasing linearly with time. Molecular weights also increased with conversion, albeit with some deviation from linearity.

Table 2.13 - Kinetics of MMA polymerisation, starting with a period of thermal initiation in the absence of monomer.

#	Time (hr)	Conversion (%)	$M_{n,th}$ (Da)	M_n (Da)	Đ
2.79	1	6	600	62800	1.89
2.80	3	16	1600	78600	1.86
2.81	6	33	3300	137800	1.68

Conditions: [MMA]:[**Fe1**]:[V-601] = 100:1.00:1.00, MMA:toluene = 1:1 (v/v). Initiation temperature of 100 °C. Initiation time of 30 minutes. Propagation temperature of 60 °C. Conversion determined by ^{1}H NMR spectroscopy. $M_{n,th} = [MMA]_0/[\mathbf{Fe1}]_0 \times M(MMA) \times$ conversion.

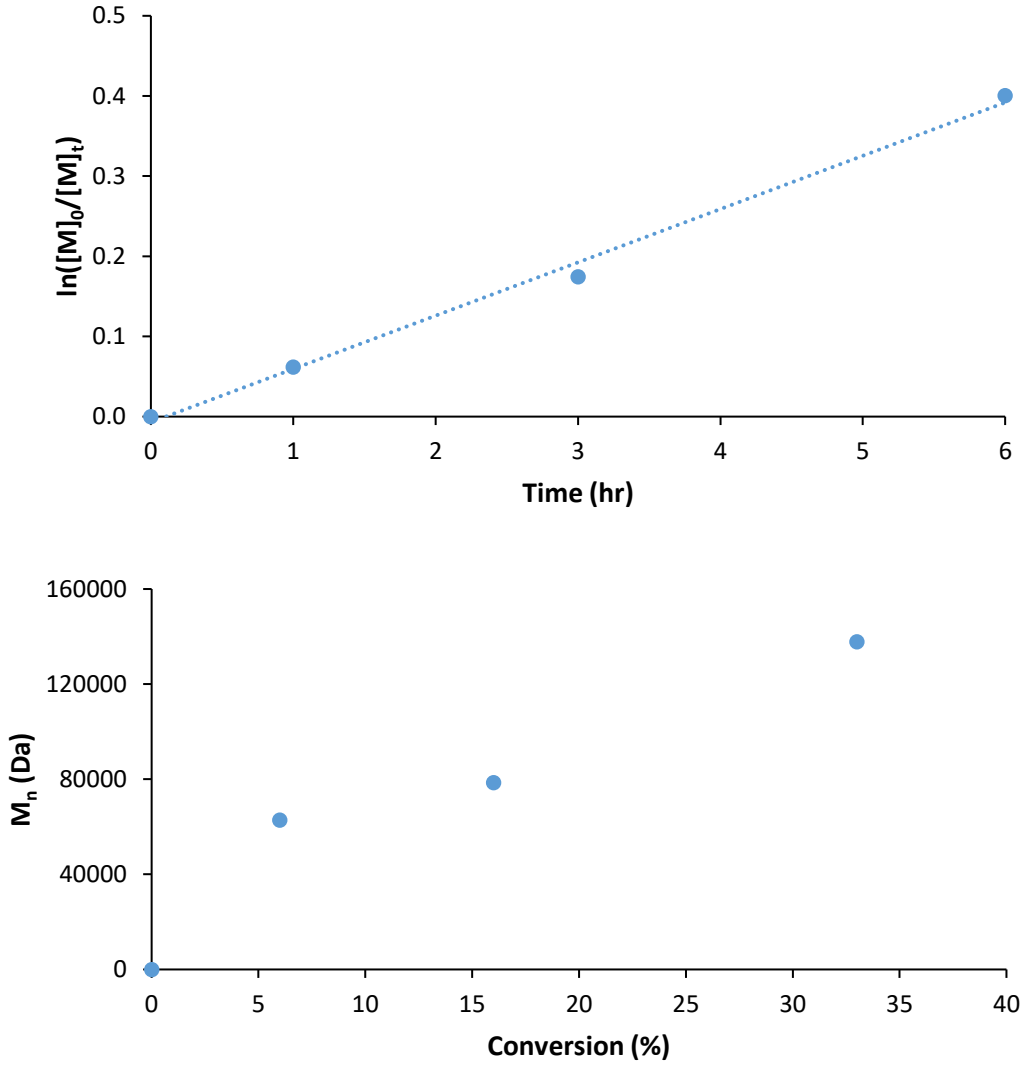

Figure 2.20 - Kinetics of MMA polymerisation at 60 °C, starting with a period of thermal initiation (100 °C) in the absence of monomer.

These results show that if a metal-alkyl species is formed, then a well-controlled polymerisation may occur. However, the challenge lies in forming this metal-alkyl complex, because the experimental results show that this iron-carbon bond is weak and easily broken. Consequently, only a few metal-alkyl species remain at the end of the initiation period, and so only a few metal centres can grow a polymer chain, which results in the very high molecular weights.

2.7 Mechanistic Implications & Conclusions

In this chapter the OMRP of styrene, MMA and vinyl acetate, mediated by the iron(II) ABP complex **Fe1**, has been thoroughly explored and the interplay between the various mechanisms active during OMRP has been demonstrated (Scheme 2.1).

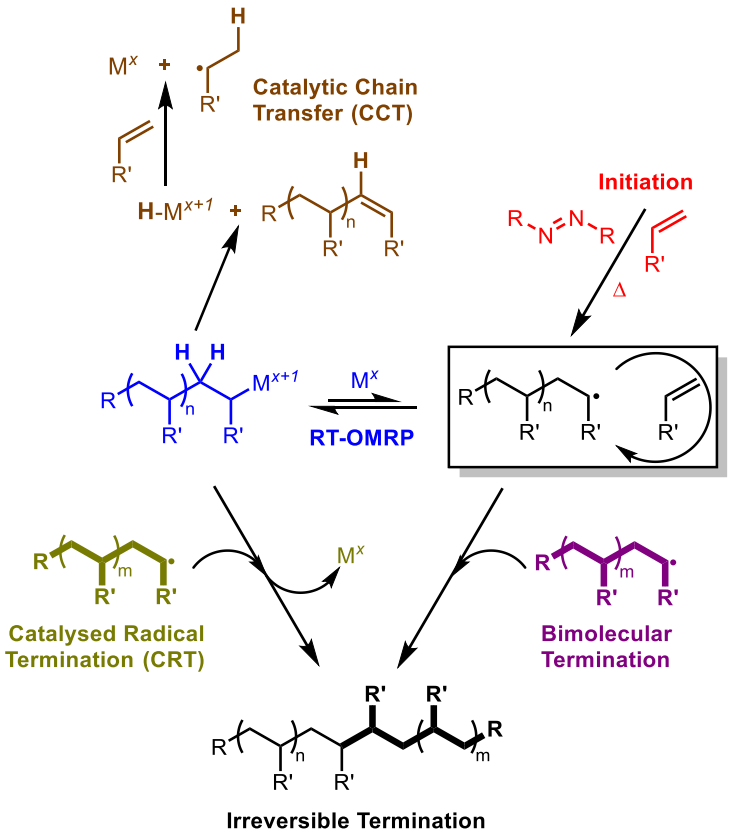

Scheme 2.1 - Overview of the mechanisms likely exhibited in the OMRP of styrene and MMA mediated by **Fe1**.

The conclusions reached following the work in this chapter can be considered to be the final piece of the "iron-mediated CRP" puzzle. The previous work covered iron-ATRP and ATRP-OMRP interplay in considerable detail, whereas this work aimed to address the lack of a detailed mechanistic understanding surrounding OMRP-only pathways. With the improved knowledge gained from this work, and a newly found awareness of the limitations of iron-mediated CRP, we now have a full picture of how iron complexes control the polymerisation of typical vinyl monomers such as styrene and MMA.

Table 2.14 - Summary of the mechanistic conclusions in this chapter.

Fe1-Mediated Polymerisation	**MMA**	**Styrene**	**Vinyl Acetate**
High Temperature (75 °C)	RT-OMRP to moderate conversion, followed by irreversible termination	Uncontrolled polymerisation	No polymerisation
Low Temperature (30 °C)	RT-OMRP to high conversion, due to CCT	Slow RT-OMRP	

As previously discussed, past work investigating the OMRP of MMA mediated by an iron ABP complex used AIBN as the thermal initiator,[8] and so a temperature in excess of 110 °C was required for fast initiation. The work in this chapter used V-70 and so a much lower polymerisation temperature could be used whilst maintaining fast initiation. This was expected to promote a more stable iron-alkyl bond and provide information to help achieve a deeper understanding of the equilibrium between propagation and termination reactions, which are fundamentally intertwined within the OMRP mechanism.

The past work achieved reasonable control and good conversions in the RT-OMRP of MMA. With AIBN at 110 °C for 1 hour, a conversion of 75% was reached with a dispersity of 1.30. The polymerisation was well-controlled, but molecular weights did not increase with conversion. It is therefore likely that this successful result was due to CCT. In this work, the reaction temperature was lowered to 75 °C in an attempt to separate out elements of control and to determine optimised conditions. Under certain conditions, the OMRP of MMA at 75 °C showed moderate control, with reasonable dispersities and some chain-end fidelity, demonstrated through chain extension.

Unfortunately, only moderate conversions were required for the equilibrium between propagation and termination to shift markedly towards irreversible termination. It is unclear whether this was in the form of bimolecular termination or CRT. Recent work by Matyjaszewski and co-workers investigated the equilibrium between bimolecular termination and CRT in the ATRP of acrylates, and set out to determine under what conditions each termination mechanism was favoured.[44,45] Using experimental and computational techniques, it was found that conditions which promoted bimolecular termination resulted in the increase of a shoulder in the chromatography data with double molecular weight relative to the macroinitiator distribution. This indicated that bimolecular termination occurred predominantly *via* radical combination. However, when CRT was promoted, the macroinitiator distribution did not shift, which suggested a disproportionation-like pathway. Further work should focus on understanding the radical termination pathways in iron-mediated polymerisations, which have not previously been studied in detail.

Lowering the polymerisation temperature even further, to 30 °C, saw very similar behaviour to that of polymerisations at 110 °C. High monomer conversions, in excess of 90%, were achieved with reasonable control over dispersity, but the molecular weight was found to be independent of conversion. However, it is likely to be possible to control the molecular weight in a CCT-dominated polymerisation by altering the monomer concentration at the start of the polymerisation.

Using a range of temperatures also allowed for a range of rates of initiation, in order to explore whether the propagation mechanism is RT-OMRP or DT-OMRP. At high temperatures the initiator decomposes rapidly, and so the only subsequent source of radicals in the polymerisation is from the dormant organometallic species. Therefore, the polymerisation of MMA at 75 °C is considerably more likely to proceed *via* RT-OMRP than DT-OMRP. Traditionally, low polymerisation temperatures and a slow rate of initiator decomposition promotes DT-OMRP, since these conditions provide the required constant influx of radicals. A characteristic behaviour of DT-OMRP is a “lag” period at the start of the polymerisation,[22,46] where no conversion is observed for a period of time, before a linear increase in conversion with time is established. In this study, neither the low temperature polymerisation of MMA nor styrene showed any evidence of a “lag” period. In both cases an immediate increase in

conversion with time is observed. This would again suggest that the low temperature polymerisation of MMA and styrene proceeds through RT-OMRP and not DT-OMRP. Given that it is not possible to promote DT-OMRP control, this would suggest that the iron(II) amine-bis(phenolate) complex is unable to undergo DT-OMRP at any temperature. This is likely to be due to a lack of a vacant coordination site on the metal, originating from the steric bulk of the *tert*-butyl substituents on the phenyl ring resulting in a coordinatively saturated complex.

For a successful well-controlled OMRP, it is imperative that the metal-alkyl bond in the dormant species is sufficiently labile for productive polymerisation to occur, whilst also being sufficiently strong for the propagation-reversible termination equilibrium to significantly favour the dormant species. Given the possibility of achieving partially controlled PMMA at all temperatures, ranging from 120 °C to 30 °C, this would suggest that the bond strength between the iron ABP complex and the growing PMMA chain is ideal for productive OMRP at a wide range of temperatures. It is therefore unlikely that the tendency to undergo termination reactions, whether that is bimolecular, CRT or CCT, is dependent on the bond strength in the dormant species.

It is also interesting to consider the bond strengths in the case of styrene. Previous work, using Mössbauer studies,[8] suggested that the absence of an iron(III)-alkyl species during the polymerisation of styrene is strong evidence for the inability of styrene to be polymerised through OMRP. At the high temperatures used in this previous work, the iron-alkyl bond is far too labile for OMRP-control. This chapter has shown that reducing the polymerisation temperature to 30 °C greatly slows the rate of propagation, and decreases the lability of the metal-alkyl bond to the extent that a controlled OMRP can occur, supporting previous computational work which suggested iron-mediated OMRP was feasible.[10] This low temperature OMRP of styrene represents the most effective iron-mediated OMRP to date, with dispersities as low as 1.27.

Attempts were made to replace V-70, which is expensive and challenging to store and handle, with alternative initiators which would improve the industrial applicability of the polymerisation method. The use of a photoinitiator to start the polymerisation was generally unsuccessful using the available experimental set-up, primarily due to difficulty in fully decomposing the initiator before commencing propagation. Attempts to form a metal-alkyl

species *in situ* from either a photoinitiator or an azo initiator, before the addition of MMA, were somewhat more promising. There was evidence of a controlled polymerisation, albeit with molecular weights significantly higher than theoretical values. This was due to the large majority of radicals being lost from the system during the attempted *in situ* synthesis of the metal-alkyl species. Further work should focus on synthesising and isolating an iron-alkyl complex, which would likely be able to initiate and mediate a controlled OMRP. However, experimental evidence suggests that the iron-carbon bond in such a species is generally weak and unlikely to be stable when isolated. There have been some previous attempts within the research group to synthesise a stable iron-alkyl complex, for example in a transmetalation reaction between an iron(III) ABP complex and an organometallic reagent, such as methyl lithium. Exploring in more detail the reactivity between organolithium reagents and iron(III) ABP complexes should form the basis of further work.

As discussed in chapter 1.2.2.1, iron complexes have been used in the polymerisation of olefins, such as ethylene and propylene, and in the ring-opening polymerisation of cyclic esters. Further work should focus on using the controlled OMRP conditions achieved for both MMA and styrene, and exploring the range of block copolymers which are able to be synthesised due to the metal-capped polymer afforded by OMRP. It may be feasible to insert an olefin or cyclic ester monomer into the iron-alkyl bond in the metal-capped polymer. This would enable the synthesis of a range of multi-mechanistic block copolymers using a single metal catalyst, in which the first block is synthesised *via* a controlled radical polymerisation, and the second block is synthesised *via* an insertion polymerisation.

2.8 References

1 R. K. Dean, C. I. Fowler, K. Hasan, K. Kerman, P. Kwong, S. Trudel, D. B. Leznoff, H. B. Kraatz, L. N. Dawe and C. M. Kozak, *Dalt. Trans.*, 2012, **41**, 4806–4816.

2 R. R. Chowdhury, A. K. Crane, C. Fowler, P. Kwong and C. M. Kozak, *Chem. Commun.*, 2008, 94–96.

3 K. Zhu, M. P. Shaver and S. P. Thomas, *European J. Org. Chem.*, 2015, **2015**, 2119–2123.

4 K. Zhu, M. P. Shaver and S. P. Thomas, *Chem. Sci.*, 2016, **7**, 3031–3035.

5 K. Zhu, M. P. Shaver and S. P. Thomas, *Chem. - An Asian J.*, 2016, **11**, 977–980.

6 L. E. N. Allan, J. P. MacDonald, A. M. Reckling, C. M. Kozak and M. P. Shaver, *Macromol. Rapid Commun.*, 2012, **33**, 414–418.

7 L. E. N. Allan, J. P. MacDonald, G. S. Nichol and M. P. Shaver, *Macromolecules*, 2014, **47**, 1249–1257.

8 H. Schroeder, B. R. M. Lake, S. Demeshko, M. P. Shaver and M. Buback, *Macromolecules*, 2015, **48**, 4329–4338.

9 H. Schroeder, M. Buback and M. P. Shaver, *Macromolecules*, 2015, **48**, 6114–6120.

10 R. Poli and M. P. Shaver, *Inorg. Chem.*, 2014, **53**, 7580–7590.

11 C. J. Whiteoak, R. Torres Martin De Rosales, A. J. P. White and G. J. P. Britovsek, *Inorg. Chem.*, 2010, **49**, 11106–11117.

12 Azo Polymerization Initiators Comprehensive Catalog (Wako), https://www.wako-chemicals.de/files/download/pdf/wako_azo_polymerization_initiators_catalog_25.pdf.

13 B. R. M. Lake and M. P. Shaver, *Dalt. Trans.*, 2016, **45**, 15840–15849.

14 G. Greyling and H. Pasch, *Anal. Chem.*, 2015, **87**, 3011–3018.

15 A. J. White and F. E. Filisko, *J. Polym. Sci. Polym. Lett. Ed.*, 1982, **20**, 525–529.

16 Y. Isobe, K. Yamada, T. Nakano and Y. Okamoto, *J. Polym. Sci. Part A Polym. Chem.*, 2000, **38**, 4693–4703.

17 C. Boyer, N. A. Corrigan, K. Jung, D. Nguyen, T. K. Nguyen, N. N. M. Adnan, S. Oliver, S. Shanmugam and J. Yeow, *Chem. Rev.*, 2016, **116**, 1803–1949.

18 S. Perrier, *Macromolecules*, 2017, **50**, 7433–7447.

19 A. Debuigne, R. Poli, C. Jérôme, R. Jérôme and C. Detrembleur, *Prog. Polym. Sci.*, 2009, **34**, 211–239.

20 A. Debuigne, C. Jérôme and C. Detrembleur, *Polymer (Guildf).*, 2017, **115**, 285–307.

21 L. E. N. Allan, M. P. Shaver, A. J. P. White and V. C. Gibson, *Inorg. Chem.*, 2007, **46**, 8963–8970.

22 L. E. N. Allan, M. R. Perry and M. P. Shaver, *Prog. Polym. Sci.*, 2012, **37**, 127–156.

23 R. Poli, *Chem. - A Eur. J.*, 2015, **21**, 6988–7001.

24 K. Matyjaszewski, *Macromolecules*, 2012, **45**, 4015–4039.

25 A. D. Asandei and I. W. Moran, *J. Am. Chem. Soc.*, 2004, **126**, 15932–15933.

26 A. D. Asandei and I. W. Moran, *J. Polym. Sci. Part A Polym. Chem.*, 2005, **43**, 6028–6038.

27 A. D. Asandei and I. W. Moran, *J. Polym. Sci. Part A Polym. Chem.*, 2005, **43**, 6039–6047.

28 A. D. Asandei, I. W. Moran, G. Saha and Y. Chen, *J. Polym. Sci. Part A Polym. Chem.*, 2006, **44**, 2015–2026.

29 A. D. Asandei, I. W. Moran, G. Saha and Y. Chen, *J. Polym. Sci. Part A Polym. Chem.*, 2006, **44**, 2156–2165.

30 Z. Xue, D. He and X. Xie, *Polym. Chem.*, 2015, **6**, 1660–1687.

31 G. Mazzotti, T. Benelli, M. Lanzi, L. Mazzocchetti and L. Giorgini, *Eur. Polym. J.*, 2016, **77**, 75–87.

32 A. N. Morin, C. Detrembleur, C. Jérôme, P. De Tullio, R. Poli and A. Debuigne, *Macromolecules*, 2013, **46**, 4303–4312.

33 Z. Xue and R. Poli, *J. Polym. Sci. Part A Polym. Chem.*, 2013, **51**, 3494–3504.

34 J. Wang, J. Zhou, H. S. E. M. Sharif, D. He, Y. S. Ye, Z. Xue and X. Xie, *RSC Adv.*, 2015, **5**, 96345–96352.

35 M. Wakioka, K.-Y. Baek, T. Ando, M. Kamigaito and M. Sawamoto, *Macromolecules*, 2002, **35**, 330–333.

36 Y. Yagci, S. Jockusch and N. J. Turro, *Macromolecules*, 2010, **43**, 6245–6260.

37 S. Dadashi-Silab, S. Doran and Y. Yagci, *Chem. Rev.*, 2016, **116**, 10212–10275.

38 M. Chen, M. Zhong and J. A. Johnson, *Chem. Rev.*, 2016, **116**, 10167–10211.

39 S. Dadashi-Silab, M. Atilla Tasdelen and Y. Yagci, *J. Polym. Sci. Part A Polym. Chem.*, 2014, **52**, 2878–2888.

40 X. Pan, N. Malhotra, S. Dadashi-Silab and K. Matyjaszewski, *Macromol. Rapid Commun.*, 2017, **38**, 1600651.

41 S. Dadashi-Silab, X. Pan and K. Matyjaszewski, *Macromolecules*, 2017, **50**, 7967–7977.

42 A. Anastasaki, V. Nikolaou, Q. Zhang, J. Burns, S. R. Samanta, C. Waldron, A. J. Haddleton, R. McHale, D. Fox, V. Percec, P. Wilson and D. M. Haddleton, *J. Am. Chem. Soc.*, 2014, **136**, 1141–1149.

43 A. Anastasaki, V. Nikolaou, G. S. Pappas, Q. Zhang, C. Wan, P. Wilson, T. P. Davis, M. R. Whittaker and D. M. Haddleton, *Chem. Sci.*, 2014, **5**, 3536–3542.

44 T. G. Ribelli, K. F. Augustine, M. Fantin, P. Krys, R. Poli and K. Matyjaszewski, *Macromolecules*, 2017, **50**, 7920–7929.

45 T. G. Ribelli, S. M. W. Rahaman, K. Matyjaszewski and R. Poli, *Chem. - A Eur. J.*, 2017, **23**, 13879–13882.

46 A. Debuigne, J.-R. Caille and R. Jérôme, *Angew. Chemie - Int. Ed.*, 2005, **44**, 1101–1104.

3 Titanium

3.1 Titanium Amino-Phenolate Complexes

As discussed in chapter 2.1, the amino-phenolate ligand framework is well-established and has been used extensively in catalysis and in controlling polymerisations. There are many examples of the use of titanium amino-phenolate complexes,[1–6] particularly within olefin polymerisation[7–11] and ring-opening polymerisation (ROP).[12–14] A select few publications will be discussed here in more detail (Figure 3.1).

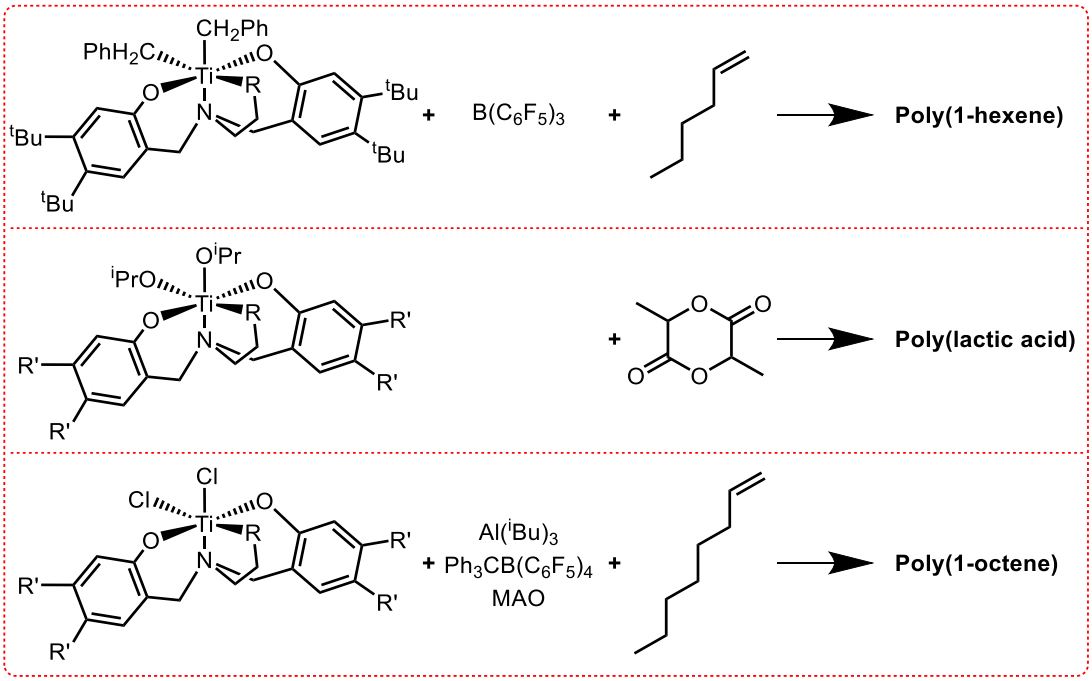

Figure 3.1 - Previous work with titanium amino-phenolate complexes in controlled polymerisations. R = NMe_2, N^iPr_2, CH_3. R' = ^{t}Bu, Cl, H, OMe.

In 2000 Kol and co-workers reported the synthesis and olefin polymerisation behaviour of a titanium complex with an amine bis(phenolate) ligand, into which was incorporated an additional amino side-arm donor.[8] Upon activation with $B(C_6F_5)_3$ at room temperature, poly(1-hexene) was synthesised with narrow dispersity (lower than 1.2) and linear first-order kinetics. In the absence of the side-arm donor, only low molecular weight polymer with a broad dispersity was obtained. Further work on the titanium-mediated polymerisation of 1-hexene was published in 2005.[11] With the aim of producing catalysts with higher activities,

amino-phenolate ligands with electron-withdrawing groups were used. These complexes were found to be highly active and led to ultrahigh-molecular-weight (in excess of 1000000 Da) poly(1-hexene) samples with varying tacticity. The tacticity was dictated by the size of the phenolate substituents. It was concluded that the combination of electron-withdrawing groups on the phenolate rings and a small titanium centre that is sensitive to ligand steric bulk leads to the high activity of the complexes.

Kol and co-workers also used a variety of tetradentate di- or tri-anionic titanium amino-phenolate complexes in the polymerisation of lactide.[12] The polymerisations were conducted in the absence of any solvent at 130 °C and were found to be reasonably well-controlled, with dispersities in some cases as low as 1.11. In general, a higher yield led to polymer with a broader dispersity. The activities of complexes derived from the di-anionic ligands were dependent on the phenolate substituents but not on the ligand backbone. Furthermore, pentacoordinate complexes were found to be more active than hexacoordinate complexes bearing the same phenolate substituents. It was concluded that a more open metal site leads to higher activity in lactide polymerisation.

Davidson and co-workers used a series of tetradentate amine bis(phenolate) ligands with group 4 metals in the ROP of ε-caprolactone and *rac*-lactide.[13] In the case of the titanium(IV) complexes, it was found that sterically demanding ligands were more effective initiators. The polymerisation of *rac*-lactide demonstrated that the titanium(IV) complexes produced atactic polymer.

Martins and co-workers reacted titanium and yttrium trichlorides with the sodium or potassium salts of a variety of diamine bis(phenolate) ligands.[1] They also found that the titanium(III) bis(phenolate) complexes do not promote nitrile coupling reactions by electron transfer. The solid-state molecular structures show that the ligand is coordinated to the metal centre by the two oxygen atoms and the two nitrogen atoms with a trans phenolate arrangement.

More recently, Białek and co-workers used monomeric titanium(IV) dichloride complexes of amine-bis(phenolate) ligands in the polymerisation of 1-octene and other higher molecular weight alkenes.[7] The complexes were activated with $[Ph_3CB(C_6F_5)_4]$ and methylaluminoxane (MAO). The activity of the complexes was found to be highly dependent on the structure of

the ligand framework, following the investigation of a variety of phenolate substituents and pendant donor arms.

To the present date, there have been no attempts to use titanium amino-phenolate complexes in controlled radical polymerisation. Furthermore, there is uncertainty as to the mechanism of the previous titanium-mediated controlled radical methods (as discussed in detail in chapter 1.2.2.2). Whilst possible mechanisms have been proposed, little supporting evidence has been provided, with no thorough mechanistic investigation or speciation analysis. This leaves unanswered questions as to whether the mechanism is truly a radical polymerisation. As discussed in the preceding paragraphs, other titanium-mediated methods typically require expensive or pyrophoric activators such as $B(C_6F_5)_3$ and MAO. This significantly limits the industrial usefulness of these methods. Building on the extensive knowledge of the amino-phenolate ligand family, it is hypothesised that the use of tetradentate amino-phenolate ligands would yield titanium complexes with one free coordination site, following dissociation of coordinated solvent. This might enable these complexes to participate in OMRP reactions of alkenes such as methacrylates, which could be initiated by a conventional azo initiator instead of by a co-catalyst or activator.

3.2 Complex Synthesis

*The following work in this section was completed by Dr Benjamin R. M. Lake: Synthesis of ligands **Lig4**H_2-**Lig7**H_3 and complexes **Ti5**-**Ti7**, growing of crystals for x-ray crystallographic analysis, collection and computational analysis of x-ray crystallographic data for all complexes.*

The amino-phenolate ligand precursors **Lig1**H_2-**Lig7**H_3 were synthesised *via* Mannich-type condensation reactions between the appropriate 2,4-subsituted phenol, amine and formaldehyde (Scheme 3.1). The characterisation data of these seven compounds was consistent with the well-established literature precedent.[5,9,15–18] The ligands were chosen so as to investigate the effect of ligand electronic and steric properties, as well as coordination geometry, on alkene polymerisation. **Lig1**H_2-**Lig3**H_2 all have dimethylamino pendant donor arms but vary in the nature of the 2,4-substituents on the aromatic group. The substituent is either electron-withdrawing chloro (**Lig3**H_2), electron-releasing methyl (**Lig2**H_2) or sterically

bulky, electron-releasing *tert*-butyl (**Lig1**H_2). **Lig4**H_2 also contains *tert*-butyl 2,4-substitutents, but instead has a tethered THF pendant donor arm in place of the dimethylamino donor arm. **Lig5**H_2 has a very similar donor set to **Lig1**H_2 but varies with regards to connectivity and is likely to have a different coordination geometry around the metal. **Lig6**H_3 and **Lig7**H_3 are potentially trianionic donors, with 2,4-dimethyl and 2,4-di-*tert*-butyl aromatic substituents.

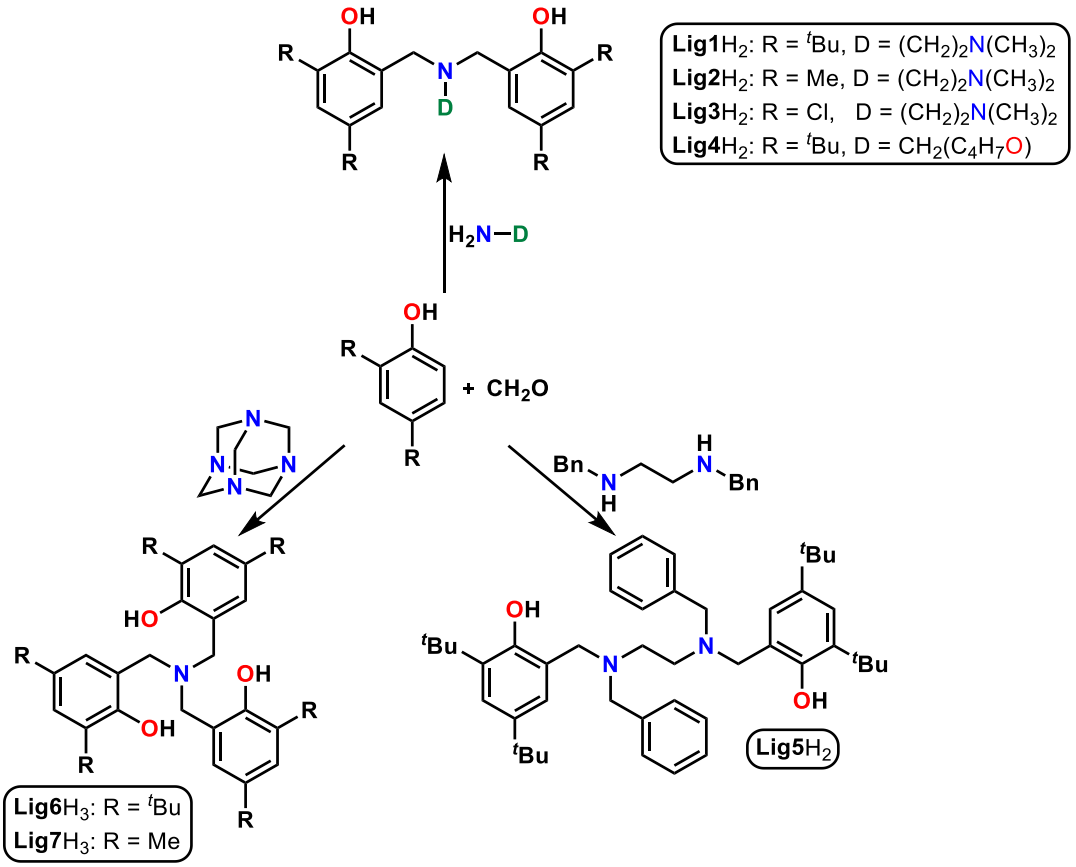

Scheme 3.1 - Synthesis of ligand precursors **Lig1**H_2-**Lig7**H_3.

Complexation of ligands **Lig1**H_2-**Lig5**H_2 was achieved using one of two methods (Scheme 3.2). One method is by a one-pot, one-step reaction of 3 equivalents of the ligand precursor with 2 equivalents of $Ti(N(SiMe_3)_2)_3$ ($Ti(HMDS)_3$)[19] and 1 equivalent of $TiCl_3(THF)_3$.[20] Complexes **Ti1**-**Ti5** (from **Lig1**H_2-**Lig5**H_2 respectively) may also be synthesised by a one-pot, two-step reaction, initially using the ligand precursor and 2 equivalents of Li(HMDS) to form the dilithiated ligand, followed by transmetalation to titanium(III) using $TiCl_3(THF)_3$ with the subsequent release of lithium chloride, which is removed by filtration.

Complexes **Ti6** and **Ti7** (from **Lig6**H_3 and **Lig7**H_3 respectively) could also be synthesised using one of two routes; either through direct reaction of the ligand precursor with 1 equivalent of

$Ti(HMDS)_3$, or *via* reaction of the ligand precursor with 3 equivalents of Li(HMDS) to form the trilithiated ligand, followed by transmetalation to $TiCl_3(THF)_3$. It was found that yields were generally higher when using the transmetalation method.

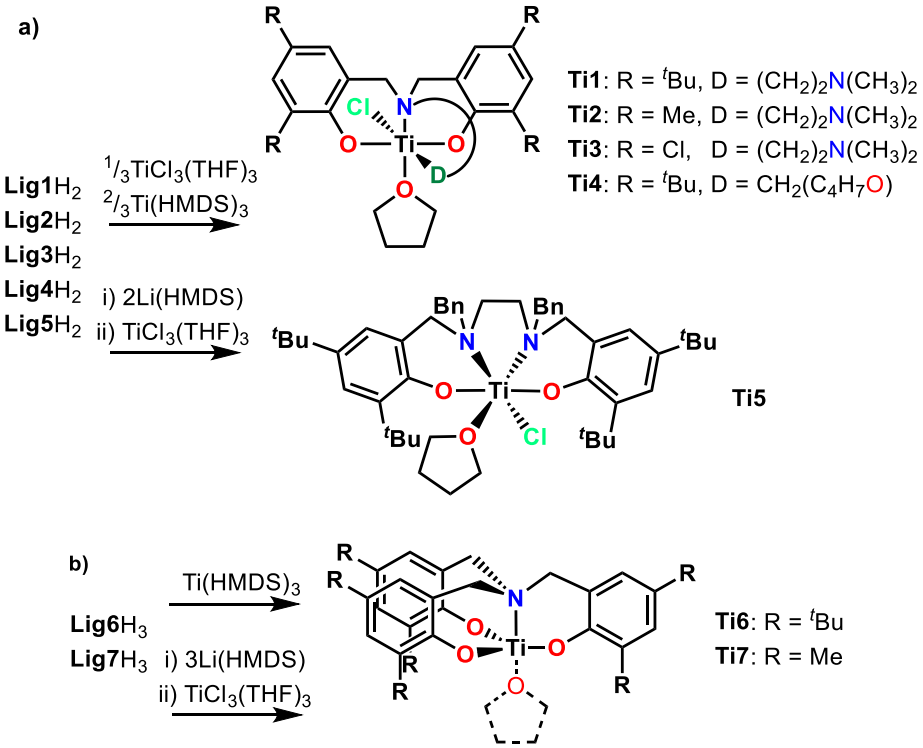

Scheme 3.2 - a) Synthesis of complexes **Ti1**-**Ti5** and b) synthesis of complexes **Ti6** and **Ti7**.

Complexes **Ti1**-**Ti5** were isolated as pale yellow solids after recrystallisation, whereas **Ti6** was obtained as a violet solid and **Ti7** as an off-white solid. Interestingly, it was found that dissolution of complexes **Ti2** and **Ti3** in a non-coordinating solvent (such as benzene or toluene) resulted in a colour change from yellow to yellow/green and was accompanied by the precipitation of a green crystalline solid. This is likely because in a non-coordinating solvent, the coordinating THF molecule dissociates and allows for the formation of a $(\mu\text{-Cl})_2$-bridged dimer. This behaviour was not exhibited for complexes **Ti1** and **Ti4**, which is likely to be due to the steric clash which would arise between the ortho *tert*-butyl groups of the two amino-phenolate ligands of a dimer.

Single crystals of complexes **Ti2** and **Ti3** were obtained by the vapour diffusion of *n*-hexane into a concentrated THF solution. Crystals of **Ti4** were obtained from a toluene/*n*-hexane solution (Figure 3.2). The solid-state structure of complex **Ti1** has already been reported by Marques, Martins and co-workers.[1]

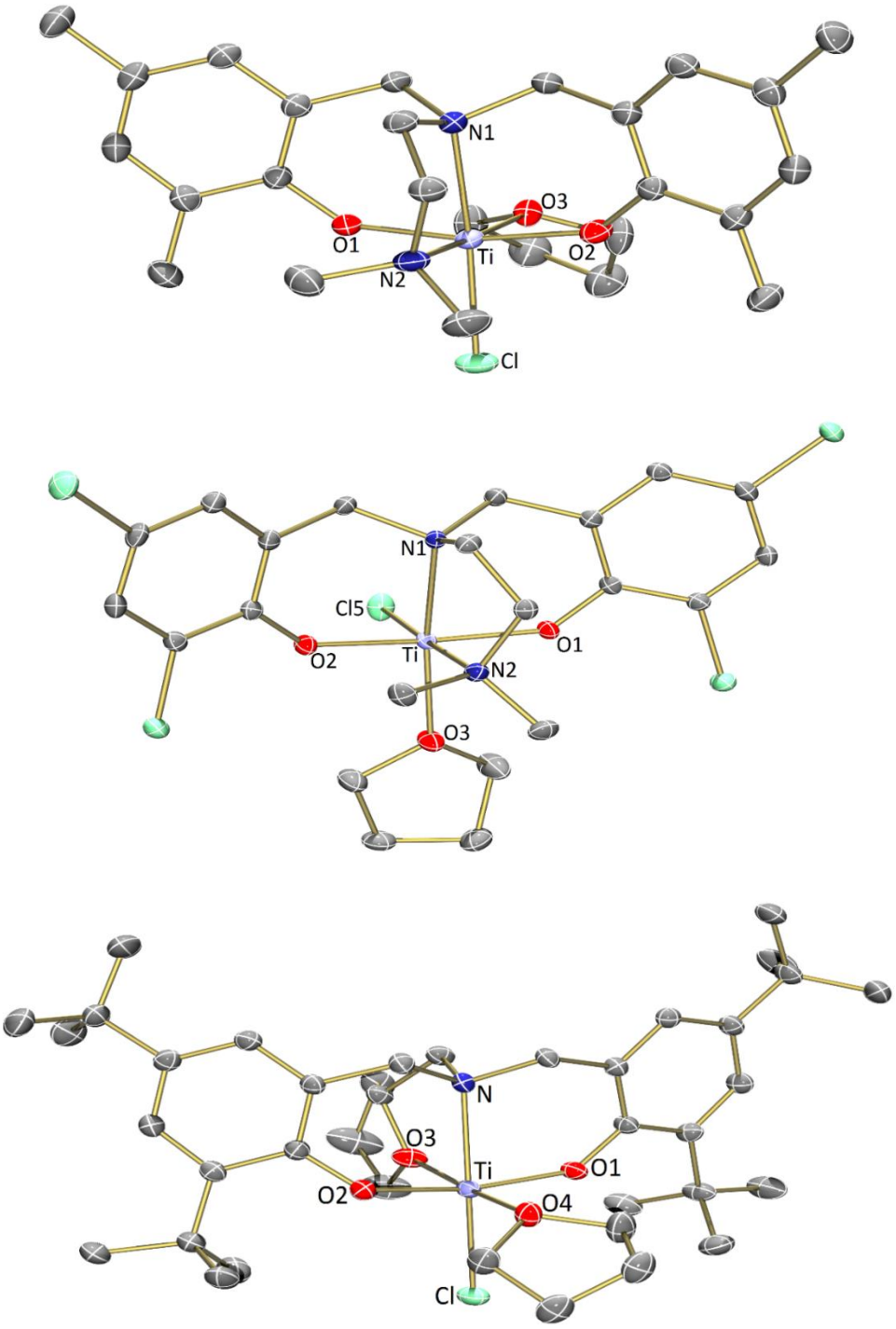

Figure 3.2 - Molecular structures of **Ti2** (top), **Ti3** (middle) and **Ti4** (bottom) with ellipsoids set at the 50% probability level. Hydrogen atoms, solvent and minor disorder components have been omitted for clarity. Selected bond lengths (Å) and angles (°): **Ti2** - Ti-Cl 2.4188(5), Ti-O1 1.8984(13), Ti-O2 1.8995(13), Ti-O3 2.2085(14), Ti-N1 2.2769(15), Ti-N2 2.2581(16), Cl-Ti-N1 175.10(4), O1-Ti-O2 167.43(6), N2-Ti-O3 175.39(6). **Ti3** - Ti-Cl5 2.4209(5), Ti-O1 1.9158(11), Ti-O2 1.9072(11), Ti-O3 2.1415(12), Ti-N1 2.2350(13), Ti-N2 2.3052(13), Cl5-Ti-N2 177.97(4), O1-Ti-O2 172.47(5), N1-Ti-O3 169.50(5). **Ti4** - Ti-Cl 2.4185(6), Ti-O1 1.8893(16), Ti-O2 1.9211(16), Ti-O3 2.1142(17), Ti-O4 2.1856(17), Ti-N 2.2847(17), Cl-Ti-N 170.48(5), O1-Ti-O2 166.07(6), O3-Ti-O4 174.28(6).

As expected, complexes **Ti2**-**Ti4** all possess slightly distorted octahedral geometries, with the coordination sphere, in all cases, comprising the tetradentate ABP ligand, a chloride and a molecule of THF. Measured bond lengths in the complexes are similar to one another, and to the previously reported titanium(III) complexes.[1]

3.3 Monomer Screening

Complexes **Ti1**-**Ti7** were screened for their efficacy as mediators in the polymerisation of MMA under OMRP conditions (Figure 3.3). As previously discussed, the azo initiator V-70 was used because it has a much lower decomposition temperature (10 hour $t_{½}$ = 30 °C) than AIBN (10 hour $t_{½}$ = 65 °C) and so polymerisations may be performed at much lower temperatures whilst maintaining fast initiation. Generally, a lower temperature during propagation improves the polymerisation control.[21] Non-coordinating toluene was chosen to be the polymerisation solvent. Theoretical molecular weights were calculated based on the ratio of initial monomer concentration to initial titanium concentration.

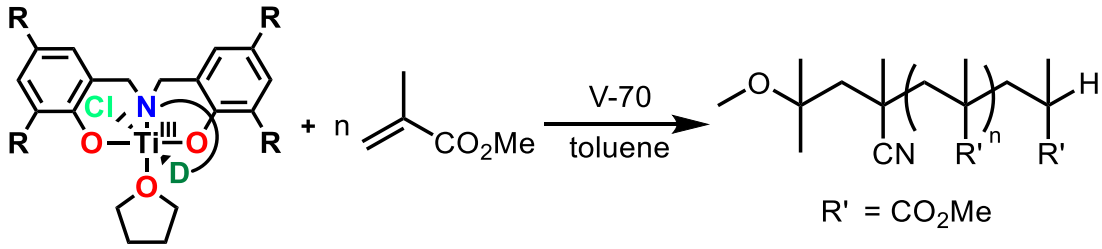

Figure 3.3 - Representative MMA polymerisation.

With complexes **Ti1**-**Ti3** (polymerisations **3.1**-**3.3**), moderate to high conversions were achieved, with the *tert*-butyl-substituted complex **Ti1** giving polymer with the lowest dispersity (Đ = 1.10), albeit with the lowest conversion. In all cases, molecular weights were much higher than the theoretical values, which typically suggests that a significant number of radicals are lost at the very beginning of the reaction. Consequently, only a fraction of the titanium complexes have a polymer chain growing from them, which results in a higher effective number of equivalents of monomer per growing chain.

Complexes **Ti5**-**Ti7** were found to be poor mediators of MMA polymerisation under these OMRP conditions, yielding polymers with a broad dispersity (polymerisations **3.5**-**3.7**). Using

the same technique as in chapter 2.3, observation of the ^{1}H NMR spectrum of the purified PMMA sample made by complex **Ti7** showed resonances in the alkene region (Figure 3.4). This suggests the presence of catalytic chain transfer or radical disproportionation.

Table 3.1 - Polymerisation screening of MMA with complexes **Ti1**-**Ti7**.

#	Complex	Conv. (%)	$M_{n,th}$ (Da)	M_n (Da)	Đ	mm:rm:rr
3.1[b]	Ti1	50	5000	19700	1.10	15:47:38
3.2[b]	Ti2	97	9700	46500	1.61	6:39:55
3.3[a]	Ti3	73	7300	20700	1.59	6:39:55
3.4[a]	Ti4	80	8000	21600	1.26	18:48:34
3.5[a]	Ti5	55	5500	16900	1.97	8:34:57
3.6[b]	Ti6	76	7600	19100	2.41	8:38:54
3.7[b]	Ti7	70	7000	29700	2.01	4:36:59

Conditions: [MMA]:[Ti(III)]:[V-70] = 100:1.0:1.0, MMA:toluene = 1:1 (v/v). 80 °C. [a]1 hour. [b]2.5 hours. Conversion determined by ^{1}H NMR spectroscopy. $M_{n,th}$ = $[MMA]_0/[Ti(III)]_0$ × M(MMA) × conversion.

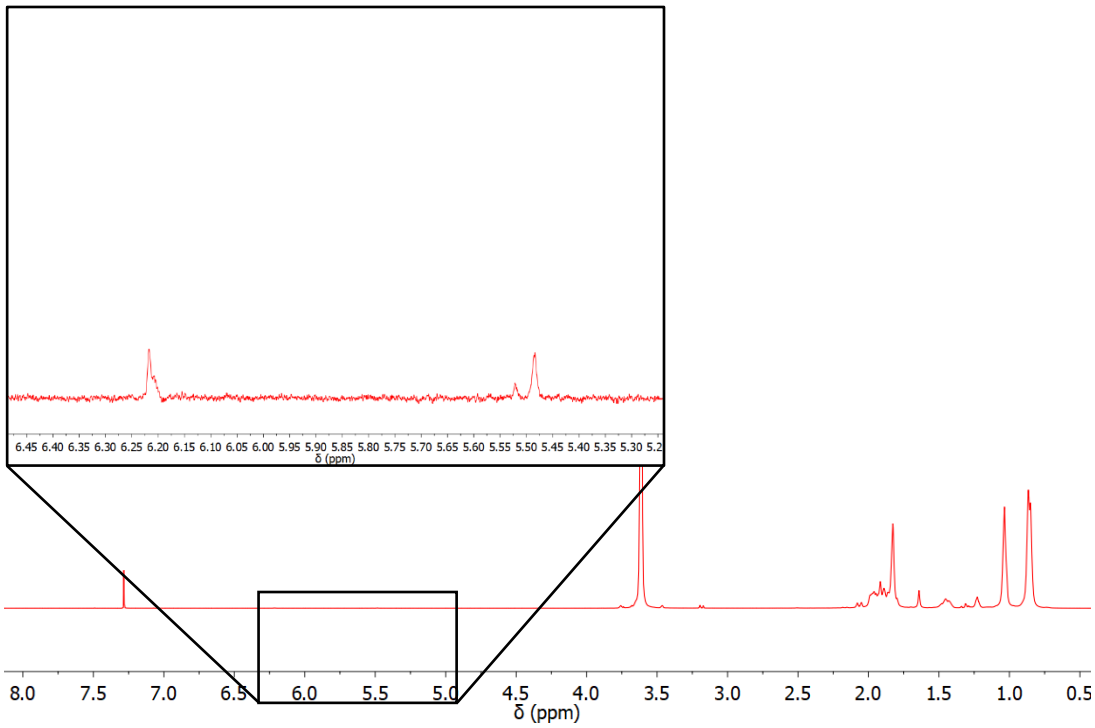

Figure 3.4 - ^{1}H NMR spectrum of purified PMMA produced by complex **Ti7** (500 MHz, $CDCl_3$).

Complexes **Ti5**-**Ti7** have a substantially more rigid and bulky ligand framework than complexes **Ti1**-**Ti4**, in which the flexible nitrogen donor arm is replaced by either a bulkier amine donor (**Ti5**) or a further phenolate donor (**Ti6** and **Ti7**). It is therefore likely that these properties are undesirable, because they prevent the formation of the dormant species necessary for polymerisation control. This therefore results in an uncontrolled polymerisation and broad dispersities.

To demonstrate the "livingness" of the MMA polymerisation, kinetics were performed using complex **Ti1** as the mediator (Table 3.2 and Figure 3.5). The polymerisation is well-controlled with linear first-order kinetics, up to approximately 90% conversion. At high conversions (and therefore high molecular weights), deviation from linearity occurs due to the solidification of the reaction mixture. At this point, diffusion-controlled kinetics become predominant. In addition, molecular weights increased linearly with conversion. However, molecular weights are approximately 4.3 times greater than theoretical values, which could be due to poor initiator efficiency. Dispersities remained almost constant throughout the polymerisation and slightly increased at conversions greater than 90%. Again, this is most likely to be due to the solidification of the reaction mixture.

Table 3.2 - Kinetics of MMA with complex **Ti1**.

#	Time (min)	Conversion (%)	$M_{n,th}$ (Da)	M_n (Da)	Đ
3.8	10	27	2700	11400	1.11
3.9	20	48	4800	19400	1.10
3.10	30	70	7000	28400	1.13
3.11	40	78	7800	33500	1.11
3.12	60	88	8800	37800	1.13
3.13	90	92	9200	40000	1.17

Conditions: [MMA]:[**Ti1**]:[V-70] = 100:1.0:1.0, MMA:toluene = 1:1 (v/v), 80 °C. Conversion determined by ^{1}H NMR spectroscopy. $M_{n,th} = [MMA]_0/[\mathbf{Ti1}]_0 \times M(MMA) \times$ conversion.

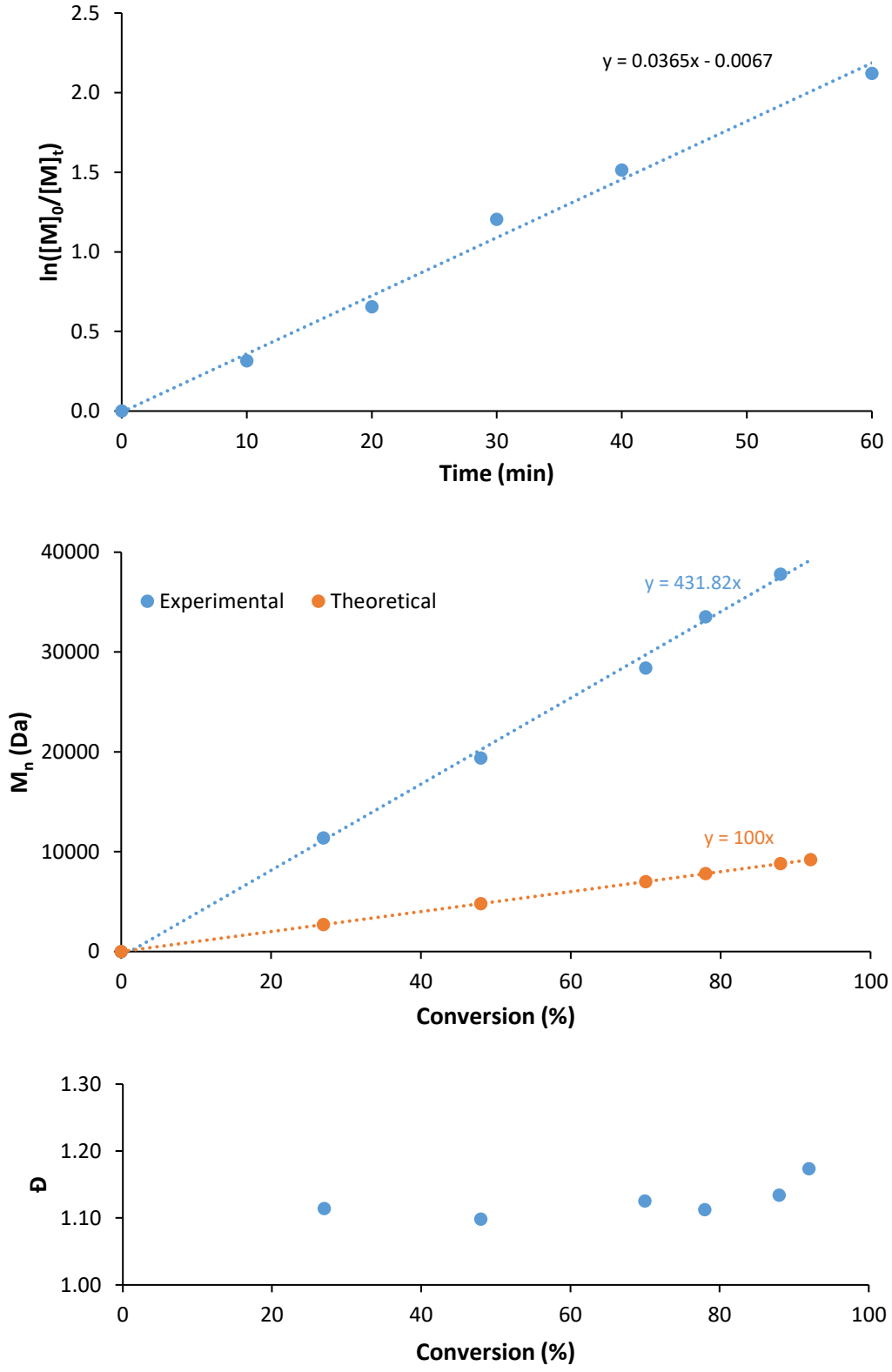

Figure 3.5 - MMA kinetics at 80 °C with complex **Ti1**. [MMA]:[**Ti1**]:[V-70] = 100:1.0:1.0, MMA:toluene = 1:1 (v/v).

Using the same technique as in chapter 2.3, it is possible to use ^{1}H NMR spectroscopy to calculate the tacticity of the resultant purified polymer sample (Figure 3.6). It was expected that the PMMA synthesised in all cases would possess an mm:rm:rr ratio of approximately 3:33:64, which is characteristic of a radical polymerisation.[22] PMMA synthesised using both chloro-substituted **Ti3** and methyl-substituted **Ti2** possesses a slight isotactic bias compared to a free-radical polymerisation (Table 3.1). The bulky *tert*-butyl-substituted **Ti1** displayed an even more pronounced isotactic bias. *Tert*-butyl-substituted **Ti4** displayed a yet further pronounced isotactic bias.

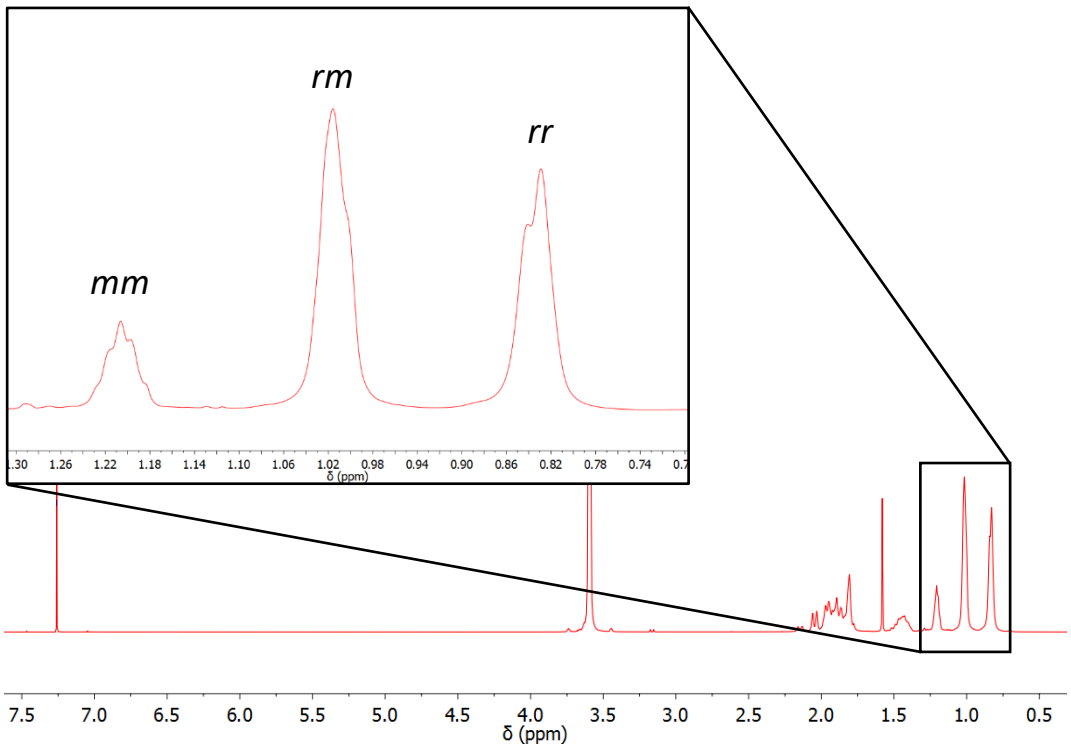

Figure 3.6 - Determination of the tacticity of purified PMMA by ^{1}H NMR spectroscopy (500 MHz, $CDCl_3$).

In a typical metal-mediated controlled radical polymerisation, one would expect the tacticity of the resultant polymer to be very similar to that of a free-radical polymerisation, since monomer addition to a radical chain end occurs away from the metal centre and thus is not influenced by the ligand framework. The fact that such a noticeable isotactic bias is present when complexes **Ti1**-**Ti4** are used as mediators suggests that the polymerisation mechanism may not be radical-based, even though a standard radical polymerisation protocol had been employed. Based on this initial tacticity data a polymerisation mechanism involving coordination-insertion, initiated by a conventional radical initiator, appears more likely.

A coordination-insertion mechanism is most commonly observed in the polymerisation of olefins with Ziegler-Natta catalysts, which are based on titanium tetrachloride and activated with organoaluminium compounds, and which are widely used in the polymerisation of ethylene and propylene.[23–25] The coordination-insertion polymerisation of MMA is much less common but has previously been reported using, for example, palladium,[26,27] samarium,[28] and nickel complexes.[29] In these examples, the MMA is typically copolymerised with ethylene. It would therefore be surprising and unique if the polymerisation of MMA, mediated by titanium complexes **Ti1**-**Ti4**, exhibits a coordination-insertion type mechanism. This is even more surprising given that the polymerisation is initiated by a conventional radical azo initiator, rather than a typical activator such as $B(C_6F_5)_3$ and MAO.

To further investigate the possibility that the polymerisation mechanism involves coordination-insertion, the polymerisation of MMA mediated by complexes **Ti1**-**Ti3** was conducted in a variety of solvents (Table 3.3 and Figure 3.7). In a non-radical polymerisation, one would expect that varying the coordinating nature of the polymerisation solvent would have a significant effect on the conversion. Inversely, in a radical polymerisation, one would expect that the coordinating nature of the polymerisation solvent would have little effect on the conversion (as exhibited in chapters 2.3 and 2.4).

Table 3.3 - Polymerisation solvent screening of MMA with complexes **Ti1**-**Ti3**.

#	Complex	Solvent	Conversion (%)	$M_{n,th}$ (Da)	M_n (Da)	Đ
3.14	Ti1	toluene	93	9300	54800	1.19
3.15	Ti2	toluene	>99	10000	95300	1.48
3.16	Ti3	toluene	76	7600	22800	1.40
3.17	Ti1	1,4-dioxane	32	3200	29400	1.13
3.18	Ti2	1,4-dioxane	>99	10000	85800	1.54
3.19	Ti3	1,4-dioxane	66	6600	22700	1.53
3.20	Ti1	THF	12	1200	15500	1.25
3.21	Ti2	THF	>99	10000	68600	1.60
3.22	Ti3	THF	54	5400	23500	1.54

Conditions: [MMA]:[Ti(III)]:[V-70] = 100:1.0:0.5, MMA:solvent = 1:1 (v/v), 75 °C, 2.5 hours. Conversion determined by ^{1}H NMR spectroscopy. $M_{n,th} = [MMA]_0/[Ti(III)]_0 \times M(MMA) \times$ conversion.

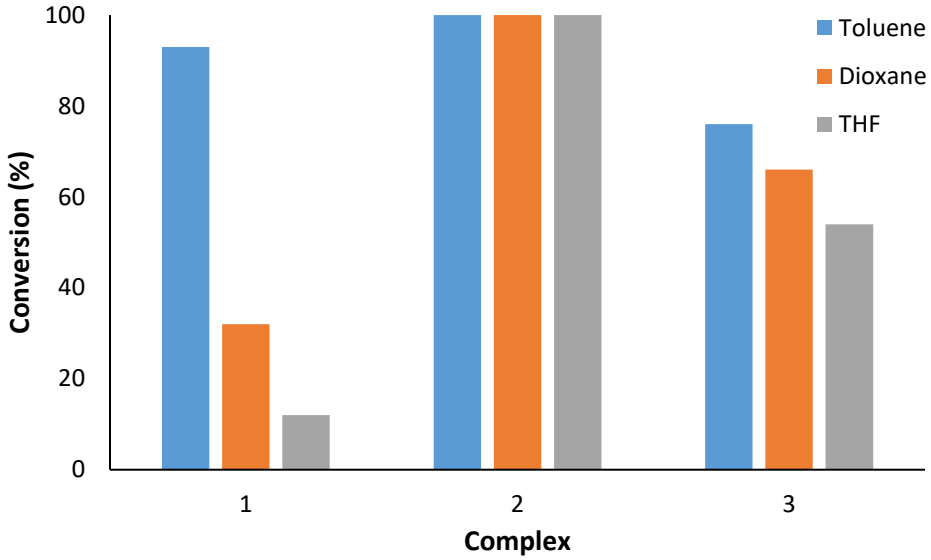

Figure 3.7 - Polymerisation solvent screening of MMA with complexes **Ti1**-**Ti3**.

As previously discussed, polymerisations were fast and moderate to high conversions were achieved when using toluene as solvent (polymerisations **3.14**-**3.16**). This rate decreased when using the more coordinating solvent dioxane (polymerisations **3.17**-**3.19**) and decreased even further using THF (polymerisations **3.20**-**3.22**). This is most clearly evidenced with complex **Ti1**, with the conversion decreasing from 93% (polymerisation **3.14**) to 12% (polymerisation **3.20**) upon the use of a more coordinating solvent. This suggests that a vacant coordination site is required on the metal for a productive polymerisation.

Interestingly, increasing the polarity/coordinating ability of the solvent from toluene to dioxane to THF decreases the conversion considerably for complexes **Ti1** and **Ti3** but apparently has no effect on complex **Ti2**, which gives a rapid polymerisation in all three solvents. In the case of complexes **Ti1** and **Ti3**, dispersities are slightly broader in dioxane and THF than in toluene. In all cases, molecular weights are significantly higher than the theoretical values. Complex **Ti1** gave a remarkably narrow dispersity (Đ = 1.13) when the polymerisation was performed in dioxane.

To further understand how the choice of solvent affects the polymerisation of MMA, kinetics were performed using complex **Ti1** as the mediator (Table 3.4 and Figure 3.8). Toluene, THF and acetonitrile were used as solvents. As previously discussed, the polymerisation in toluene rapidly reached high conversion, with dispersities remaining below 1.20 throughout the polymerisation. In the case of THF the polymerisation is essentially prohibited, with

conversions unable to exceed 6% even after 3 days. At this time, the molecular weight is very high and the dispersity is extremely broad, suggesting numerous uncontrolled termination reactions. Similarly, the polymerisation is essentially prohibited in acetonitrile, with conversion unable to exceed 10%. These kinetic results support the theory that, at least in the case of **Ti1**, a vacant coordination site is required on the metal for productive polymerisation. This is because THF and acetonitrile are coordinating with the titanium and thus block this coordination site from participating in the polymerisation.

Table 3.4 - MMA kinetics, with complex **Ti1**, using different solvents.

#	Solvent	Time (min)	Conv. (%)	$M_{n,th}$ (Da)	M_n (Da)	Đ
3.23	toluene	5	26	2600	13500	1.20
3.24	toluene	7	46	4600	23900	1.14
3.25	toluene	10	60	6000	30800	1.13
3.26	toluene	15	74	7400	40100	1.11
3.27	toluene	20	83	8300	43700	1.14
3.28	toluene	24	87	8700	44600	1.20
3.29	THF	60	1	100	14500	1.55
3.30	THF	420	6	600	40600	1.40
3.31	THF	4440	6	600	85100	5.34
3.32	acetonitrile	60	6	600	-	-
3.33	acetonitrile	420	10	1000	-	-

Conditions: [MMA]:[**Ti1**]:[V-70] = 100:1.0:0.5, MMA:solvent = 1:1 (v/v), 80 °C. Conversion determined by ^{1}H NMR spectroscopy. $M_{n,th} = [MMA]_0/[\mathbf{Ti1}]_0 \times M(MMA) \times$ conversion.

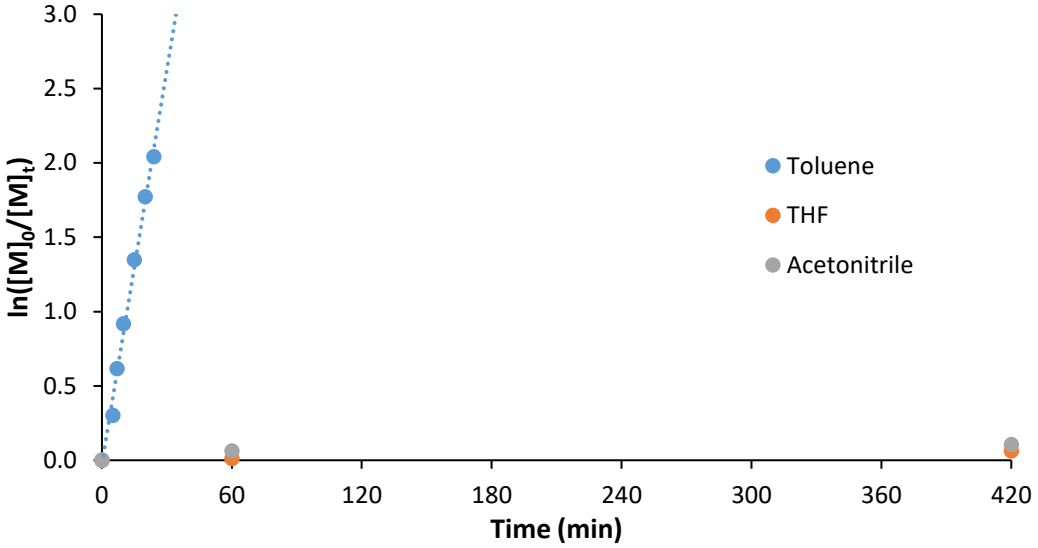

Figure 3.8 - MMA kinetics at 80 °C, with complex **Ti1**, using different solvents. [MMA]:[**Ti1**]:[V-70] = 100:1.0:0.5, MMA:solvent = 1:1 (v/v).

3.4 DFT Study - Possible Pathways

All the DFT calculations were completed during a research placement with Professor Rinaldo Poli at the Laboratoire de Chimie de Coordination, Toulouse, France.

To better understand how the titanium(III) amino-phenolate complexes **Ti1**-**Ti4** control the polymerisation of MMA, DFT studies were performed. Firstly, before starting the DFT calculations, it is necessary to benchmark the many DFT functionals with some known data relating to the complexes. For example, this may be a crystal structure or some physical data, such as an equilibrium constant. In order to identify the functional to be used for the DFT study, three common DFT functionals were used to optimise the structure of the literature-published complex **Ti1** (Figure 3.9).[1] However, to save computational time, the *tert*-butyl groups were replaced with methyl groups. It was anticipated that this substitution would have little effect on the coordination geometry. Key bond lengths and bond angles from the optimised structure (Figure 3.10) were compared with the two isomers in the published crystal structure (Table 3.5). It was found that there is little difference between the functionals, in terms of bond lengths and bond angles. As a result, M06 was chosen as the DFT functional to use throughout this study, partly because of the inclusion of dispersion corrections.

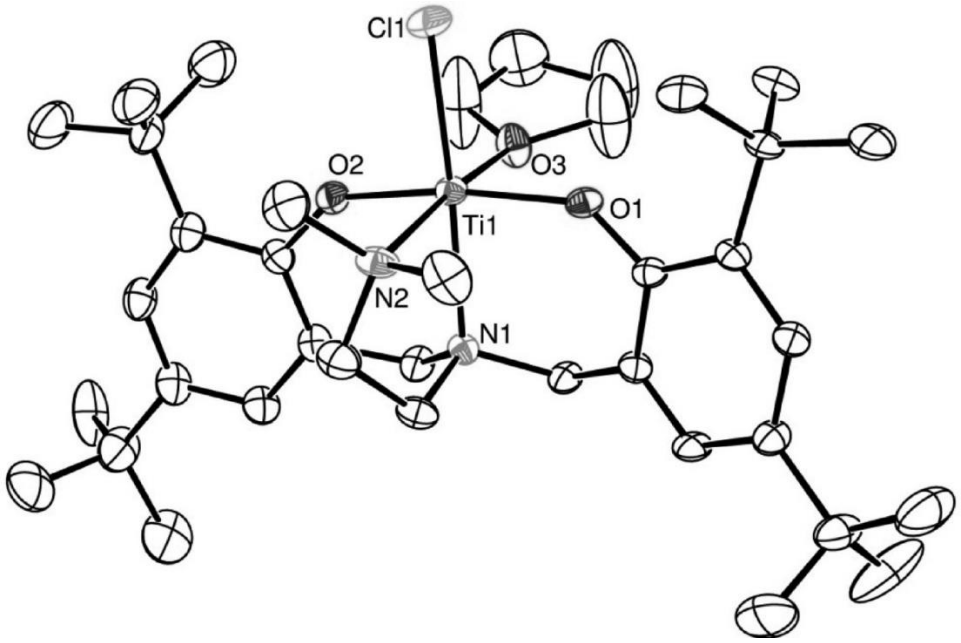

Figure 3.9 - Molecular structure of **Ti1**.[1]

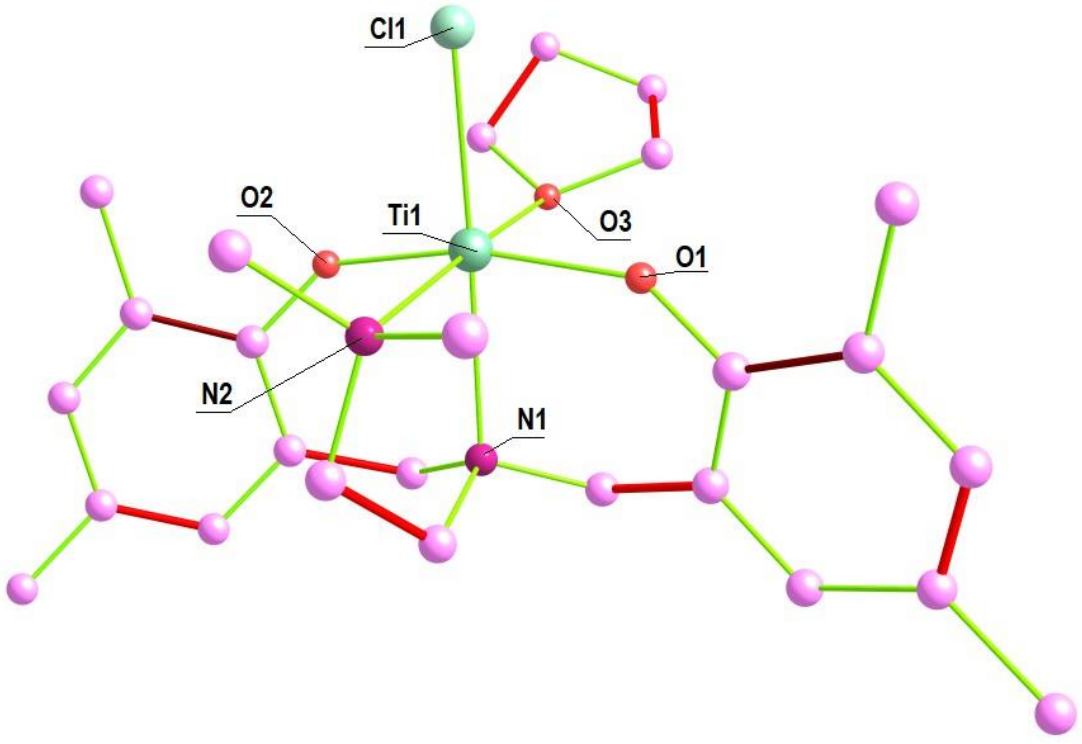

Figure 3.10 - Optimised DFT structure of **Ti2**.

Table 3.5 - Benchmarking of three functionals against the published crystal structure.

Bond/Angle	Structure 1	Structure 2	B3LYP	BP86	M06
Ti-Cl	2.41831	2.41862	2.40054	2.39643	2.37623
Ti-O1	1.90541	1.89781	1.91068	1.91708	1.90251
Ti-O2	1.90628	1.90855	1.91652	1.92144	1.91521
Ti-O(THF)	2.22565	2.22425	2.25951	2.26529	2.21958
Ti-N(pivot)	2.27749	2.27879	2.40697	2.3897	2.36881
Ti-N(arm)	2.28153	2.28388	2.33739	2.32005	2.2939
Cl-Ti-N(pivot)	173.946	173.835	173.08	173.051	173.808
O1-Ti-O2	167.546	167.453	162.884	163.762	164.258
N(arm)-Ti-O(THF)	172.251	172.33	176.281	176.528	176.441

The first system explored was the methyl-substituted **Ti2** (Scheme 3.3), due to the simplicity of the methyl group compared to the *tert*-butyl group. Calculations using the methyl group require less computational time than calculations using the *tert*-butyl group. All the energy differences are relative to the free 5-coordinate Ti(III) complex, which is always higher in energy than the 6-coordinate bound species. The binding energies between the titanium complex and THF, R_0 (primary radical of V-70) and MMA_n-R_0 (representative of the dormant OMRP species) were found to all be approximately the same. ΔG of 17.72-18.66 kcal/mol suggests a weak bond and low energy barrier to the breaking of this bond. This confirms the previously observed behaviour of complexes **Ti2** and **Ti3** in changing colour upon dissolution in toluene, because the THF molecule bound to these complexes when synthesised readily dissociates and is unable to re-associate due to the vast excess of toluene. Furthermore, it is understood that the bond strength of 18.66 kcal/mol in the Ti(IV)Cl-MMA_n-R_0 species is insufficient for OMRP to occur.

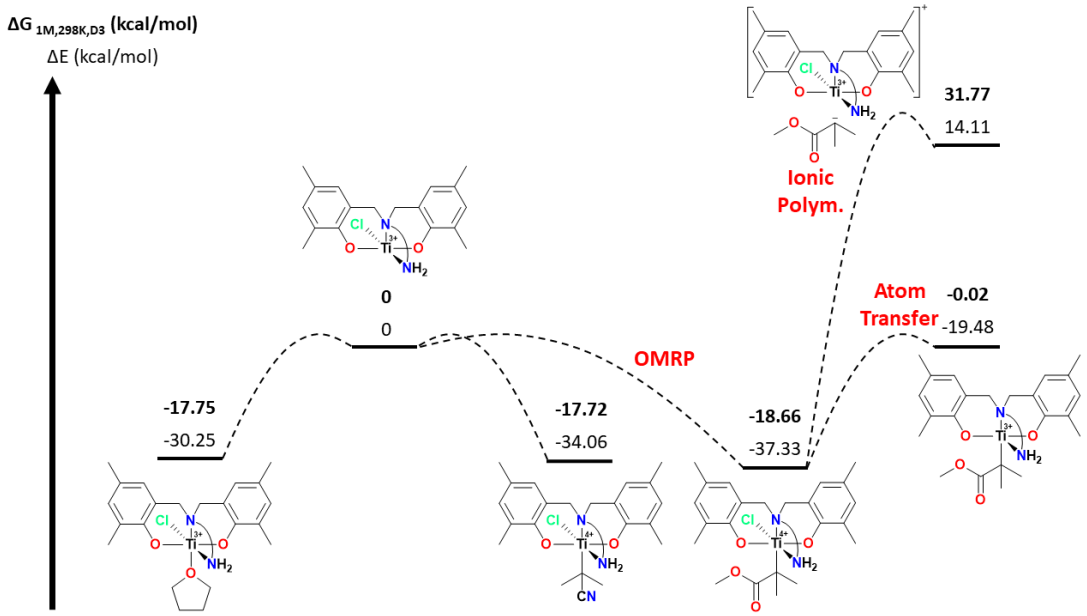

Scheme 3.3 - Energy diagram showing the relative stability of 6-coordinate titanium species, relative to the 5-coordinate complex **Ti2**.

To discount the possibility of polymerisation control *via* an ionic mechanism, the ion pair of $PMMA^-$ and Ti^+ was optimised, using the bulky ligand framework to isolate the anionic PMMA away from the titanium centre and prevent re-association. The calculated ΔG of +31.77 kcal/mol is prohibitively high for ionic polymerisation to occur, and it is therefore unlikely that the polymerisation mechanism is ionic.

To discount the possibility of polymerisation control *via* ATRP, the Ti(III)-MMA_n-R_0 species, in which the halide has transferred to an MMA radical, was optimised. One would expect this to be lower in energy than the analogous Ti(IV)Cl-MMA_n-R_0 species if ATRP was feasible as a polymerisation mechanism. This is because Ti(IV)Cl-MMA_n-R_0 corresponds with the "active" ATRP species and Ti(III)-MMA_n-R_0 corresponds with the "dormant" ATRP species. However, the opposite was found to be true, suggesting that ATRP is not occurring in the MMA polymerisation.

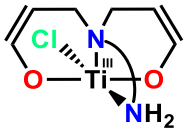

Figure 3.11 - Simplified titanium(III) complex used in the DFT studies.

In view of the significant computational time required for the calculations performed on the full methyl-substituted **Ti2** system, a greatly simplified ligand framework was used (Figure 3.11). The coordination environment around the titanium centre was the same as in the full ligand framework (N_2O_2Cl). However, much of the steric bulk on the ligand was removed. In particular, the substituted phenyl ring was simply replaced by an alkene bond. All the structures in Scheme 3.3 were re-optimised using this simplified ligand framework (Scheme 3.4). There is no change in the observed trends, and in most cases the energy differences were virtually identical, suggesting that this simplified ligand framework is a good model for the full system. The main differences, when compared with the methyl-substituted **Ti2** system, are a small increase in Ti-MMA_n-R_0 and Ti-THF bond strength and a small decrease in Ti-R_0 bond strength. However, due to the lack of steric bulk on the simplified ligand, it was not possible to calculate a value for the ion pair species. Since the energy differences are virtually identical and the observed trends are the same, this simplified ligand framework was adopted for the rest of the DFT study. However, care was taken when drawing mechanistic conclusions, recognising that this simplified ligand framework is only representative and not fully accurate. Clearly the steric and electronic effects of the full ligand framework will be different to those of the simplified ligand framework.

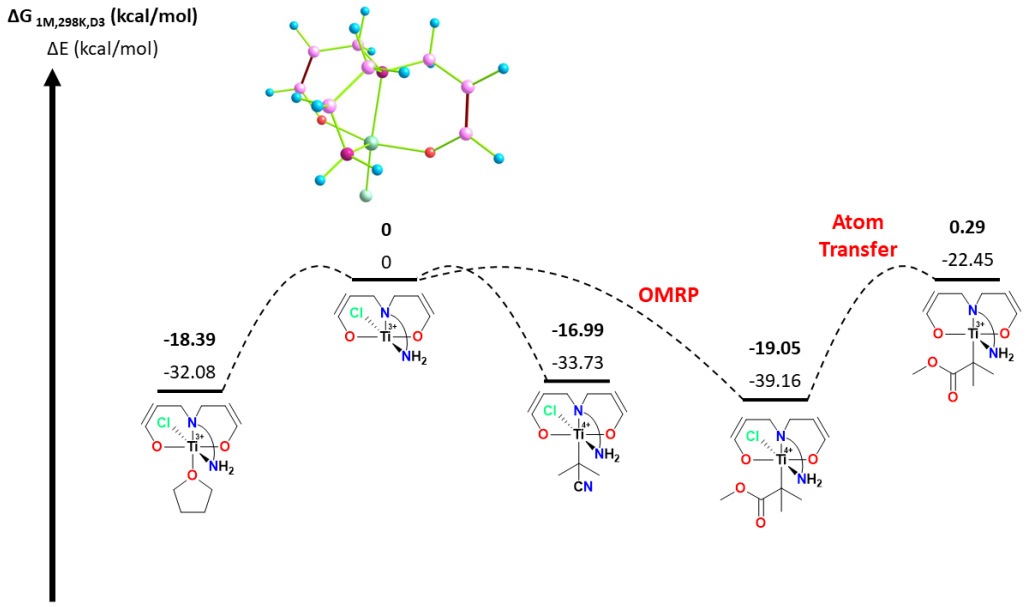

Scheme 3.4 - Energy diagram showing the relative stability of 6-coordinate titanium species, relative to the 5-coordinate complex, using a simplified ligand framework.

From the 5-coordinate Ti(III) species, MMA can interact with the metal in several ways, including olefin coordination and formation of a metal-carbon bond *via* OMRP (Scheme 3.5). In both cases reforming a 6-coordinate complex is most favourable, although OMRP results in a larger energy decrease and a more stabilised species than simple MMA olefin coordination. Furthermore, in both cases, there is an increase in energy with dissociation of the pendant donor arm on the ligand framework; a step that is required to yield a vacant coordination site for coordination polymerisation. This energy increase is significantly larger when MMA is coordinated through the olefin as opposed to *via* a metal-carbon bond. The lower energy gap in the OMRP case is due to stabilisation of the "no-arm" complex through coordination of the MMA carbonyl to the titanium, reforming a 6-coordinate species. This does not occur in the olefin coordination species.

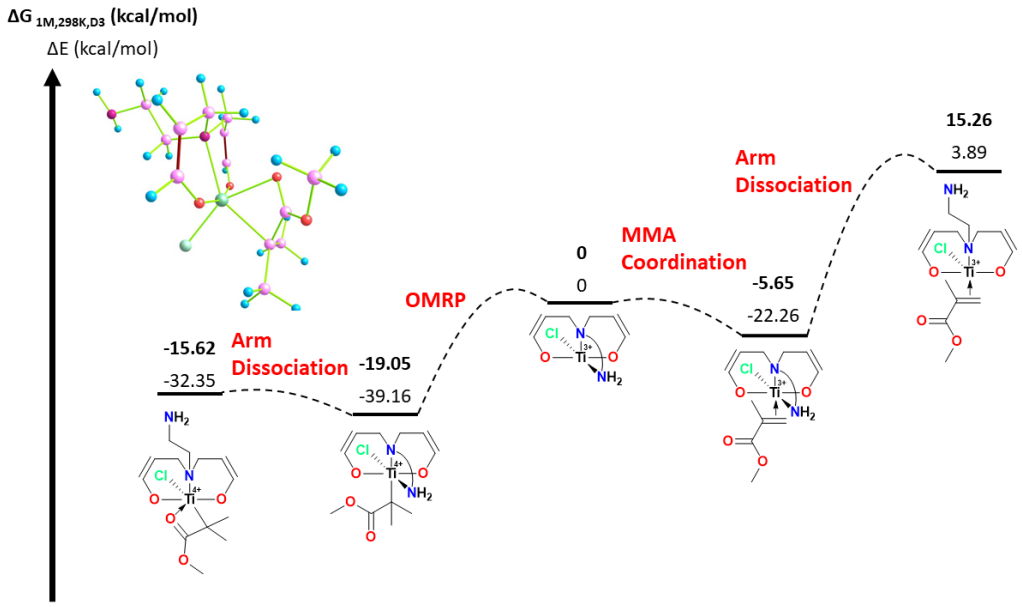

Scheme 3.5 - Energy diagram showing the binding energies of MMA to the titanium as a radical and as an olefin, with and without the pendant donor arm.

One hypothesis for the polymerisation is that the mechanism is a classical coordination-insertion polymerisation, involving a Ti(IV)-MMA_n-R_0 species and a further MMA monomer unit coordinating *via* the olefin. The pendant donor arm dissociates providing the vacant coordination site necessary for this mechanism to be feasible. However, despite many different starting geometries and optimisation attempts, it was not sterically possible to have the MMA monomer in close enough proximity to the Ti(IV)-MMA_n-R_0 species for coordination

to occur. It was therefore concluded that coordination-insertion polymerisation was sterically unfavourable, and that this was unlikely to be the polymerisation mechanism.

The 6-coordinate species Ti(IV)-MMA_n-R_0 species mentioned above, with the arm dissociated and the carbonyl coordination stabilising the complex, was explored further (Scheme 3.6). A further hypothesis is that the polymerisation mechanism is radical but in close proximity to the metal, which would influence the polymer tacticity and account for the observed isotactic bias. This mechanism may be facilitated by the aforementioned carbonyl coordination. To explore this, the same structure was re-optimised as a triplet instead of a singlet, with the intention to place an unpaired electron on both the titanium and the MMA carbon. This required an increase in ΔG of approximately 19 kcal/mol. Spin density was indeed observed on both the titanium and the MMA carbon. This complex can be stabilised by re-coordination of the pendant donor arm, reforming a 6-coordinate complex.

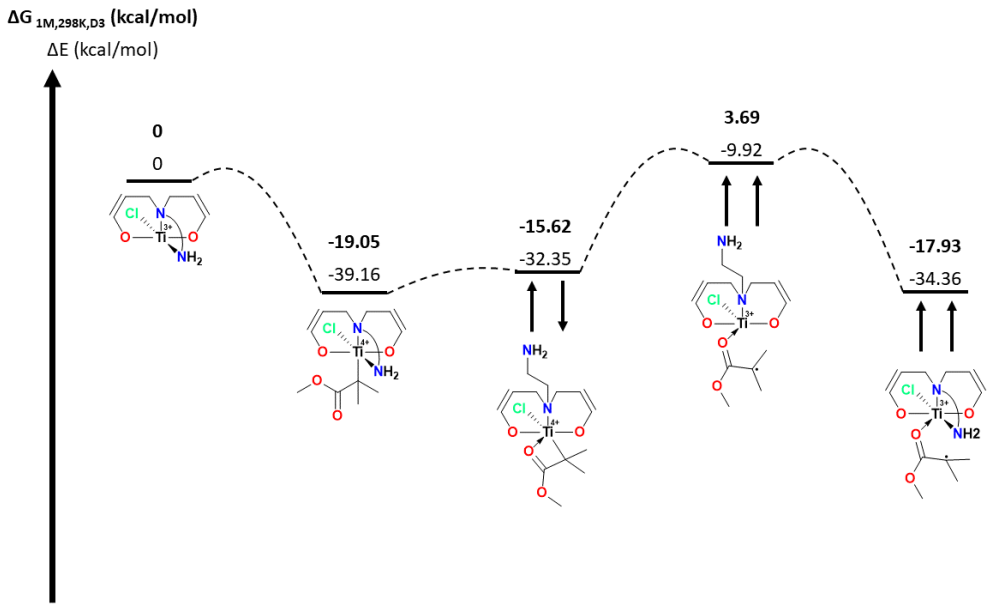

Scheme 3.6 - Energy diagram showing the energy difference between the singlet and triplet species.

To verify the validity of this conclusion, the triplet complexes were re-optimised as broken symmetry singlets - an overall singlet but specifying local spin density (Scheme 3.7). However, upon optimisation, the local spin density was not retained, and instead the structures were optimised to singlet complexes *i.e.* Ti(IV)-enolates. These TI(IV)-enolates are significantly lower in energy than the analogous triplet species and are, by far, the most stable species

identified thus far. Therefore, it is very likely that these Ti(IV)-enolate species play a key role in the polymerisation mechanism.

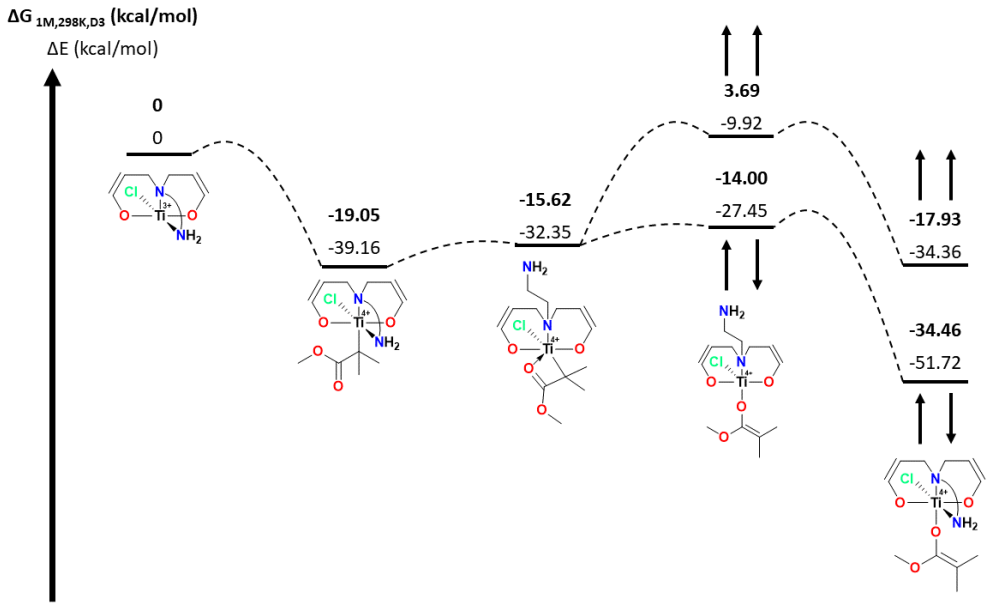

Scheme 3.7 - Energy diagram showing the stability of the Ti(IV)-enolate complexes.

3.5 Polymerisation Kinetics

To elucidate the polymerisation mechanism, it is important to conduct further kinetic studies to understand how different parameters have an impact on the polymerisation.

Table 3.6 and Figure 3.12 explore the difference in kinetics between free-radical and **Ti1**-mediated MMA polymerisation. It is typical for a controlled radical polymerisation to be slower than a free-radical polymerisation, because the equilibrium between dormant and active species lies heavily towards the dormant species. Therefore, for most of the time, the polymer chains are not propagating and so the polymerisation rate is lower. However, using **Ti1** as a mediator (blue plot in Figure 3.12) results in a faster polymerisation than without (orange plot in Figure 3.12). This is strong experimental evidence that the polymerisation mechanism is not radical, and that **Ti1** both controls and catalyses the polymerisation. This catalytic behaviour is uncharacteristic of a controlled radical polymerisation.

Table 3.6 - MMA kinetics, with and without complex **Ti1**, using different concentrations of initiator.

#	[MMA]:[Ti1]:[V-70]	Time (min)	Conv. (%)	$M_{n,th}$ (Da)	M_n (Da)	Đ
3.34	100:1:1	10	33	3300	14300	1.10
3.35	100:1:1	20	62	6200	25600	1.11
3.36	100:1:1	30	77	7700	31700	1.14
3.37	100:1:1	40	84	8400	34200	1.13
3.38	100:1:0.2	3	27	6800	21000	1.22
3.39	100:1:0.2	8	68	17000	50600	1.28
3.40	100:1:0.2	10	75	18800	58100	1.31
3.41	100:0:1	10	34	-	19200	1.56
3.42	100:0:1	20	48	-	17900	1.49
3.43	100:0:1	40	56	-	18200	1.77
3.44	100:0:0.2	10	23	-	24400	1.85
3.45	100:0:0.2	20	29	-	29300	2.08
3.46	100:0:0.2	40	35	-	30100	2.65

Conditions: [MMA]:[**Ti1**]:[V-70] = 100:x:y, MMA:toluene = 1:1 (v/v), 80 °C. Conversion determined by ^{1}H NMR spectroscopy. $M_{n,th}$ = $[MMA]_0/[\mathbf{Ti1}]_0$ × M(MMA) × conversion.

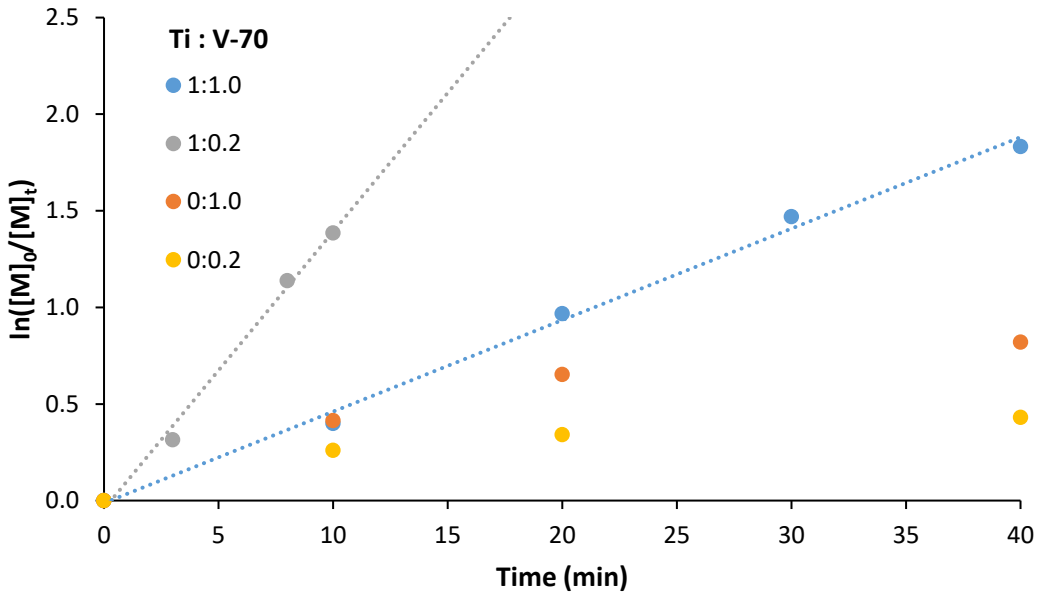

Figure 3.12 - MMA kinetics at 80°C, with and without complex **Ti1**, using different concentrations of initiator. [MMA]:[**Ti1**]:[V-70] = 100:x:y, MMA:toluene = 1:1 (v/v).

Furthermore, in a typical free-radical polymerisation it is expected that the polymerisation rate increases with increased initiator concentration. This is because the rate of propagation

is proportional to the concentration of propagating radicals. Increasing the concentration of initiator increases the concentration of radicals entering the system, and thus increases the concentration of propagating radicals. This is illustrated in Figure 3.12, in which the MMA polymerisation with 1.0 equivalents of V-70 (orange plot) is faster than the polymerisation with 0.2 equivalents of V-70 (yellow plot). In both cases the polymerisation rate is greatest at the start, before slowing over the course of the polymerisation. This behaviour is typical of a free-radical and uncontrolled polymerisation.

However, and unusually, the opposite trend to this is observed when the MMA polymerisation is mediated by **Ti1**. Here, the polymerisation rate decreased as the initiator concentration increased from 0.2 equivalents of V-70 (grey plot in Figure 3.12) to 1.0 equivalents of V-70 (blue plot in Figure 3.12). To understand this unusual behaviour, kinetics were performed using complex **Ti1** as the mediator in the polymerisation of MMA at a range of different initial concentrations of initiator (Table 3.7 and Figure 3.13). The lowest concentration of initiator used was 0.2 equivalents of V-70, which produces 0.4 equivalents of radical, and therefore the titanium is in excess. At the other end of the scale, the highest concentration of initiator used was 4 equivalents of V-70, and therefore the initiator was in excess.

It can clearly be seen in Figure 3.13 that as the concentration of initiator increases, the polymerisation rate decreases. The rate of polymerisation varies significantly, from 0.1436 min^{-1} at 0.2 equivalents of V-70 to 0.0094 min^{-1} and 0.0015 min^{-1} at 2 and 4 equivalents of V-70 respectively. Molecular weights decreased (closer to theoretical values) with increased initiator concentration. This trend is typical for a controlled radical polymerisation. However, this trend is only valid until approximately 1.5 equivalents of V-70. After this point, increasing the concentration of initiator further has no effect on the molecular weight. There is therefore an optimal concentration of initiator, which gives both fast polymerisations and molecular weights as close to theoretical values as possible. This was determined to be 1.0 equivalents of V-70.

Attempts to produce reliable kinetics with 0.1 equivalents of V-70 were unsuccessful, primarily due to the very short polymerisation time and the variability in the results that consequently arise.

Table 3.7 - MMA kinetics, with complex **Ti1**, using different concentrations of initiator.

#	Equiv. V-70	Time (min)	Conv. (%)	$M_{n,th}$ (Da)	M_n (Da)	Đ	Rate (min^{-1})
3.47	0.2	3	27	6800	21000	1.22	
3.48	0.2	8	68	17000	50600	1.28	0.1436
3.49	0.2	10	75	18800	58100	1.31	
3.50	0.5	5	26	2600	13500	1.20	
3.51	0.5	7	46	4600	23900	1.14	
3.52	0.5	10	60	6000	30800	1.13	0.0884
3.53	0.5	15	74	7400	40100	1.11	
3.54	0.5	20	83	8300	43700	1.14	
3.55	0.5	24	87	8700	44600	1.20	
3.56	1.0	10	27	2700	11400	1.11	
3.57	1.0	20	48	4800	19400	1.10	
3.58	1.0	30	70	7000	28400	1.13	0.0365
3.59	1.0	40	78	7800	33500	1.11	
3.60	1.0	60	88	8800	37800	1.13	
3.61	1.5	20	35	3500	11200	1.10	
3.62	1.5	40	57	5700	19300	1.10	0.0206
3.63	1.5	60	73	7300	25200	1.09	
3.64	1.5	90	84	8400	28400	1.17	
3.65	2.0	20	16	1600	5900	1.12	
3.66	2.0	40	32	3200	10600	1.10	
3.67	2.0	60	43	4300	14400	1.11	
3.68	2.0	90	58	5800	19400	1.12	0.0094
3.69	2.0	120	68	6800	23800	1.12	
3.70	2.0	180	83	8300	30300	1.14	
3.71	2.0	240	89	8900	32200	1.16	
3.72	4.0	420	47	4700	15500	1.20	0.0015

Conditions: [MMA]:[**Ti1**]:[V-70] = 100:1.00:x, MMA:toluene = 1:1 (v/v), 80 °C. Conversion determined by ^{1}H NMR spectroscopy. $M_{n,th} = [MMA]_0/[\mathbf{Ti1}]_0 \times M(MMA) \times$ conversion.

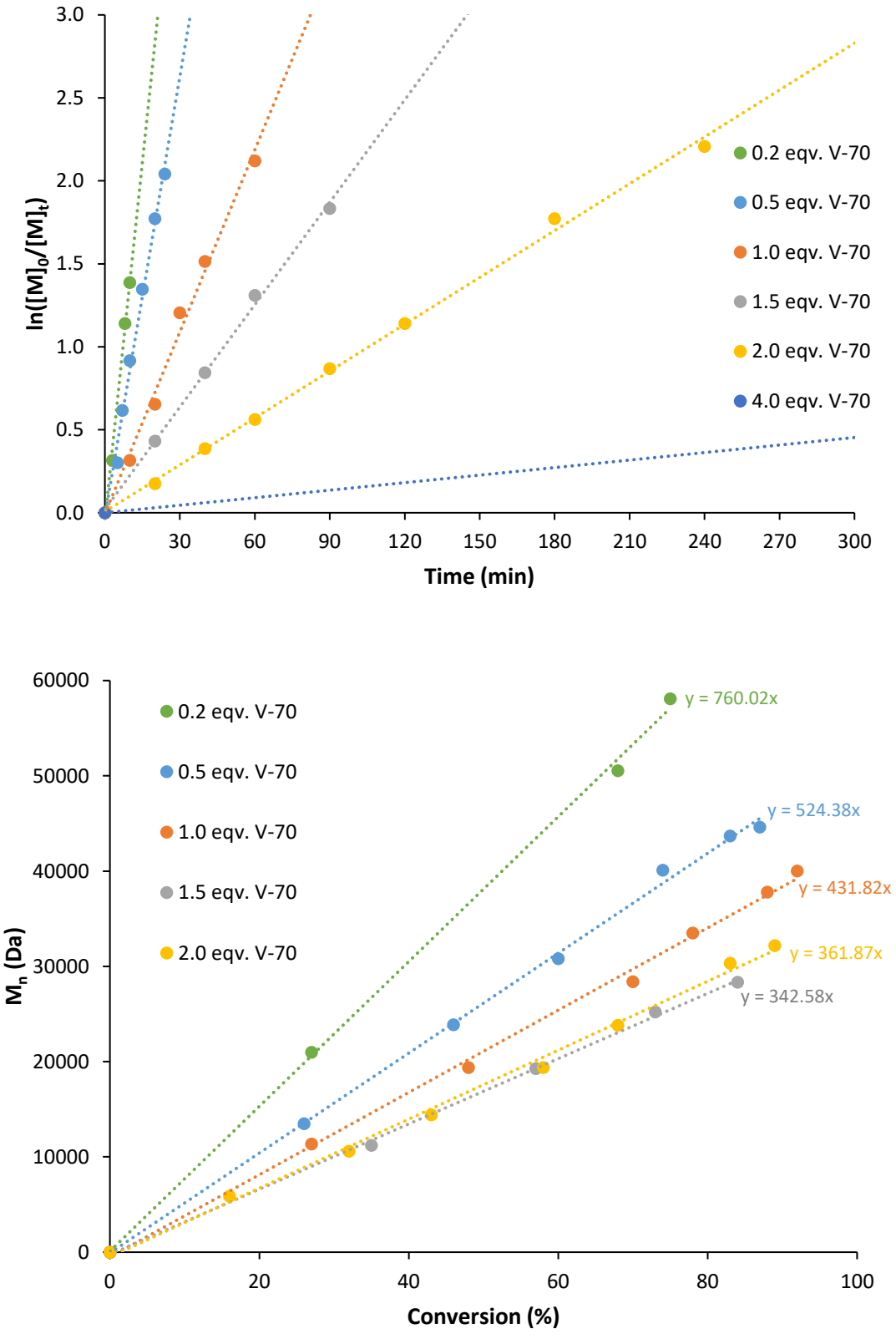

Figure 3.13 - MMA kinetics at 80 °C, with complex **Ti1**, using different concentrations of initiator. [MMA]:[**Ti1**]:[V-70] = 100:1.00:x, MMA:toluene = 1:1 (v/v).

In addition, kinetics were performed using complex **Ti1** as the mediator in the polymerisation of MMA at a range of different initial concentrations of complex **Ti1** (Table 3.8 and Figure 3.14). In particular, 0.2, 0.5 and 1.0 equivalents of **Ti1** were used in the polymerisation. As the concentration of titanium decreased, the rate of polymerisation decreased. This behaviour is typical of a controlled polymerisation, as fewer metal complexes present in the polymerisation permits fewer growing chains, and therefore a decrease in polymerisation rate.

Dispersities remained broadly constant and below 1.25, which represents excellent control over the polymerisation. However, dispersities increased slightly at low titanium concentration. Furthermore, in all cases, molecular weights were approximately 3-4 times greater than theoretical values.

Table 3.8 - MMA kinetics using different concentrations of complex **Ti1**.

#	Equivalents Ti1	Time (min)	Conv. (%)	$M_{n,th}$ (Da)	M_n (Da)	Đ
3.73	1.0	10	33	3300	14300	1.10
3.74	1.0	20	62	6200	25600	1.11
3.75	1.0	30	77	7700	31700	1.14
3.76	1.0	40	84	8400	34200	1.13
3.77	0.5	10	28	5600	17700	1.17
3.78	0.5	20	57	11400	36900	1.13
3.79	0.5	30	69	13800	44700	1.19
3.80	0.5	40	79	15800	56500	1.20
3.81	0.2	20	32	16000	50900	1.23
3.82	0.2	30	43	21500	69500	1.23
3.83	0.2	40	48	24000	70400	1.19

Conditions: [MMA]:[**Ti1**] = 100:x, [**Ti1**]:[V-70] = 1.0:1.0, MMA:toluene = 1:1 (v/v). 80 °C. Conversion determined by ^{1}H NMR spectroscopy. $M_{n,th} = [MMA]_0/[\mathbf{Ti1}]_0 \times M(MMA) \times$ conversion.

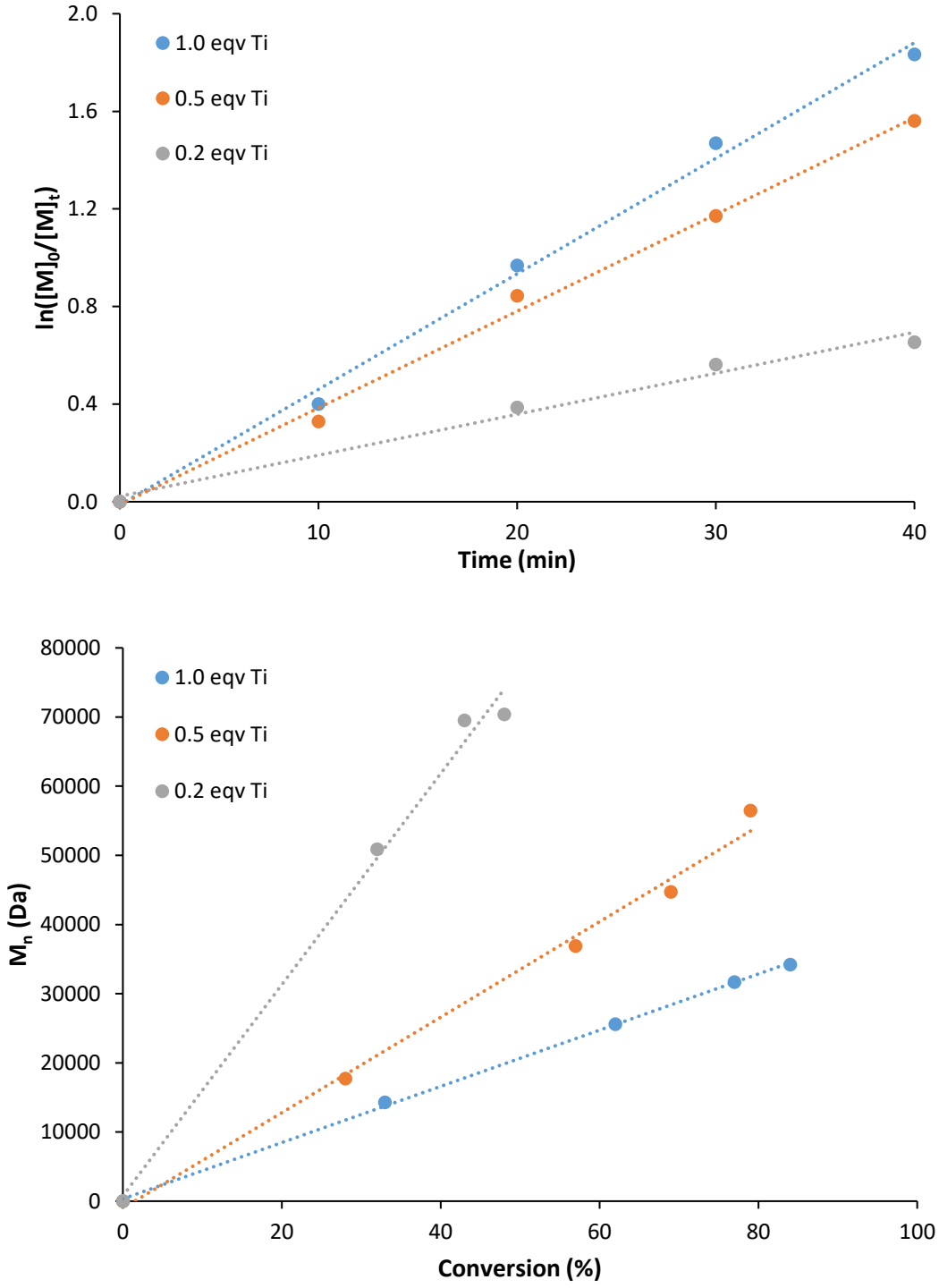

Figure 3.14 - MMA kinetics using different concentrations of complex **Ti1**. [MMA]:[**Ti1**] = 100:x, [**Ti1**]:[V-70] = 1.0:1.0, MMA:toluene = 1:1 (v/v).

Kinetics were performed using complex **Ti1** and **Ti4** as mediators in the polymerisation of MMA to investigate the effect of the pendant donor arm (Table 3.9 and Figure 3.15). In **Ti1** the donor on the pendant arm is a dimethylamino group (NMe_2), whereas in **Ti4** the donor is

a tethered THF. It is clear to see from Figure 3.15 that the rate of MMA polymerisation is greater when using **Ti4** instead of **Ti1**. Furthermore, molecular weights are lower and closer to theoretical values when using **Ti4** instead of **Ti1**.

This rate difference is most likely to be due to the strength of the donor arm. The THF in **Ti4** is a stronger donor than the dimethylamino in **Ti1**. This results in a stronger stabilisation of the titanium centre and, consequently, a more stabilised dormant titanium species. The fact that the dormant species is more stable in **Ti4** than **Ti1** means that more polymer chains are captured and reversibly terminated by the titanium complex, and therefore more polymer chains are undergoing controlled propagation. Therefore, the polymerisation is faster and the molecular weights are lower.

The polymer synthesised using complex **Ti4** has a slightly more isotactic bias than the polymer synthesised using complex **Ti1**, possibly due to the increased steric bulk of the THF in **Ti4** compared to the dimethylamino group of **Ti1**. However, the dispersity of the polymer is slightly broader using **Ti4** instead of **Ti1**.

Table 3.9 - MMA kinetics with complex **Ti1** and **Ti4**.

#	Complex	Time (min)	Conv. (%)	$M_{n,th}$ (Da)	M_n (Da)	Đ	mm:rm:rr
3.84	Ti1	10	27	2700	11400	1.11	-
3.85	Ti1	20	48	4800	19400	1.10	15:47:38
3.86	Ti1	30	70	7000	28400	1.13	-
3.87	Ti1	40	78	7800	33500	1.11	-
3.88	Ti1	60	88	8800	37800	1.13	-
3.89	Ti4	5	37	3700	11700	1.27	18:48:34
3.90	Ti4	10	57	5700	15800	1.26	-
3.91	Ti4	20	76	7600	19700	1.26	18:47:35

Conditions: [MMA]:[Ti(III)]:[V-70] = 100:1.0:1.0, MMA:toluene = 1:1 (v/v), 80 °C. Conversion determined by ^{1}H NMR spectroscopy. $M_{n,th} = [MMA]_0/[Ti(III)]_0 \times M(MMA) \times$ conversion.

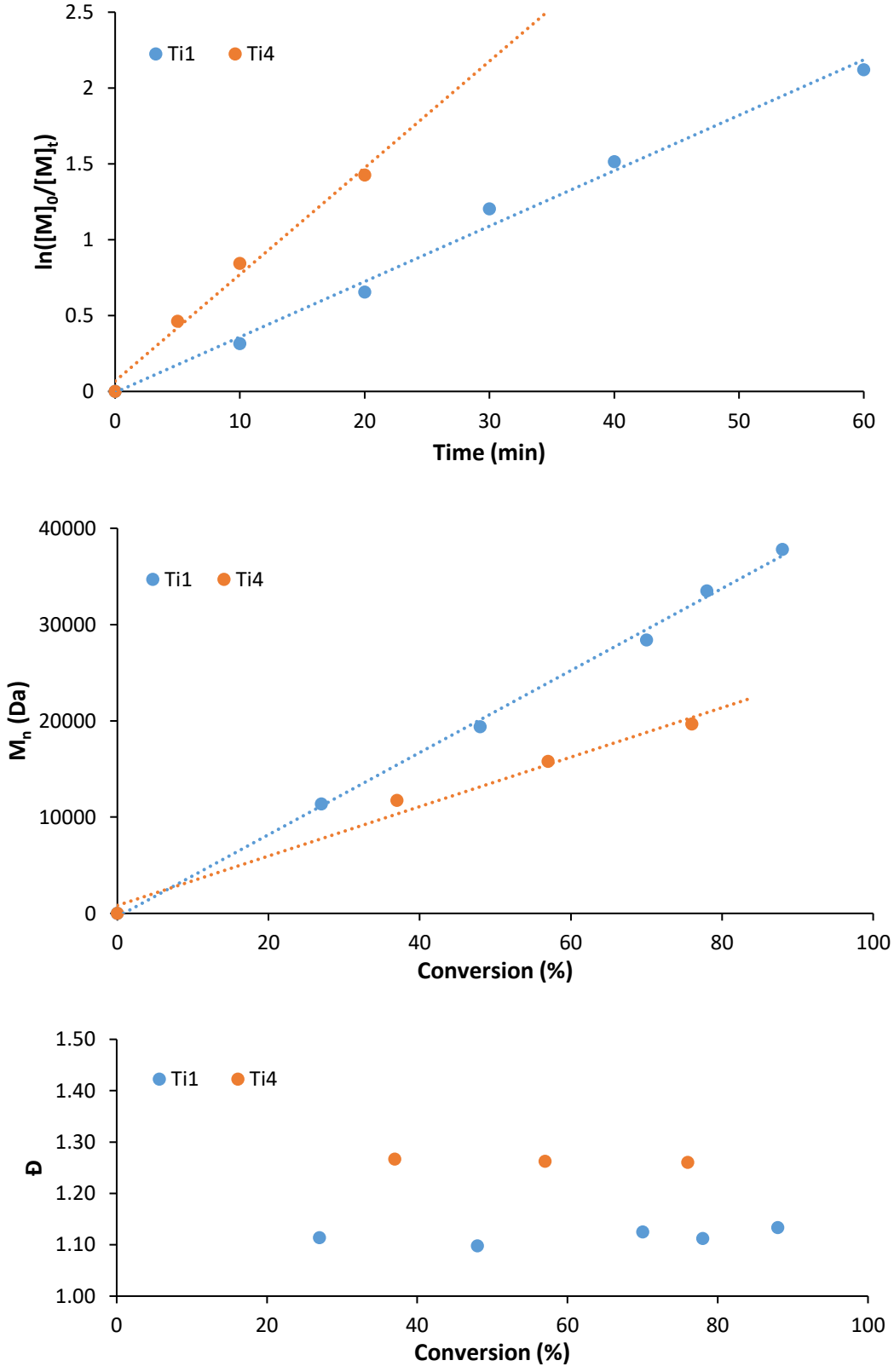

Figure 3.15 - MMA kinetics at 80 °C with complex **Ti1** and **Ti4**. [MMA]:[Ti(III)]:[V-70] = 100:1.0:1.0, MMA:toluene = 1:1 (v/v).

It has already been demonstrated how complexes **Ti1**-**Ti4** are effective mediators of the polymerisation of MMA. Complexes **Ti1** and **Ti2** were also used as mediators in the polymerisation of other (meth)acrylates (Table 3.10). The attempted polymerisation of methyl acrylate (MA, polymerisation **3.92**) with **Ti1** was poorly-controlled, yielding poly(methyl acrylate) with a broad dispersity. No polymer was produced during the attempted polymerisation of *tert*-butyl methacrylate (^{t}BuMA) using either **Ti1** (polymerisation **3.93**) or **Ti2** (polymerisation **3.94**). This is perhaps a little surprising, given the relatively small steric difference between MMA and ^{t}BuMA compared to the large bulky ligand framework of **Ti1** and **Ti2**. It is presumed that the necessity for an additional two *tert*-butyl-containing molecules to interact with the metal centre is too energetically unfavourable for polymerisation.

The polymerisation of *n*-butyl methacrylate (^{n}BuMA) gave interesting results and was highly dependent on the ligand framework of the metal. Use of **Ti1** as mediator led to a well-controlled polymerisation with a narrow dispersity (Đ = 1.14). However, use of **Ti2** as mediator led to a poorly-controlled polymerisation with a much broader dispersity (Đ = 2.12). In both cases molecular weights were considerably higher than theoretical values, and high conversions were achieved, with the polymerisation using **Ti2** reaching full conversion in 2.5 hours.

Interestingly, it was also found that performing the polymerisation of MMA using complex **Ti1** in the absence of any additional solvent (polymerisation **3.97**) gave an extremely well-controlled polymerisation, with the resultant PMMA having a very narrow dispersity of 1.09.

Table 3.10 - Additional polymerisation screening.

#	Complex	Monomer	Conv. (%)	$M_{n,th}$ (Da)	M_n (Da)	Đ
3.92	Ti1	MA	81	7000	23800	2.68
3.93	Ti1	^{t}BuMA	<1	-	-	-
3.94	Ti2	^{t}BuMA	<1	-	-	-
3.95	Ti1	^{n}BuMA	81	11500	58500	1.14
3.96	Ti2	^{n}BuMA	>99	14200	45000	2.12
3.97[a]	Ti1	MMA	80	8000	30000	1.09

Conditions: [Monomer]:[Ti(III)]:[V-70] = 100:1.0:1.0, monomer:toluene = 1:1 (v/v). 80 °C. 2.5 hours. [a]No added solvent. Conversion determined by ^{1}H NMR spectroscopy. $M_{n,th}$ = $[monomer]_0/[Ti(III)]_0$ × M(monomer) × conversion.

Table 3.11 - ^{n}BuMA kinetics with complex **Ti1**.

#	Time (min)	Conv. (%)	$M_{n,th}$ (Da)	M_n (Da)	Đ
3.98	30	32	4600	18600	1.13
3.99	60	57	8100	31800	1.18
3.100	120	77	10900	43300	1.27
3.101	150	82	11700	48000	1.27

Conditions: [^{n}BuMA]:[**Ti1**]:[V-70] = 100:1.0:1.0, ^{n}BuMA:toluene = 1:1 (v/v). 80 °C. Conversion determined by ^{1}H NMR spectroscopy. $M_{n,th}$ = [^{n}BuMA]$_0$/[**Ti1**]$_0$ × M(^{n}BuMA) × conversion.

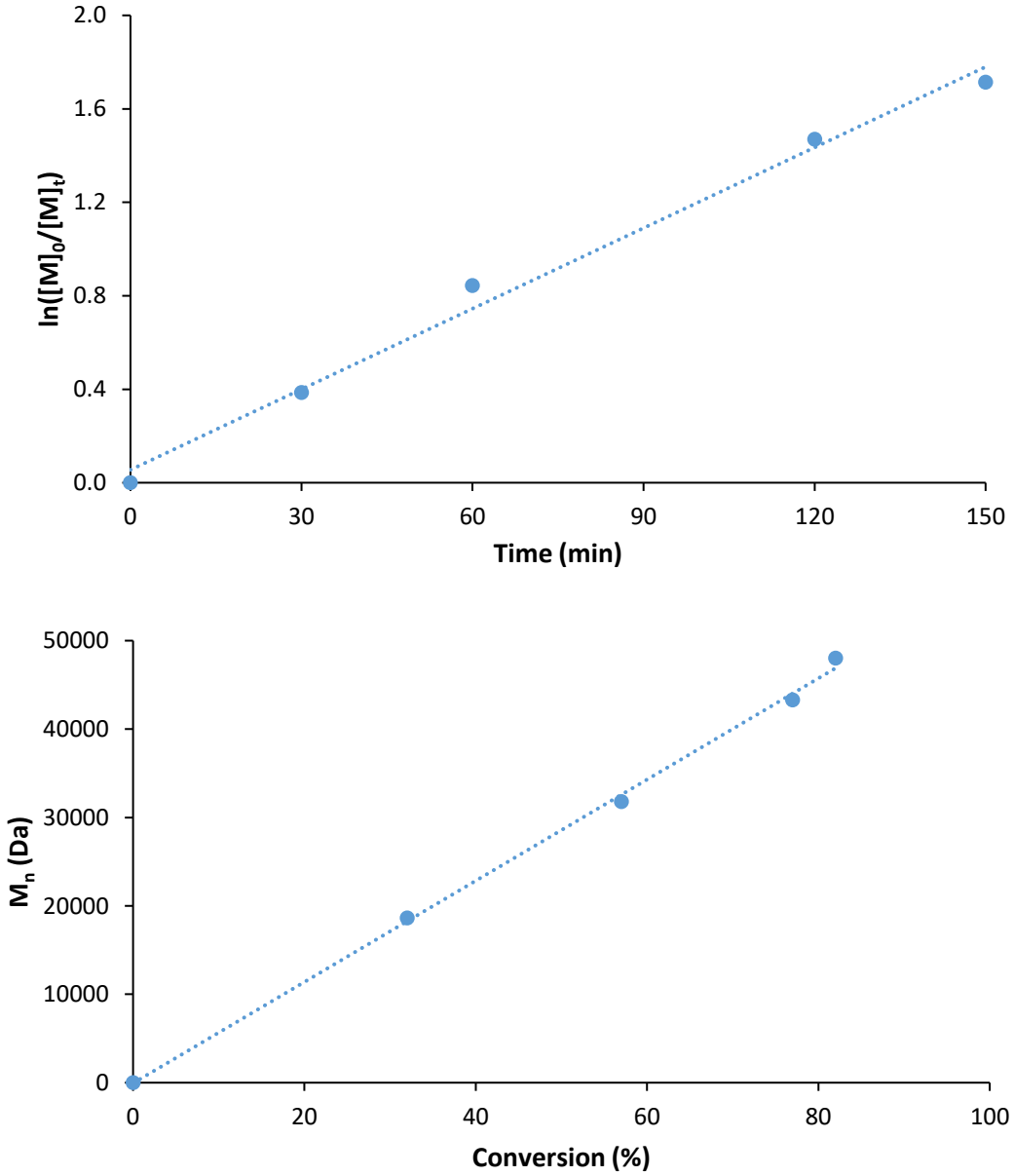

Figure 3.16 - ^{n}BuMA kinetics at 80 °C with complex **Ti1**. [^{n}BuMA]:[**Ti1**]:[V-70] = 100:1.0:1.0, ^{n}BuMA:toluene = 1:1 (v/v).

To demonstrate the "livingness" of the ^{n}BuMA polymerisation, kinetics were performed using complex **Ti1** as the mediator (Table 3.11 and Figure 3.16). The polymerisation is well-controlled with linear first-order kinetics, with conversions reaching at least 80%. In addition, molecular weights increased linearly with conversion. However, and as with MMA, molecular weights are approximately 4 times greater than theoretical values. Dispersities increased very slightly over the course of the polymerisation, perhaps suggesting the late onset of termination reactions.

3.6 DFT Study - Group Transfer Polymerisation

As discussed in chapter 3.4, radical, ionic and classical coordination-insertion mechanisms have all been discounted as the possible polymerisation mechanism. Furthermore, the initial DFT studies suggested that Ti(IV)-enolates play a key role in the polymerisation mechanism.

From analysis of the kinetic and computational data, a further hypothesis for the polymerisation mechanism was developed. It is proposed that the mechanism is bimetallic and involves both a titanium(IV) and titanium(III) species. This mechanism has previously been termed group transfer polymerisation (GTP), and it is understood that this mechanism has not previously been observed with titanium.

Group transfer polymerisation was first discovered in 1983, through a desire for controlled "living" polymerisations of acrylates and methacrylates. Webster and co-workers used dimethylketene methyl trimethylsilyl acetal as the initiator of the polymerisation of MMA.[30] The mechanism was termed GTP since the trimethylsilyl group is transferred from the initiator to the incoming monomer. A nucleophilic catalyst is required for the polymerisation to proceed, and bifluorides were found to be effective (Scheme 3.8). The polymerisation was conducted at room temperature and was found to be living, yielding narrow dispersity PMMA. Detailed reviews by Webster have been published which discuss the extensive research and subsequent commercialisation successes of GTP since its discovery.[31,32]

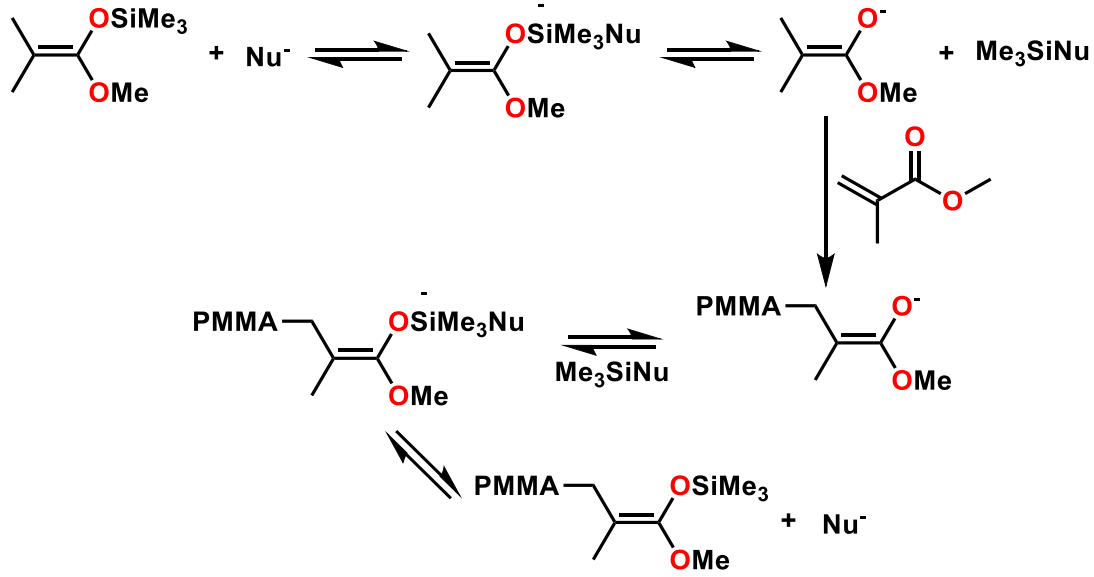

Scheme 3.8 - Group transfer polymerisation mechanism.[32]

Following the seminal work on GTP, various parameters of the polymerisation were explored. Work published in 1984 by Webster and co-workers looked at the use of zinc halides and dialkylaluminium halides and oxides as Lewis acid catalysts for GTP.[33] They were found to be effective catalysts for the polymerisation of acrylates and methacrylates, with initiation by the ketene silyl acetal. More detailed work published in 1987 looked at the polymerisation of several acrylic monomers, such as *n*-butyl methacrylate and allyl methacrylate, with a variety of initiators and catalysts.[34] In particular, tris(dimethylamino)-sulfonium ($TASHF_2$) was identified as an effective catalyst of GTP. In later work, Dicker, Sogah and co-workers used oxyanions as catalysts for the GTP of acrylic monomers.[35] Active catalysts were found to be aliphatic and aromatic carboxylates, phenolates, sulfinates, phosphinates, sulfonamidates, perfluoroalkoxides, nitrite and cyanate.

It is proposed here that during the initiation phase of the titanium-mediated polymerisation, a titanium(IV) enolate species is formed, most likely after a few radical monomer additions. This initial process would account for the imperfect PMMA dispersity. The polymerisation then proceeds *via* a reaction between this Ti(IV)-enolate species and a Ti(III)-MMA adduct, with the MMA coordinating *via* the carbonyl (Scheme 3.9). Once in close proximity, the polymer chain and the monomer unit undergo a one-electron Michael-type addition, with the Ti(IV) metal centre becoming Ti(III) and *vice versa*. The carbonyl bound to the new Ti(III)

metal centre then dissociates, allowing the subsequent coordination of a new monomer unit, and completion of the catalytic cycle.

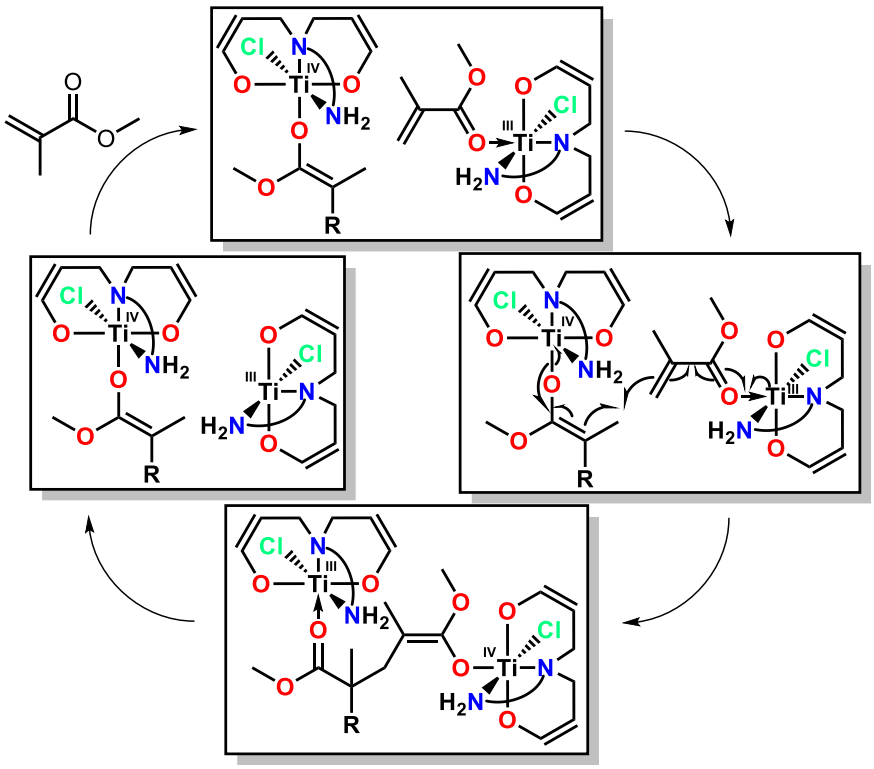

Scheme 3.9 - Proposed bimetallic group transfer polymerisation mechanism. R = MMA_{n-1}-R_0.

Further DFT studies (Scheme 3.10) show that this starting Ti(IV)-enolate is considerably more energetically favourable (ΔG = -34.46 kcal/mol) than the other previously-discussed 6-coordinate titanium(IV) species, such as Ti-R_0 (R_0 = primary radical of V-70) and Ti-MMA_n-R_0 (with a Ti-C bond) adducts. This suggests that the proposed mechanism is energetically preferred to an OMRP mechanism. Scheme 3.10 also shows that it is energetically favourable to form the Ti(III)-MMA adduct (ΔG = -16.48 kcal/mol), where the MMA monomer binds to the titanium *via* the carbonyl group.

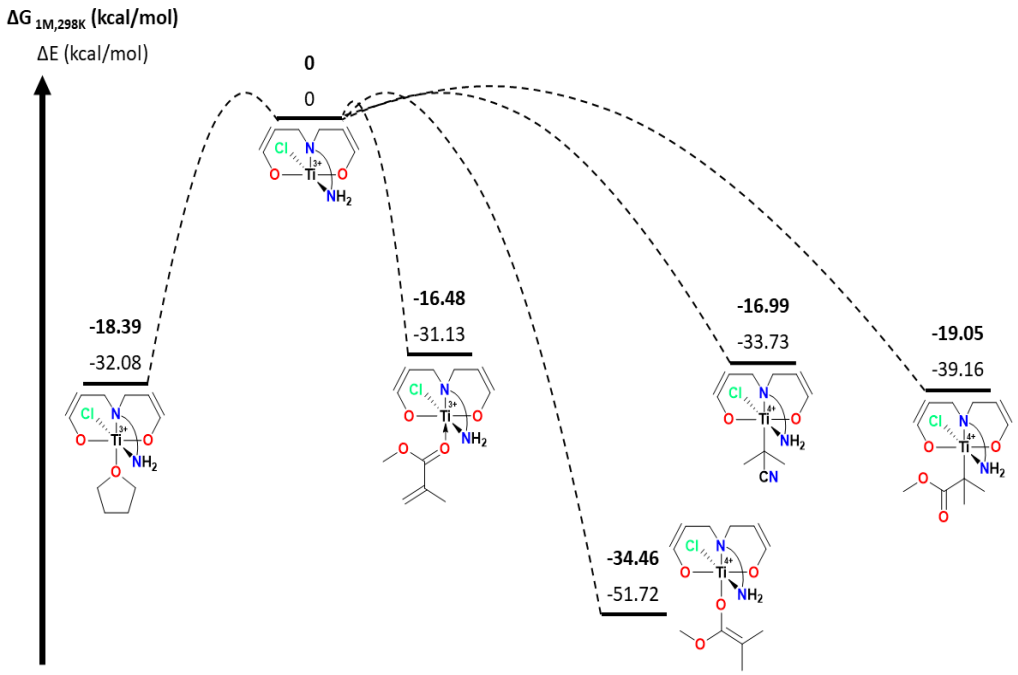

Scheme 3.10 - Energy diagram showing the relative stability of the Ti(IV)-enolate species compared to other 6-coordinate titanium species.

Additional DFT calculations were performed to understand this proposed bimetallic mechanism in greater detail, and to determine whether the mechanism is theoretically feasible (Scheme 3.11). After formation of the Ti(IV)-enolate and the Ti(III)-MMA adduct, there is a very small energy barrier to overcome (ΔG = +6.21 kcal/mol) to bring the two species into close proximity. Following this, there is an accessible transition state ($\Delta G^{\ddagger}$ = +21.86 kcal/mol) for the chain propagation step. The overall reaction (*i.e.* the addition of a monomer unit to the polymer chain) has a ΔG of -5.19 kcal/mol, which is as expected for a typical polymerisation.

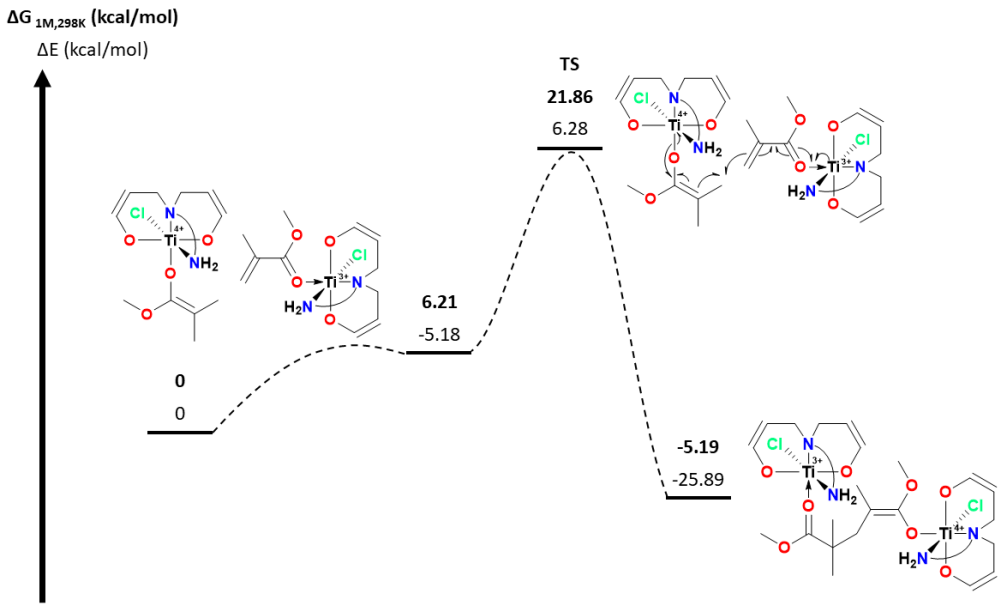

Scheme 3.11 - Energy diagram showing the proposed bimetallic group transfer polymerisation mechanism.

DFT additionally supports the presence of a monometallic GTP mechanism, also starting from a Ti(IV)-enolate (Scheme 3.12). The necessary vacant coordination site for monomer activation arises from dissociation of the pendant amine donor arm on the ligand framework. There is a ΔG of +20.46 kcal/mol to overcome to achieve the arm dissociation. The species is then stabilised by the arrival and activation of MMA monomer, as a 6-coordinate complex is reformed. Following this, the one-electron Michael-type addition of monomer to the polymer chain is then able to occur on a single metal centre. The chain propagation transition state was found to have a $\Delta G^{\ddagger}$ of +24.61 kcal/mol. Finally, after the monomer addition step, the pendant donor arm re-associates with the titanium centre to reform the 6-coordinate complex, and thus complete the catalytic cycle.

It is important to note that the chain propagation transition state of this monometallic pathway yields a $\Delta G^{\ddagger}$ of +24.61 kcal/mol, which is significantly higher than for the bimetallic pathway (+21.86 kcal/mol). This suggests that the bimetallic mechanism is preferred to the monometallic mechanism.

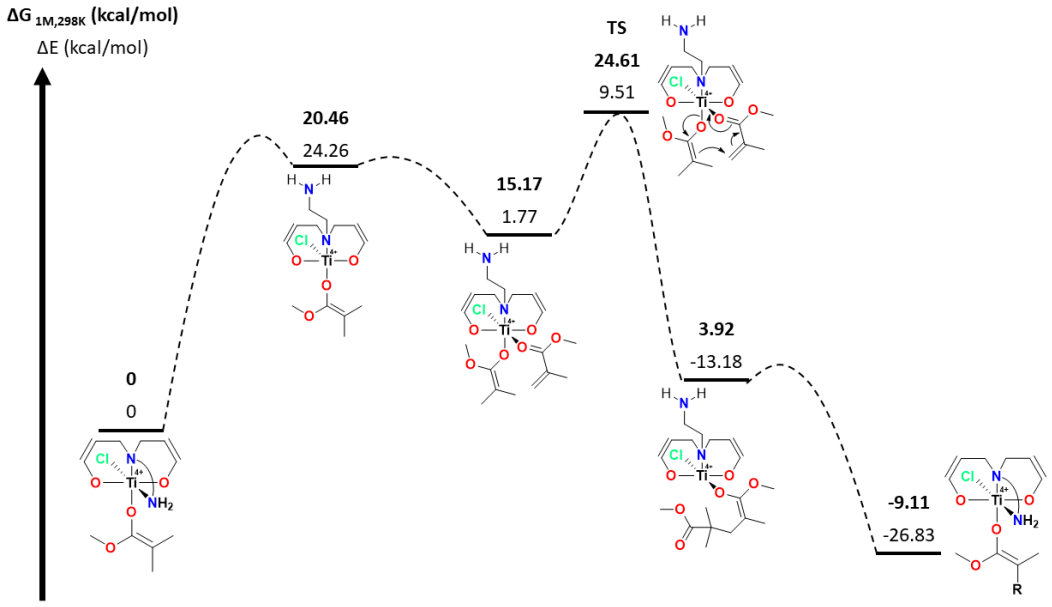

Scheme 3.12 - Energy diagram showing the proposed monometallic group transfer polymerisation mechanism with the simplified ligand framework.

The majority of the DFT calculations in this chapter have been performed on the simplified ligand framework, in order to considerably save computational time. However, it is important to also check the feasibility of the group transfer mechanism on the full ligand framework and compare the energy values to those of the simplified ligand framework.

Rather than recalculate the energy values of each of the species in Scheme 3.12, only the two most important species were calculated; that is, the transition state corresponding to the arm dissociation and the transition state corresponding to the polymerisation step. It is the energy values of these two transition states which determine whether or not the mechanism is feasible. The energy values of these two species were calculated for the methyl-substituted **Ti2** system (Scheme 3.13) and the *tert*-butyl-substituted **Ti1** system (Scheme 3.14). Unfortunately, despite numerous attempts it was not possible to calculate the energy value of the transition state for the polymerisation step with the *tert*-butyl-substituted system. This is most likely to be due to the large number of atoms in the species and consequently the considerable difficulty in the calculation converging to a solution and an optimised structure.

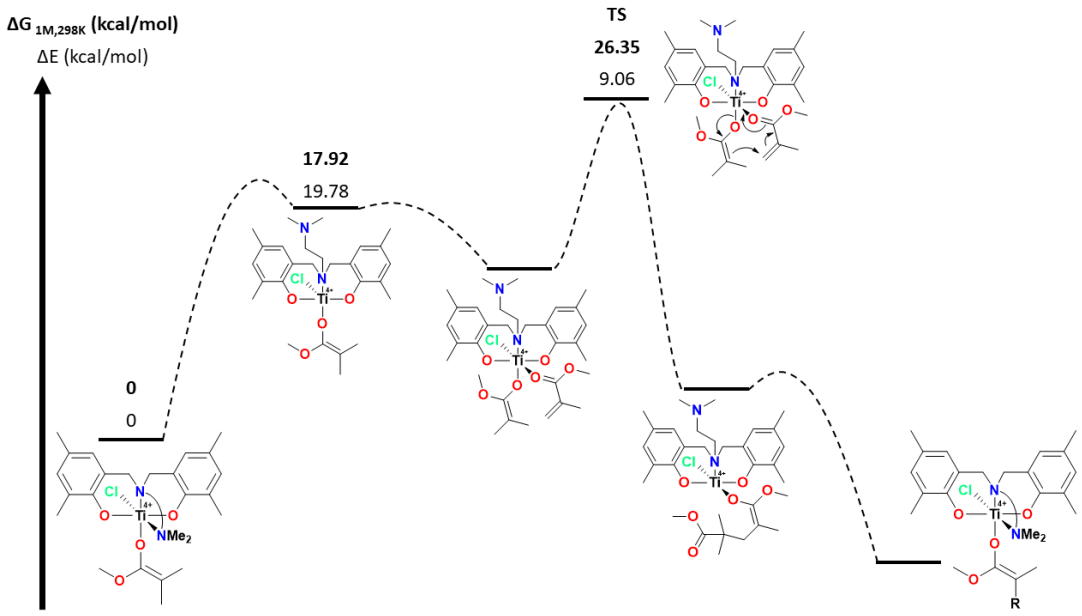

Scheme 3.13 - Energy diagram showing the proposed monometallic group transfer polymerisation mechanism with the methyl-substituted ligand framework. R = MMA.

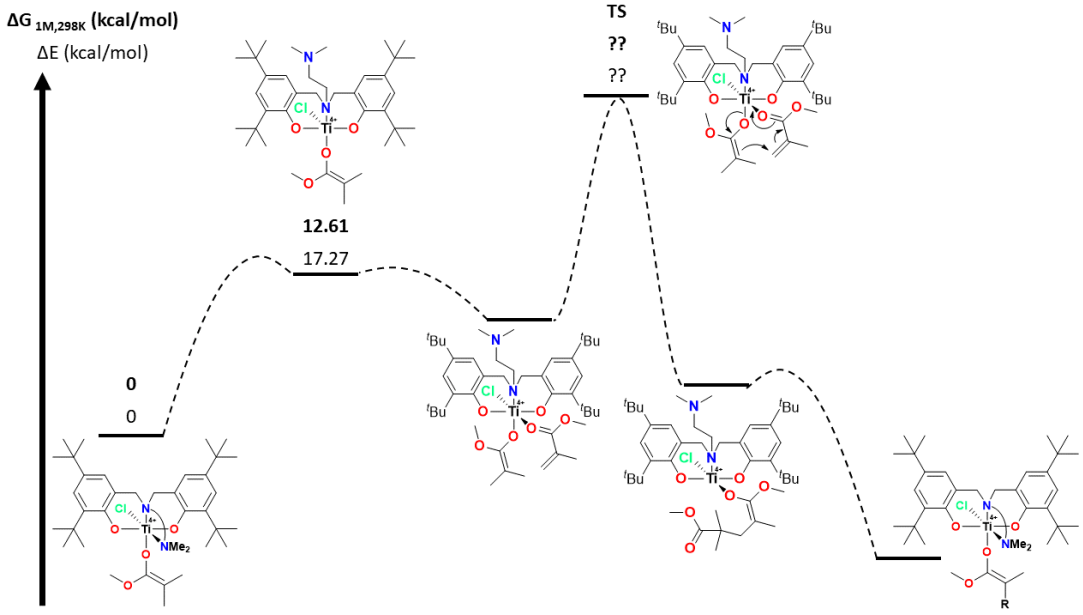

Scheme 3.14 - Energy diagram showing the proposed monometallic group transfer polymerisation mechanism with the *tert*-butyl-substituted ligand framework. R = MMA.

It is interesting to compare the difference in energy values of the transition states as the ligand framework changes (Table 3.12). As the size of the ligand framework increases, the energy barrier to dissociation of the pendant arm considerably decreases. On the other hand, as the size of the ligand framework increases, the energy barrier to the group transfer polymerisation step increases. It would therefore be expected that the energy value for the

tert-butyl-substituted system is considerably greater than 26.56 kcal/mol. This suggests that as the size of the ligand framework increases, the rate of polymerisation decreases. This difference in energy barrier correlates with the experimental result that polymerisations mediated by **Ti2** are faster than polymerisations mediated by **Ti1** (polymerisations **3.1** and **3.2** in Table 3.1)

Table 3.12 - Comparing the transition state energy values of the three ligand frameworks, in the proposed monometallic group transfer polymerisation mechanism.

Ligand Framework	$\Delta G^{\ddagger}_{1M,298K}$ TS 1 (kcal/mol)	$\Delta G^{\ddagger}_{1M,298K}$ TS 2 (kcal/mol)
Simplified	20.46	24.61
Lig2 (Me-substituted)	17.92	26.35
Lig1 (^{t}Bu-substituted)	12.61	-

Given the difficulty in optimising the transition state for the monometallic GTP mechanism using the *tert*-butyl-substituted ligand, no attempt was made to investigate the bimetallic GTP mechanism using a ligand other than the simplified framework. It is expected that there would be too many atoms in each of the species for an energy value to be accurately calculated.

3.7 Experimental Evidence of Group Transfer Polymerisation

Whilst theoretical DFT studies show that the likely polymerisation mechanism is bimetallic (and monometallic) group transfer polymerisation, it is important to demonstrate this experimentally.

One possible way to demonstrate a non-radical pathway is through the addition of a radical scavenger. It was expected that a radical scavenger, when added at the start of the polymerisation, would react with the initiator radicals and prevent any polymerisation whatsoever. However, in theory, the addition of the scavenger midway through the polymerisation would stop a radical polymerisation but have no effect on an insertion polymerisation.

Initial attempts made use of (2,2,6,6-tetramethylpiperidin-1-yl)oxyl (TEMPO), a well known stable radical. However, addition of TEMPO to the polymerisation of MMA mediated by **Ti1** merely terminated the polymerisation. This is not wholly unexpected, as TEMPO is known to directly react with titanium complexes.[36,37]

Next, it was thought that silanes may be effective at radical scavenging, because their reactivity in radical chemistry is well known.[38,39] It was also thought that they would be less reactive with titanium than TEMPO. However, it was found that diphenylsilane had no effect on the free-radical polymerisation of MMA (Table 3.13). There was negligible change in conversion even at very high concentrations of diphenylsilane. If diphenylsilane is unable to terminate a polymerisation mechanism which is known to be radical, then it will certainly not work as a radical scavenger in the titanium-mediated polymerisation.

Table 3.13 - Free-radical polymerisation of MMA, with and without diphenylsilane (Ph_2SiH_2).

#	Equivalents Ph_2SiH_2	Conversion (%)
3.102	0	56
3.103	5	58
3.104	50	54

Conditions: [MMA]:[V-70]:[Ph_2SiH_2] = 100:1.0:x, MMA:toluene = 1:1 (v/v), 80 °C, 40 min. Ph_2SiH_2 is added at the start of the polymerisation. Conversion determined by ^{1}H NMR spectroscopy.

A further attempt was made using dihydroanthracene (DHA, Figure 3.17), which is known to be a useful compound to test for the presence of radicals.[40]

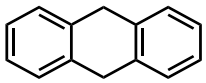

Figure 3.17 - Dihydroanthracene (DHA).

Table 3.14 shows the effect of DHA in both the free-radical and **Ti1**-mediated polymerisation of MMA. Free-radical polymerisations **3.105**-**3.107** show that the introduction of the radical scavenger results in a lower monomer conversion, as the radical chain ends irreversibly terminate by reacting with the scavenger. If the radical scavenger was fully effective, the conversion should be zero, because ideally all radicals produced would immediately react with the scavenger. However, DHA is slow to react and only partially reactive, and therefore does not quench the primary radicals of V-70. As a result, DHA is only able to lower monomer conversion, and not prevent it entirely.

However, polymerisations **3.108**-**3.109** demonstrate that the use of DHA in a polymerisation mediated by **Ti1** results in a negligible change in monomer conversion, which suggests that there are no radical chain ends for the scavenger to react with. This is strong evidence for the absence of a radical-based polymerisation mechanism.

Table 3.14 - Polymerisation of MMA, with and without complex **Ti1** and radical scavenger dihydroanthracene.

#	Equivalents Ti1	Equivalents DHA	Conversion (%)
3.105	0	0	56
3.106	0	5	33
3.107	0	20	20
3.108	1	0	84
3.109	1	5	81

Conditions: [MMA]:[**Ti1**]:[V-70]:[DHA] = 100:x:1.0:y, MMA:toluene = 1:1 (v/v), 80 °C, 40 min. DHA is added at the start of the polymerisation. Conversion determined by ^{1}H NMR spectroscopy.

The theory that the polymerisation mechanism is bimetallic group transfer helps to explain the strange kinetic data previously seen in Figure 3.13, where the polymerisation rate decreased as the concentration of initiator increased. By increasing the concentration of initiator, the concentration of Ti(IV)-enolate, from which the chains grow, also increases. Therefore, the concentration of Ti(IV)-enolate dictates the molecular weight, which is consistent with the experimental data. However, increasing Ti(IV) concentration is concurrent with a decreased Ti(III) concentration. As both are required in the bimetallic mechanism, the low polymerisation rate with high V-70 concentration can be attributed to the low Ti(III) concentration.

If this is true, and the concentration of Ti(IV)-enolate controls the molecular weight and the relative concentration of Ti(IV) to Ti(III) controls the polymerisation rate, it would be expected that adding additional Ti(III) complex **Ti1** midway through the polymerisation would result in a higher polymerisation rate with no new chains being formed. To explore this further, several kinetic experiments were performed (Table 3.15 and Figure 3.18). To begin each kinetic experiment, the standard polymerisation method of this study was applied (polymerisation **3.110**, [MMA]:[**Ti1**]:[V-70] = 100:1.00:2.00) and the polymerisation was allowed to proceed for 20 minutes. This duration was chosen so as to have a low conversion whilst ensuring that all of the V-70 had decomposed. This is important because it means that

the newly-added **Ti1** would not be able to react with any initiator radicals. After this time, the polymerisation mixture was returned to the glovebox, and additional amounts of **Ti1** were added (0, 0.5 or 1.0 equivalents, yielding a total concentration of titanium in the system of 1.0, 1.5 or 2.0 equivalents respectively).

It is clear to see from Figure 3.18 that upon the addition of the extra Ti(III) complex the polymerisation rate increases. Adding an additional 0.5 equivalents of **Ti1** almost doubles the polymerisation rate from 0.0105 min^{-1} to 0.019 min^{-1}. A further 0.5 equivalents of **Ti1** does not give a substantial increase in rate, suggesting that there is a limit to how fast the polymerisation can be at a fixed Ti(IV) concentration.

Table 3.15 - Addition of extra **Ti1** during MMA polymerisation.

#	Extra Equiv. Ti1	Time (min)	Conv. (%)	$M_{n,th}$ (Da)	M_n (Da)	Đ
3.110	Start	20	17	1700	6300	1.17
3.111	0	40	35	3500	11300	1.10
3.112	0	60	45	4500	13500	1.10
3.113	0	75	56	5600	18100	1.15
3.114	0	90	58	5800	18000	1.11
3.115	0	180	85	8500	27300	1.13
3.116	0.5	40	47	4700	15200	1.10
3.117	0.5	60	62	6200	19200	1.10
3.118	0.5	75	73	7300	25800	1.13
3.119	0.5	90	79	7900	24000	1.17
3.120	0.5	110	85	8500	28600	1.10
3.121	1.0	40	53	5300	18100	1.17
3.122	1.0	60	68	6800	22000	1.11
3.123	1.0	75	76	7600	24900	1.16
3.124	1.0	90	82	8200	26000	1.14

Conditions: [MMA]:[**Ti1**]:[V-70] = 100:1.00:2.00, MMA:toluene = 1:1 (v/v), 80 °C, 20 min. Subsequently, add x equiv. **Ti1** and continue heating. Conversion determined by ^{1}H NMR spectroscopy. $M_{n,th}$ = $[monomer]_0/[\mathbf{Ti1}]_0 \times M(monomer) \times conversion$.

More importantly, the molecular weights attained in all the polymerisations (**3.110**-**3.124**) lie on the same line in the graph of molecular weight versus conversion. This is crucial because it means that despite the introduction of additional Ti(III) midway through the

polymerisation, no new chains are formed. Therefore, the polymerisation must be radically-initiated by the V-70 and the polymer chains must be growing from the Ti(IV) species.

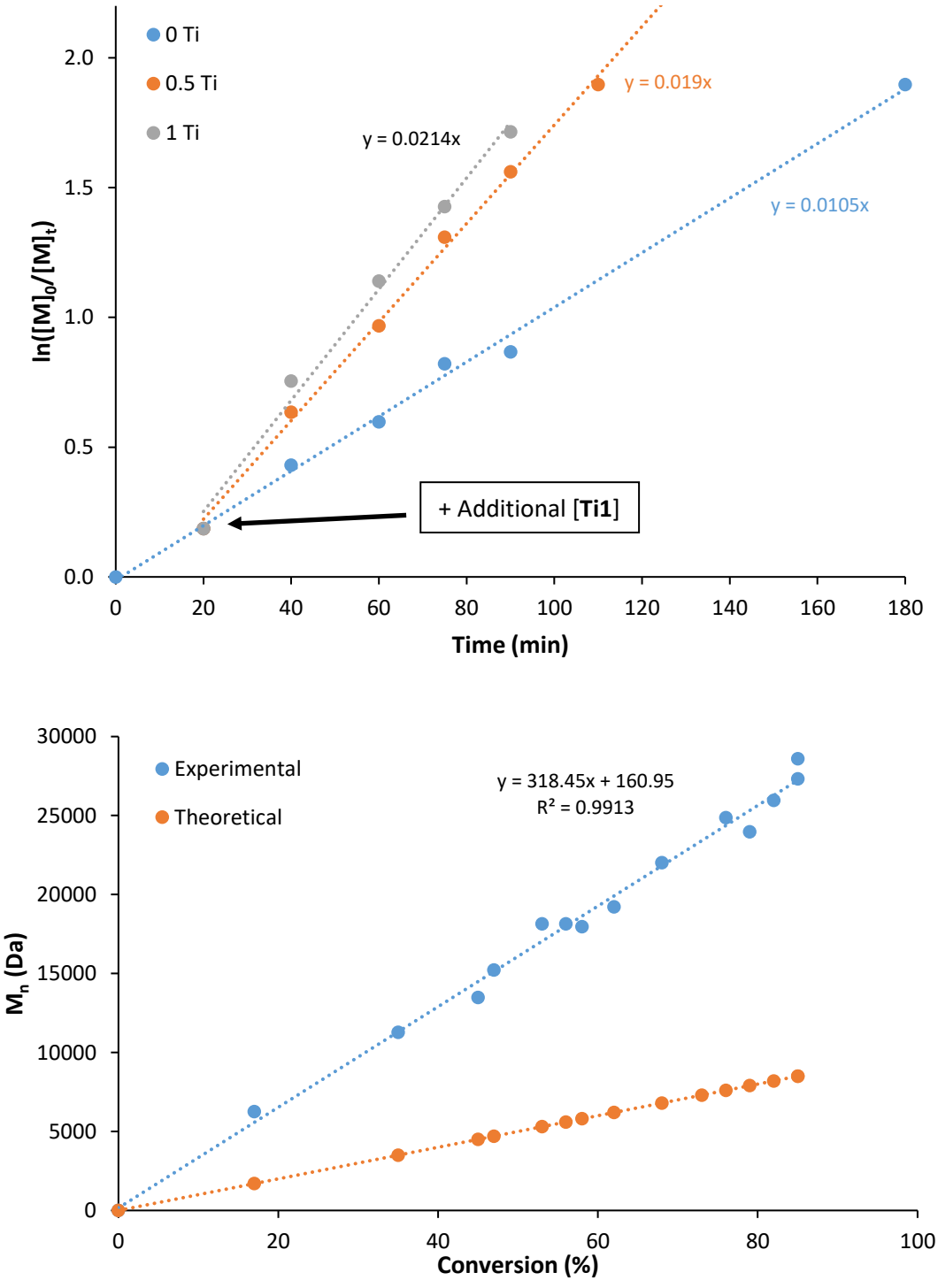

Figure 3.18 - Addition of extra **Ti1** during MMA polymerisation at 80 °C. [MMA]:[**Ti1**]:[V-70] = 100:1.00:2.00, MMA:toluene = 1:1 (v/v). After 20 mins, add x equiv. **Ti1** and continue heating.

In order to definitively prove that the Ti(IV)-enolate is the key species in the polymerisation mechanism, it would be preferable to synthesise and isolate the complex. In theory, this complex would then be able to both initiate and mediate the MMA polymerisation. Numerous attempts were made to synthesise the Ti(IV)-enolate analogue of **Ti1**, taking inspiration from previously-published group 4 enolates.[41–43] Firstly, the Ti(IV) equivalent of **Ti1**, $^{t\text{-}Bu,t\text{-}Bu,NMe2}[O_2NN']TiCl_2$ **Ti1-Cl**, was reacted with lithium methyl isobutyrate (LiMIB) in THF at -78 °C. Secondly, the same method was used but refluxed in THF overnight. Thirdly, LiMIB was first reacted with $TiCl_4$.THF in THF at -78 °C, followed by addition of a pre-reacted mixture of **Lig1** and Li(HMDS) at -78 °C. However, in all cases the resultant ^{1}H NMR spectra were unclean, suggesting that there were multiple reaction products. Furthermore, a sample of the reaction products was unable to initiate the polymerisation of MMA under the standard conditions used in this work.

However, it was possible to generate a macroinitiator comprising approximately 30 monomer units, by polymerising MMA ([MMA]:[**Ti1**]:[V-70] = 100:1.00:2.00) for a short period of time (10 minutes at 80 °C) and precipitating the resultant product from *n*-hexane. This macroinitiator was then used as initiator and mediator of the polymerisation of MMA without the addition of any V-70 (Table 3.16 and Figure 3.19). This macroinitiator is represented by polymerisation **3.125**, which had an "effective" MMA conversion of 5% when added to excess MMA (0.2002 g). Attempts to use ^{1}H NMR spectroscopy to identify characteristic enolate resonances in the macroinitiator were unsuccessful, because it was not possible to synthesise a macroinitiator small enough for the relevant resonances to be sufficiently visible. However, the resonances which are characteristic of PMMA were present in the ^{1}H NMR spectrum. Furthermore, it is unlikely that the macroinitiator contains any residual Ti(III) complex, because **Ti1** is soluble in *n*-hexane. Whilst it is likely that the macroinitiator is intact (the polymer chain is still bound to the metal centre *via* an enolate), further spectroscopic evidence is required to confirm this.

In the presence of this macroinitiator and excess monomer, but the absence of **Ti1**, chains grew slowly (polymerisation **3.126**). This slow polymerisation illustrates the presence of the monometallic mechanism, because there is no Ti(III) present for the bimetallic pathway to be active. The fact that the macroinitiator was able to undergo polymerisation, in the absence of any initiator, is strong evidence that the macroinitiator is still intact.

However, upon addition of **Ti1** (0.0136 g), the polymerisation rate increased by an approximate factor of nine (polymerisation **3.127**). Now that there is excess Ti(III) in the system, the polymerisation can proceed *via* the bimetallic pathway. The fact that the polymerisation rate increases by so much demonstrates that the bimetallic pathway is significantly more favoured.

Table 3.16 - Use of a macroinitiator, with and without added **Ti1**.

#	Time (min)	Conversion (%)
3.125	0	5
3.126	60	18
3.127	90	57

Conditions: MMA:toluene = 1:1 (v/v), 80 °C. Conversion determined by ^{1}H NMR spectroscopy.

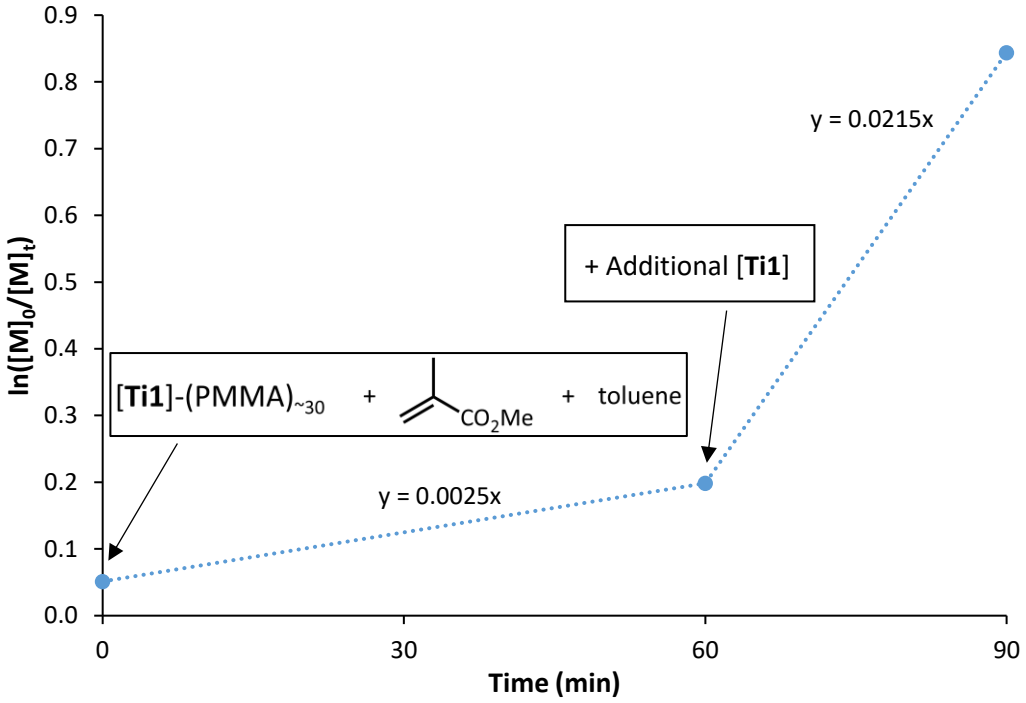

Figure 3.19 - Use of a macroinitiator, with and without added **Ti1**.

Polymerisation kinetics were not performed, primarily because only a very limited quantity of macroinitiator was synthesised and isolated. Furthermore, taking samples whilst the polymerisation was ongoing was avoided in order to minimise contact with air and moisture. Future work should focus on performing kinetics using the macroinitiator to better

understand and quantify the relative rates of polymerisation of the monometallic and bimetallic pathways.

Finally, the bimetallic (and monometallic) group transfer polymerisation mechanism is supported by the inability of the polymer to undergo copolymerisation with monomers other than methacrylates. In a classical coordination-insertion mechanism, it is theoretically possible that adding a further alkene monomer, such as ethylene or isoprene, would yield a poly(methyl methacrylate)-poly(olefin) block copolymer. However, with the proposed group transfer mechanism, polymerisation of an alkene monomer such as isoprene would not be possible. Table 3.17 shows that this assumption is correct and, whilst a high MMA conversion was reached, no isoprene conversion was observed.

Table 3.17 - MMA and isoprene (IP) copolymerisation.

#	Equiv. MMA	Equiv. IP	Temp. (°C)	Time (min)	MMA Conv. (%)	IP Conv. (%)
3.128	100	100	80	180	91	<1

Conditions: [MMA]:[Isoprene]:[**Ti1**]:[V-70] = x:y:1.00:1.00, MMA:toluene = 1:1 (v/v), 80 °C, 3 hours. Conversion determined by ^{1}H NMR spectroscopy. Both MMA and isoprene were added together at the start of the polymerisation.

3.8 Conclusions

The use of titanium complexes in controlled radical polymerisation has received relatively little attention, especially in comparison with other first-row transition metals. Furthermore, there is uncertainty as to the mechanism of the previous titanium-mediated controlled radical methods. Other titanium-mediated methods typically require expensive or pyrophoric activators. In contrast, in this chapter the excellent control that “easy to make” titanium(III) amino-phenolate complexes have over the polymerisation of methacrylates, without the need for any co-catalyst or activator, has been demonstrated. A variety of amino-phenolate ligands **Lig1**H_2-**Lig7**H_3 and their respective titanium(III) complexes **Ti1**-**Ti7** were synthesised to investigate the effect of ligand electronic and steric properties, as well as coordination geometry, on the polymerisation. The complexes were all straightforward to synthesise under inert conditions and were all produced with high yields. The novel

complexes were characterised and shown to display geometries similar to previously published titanium(III) amino-phenolate complexes.

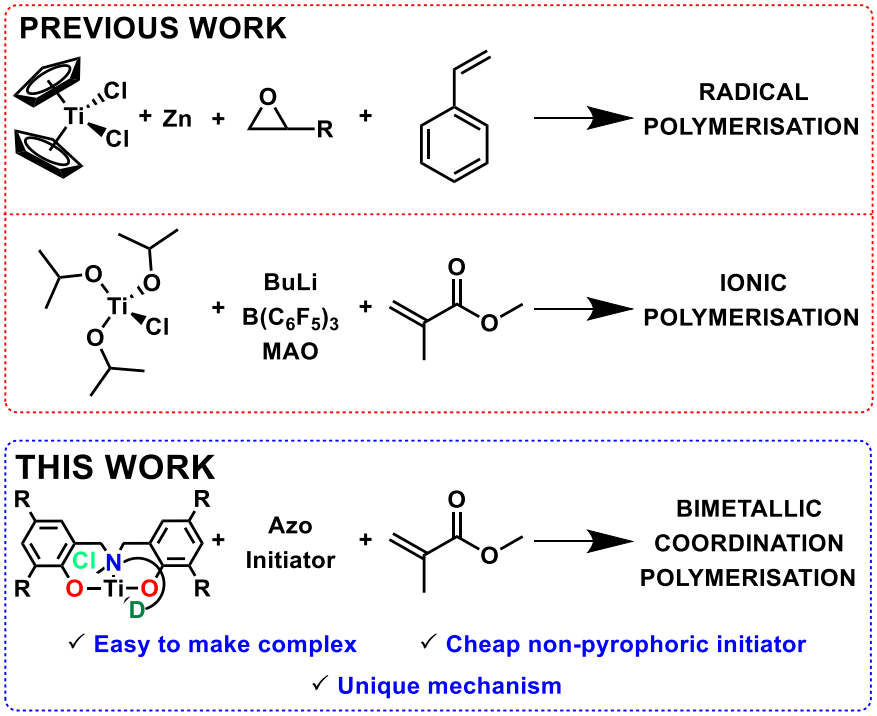

Figure 3.20 - Comparing the titanium-mediated methods of previous work and of this work.

The complexes were screened for their efficacy as mediators in the polymerisation of MMA under OMRP conditions, with complexes **Ti1**-**Ti4** particularly showing excellent control with linear first-order kinetics. Conversions in excess of 90% and dispersities lower than 1.10 were achieved. Interestingly, it was found that the tacticity deviated from that which is typical for a free-radical polymerisation, suggesting that the polymerisation mechanism is not radical-based despite using a conventional azo initiator.

Through a combination of experimental and DFT studies, it has been shown that the polymerisation most likely proceeds *via* a group transfer mechanism, with a primary bimetallic and secondary monometallic mode of operation. The key species in the catalytic cycle is a Ti(IV)-enolate complex, which is formed after a few radical monomer additions. DFT calculations show that this enolate species is considerably more energetically favourable than other 6-coordinate titanium(IV) species. Furthermore, DFT calculations also show that OMRP, ionic and coordination-insertion mechanisms are all unlikely to be present. In the case of the group transfer mechanism, both the bimetallic and monometallic pathways are

accessible and feasible, with a transition state of +21.86 kcal/mol and +24.61 kcal/mol respectively.

Kinetic studies strongly support the proposed group transfer mechanism. It has been found that the titanium complex is catalytic, and that the polymerisation rate is faster than that observed in a free-radical polymerisation. Furthermore, increasing the concentration of initiator decreases the rate of the titanium-mediated polymerisation. Both trends are uncharacteristic of a typical controlled radical polymerisation

The use of a radical scavenger highlights the absence of radicals present during the polymerisation, as dihydroanthracene suppresses the free-radical MMA polymerisation but has negligible effect on the **Ti1**-mediated polymerisation. Furthermore, it is possible to introduce additional titanium(III) complex midway through the polymerisation to increase the propagation rate, whilst having no effect on the number of growing polymer chains.

It can also be concluded that for effective polymerisation control, there are some constraints over the ligand framework. A strongly donating or overly bulky framework prohibits the proposed group transfer mechanism, with ligand flexibility promoting formation of the required Ti(IV)-enolate species. On the other hand, steric bulk on the phenolate has the positive effect of increasing isotactic bias in the resultant PMMA.

Attempts to isolate the Ti(IV)-enolate complex were unsuccessful. However, a macroinitiator was synthesised and used to initiate and mediate MMA polymerisation. Further work should focus on synthesising this Ti(IV)-enolate complex using other methods. Initial attempts should focus on using a silyl enol ether precursor (Figure 3.21). Further attempts could focus on synthesising the Ti(IV)-enolate directly from the carbonyl precursor in the presence of titanium(IV) chloride and a tertiary amine.[44] If a stable Ti(IV)-enolate complex could be isolated and used to initiate and mediate MMA polymerisation, this would provide an even more straightforward method to synthesise well-controlled MMA using an environmentally friendly metal complex.

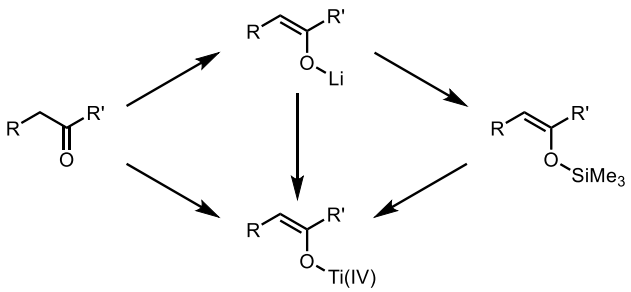

Figure 3.21 - General methods for the preparation of titanium(IV) enolates.[44]

As shown in chapter 3.6, DFT calculations suggest that as the size of the ligand framework increases, the energy barrier to the GTP transition state increases and consequently the polymerisation rate decreases. These DFT calculations therefore suggest that the simplified ligand framework, which was used in the majority of the calculations, would have the greatest polymerisation rate. It would be interesting to synthesise ligands and complexes based on the simplified ligand framework and explore their efficacy as mediators of the polymerisation of MMA. Whilst it is expected that the polymerisation would still proceed *via* the bimetallic and monometallic GTP mechanisms, the lack of steric bulk on the ligand would likely result in a loss of the tacticity bias towards isotactic PMMA. However, the lack of steric bulk on the ligand may also permit the polymerisation of more sterically bulky monomers such as ^{t}BuMA.

Attempts to synthesise copolymers of MMA and another alkene monomer, such as isoprene, were unsuccessful. The DFT calculations suggest that the Ti(IV)-enolate species is the important starting point in the polymerisation mechanism. Therefore, it is not possible to polymerise isoprene *via* this mechanism, because it cannot form this necessary enolate species. However, it is reasonable to expect that other monomers, aside from simple alkyl methacrylates, which are able to form Ti(IV)-enolate species would also be polymerisable *via* the proposed group transfer mechanism. Chen and co-workers recently reported the group transfer polymerisation of cyclic γ-methyl-α-methylene-γ-butyrolactone (MMBL) and α-methylene-γ-butyrolactone (MBL) using a silyl ketene acetal/Al(C_6F_5)$_3$ system.[45] Kakuchi and co-workers have used B(C_6F_5)$_3$-catalysed group transfer to polymerise N,N-diethylacrylamide (DEAA).[46] They have also recently polymerised a range of functional acrylates, including 2-methoxyethyl, 2-(2-ethoxyethoxy)ethyl, tetrahydrofurfuryl, allyl, triisopropylsilyl, and 2-(triisopropylsiloxy)ethyl acrylates.[47] Further work should focus on exploring the monomer

scope, using this previous work as inspiration, and expand the range of polymers and materials that can be synthesised through this titanium-mediated method.

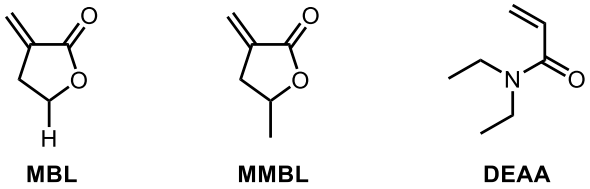

Figure 3.22 - α-Methylene-γ-butyrolactone (MBL), γ-methyl-α-methylene-γ-butyrolactone (MMBL) and N,N-diethylacrylamide (DEAA).

It was suggested in chapter 3.7 that the relative concentration of Ti(IV) to Ti(III) controls the polymerisation rate. However, this has not been fully quantified and further work should focus on determining the exact rate equation of the propagation step of the polymerisation. With this information, the reaction parameters could be accurately tuned to further optimise the polymerisation.

Finally, there has been no work to date to investigate the physical properties of the PMMA synthesised throughout this work. It has been shown that the synthesised PMMA has an isotactic bias, with the extent to which this bias is present dependent on the ligand framework. Whilst the tacticity is not considerably different to that of free-radical PMMA, the difference in displayed physical properties may be significant. Studies into the properties of the synthesised PMMA would further ascertain the industrial usefulness of this titanium-mediated method.

3.9 References

1 S. Barroso, J. Cui, J. M. Carretas, A. Cruz, I. C. Santos, M. T. Duarte, J. P. Telo, N. Marques and A. M. Martins, *Organometallics*, 2009, **28**, 3449–3458.

2 S. Barroso, A. M. Coelho, S. Gómez-Ruiz, M. J. Calhorda, Ž. Žižak, G. N. Kaluđerović and A. M. Martins, *Dalt. Trans.*, 2014, **43**, 17422–17433.

3 E. Y. Tshuva, M. Versano, I. Goldberg, M. Kol, H. Weitman and Z. Goldschmidt, *Inorg. Chem. Commun.*, 1999, **2**, 371–373.

4 E. Y. Tshuva, I. Goldberg, M. Kol and Z. Goldschmidt, *Inorg. Chem.*, 2001, **40**, 4263–

4270.

5 E. Hayut-Salant, M. Kol, Z. Goldschmidt, M. Shamis, I. Goldberg and S. Alfi, *Inorg. Chem. Commun.*, 2002, **4**, 177–179.

6 G. Bernardinelli, T. M. Seidel, E. P. Kündig, L. J. Prins, A. Kolarovic, M. Mba, M. Pontini and G. Licini, *Dalt. Trans.*, 2007, 1573–1576.

7 M. Białek and E. Bisz, *Appl. Catal. A Gen.*, 2016, **525**, 137–144.

8 E. Y. Tshuva, I. Goldberg, M. Kol and Z. Goldschmidt, *Inorg. Chem. Commun.*, 2000, **3**, 611–614.

9 S. Groysman, I. Goldberg, M. Kol, E. Genizi and Z. Goldschmidt, *Inorganica Chim. Acta*, 2003, **345**, 137–144.

10 E. Y. Tshuva, I. Goldberg, M. Kol and Z. Goldschmidt, *Chem. Commun.*, 2001, 2120–2121.

11 S. Segal, I. Goldberg and M. Kol, *Organometallics*, 2005, **24**, 200–202.

12 S. Gendler, S. Segal, I. Goldberg, Z. Goldschmidt and M. Kol, *Inorg. Chem.*, 2006, **45**, 4783–4790.

13 A. J. Chmura, M. G. Davidson, M. D. Jones, M. D. Lunn, M. F. Mahon, A. F. Johnson, P. Khunkamchoo, S. L. Roberts and S. S. F. Wong, *Macromolecules*, 2006, **39**, 7250–7257.

14 J. M. E. P. Cols, C. E. Taylor, K. J. Gagnon, S. J. Teat and R. D. McIntosh, *Dalt. Trans.*, 2016, **45**, 17729–17738.

15 S. Groysman, I. Goldberg, M. Kol, E. Genizi and Z. Goldschmidt, *Organometallics*, 2004, **23**, 1880–1890.

16 E. Y. Tshuva, I. Goldberg, M. Kol and Z. Goldschmidt, *Organometallics*, 2001, **20**, 3017–3028.

17 P. Hormnirun, E. L. Marshall, V. C. Gibson, A. J. P. White and D. J. Williams, *J. Am. Chem. Soc.*, 2004, **126**, 2688–2689.

18 T. R. Dargaville, P. J. De Bruyn, A. S. C. Lim, M. G. Looney, A. C. Potter, D. H. Solomon and X. Zhang, *J. Polym. Sci. Part A Polym. Chem.*, 1997, **35**, 1389–1398.

19 R. Minhas, R. Duchateau, S. Gambarotta and C. Bensimon, *Inorg. Chem.*, 1992, **31**, 4933–4938.

20 N. A. Jones, S. T. Liddle, C. Wilson and P. L. Arnold, *Organometallics*, 2007, **26**, 755–757.

21 L. E. N. Allan, J. P. MacDonald, G. S. Nichol and M. P. Shaver, *Macromolecules*, 2014, **47**, 1249–1257.

22 Y. Isobe, K. Yamada, T. Nakano and Y. Okamoto, *J. Polym. Sci. Part A Polym. Chem.*, 2000, **38**, 4693–4703.

23 H. H. Brintzinger, D. Fischer, R. Mülhaupt, B. Rieger and R. M. Waymouth, *Angew. Chemie Int. Ed. English*, 1995, **34**, 1143–1170.

24 Y. Qian, J. Huang, M. D. Bala, B. Lian, H. Zhang and H. Zhang, *Chem. Rev.*, 2003, **103**, 2633–2690.

25 V. C. Gibson and S. K. Spitzmesser, *Chem. Rev.*, 2003, **103**, 283–315.

26 T. Rünzi, D. Guironnet, I. Göttker-Schnetmann and S. Mecking, *J. Am. Chem. Soc.*, 2010, **132**, 16623–16630.

27 H. Yasuda, R. Nakano, S. Ito and K. Nozaki, *J. Am. Chem. Soc.*, 2018, **140**, 1876–1883.

28 C. Cui, A. Shafir, C. L. Reeder and J. Arnold, *Organometallics*, 2003, **22**, 3357–3359.

29 X.-F. Li, Y.-G. Li, Y.-S. Li, Y.-X. Chen and N.-H. Hu, *Organometallics*, 2005, **24**, 2502–2510.

30 O. W. Webster, W. R. Hertler, D. Y. Sogah, W. B. Farnham and T. V. RajanBabu, *J. Am. Chem. Soc.*, 1983, **105**, 5706–5708.

31 O. W. Webster, *J. Polym. Sci. Part A Polym. Chem.*, 2000, **38**, 2855–2860.

32 O. W. Webster, in *New Synthetic Methods*, Springer, Berlin, Heidelberg, 2003, pp. 1–34.

33 W. R. Hertler, D. Y. Sogah, O. W. Webster and B. M. Trost, *Macromolecules*, 1984, **17**, 1415–1417.

34 D. Y. Sogah, W. R. Hertler, O. W. Webster and G. M. Cohen, *Macromolecules*, 1987, **20**, 1473–1488.

35 I. B. Dicker, G. M. Cohen, W. B. Farnham, W. R. Hertler, E. D. Laganis and D. Y. Sogah, *Macromolecules*, 1990, **23**, 4034–4041.

36 M. K. Mahanthappa, A. P. Cole and R. M. Waymouth, *Organometallics*, 2004, **23**, 1405–1410.

37 T. Kurogi, P. J. Carroll and D. J. Mindiola, *Chem. Commun.*, 2017, **53**, 3412–3414.

38 M. Ballestri, C. Chatgilialoglu, K. B. Clark, D. Griller, B. Giese and B. Kopping, *J. Org. Chem.*, 1991, **56**, 678–683.

39 C. Chatgilialoglu and J. Lalevée, *Molecules*, 2012, **17**, 527–555.

40 P. L. Arnold, S. M. Mansell, L. Maron and D. McKay, *Nat. Chem.*, 2012, **4**, 668–674.

41 A. D. Bolig and E. Y. X. Chen, *J. Am. Chem. Soc.*, 2004, **126**, 4897–4906.

42 A. Rodriguez-Delgado, W. R. Mariott and E. Y. X. Chen, *Macromolecules*, 2004, **37**, 3092–3100.

43 B. Lian, T. P. Spaniol and J. Okuda, *Organometallics*, 2007, **26**, 6653–6660.

44 D. Ciez, A. Pałasz and B. Trzewik, *European J. Org. Chem.*, 2016, **2016**, 1476–1493.

45 L. Hu, J. He, Y. Zhang and E. Y. X. Chen, *Macromolecules*, 2018, **51**, 1296–1307.

46 S. Kikuchi, Y. Chen, E. Ichinohe, K. Kitano, S. I. Sato, Q. Duan, X. Shen and T. Kakuchi, *Macromolecules*, 2016, **49**, 4828–4838.

47 Y. Chen, Q. Jia, Y. Ding, S. Sato, L. Xu, C. Zang, X. Shen and T. Kakuchi, *Macromolecules*, 2019, **52**, 844–856.

4 Conclusions & Future Work

The purpose of this research was to develop iron and titanium complexes which could be used as environmentally-friendly mediators in the controlled polymerisation of alkenes. In particular, the research aimed to build on the extensive knowledge and experience of the amino-phenolate ligand framework in order to further understand how complexes of this family mediate polymerisations. The polymerisations were studied in detail to understand the mechanisms involved, with a focus on the balance between competing propagation and termination reactions. A set of optimal experimental conditions were targeted, under which the polymerisation of some common alkene monomers was controlled.

In Chapter 2, a novel *tert*-butyl substituted iron(II) amine−bis(phenolate) complex was synthesised and used in the OMRP of styrene, methyl methacrylate and vinyl acetate. Under certain conditions, the OMRP of MMA at 75 °C showed moderate control, with reasonable dispersities and some chain-end fidelity, demonstrated through chain extension. However, only moderate conversions were required before irreversible radical termination became prevalent. At low temperatures, the OMRP of MMA was dominated by catalytic chain transfer, although high conversions and reasonable dispersities were achieved. It is likely to be possible to control the molecular weight in a CCT-dominated polymerisation by altering the monomer concentration at the start of the polymerisation. The polymerisation of vinyl acetate was unsuccessful, which was most likely to be due to the formation of a highly stable deactive species upon the reaction of a vinyl acetate radical with the iron(II) complex.

Previous work suggested that at high temperatures the iron-alkyl bond is far too labile for OMRP-control of styrene. However, lowering the polymerisation temperature to 30 °C significantly reduced the rate of propagation, and decreased the lability of the metal-alkyl bond to the extent that a controlled OMRP could occur. The OMRP of styrene, at low temperature, represents the most effective iron-mediated OMRP to date, with dispersities as low as 1.27.

In Chapter 3, a family of titanium(III) amino-phenolate complexes were synthesised and used to provide excellent control over the polymerisation of methacrylates. Conversions in excess of 90% and dispersities lower than 1.10 were achieved. Through a combination of

experimental and DFT studies it was shown that the polymerisation does not proceed *via* a radical mechanism, as would be expected, but most likely proceeds *via* a group transfer mechanism, with a primary bimetallic and secondary monometallic mode of operation. The key species in the catalytic cycle was found to be a Ti(IV)-enolate complex. In addition to controlling the polymerisation, the titanium complex is catalytic, given that the polymerisation rate was greater than that observed in a free-radical polymerisation.

Furthermore, the titanium-mediated polymerisation was advantageously activated using a conventional azo initiator instead of typical expensive or pyrophoric alternatives, which is unusual for a titanium-mediated coordination polymerisation. This feature considerably increases the industrial applicability of titanium-mediated methods, because an azo initiator is far easier and safer to store, handle and use.

With regard to error analysis and the reproducibility of this research, the majority of the polymerisations were performed once only and were not repeated. Whilst it is acknowledged that repetition would help to confirm the reliability of the results, many of the conclusions of this research are based on trends. Therefore, calculating the exact molecular weight and dispersity to a precise degree of accuracy is not important. The lack of repeated data points is further counterbalanced by the numerous kinetic experiments, in which linear trends are identified based on a series of data points. Those points which are incorrect are then easily spotted. In addition, it is worth noting that GPC analysis has an inherent error of approximately 10%, which is unavoidable regardless of the number of times a polymerisation is repeated.

Controlled radical polymerisation, and other methods of polymerisation control, have contributed considerably to the field of polymer chemistry. This is due to the functional group tolerance, facile process conditions and the ability to develop a wide range of (co)polymers from a variety of vinyl monomers. However, there is an ever-increasing public awareness of the problems relating to plastic waste and the processes involved in making plastics. Consequently, there is an economic and political demand for increased sustainability within the plastics industry. This research has shown that control over the polymerisation of common alkenes can be achieved using more environmentally-friendly metals and complexes than the alternatives currently available.

With this in mind, there are several areas in which further work should be focused in order to build upon this research. This work has provided a set of experimental conditions in which iron and titanium amino-phenolate complexes have optimal control over polymerisations. It would be of interest to explore the range of block copolymers which are able to be synthesised due to the metal-capped polymer afforded by OMRP (in the case of iron) or GTP (in the case of titanium). Block copolymers is a particular field which has been driven forward by the development of controlled methodologies. The results in this work pave the way for new research in this field, perhaps through the synthesis of multi-mechanistic copolymers. This would allow for the facile synthesis of copolymers which would typically require multiple process steps.

Furthermore, DFT calculations were used in this work to investigate the use of titanium amino-phenolate complexes in controlled polymerisations from a theoretical viewpoint. Further work should focus on the lessons learnt from the results of these calculations to intelligently design new ligand frameworks, and their respective complexes, with the aim of improving polymerisation rates and control over the molecular weight, dispersity and tacticity of the polymer.

Finally, further work should focus on increased efforts to synthesise, isolate and characterise iron-alkyl and titanium-enolate complexes, which have been shown to be the important species in their respective control mechanisms. Such complexes would, in theory, be able to both initiate and mediate a polymerisation. This would provide a simpler method to a controlled polymer than the current alternatives. Furthermore, the polymerisation would likely be more controlled because the need for a radical initiation step, which typically broadens dispersities, is removed.

5 Experimental

5.1 General Considerations

All experiments involving moisture- and air-sensitive compounds were performed under a nitrogen atmosphere using an MBraun LABmaster sp glovebox system equipped with a -35 °C freezer and [H_2O] and [O_2] analysers or using standard Schlenk techniques. Gel permeation chromatography (GPC) was carried out in THF at a flow rate of 1 mL min^{-1} at 35 °C on a Malvern Instruments Viscotek 270 GPC Max triple detection system with 2× mixed bed styrene/DVB columns (300 × 7.5 mm). Absolute molar masses were obtained using dn/dc values of 0.088 for poly(methyl methacrylate),[1] 0.068 for poly(methyl acrylate),[2] 0.076 for poly(*n*-butyl methacrylate),[3] 0.185 for poly(styrene),[4] and 0.052 for poly(vinyl acetate).[4] NMR spectra were obtained on either a 400 MHz, 500 MHz or 600 MHz Bruker Avance III spectrometer. ^{1}H and ^{13}C chemical shifts are reported as δ (in ppm) and referenced to the residual proton signal and to the ^{13}C signal of the deuterated solvent, respectively. The following abbreviations have been used for multiplicities: s (singlet), d (doublet), t (triplet), m (unresolved multiplet), br (broad). Solution magnetic moments were determined *via* NMR spectroscopy using Evans' method.[5] Elemental analyses were performed by Stephen Boyer at London Metropolitan University.

X-Ray diffraction data was collected on an Agilent SuperNova diffractometer fitted with an Atlas CCD detector with Mo-K_α radiation (λ = 0.7107 Å) or Cu-K_α radiation (λ = 1.5418 Å). Crystals were mounted under paratone on MiTeGen loops. The structures were solved by direct methods using SHELXS or SHELXT interfaced through Olex2 and refined by full-matrix least-squares on F2 using SHELXL, interfaced through Olex2.[6–8] Molecular graphics for all structures were generated using POV-RAY, POVLabel and Ortep.

5.2 Materials

Solvents used were obtained from a solvent purification system (Innovative Technologies) consisting of columns of alumina and copper catalyst and were further degassed by three freeze-pump-thaw cycles prior to use. Benzene-d_6 and THF-d_8 were dried by stirring over sodium/benzophenone, before being collected by distillation and degassed by three freeze-pump-thaw cycles. Chloroform-d_1 was used as received. Styrene (Sty), vinyl acetate (VAc), methyl methacrylate (MMA), methyl acrylate (MA), *tert*-butyl methacrylate (^{t}BuMA), *n*-butyl methacrylate (^{n}BuMA) and isoprene (IP) were dried by stirring over calcium hydride for a minimum of 24 hours, before being vacuum transferred and stored at -35 °C. 2,2'-Azobis(4-methoxy-2,4-dimethylvaleronitrile) (V-70, Wako) was suspended in dry acetone at -10°C, stirred vigorously for ca. 30 minutes before collection by filtration and drying *in vacuo* followed by storage at -35 °C under an inert atmosphere. At large scale V-70 should be used with considerable caution. 2,2'-Azobis(2-methylpropionitrile) (AIBN) and dimethyl 2,2'-azobis(2-methylpropionate) (V-601, Wako) were recrystallised from DCM/hexane, dried under vacuum and stored at -35 °C.

5.3 Complex Synthesis

5.3.1 Ligands

5.3.1.1 Synthesis of $^{t\text{-}Bu,t\text{-}Bu,NMe2}[O_2NN']H_2$ (Lig1H_2)

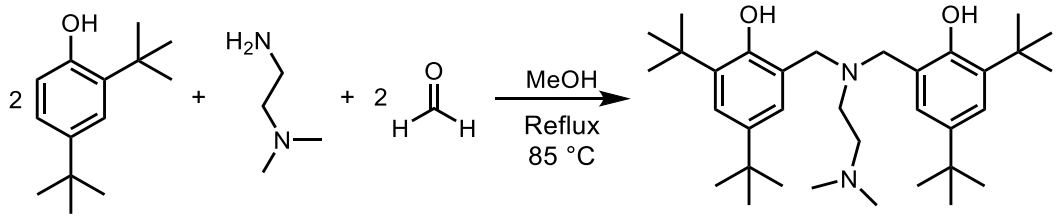

Lig1H_2 was synthesised following a modified literature procedure.[9,10] 2,4-Di-*tert*-butylphenol (6.19 g, 30 mmol) was weighed into a round-bottom flask. To this, N,N'-dimethylethylenediamine (1.65 mL, 15 mmol), formaldehyde (3.5 mL, 42.0 mmol) and methanol (10 mL, solvent) were added. The contents were stirred and heated at reflux (85

°C) overnight. A white precipitate formed. After this period of time, the flask was cooled to room temperature, and the precipitate was filtered, washed with ice cold methanol and dried under vacuum to give a white powder (5.17 g, 67%). ^{1}H NMR (500 MHz, $CDCl_3$) δ 9.80 (s, 2H), 7.22 (s, 2H), 6.90 (s, 2H), 3.62 (s, 4H), 2.57-2.68 (m, 4H), 2.34 (s, 6H), 1.41 (s, 18H), 1.29 (s, 18H). ^{13}C NMR (500 MHz, $CDCl_3$) δ 153.3, 140.1, 136.0, 124.8, 123.3, 121.6, 56.6, 55.9, 49.0, 44.9, 35.0, 34.0, 31.7, 29.5.

5.3.1.2 Synthesis of $^{Me,Me,NMe2}[O_2NN']H_2$ (Lig2H_2)

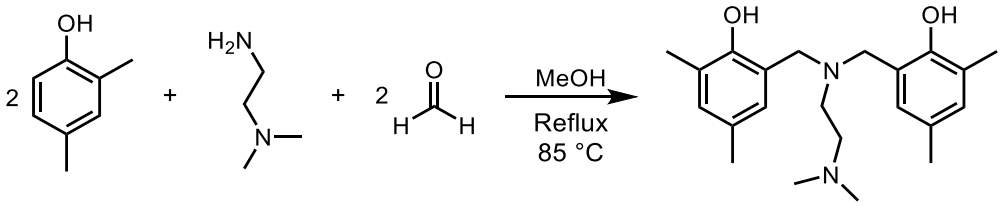

Lig2H_2 was synthesised following a modified literature procedure.[10] 2,4-Dimethylphenol (3.66 g, 30 mmol) was weighed into a round-bottom flask. To this, N,N'-dimethylethylenediamine (1.65 mL, 15 mmol), formaldehyde (3.5 mL, 42.0 mmol) and methanol (10 mL, solvent) were added. The contents were stirred and heated at reflux (85 °C) overnight. A white precipitate formed. After this period of time, the flask was cooled to room temperature, and the precipitate was filtered, washed with ice cold methanol and dried under vacuum to give a white powder (4.60 g, 86%). ^{1}H NMR (500 MHz, $CDCl_3$) δ 9.45 (s, 2H), 6.87 (s, 2H), 6.69 (s, 2H), 3.60 (s, 4H), 2.57 (s, 4H), 2.33 (s, 6H), 2.21 (s, 12H). ^{13}C NMR (500 MHz, $CDCl_3$) δ 152.6, 131.2, 128.2, 127.5, 125.4, 121.6, 56.4, 56.0, 49.1, 45.0, 20.4, 16.1.

5.3.1.3 Synthesis of $^{Cl,Cl,NMe2}[O_2NN']H_2$ (Lig3H_2)

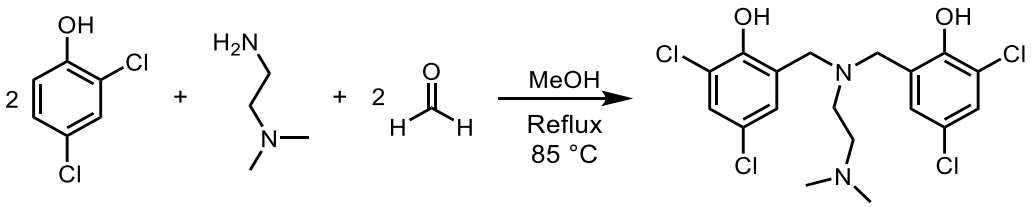

Lig3H_2 was synthesised following a modified literature procedure.[11] 2,4-Dichlorophenol (4.89 g, 30 mmol) was weighed into a round-bottom flask. To this, N,N'-dimethylethylenediamine

(1.65 mL, 15 mmol), formaldehyde (3.5 mL, 42.0 mmol) and methanol (10 mL, solvent) were added. The contents were stirred and heated at reflux (85 °C) overnight. A white precipitate formed. After this period of time, the flask was cooled to room temperature, and the precipitate was filtered, washed with ice cold methanol and dried under vacuum to give a white powder (3.14 g, 58%). ^{1}H NMR (500 MHz, $CDCl_3$) δ 7.29 (d, 2H), 7.28 (s, 2H), 6.94 (s, 2H), 3.66 (s, 4H), 2.66 (s, 4H), 2.40 (s, 6H). ^{13}C NMR (500 MHz, $CDCl_3$) δ 150.6, 128.6, 128.5, 124.7 , 124.3, 121.0, 55.5, 55.1, 18.9, 11.6.

5.3.2 Iron Complexes

The precursor [Fe(N($SiMe_3$)$_2$)$_2$THF] was synthesised following a modified literature procedure.[12] A large ampoule was charged with $FeBr_2$ (4.60 g, 21.34 mmol) and LiN($SiMe_3$)$_2$ (7.14 g, 42.68 mmol). To this, anhydrous THF (50 mL) was added at -35 °C. The resulting brown suspension was stirred vigorously at -35 °C for 15 minutes, before being heated at reflux for 30 minutes. The volatiles were removed *in vacuo* and the pure product (a dark green oil) was collected through distillation (120 °C under full vacuum) and stored under an inert atmosphere (6.43 g, 67%).

5.3.2.1 Synthesis of $^{t\text{-}Bu,t\text{-}Bu,NMe2}$[$O_2$NN']Fe(II) (Fe1)

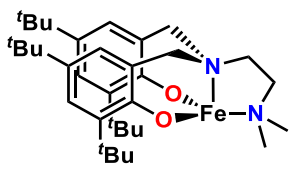

The ligand **Lig1**H_2 (0.31 g, 0.60 mmol) was taken up in anhydrous toluene (10 mL) in a glovebox. To this was added, with stirring, a solution of [Fe(N($SiMe_3$)$_2$)$_2$THF] (0.27 g, 0.60 mmol) in toluene (5 mL). The resultant pale green solution was stirred vigorously at ambient temperature for 30 minutes. After this time, the extremely air-sensitive solid was isolated through the removal of volatiles *in vacuo* (0.28 g, 0.48 mmol, 81%). ^{1}H NMR (500 MHz, C_6D_6) δ: 88.11 (br), 64.30 (br), 43.45 (br), 39.39 (br), 26.58 (br), 20.83 (br), 8.03 (br), 4.99 (br), 2.46 (br), -1.49 (br). μ_{eff} (Evans' Method, C_6D_6) = 4.8 μ_B. Analysis Calculated for $C_{34}H_{54}FeN_2O_2$: C, 70.57; H, 9.41; N, 4.84. Found: C, 70.51; H, 9.58; N, 4.88.

5.3.3 Titanium Complexes

The precursor $TiCl_3(THF)_3$ was synthesised by Dr Benjamin R. M. Lake following a modified literature procedure and subsequently stored under an inert atmosphere.[13]

5.3.3.1 Synthesis of $^{t\text{-}Bu,t\text{-}Bu,NMe2}[O_2NN']TiCl(THF)$ (Ti1)

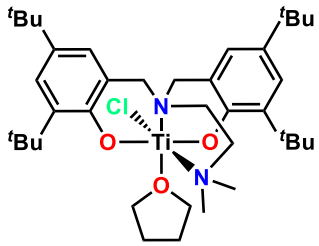

Synthesised following a modified literature procedure.[14] A solution of **Lig1**H_2 (0.60 g, 1.14 mmol) and Li(HMDS) (0.38 g, 2.27 mmol) in THF (5 ml) was stirred at ambient temperature for 30 minutes. To this was added a suspension of $TiCl_3(THF)_3$ (0.42 g, 1.14 mmol) in THF (5 ml). The resulting mixture was stirred for 4 hours. After this time, the volatiles were removed *in vacuo*, and the residue taken-up in to toluene (15 ml), filtered through Celite and the solvent removed *in vacuo* to yield a pale yellow crystalline solid (0.62 g, 0.92 mmol, 80 %). Complex was found to be essentially NMR-silent in both d_8-THF and C_6D_6. μ_{eff} (Evans' Method, C_6D_6) = 1.7 μ_B.

5.3.3.2 Synthesis of $^{Me,Me,NMe2}[O_2NN']TiCl(THF)$ (Ti2)

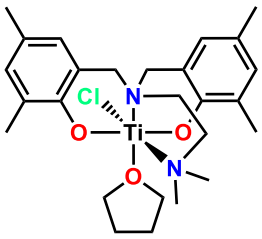

A solution of **Lig2**H_2 (0.20 g, 0.56 mmol) and Li(HMDS) (0.19 g, 1.12 mmol) in toluene (10 ml) was stirred at ambient temperature for 30 minutes. To this was added a suspension of $TiCl_3(THF)_3$ (0.21 g, 0.56 mmol) in THF (5 ml). The resulting mixture was stirred for 24 hours. After this time, the volatiles were removed *in vacuo*, and the residue taken-up in to toluene (15 ml), filtered through Celite and the solvent removed *in vacuo*. Recrystallisation of the complex from THF/*n*-hexane at -35 °C produced the pure complex as pale yellow crystals (0.26 g, 0.51 mmol, 91 %). Single crystals of **Ti2** suitable for x-ray diffraction analysis could be obtained by the vapour diffusion of n-hexane in to a concentrated THF solution. Single crystals of **2(μ-Cl)$_2$** could be obtained on prolonged standing of a concentrated solution of **2** in C_6D_6. ^{1}H NMR (500 MHz, C_6D_6) δ 6.99 (br), 6.59 (br), 4.60 (br), 3.44 (br), 2.33 (br), 2.22

(br), 2.16 (br), 1.79 (br) ppm. μ_{eff} (Evans' Method, d_8-THF) = 1.6 μ_B. Analysis Calculated for $C_{26}H_{38}ClN_2O_3Ti$: C, 61.24; H, 7.51; N, 5.49. Found: C, 61.09; H, 7.61; N, 5.41.

5.3.3.3 Synthesis of ^{Cl,Cl,NMe2}[O_2NN']TiCl(THF) (Ti3)

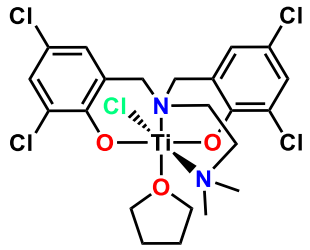

A solution of **Lig3**H_2 (0.20 g, 0.46 mmol), Ti(HMDS)$_3$ (0.16 g, 0.30 mmol) and $TiCl_3(THF)_3$ (0.056 g, 0.15 mmol) in THF (5 ml) was stirred at ambient temperature for 1 hour. After this time, the volatiles were removed *in vacuo*, and the residue taken-up in to a minimum of THF. Precipitation with an excess of *n*-hexane gave the pure product as a pale yellow crystalline solid (0.19 g, 0.32 mmol, 70 %). ^{1}H NMR (500 MHz, C_6D_6) δ 7.35 (br), 7.11 (br), 6.60 (br), 6.43 (br), 4.18 (br), 2.99 (br), 2.54 (br), 2.21 (br), 1.81 (br), 1.65 (br) ppm. μ_{eff} (Evans' Method, d_8-THF) = 1.7 μ_B. Analysis Calculated for $C_{22}H_{26}Cl_5N_2O_3Ti$: C, 44.67; H, 4.43; N, 4.74. Found: C, 44.59; H, 4.56; N, 4.75.

5.3.3.4 Synthesis of $^{t\text{-}Bu,t\text{-}Bu,THF}$[$O_2$NO']TiCl(THF) (Ti4)

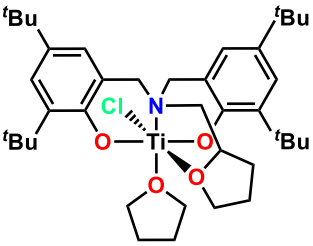

A solution of **Lig4**H_2 (0.20 g, 0.37 mmol) and Li(HMDS) (0.12 g, 0.74 mmol) in toluene (10 ml) was stirred at ambient temperature for 30 minutes. To this was added a suspension of $TiCl_3(THF)_3$ (0.14 g, 0.37 mmol) in THF (5 ml). The resulting mixture was stirred for 24 hours. After this time, the volatiles were removed *in vacuo*, and the residue taken-up in to toluene (15 ml), filtered through Celite and the solvent removed *in vacuo*. Recrystallisation of the complex from toluene/*n*-hexane at reflux produced the pure complex as a pale yellow crystalline solid (0.22 g, 0.31 mmol, 84 %). Single crystals of **Ti4** suitable for x-ray diffraction analysis could be obtained by the vapour diffusion of *n*-hexane in to a concentrated toluene solution. Complex was found to be essentially NMR-silent in both d_8-THF and C_6D_6. μ_{eff} (Evans' Method, C_6D_6) = 1.7 μ_B. Analysis Calculated for $C_{39}H_{61}ClNO_4Ti$: C, 67.77; H, 8.90; N, 2.03. Found: C, 67.89; H, 9.01; N, 2.14.

5.3.3.5 Synthesis of $^{t\text{-}Bu,t\text{-}Bu,Bn}[O_2N_2]TiCl(THF)$ (Ti5)

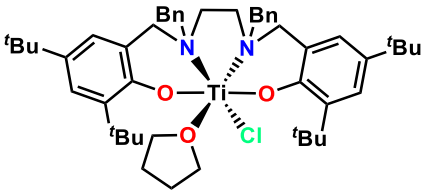

A solution of **Lig5**H_2 (0.20 g, 0.30 mmol) and Li(HMDS) (0.10 g, 0.59 mmol) in toluene (10 ml) was stirred at ambient temperature for 30 minutes. To this was added a suspension of $TiCl_3(THF)_3$ (0.11 g, 0.30 mmol) in THF (5 ml). The resulting mixture was stirred for 24 hours. After this time, the volatiles were removed *in vacuo*, and the residue taken-up in to toluene (15 ml), filtered through Celite and the solvent removed *in vacuo*. Recrystallisation of the complex from toluene/*n*-hexane at reflux produced the pure complex as a pale yellow crystalline solid (0.24 g, 0.29 mmol, 97 %). Complex was found to be essentially NMR-silent in both d_8-THF and C_6D_6. μ_{eff} (Evans' Method, C_6D_6) = 1.5 μ_B. Analysis Calculated for $C_{50}H_{70}ClN_2O_3Ti$: C, 72.32; H, 8.50; N, 3.37. Found: C, 67.62; H, 8.41; N, 3.36.[15]

5.3.3.6 Synthesis of $^{t\text{-}Bu,t\text{-}Bu}[O_3N]Ti(THF)$ (Ti6)

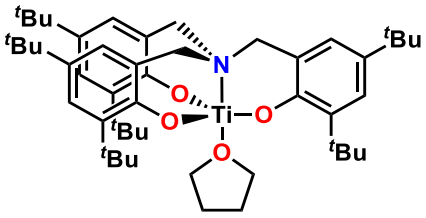

A solution of **Lig6**H_3 (0.32 g, 0.48 mmol) and Li(HMDS) (0.24 g, 1.43 mmol) in toluene was stirred at ambient temperature for 2 hours. Solid $TiCl_3(THF)_3$ (0.18 g, 0.48 mmol) was then added and the resulting suspension was stirred at ambient temperature for 18 hours. After this time, the volatiles were removed *in vacuo*, and the residue taken-up in to toluene (15 ml), filtered through Celite and the solvent removed *in vacuo*. The resulting off-white solid was washed with *n*-hexane (2 x 10 ml) and dried *in vacuo* (0.33 g, 0.42 mmol, 89 %).^{1}H NMR (500 MHz, C_6D_6) δ 7.40 (br), 5.26 (br), 4.86 (br), 4.65 (br), 1.58 (br), 1.34 (br) ppm. μ_{eff} (Evans' Method, C_6D_6) = 1.6 μ_B. Analysis Calculated for $C_{49}H_{74}NO_4Ti$: C, 74.59; H, 9.45; N, 1.78. Found: C, 68.99; H, 9.12; N, 2.04.[15]

5.3.3.7 Synthesis of $^{Me,Me}[O_3N]Ti$ (Ti7)

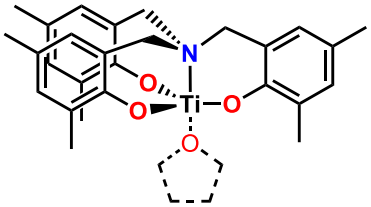

Synthesised using a modified literature procedure.[16] A solution of **Lig7**H_3 (0.20 g, 0.48 mmol) and Li(HMDS) (0.24 g, 1.43 mmol) in toluene was stirred at ambient temperature for 2 hours. Solid $TiCl_3(THF)_3$ (0.18 g, 0.48 mmol) was then added and the resulting suspension was stirred at ambient temperature for 18 hours. After this time, the volatiles were removed *in vacuo*, and the residue taken-up in to toluene (15 ml), filtered through Celite and the solvent removed *in vacuo*. The resulting violet solid was washed with *n*-hexane (2 x 10 ml) and dried *in vacuo* (0.18 g, 0.39 mmol, 82 %). ^{1}H NMR (500 MHz, C_6D_6) δ 6.80 (s, 3H, ArH), 6.61 (d, J = 1.8 Hz, 1H, ArH), 6.53 (s, 2H, ArH), 3.70 (br), 3.04 (br), 2.19 (s, 9H, CH_3), 2.17 (s, 6H, CH_3), 2.11 (s, 3H, CH_3) ppm. $^{13}C(^1H)$ NMR (126 MHz, C_6D_6) δ 133.0, 131.6, 130.1, 129.9, 127.4, 126.0, 125.0, 123.9, 123.4, 60.2, 59.7, 20.8, 20.5, 19.3, 16.5 ppm. μ_{eff} (Evans' Method, C_6D_6) = 0 μ_B (diamagnetic). Analysis Calculated for $C_{27}H_{30}NO_3Ti.2H_2O$: C, 64.80; H, 6.85; N, 2.80. Found: C, 64.34; H, 6.90; N, 2.85.

5.4 Polymer Synthesis

In all polymerisations involving styrene, methacrylates and isoprene, conversion was determined by integration of the monomer *versus* polymer backbone resonances in the ^{1}H NMR spectrum of the crude polymer product in $CDCl_3$. In all polymerisations involving vinyl acetate, conversion was determined gravimetrically. At the end of the polymerisation, excess monomer and solvent were removed *in vacuo*. The remainder of the reaction mixture was taken-up in a small volume of THF (ca. 2 ml) and left to evaporate in a vial overnight. The remaining mass was compared to the initial mass of complex and initiator.

5.4.1 General Polymerisation Procedure

In a glovebox, a small ampoule was charged with a microstirrer bar, complex (20.0 µmol), monomer (2.00 mmol), solvent (solvent:monomer, 1:1 v/v) and V-70 (20.0 µmol). The ampoule was brought out of the glovebox and heated for a period of time with a stir-rate of

500 rpm. After this time, the ampoule was cooled rapidly to ambient temperature, and an aliquot removed for analysis by ^{1}H NMR spectroscopy to determine monomer conversion. The remainder of the reaction mixture was taken-up in a small volume of THF (ca. 2 ml), and the polymer precipitated by addition of the THF solution to acidified methanol (MeOH:$HCl_{(aq)}$, ca. 75 ml:1 ml). The polymer was collected by filtration and dried *in vacuo*. The polymer was then analysed by GPC. It is acknowledged that precipitation of the polymer may remove oligomers from the sample and these will therefore not appear in the GPC analysis.

In some cases, too little purified polymer was obtained in order to be able to analyse the sample using GPC. Whilst it was possible to analyse a crude sample, this was challenging and gave unreliable results because of low monomer conversion, and residual monomer and complex peaks in the chromatography data.

5.4.2 Representative Iron Polymerisation Procedure

$^{t\text{-}Bu,t\text{-}Bu,NMe2}$[$O_2$NN']Fe(II), **Fe1** (0.012 g, 0.02 mmol), V-70 (0.006 g, 0.02 mmol), methyl methacrylate (0.200 g, 2 mmol) and toluene (0.37 g, 1:2 v/v) were added to an ampoule containing a microstirrer bar under inert atmosphere, which was then sealed and heated at 75 °C with stirring for 30 minutes. ^{1}H NMR spectroscopic analysis of the crude residue indicated 34% monomer conversion. Precipitation into acidified methanol gave white poly(methyl methacrylate), with M_n = 14800 and Đ = 1.56.

5.4.3 Representative Titanium Polymerisation Procedure

$^{t\text{-}Bu,t\text{-}Bu,NMe2}$[$O_2$NN']TiCl(THF), **Ti1** (0.014 g, 0.02 mmol), V-70 (0.006 g, 0.02 mmol), methyl methacrylate (0.200 g, 2 mmol) and toluene (0.185 g, 1:1 v/v) were added to an ampoule containing a microstirrer bar under inert atmosphere, which was then sealed and heated at 80 °C with stirring for 60 minutes. ^{1}H NMR spectroscopic analysis of the crude residue indicated 88% monomer conversion. Precipitation into acidified methanol gave white poly(methyl methacrylate), with M_n = 37800 and Đ = 1.13.

5.4.4 General Polymerisation Kinetics Procedure

In a glovebox, a vial was charged with complex (80.0 μmol), monomer (8.00 mmol), solvent (solvent:monomer, 1:1 v/v) and V-70 (80.0 μmol). The mixture in the vial was shaken vigorously for a few seconds, to ensure all the solid components had dissolved. The mixture was then evenly distributed into four ampoules, each containing a microstirrer bar. The ampoules were brought out of the glovebox and heated for a period of time with a stir-rate of 500 rpm. At pre-determined intervals during the polymerisation, an ampoule was removed from the heat source and cooled rapidly to ambient temperature. An aliquot was removed for analysis by ^{1}H NMR spectroscopy to determine monomer conversion. The remainder of the reaction mixture was taken-up in a small volume of THF (ca. 2 ml), and the polymer precipitated by addition of the THF solution to acidified methanol (MeOH:$HCl_{(aq)}$, ca. 75 ml:1 ml). The polymer was collected by filtration and dried *in vacuo*. The polymer was then analysed by GPC.

5.4.5 Representative Co-Polymerisation of MMA and IP

$^{t\text{-}Bu,t\text{-}Bu,NMe2}$[$O_2$NN']TiCl(THF), **Ti1** (0.014 g, 0.02 mmol), V-70 (0.006 g, 0.02 mmol), methyl methacrylate (0.200 g, 2 mmol), toluene (0.185 g, 1:1 v/v) and isoprene (0.136 g, 2 mmol) were added to an ampoule containing a microstirrer bar under inert atmosphere, which was then sealed and heated at 80 °C with stirring for 180 minutes. ^{1}H NMR spectroscopic analysis of the crude residue indicated 91% MMA conversion and negligible IP conversion.

5.5 X-Ray Crystallographic Data

5.5.1 $^{t\text{-}Bu,t\text{-}Bu,NMe2}[O_2NN']Fe(II)$ (Fe1)

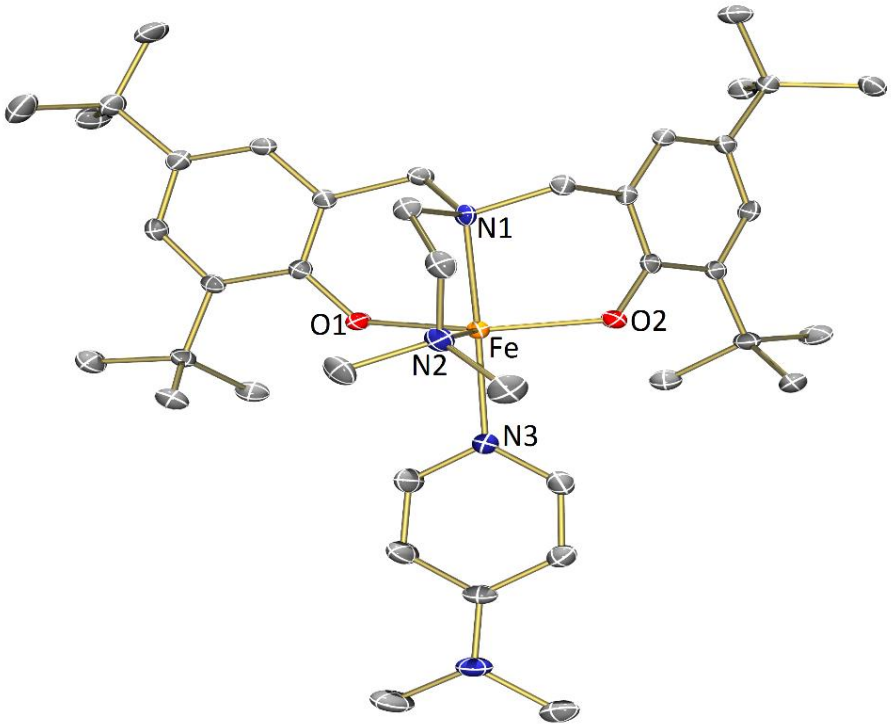

Figure 5.1 - Molecular structure of complex **Fe1·DMAP** with ellipsoids set at the 50% probability level. Hydrogen atoms and co-crystallised MeCN have been omitted for clarity.

Table 5.1 - Crystal data and structure refinement.

CCDC code	1550332	
Formula	$C_{43}H_{67}FeN_5O_2$	
Formula weight	741.86	
Size	0.397 x 0.096 x 0.073 mm	
Crystal morphology	Pale yellow needle	
Temperature	120.01(10) K	
Wavelength	0.71073 Å [Mo-K_α]	
Crystal system	Monoclinic	
Space group	$P2_1/c$	
Unit cell dimensions	a = 12.0706(7) Å	α = 90°
	b = 19.5492(10) Å	β = 102.817(5)°

	c = 18.0680(8) Å γ = 90°
Volume	4157.3(4) Å^3
Z	4
Density (calculated)	1.185 Mg/m^3
Absorption coefficient	0.403 mm^{-1}
F(000)	1608
Data collection range	3.093 ≤ θ ≤ 29.735°
Index ranges	-16 ≤ h ≤13, -26 ≤ k ≤ 26, -24 ≤ l ≤ 23
Reflections collected	47650
Independent reflections	10676 [R(int) = 0.0844]
Observed reflections	7586 [I >2σ(I)]
Absorption correction	multi-scan
Max. and min. transmission	0.98719 and 0.98719
Refinement method	Full
Data / restraints / parameters	10676 / 0 / 477
Goodness of fit	1.051
Final R indices [I >2σ(I)]	R_1 = 0.0629, wR_2 = 0.114
R indices (all data)	R_1 = 0.1004, wR_2 = 0.1295
Largest diff. peak and hole	0.486 and -0.392e.Å^{-3}

5.5.2 $^{Me,Me,NMe2}[O_2NN']TiCl(THF)$ (Ti2)

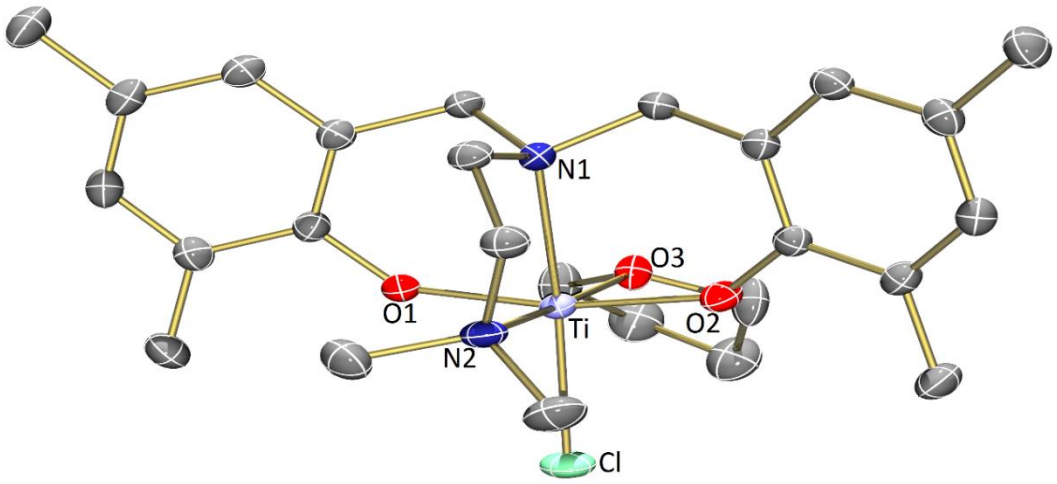

Figure 5.2 - Molecular structure of **Ti2** with ellipsoids set at the 50% probability level. Hydrogen atoms and disordered solvent have been omitted for clarity.

Note. Residual electron density could be modelled as part of a molecule of THF. 'Growing' the THF reveals that the THF molecule is in fact disordered over two positions about an inversion centre. One atom of the THF (C27B) was found to be common to both components of the disorder, and hence was assigned an SOF of 1. The other atoms (O4, C28, C29) were assigned SOFs of 0.5. A number of 'FREE' and 'BIND' commands were required to allow chemically sensible placement of H atoms.

Table 5.2 - Crystal data and structure refinement.

CCDC code	1889717	
Formula	$C_{56}H_{84}Cl_2N_4O_7Ti_2$	
Formula weight	1091.91	
Size	0.2663 x 0.0972 x 0.0344 mm	
Crystal morphology	Yellow plate	
Temperature	120.00(10) K	
Wavelength	1.54184 Å [Cu-K_α]	
Crystal system	Monoclinic	
Space group	$P2_1/c$	
Unit cell dimensions	a = 8.61539(7) Å	α = 90°
	b = 15.80257(11) Å	β = 96.8755(8)°
	c = 20.58955(17) Å	γ = 90°

Volume	2783.01(4) $Å^3$
Z	2
Density (calculated)	1.303 Mg/m^3
Absorption coefficient	3.751 mm^{-1}
F(000)	1164
Data collection range	$3.535 \leq \theta \leq 76.187°$
Index ranges	$-10 \leq h \leq 10$, $-19 \leq k \leq 16$, $-25 \leq l \leq 25$
Reflections collected	44749
Independent reflections	5809 [*R*(int) = 0.0718]
Observed reflections	5526 [$I > 2\sigma(I)$]
Absorption correction	multi-scan
Max. and min. transmission	1 and 0.62598
Refinement method	Full
Data / restraints / parameters	5809 / 3 / 346
Goodness of fit	1.042
Final *R* indices [$I > 2\sigma(I)$]	$R_1 = 0.0491$, $wR_2 = 0.1365$
R indices (all data)	$R_1 = 0.0507$, $wR_2 = 0.1386$
Largest diff. peak and hole	0.604 and $-0.551 e.Å^{-3}$

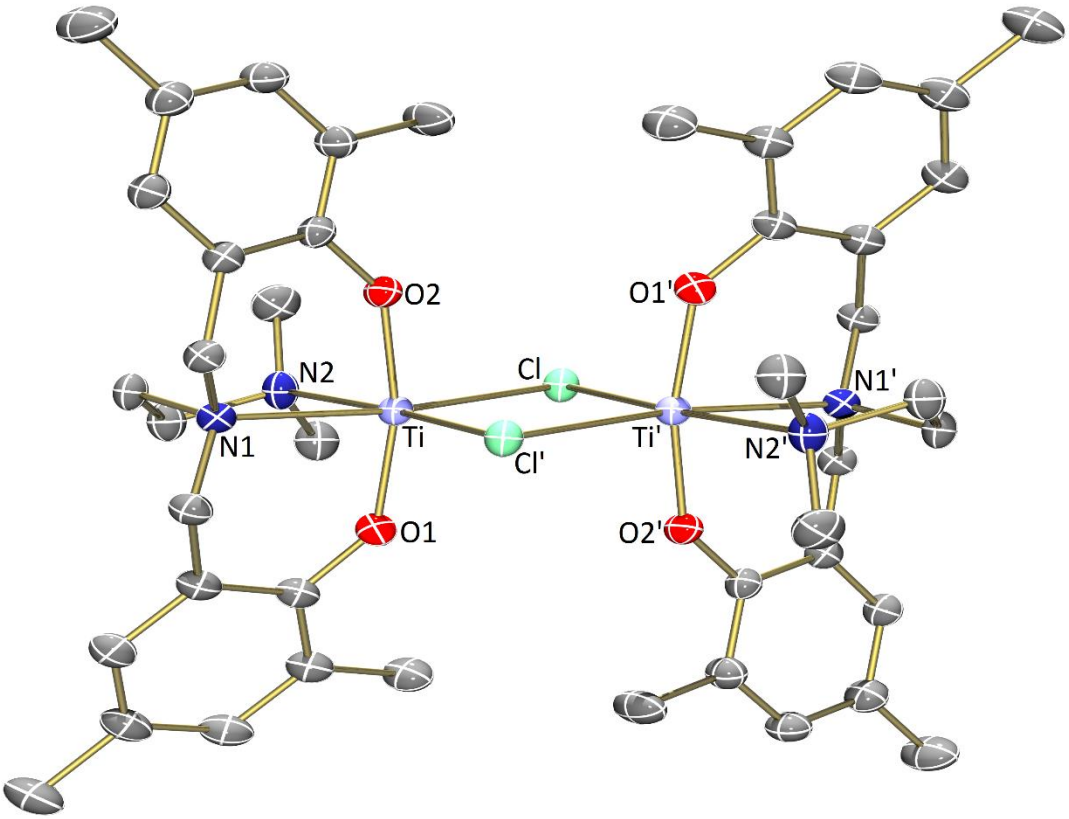

Figure 5.3 - Molecular structure of **Ti2(μ-Cl)$_2$** with ellipsoids set at the 50% probability level. Hydrogen atoms have been omitted for clarity.

Table 5.3 - Crystal data and structure refinement.

CCDC code	1889718	
Formula	$C_{44}H_{60}Cl_2N_4O_4Ti_2$	
Formula weight	875.66	
Size	0.217 x 0.0685 x 0.0393 mm	
Crystal morphology	Light green prism	
Temperature	120.00(10) K	
Wavelength	1.54184 Å [Cu-K_α]	
Crystal system	Monoclinic	
Space group	$P2_1/n$	
Unit cell dimensions	a = 8.24598(11) Å	α = 90°
	b = 19.1270(3) Å	β = 90.3456(14)°
	c = 13.8373(2) Å	γ = 90°
Volume	2182.38(6) Å^3	

Z	2
Density (calculated)	1.333 Mg/m^3
Absorption coefficient	4.599 mm^{-1}
F(000)	924
Data collection range	$3.943 \leq \theta \leq 76.546°$
Index ranges	$-8 \leq h \leq 10$, $-24 \leq k \leq 23$, $-17 \leq l \leq 17$
Reflections collected	44176
Independent reflections	4553 [*R*(int) = 0.0781]
Observed reflections	4270 [$I > 2\sigma(I)$]
Absorption correction	multi-scan
Max. and min. transmission	1 and 0.51912
Refinement method	Full
Data / restraints / parameters	4553 / 0 / 259
Goodness of fit	1.066
Final *R* indices [$I > 2\sigma(I)$]	$R_1 = 0.0481$, $wR_2 = 0.1325$
R indices (all data)	$R_1 = 0.0501$, $wR_2 = 0.1347$
Largest diff. peak and hole	0.856 and -0.565e.$Å^{-3}$

5.5.3 ^{Cl,Cl,NMe2}[O_2NN']TiCl(THF) (Ti3)

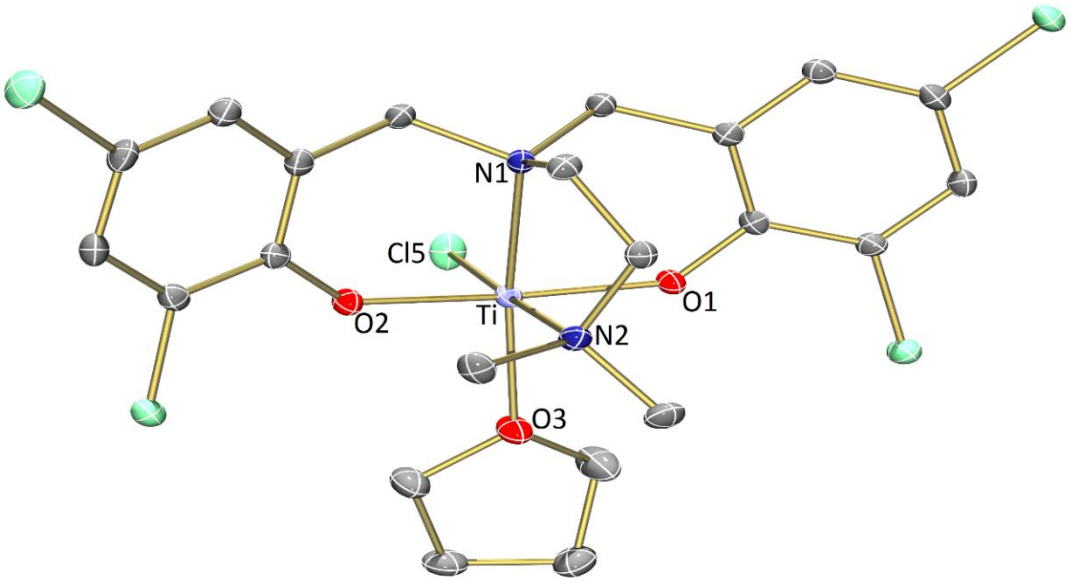

Figure 5.4 - Molecular structure of **Ti3** with ellipsoids set at the 50% probability level. Hydrogen atoms and minor disorder component have been omitted for clarity.

Note. One carbon atom ('C21') of the coordinated THF molecule was found to be disordered over two positions. The two modelled sites (C21A and C21B) could be refined satisfactorily with SOFs of 0.616 and 0.384 respectively.

Table 5.4 - Crystal data and structure refinement.

CCDC code	1889719	
Formula	$C_{22}H_{26}Cl_5N_2O_3Ti$	
Formula weight	591.6	
Size	0.3517 x 0.1178 x 0.0475 mm	
Crystal morphology	Yellow prism	
Temperature	120.00(10) K	
Wavelength	0.71073 Å [Mo-K_α]	
Crystal system	Orthorhombic	
Space group	*Pbca*	
Unit cell dimensions	*a* = 15.9365(3) Å	α = 90°
	b = 14.9569(2) Å	β = 90°
	c = 21.2219(3) Å	γ = 90°
Volume	5058.45(14) Å^3	

Z	8
Density (calculated)	1.554 Mg/m^3
Absorption coefficient	0.894 mm^{-1}
F(000)	2424
Data collection range	$2.888 \leq \theta \leq 32.959°$
Index ranges	$-24 \leq h \leq 24$, $-22 \leq k \leq 22$, $-32 \leq l \leq 32$
Reflections collected	248707
Independent reflections	9356 [*R*(int) = 0.071]
Observed reflections	8471 [$I > 2\sigma(I)$]
Absorption correction	multi-scan
Max. and min. transmission	1 and 0.78809
Refinement method	Full
Data / restraints / parameters	9356 / 0 / 310
Goodness of fit	1.223
Final *R* indices [$I > 2\sigma(I)$]	$R_1 = 0.0473$, $wR_2 = 0.0869$
R indices (all data)	$R_1 = 0.0575$, $wR_2 = 0.0899$
Largest diff. peak and hole	0.634 and -0.356e.$Å^{-3}$

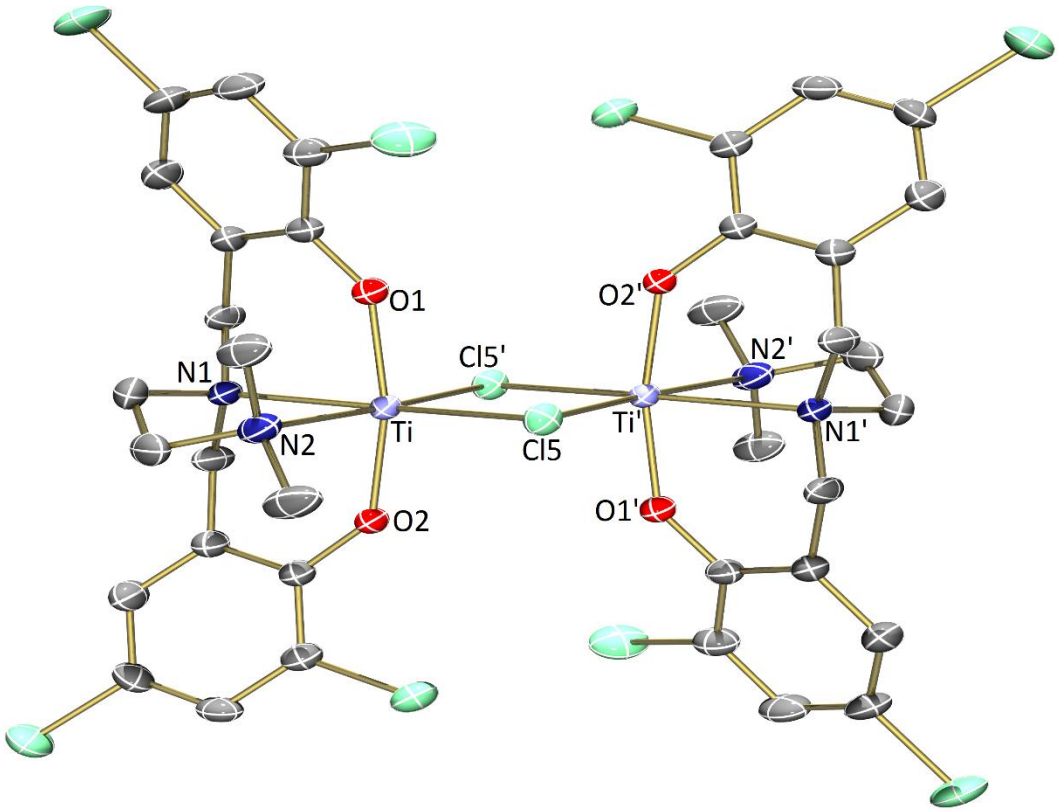

Figure 5.5 - Molecular structure of **Ti3(μ-Cl)$_2$** with ellipsoids set at the 50% probability level. Hydrogen atoms and disordered solvent have been omitted for clarity.

Note. Significant residual electron density in the vicinity of the Ti complex could be refined as 1 molecule of toluene with full positional disorder over two positions. Assignment of SOFs of 0.65 and 0.35 respectively for the two independent molecules gave stable refinement and convergence. It was necessary to refine the minor component as a rigid hexagon to ensure a chemically sensible structure was obtained.

Table 5.5 - Crystal data and structure refinement.

CCDC code	1889720
Formula	$C_{50}H_{52}Cl_{10}N_4O_4Ti_2$
Formula weight	1223.25
Size	0.3408 x 0.2758 x 0.046 mm
Crystal morphology	Green plate
Temperature	120.00(10) K
Wavelength	0.71073 Å [Mo-K_α]
Crystal system	Monoclinic

Space group	*C*2/*c*	
Unit cell dimensions	*a* = 15.1807(5) Å	α = 90°
	b = 19.7102(6) Å	β = 98.694(4)°
	c = 18.0932(7) Å	γ = 90°
Volume	5351.5(3) Å^3	
Z	4	
Density (calculated)	1.518 Mg/m^3	
Absorption coefficient	0.846 mm^{-1}	
F(000)	2504	
Data collection range	$3.076 \leq \theta \leq 29.613°$	
Index ranges	$-20 \leq h \leq 21$, $-26 \leq k \leq 25$, $-24 \leq l \leq 24$	
Reflections collected	47257	
Independent reflections	7083 [*R*(int) = 0.0677]	
Observed reflections	5393 [$I > 2\sigma(I)$]	
Absorption correction	gaussian	
Max. and min. transmission	0.953 and 0.743	
Refinement method	Full	
Data / restraints / parameters	7083 / 0 / 371	
Goodness of fit	1.088	
Final *R* indices [$I > 2\sigma(I)$]	R_1 = 0.0541, wR_2 = 0.0924	
R indices (all data)	R_1 = 0.0813, wR_2 = 0.1014	
Largest diff. peak and hole	0.435 and -0.4e.Å^{-3}	

5.5.4 $^{t\text{-}Bu,t\text{-}Bu,THF}[O_2NO']TiCl(THF)$ (Ti4)

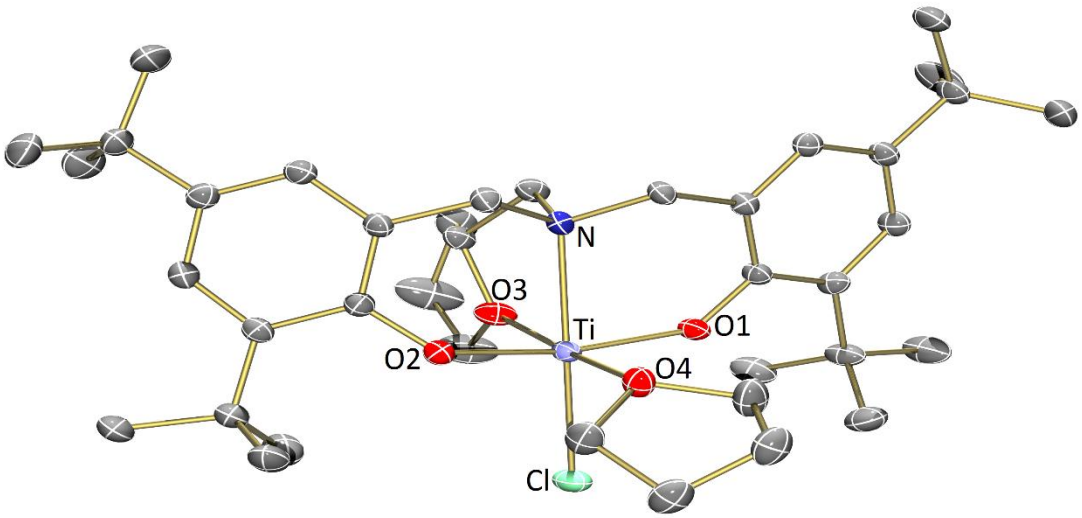

Figure 5.6 - Molecular structures **Ti4** with ellipsoids set at the 50% probability level. Hydrogen atoms, disordered solvent and minor disorder components have been omitted for clarity.

Note. Three atoms of the pendant THF donor (C32, C33 & C34) were found to be disordered over two positions, and were successfully modelled with a SOF of 0.652 (C32A, C33A & C34A) for the major component and 0.348 (C32B, C33B & C34B) for the minor component. The disorder likely originates from the use of a racemic starting material (tetrahydrofurfurylamine) and thus due to the cocrystallisation of the two possible enantiomers (R and S). In addition, further residual electron density could be modelled as a molecule of toluene, which was found to be positionally disordered over an inversion centre. Thus, the toluene was modelled with a PART -1 command and a SOF of 0.5.

Table 5.6 - Crystal data and structure refinement.

CCDC code	1889721
Formula	$C_{85}H_{130}Cl_2N_2O_8Ti_2$
Formula weight	1474.6
Size	0.661 x 0.12 x 0.023 mm
Crystal morphology	Colourless plate
Temperature	120.01(10) K
Wavelength	1.54184 Å [Cu-K_α]
Crystal system	Monoclinic
Space group	$P2_1/c$

Unit cell dimensions	a = 12.7740(4) Å	α = 90°
	b = 20.1276(6) Å	β = 94.834(3)°
	c = 16.5375(4) Å	γ = 90°
Volume	4236.8(2) Å^3	
Z	2	
Density (calculated)	1.156 Mg/m^3	
Absorption coefficient	2.586 mm^{-1}	
F(000)	1592	
Data collection range	3.466 ≤ θ ≤ 76.105°	
Index ranges	-15 ≤ h ≤16, -25 ≤ k ≤ 25, -10 ≤ l ≤ 20	
Reflections collected	34874	
Independent reflections	8785 [R(int) = 0.0855]	
Observed reflections	7216 [I >2σ(I)]	
Absorption correction	gaussian	
Max. and min. transmission	1 and 0.348	
Refinement method	Full	
Data / restraints / parameters	8785 / 4 / 519	
Goodness of fit	1.038	
Final R indices [I >2σ(I)]	R_1 = 0.0567, wR_2 = 0.1446	
R indices (all data)	R_1 = 0.069, wR_2 = 0.1549	
Largest diff. peak and hole	0.466 and -0.721e.Å^{-3}	

5.5.5 $^{t\text{-}Bu,t\text{-}Bu}[O_3N]Ti(THF)$ (Ti6)

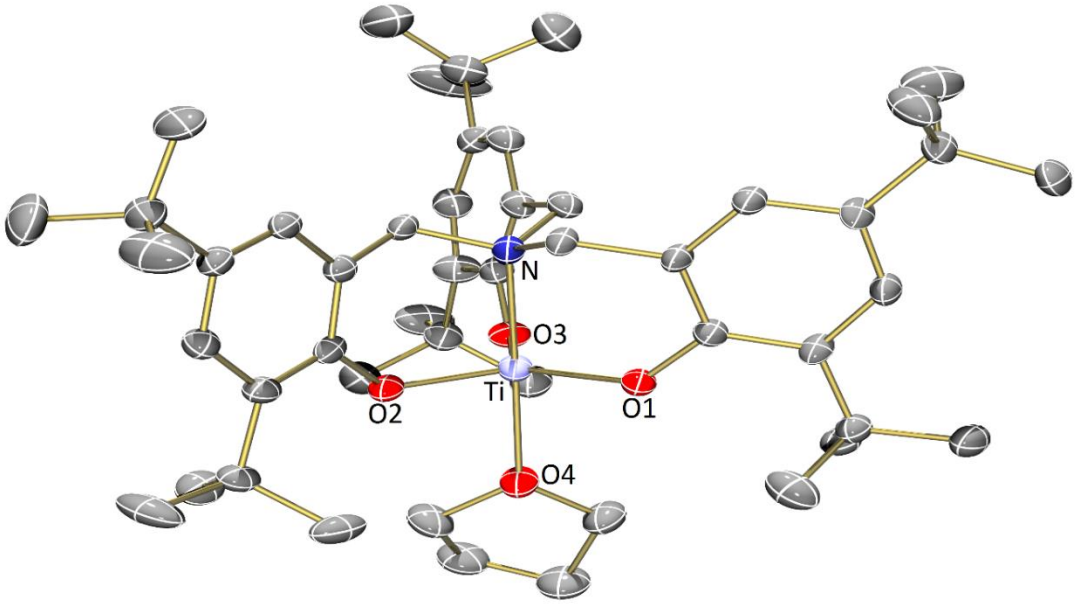

Figure 5.7 - Molecular structure of **Ti6** with ellipsoids set at the 50% probability level. Hydrogen atoms and the minor disorder component have been omitted for clarity.

Note. This complex is structurally analogous to a vanadium(III) complex reported by Goldschmidt, Kol and co-workers.[17] *In this report, the overall quality of the reported structure was low, which was explained to be mainly due to twinning effects. For our dataset, no suitable twin laws could be discerned. Rather, the structure was simply found to be heavily positionally disordered (40% disorder) over two positions. While the donor THF, Ti, N atom and most of the tert-butyl groups were common to both components of the disorder, most of the phenolate ring atoms were disordered, as were the benzylic carbon atoms and phenolate O atoms. Free refinement of the two disorder components (which were both clear in the diff. map) gave convergence at SOFs of 0.61 and 0.39 respectively (for the major and minor components, PART 1 and PART 2). Use of SADI restraints on the disordered components ensured that bond parameters were chemically sensible. In one case, it was unfortunately necessary to use an EADP constraint (since the use of softer SIMU, DELU, ISOR constraints was ineffective). Additionally, one of the tert-butyl groups was found to be disordered over two positions. Refinement of the two disorder components with SOFs of 0.72 and 0.28 gave a satisfactory outcome.*

Table 5.7 - Crystal data and structure refinement.

CCDC code	1889722	
Formula	$C_{49}H_{74}NO_4Ti$	
Formula weight	788.99	
Size	0.263 x 0.105 x 0.033 mm	
Crystal morphology	Colourless plate	
Temperature	120.01(10) K	
Wavelength	1.54184 Å [Cu-K_α]	
Crystal system	Triclinic	
Space group	*P*-1	
Unit cell dimensions	*a* = 10.3781(2) Å	α = 91.943(2)°
	b = 11.0454(2) Å	β = 100.093(2)°
	c = 20.6189(5) Å	γ = 96.4710(10)°
Volume	2308.67(8) $Å^3$	
Z	2	
Density (calculated)	1.135 Mg/m^3	
Absorption coefficient	1.884 mm^{-1}	
F(000)	858	
Data collection range	$4.034 \leq \theta \leq 76.395°$	
Index ranges	$-11 \leq h \leq 12$, $-13 \leq k \leq 13$, $-25 \leq l \leq 25$	
Reflections collected	44555	
Independent reflections	9466 [*R*(int) = 0.0703]	
Observed reflections	8262 [$I > 2\sigma(I)$]	
Absorption correction	gaussian	
Max. and min. transmission	1 and 0.653	
Refinement method	Full	
Data / restraints / parameters	9466 / 14 / 711	
Goodness of fit	1.087	
Final *R* indices [$I > 2\sigma(I)$]	R_1 = 0.068, wR_2 = 0.1763	
R indices (all data)	R_1 = 0.0761, wR_2 = 0.183	
Largest diff. peak and hole	0.755 and -0.624e.$Å^{-3}$	

5.6 Computational Procedures & Data

Initial structures were built using Chemcraft and used as starting points for geometry optimisations. The computational work was carried out using the Gaussian09.E01 suite of programs.[18] The geometry optimisations were performed without any symmetry constraint using the M06, B3LYP and BP86 functionals. The SVP basis functions were used for all atoms. The unrestricted formulation was used for all open-shell molecules, yielding only minor spin contamination. Maximum deviations for $\langle S^2 \rangle$ at convergence were 0.766 (vs the theoretical value of 0.75) for spin doublets and 2.013 (vs 2.00) for triplets. All final geometries were characterised as local minima by verifying that all second derivatives of the energy were positive. Thermochemical corrections were obtained at 298.15 K on the basis of frequency calculations, using the standard approximations (ideal gas, rigid rotor and harmonic oscillator). A correction of 1.95 kcal/mol was applied to all G values to change the standard state from the gas phase (1 atm) to solution (1 M).[19] Molecular graphics for all structures were generated using Chemcraft.

In all calculations PMMA (with degree of polymerisation "n") is modelled as a single monomer unit, in which the rest of the polymer chain ("n-1" monomer units) is replaced by a hydrogen atom.

Some of the calculations were performed as broken symmetry singlets, which involved optimising a structure as an overall singlet but specifying local spin density. This calculation was done over several stages. Firstly, the triplet state structure was optimised. Then, the structure was "split" into two fragments, the metal complex and the alkyl species, with local spin density on each fragment. This fragmented structure was used to perform a broken symmetry singlet fragment guess calculation. Subsequently, a stability check on the antiferromagnetic broken symmetry solution was carried out. Finally, geometry optimisation on the open shell singlet was performed.

All energy values are provided in hartrees for all optimised geometries. The M06 functional was used for all structures in the following tables. E values are electronic energies in the gas phase. H values are enthalpic energies in the gas phase. G values are at 298K and have also been adjusted for 1 M solution.

	Formula	C	M	S(S+1)	E	H	G	G, 1 M
Organic Molecules	$CH_2=C(CH_3)COOCH_3$ - *MMA monomer*	0	1	0.000	-345.308729	-345.177334	-345.219224	-345.216117
	$(CH_3)_2C^{\bullet}(COOCH_3)$ - *MMA radical*	0	2	0.756	-345.889640	-345.748195	-345.793012	-345.789905
	$(CH_3)_2CCl(COOCH_3)$ - *MMA-Cl adduct*	0	1	0.000	-805.980996	-805.833887	-805.878660	-805.875553
	$(CH_3)_2C^{\bullet}(CN)$ - *V-70 radical*	0	2	0.765	-210.413718	-210.319082	-210.356689	-210.353582
	$(CH_2)_4O$ - *THF*	0	1	0.000	-232.113192	-231.991514	-232.024463	-232.021355
	The organic molecules used in the DFT study.							
Complexes in Scheme 3.3	[Me-ABP]$ClTi^{III}$ - *Ti complex with no THF*	0	2	0.758	-2424.339361	-2423.825801	-2423.912178	-2423.909071
	[Me-ABP]$ClTi^{III}(O(CH_2)_4)$ - *Complex **Ti2***	0	2	0.760	-2656.500758	-2655.862855	-2655.961823	-2655.958715
	[Me-ABP]$ClTi^{IV}(C(CH_3)_2CN)$ - *Ti-R_0*	0	1	0.000	-2634.807361	-2634.195703	-2634.294003	-2634.290895
	[Me-ABP]$ClTi^{IV}(C(CH_3)_2COOCH_3)$ - *Ti-MMA_n-R_0*	0	1	0.000	-2770.288485	-2769.629404	-2769.731822	-2769.728714
	[Me-ABP]$Ti^{III}(C(CH_3)_2COOCH_3)$ - *Atom transfer polym.*	0	2	0.766	-2310.168682	-2309.514840	-2309.616474	-2309.613366
	$[[Me\text{-}ABP]ClTi^{III}]^+ [(C(CH_3)_2COOCH_3)]^-$ - *Ionic polym.*	0	1	0.000	-2770.206521	-2769.548468	-2769.651450	-2769.648342
	Various 5- and 6-coordinate titanium species with the methyl-substituted ligand framework.							

	Formula	C	M	S(S+1)	E	H	G	G, 1 M
Complexes in Scheme 3.4	[ABP]ClTi^{III} - *Simplified Ti complex*	0	2	0.758	-1881.948508	-1881.708320	-1881.766026	-1881.762918
	[ABP]ClTi^{III}(O$(CH_2)_4$) - *Ti-THF*	0	2	0.759	-2114.112821	-2113.748027	-2113.816682	-2113.813575
	[ABP]ClTi^{IV}(C$(CH_3)_2$CN) - *Ti-R_0*	0	1	0.000	-2092.415972	-2092.077035	-2092.146686	-2092.143578
	[ABP]ClTi^{IV}(C$(CH_3)_2$COOCH_3) - *Ti-MMA_n-R_0*	0	1	0.000	-2227.900559	-2227.513871	-2227.586296	-2227.583188
	[ABP]Ti^{III}(C$(CH_3)_2$COOCH_3) - *Atom transfer polym.*	0	2	0.766	-1767.782564	-1767.400798	-1767.469818	-1767.466711
	Various 5- and 6-coordinate titanium species with the simplified ligand framework.							
Complexes in Scheme 3.5	[^{N,N,O,O}ABP]ClTi^{III}	0	2	0.758	-1881.948508	-1881.708320	-1881.766026	-1881.762918
	[^{N,N,O,O}ABP]ClTi^{IV}(C$(CH_3)_2$COOCH_3) - *OMRP*	0	1	0.000	-2227.900559	-2227.513871	-2227.586296	-2227.583188
	[^{N,O,O}ABP]ClTi^{IV}(C$(CH_3)_2$COOCH_3) - *OMRP + arm dissociation*	0	1	0.000	-2227.889701	-2227.504569	-2227.580817	-2227.577709
	[^{N,N,O,O}ABP]ClTi^{III}(CH_2=C(CH_3)COOCH_3) - *MMA alkene coordination*	0	2	0.761	-2227.292713	-2226.917762	-2226.991141	-2226.988033
	[^{N,O,O}ABP]ClTi^{III}(CH_2=C(CH_3)COOCH_3) - *MMA alkene coordination + arm dissociation*	0	2	0.759	-2227.251031	-2226.878206	-2226.957816	-2226.954709
	Understanding the binding energies of MMA to the titanium as a radical and as an olefin, with and without the pendant donor arm.							

	Formula	C	M	S(S+1)	E	H	G	G, 1 M
Complexes in Scheme 3.6	$[^{N,N,O,O}ABP]ClTi^{III}$	0	2	0.758	-1881.948508	-1881.708320	-1881.766026	-1881.762918
	$[^{N,N,O,O}ABP]ClTi^{IV}(C(CH_3)_2COOCH_3)$ - *OMRP*	0	1	0.000	-2227.900559	-2227.513871	-2227.586296	-2227.583188
	$[^{N,O,O}ABP]ClTi^{IV}(C(CH_3)_2COOCH_3)$ - *OMRP + arm dissociation*	0	1	0.000	-2227.889701	-2227.504569	-2227.580817	-2227.577709
	$[^{N,O,O}ABP]ClTi^{III}$ & $(C^{\bullet}(CH_3)_2COOCH_3)$ - *Ti + MMA radical with carbonyl coordination + arm dissociation*	0	3	2.011	-2227.853964	-2227.469932	-2227.550055	-2227.546947
	$[^{N,N,O,O}ABP]ClTi^{III}$ & $(C^{\bullet}(CH_3)_2COOCH_3)$ - *Ti + MMA radical with carbonyl coordination*	0	3	2.013	-2227.892896	-2227.507980	-2227.584511	-2227.581403
	Understanding the energy difference between the singlet and triplet species, with an unpaired electron on both the titanium and the MMA carbon.							
Complexes in Scheme 3.7	$[^{N,N,O,O}ABP]ClTi^{III}$	0	2	0.758	-1881.948508	-1881.708320	-1881.766026	-1881.762918
	$[^{N,N,O,O}ABP]ClTi^{IV}(C(CH_3)_2COOCH_3)$ - *OMRP*	0	1	0.000	-2227.900559	-2227.513871	-2227.586296	-2227.583188
	$[^{N,O,O}ABP]ClTi^{IV}(C(CH_3)_2COOCH_3)$ - *OMRP + arm dissociation*	0	1	0.000	-2227.889701	-2227.504569	-2227.580817	-2227.577709
	$[^{N,O,O}ABP]ClTi^{IV}(OC(OCH_3)C(CH_3)_2)$ - *Ti-enolate + arm dissociation*	0	1	0.000	-2227.881903	-2227.497421	-2227.578238	-2227.575130
	$[^{N,N,O,O}ABP]ClTi^{IV}(OC(OCH_3)C(CH_3)_2)$ - *Ti-enolate*	0	1	0.000	-2227.920567	-2227.535014	-2227.610846	-2227.607738
	Understanding the stability of the Ti(IV)-enolate complexes compared to the Ti-MMA_n-R_0 OMRP species.							

	Formula	C	M	S(S+1)	E	H	G	G, 1 M
Complexes in Scheme 3.10	[ABP]ClTi^{III} - *Simplified Ti complex with no THF*	0	2	0.758	-1881.948508	-1881.708320	-1881.766026	-1881.762918
	[ABP]ClTi^{III}($O(CH_2)_4$) - *Ti-THF*	0	2	0.759	-2114.112821	-2113.748027	-2113.816682	-2113.813575
	[ABP]ClTi^{III}($OC(OCH_3)C(CH_2)(CH_3)$) - *Ti-MMA with carbonyl coordination*	0	2	0.760	-2227.306852	-2226.932576	-2227.008406	-2227.005299
	[ABP]ClTi^{IV}($C(CH_3)_2CN$) - *Ti-R_0*	0	1	0.000	-2092.415972	-2092.077035	-2092.146686	-2092.143578
	[ABP]ClTi^{IV}($C(CH_3)_2COOCH_3$) - *Ti-MMA_n-R_0*	0	1	0.000	-2227.900559	-2227.513871	-2227.586296	-2227.583188
	[ABP]ClTi^{IV}($OC(OCH_3)C(CH_3)_2$) - *Ti-enolate*	0	1	0.000	-2227.920567	-2227.535014	-2227.610846	-2227.607738
	Demonstrating the stability of the Ti(IV)-enolate species compared to other 6-coordinate titanium species.							
Complexes in Scheme 3.11	[ABP]ClTi^{IV}($OC(OCH_3)C(CH_3)_2$) & [ABP]ClTi^{III}($OC(OCH_3)C(CH_2)(CH_3)$) - *T(IV)-enolate + Ti(III)-MMA*	0	2	0.760	-4455.235673	-4454.473491	-4454.606242	-4454.603135
	[ABP]ClTi^{IV}($OC(OCH_3)C(CH_3)_2$) & [ABP]ClTi^{III}($OC(OCH_3)C(CH_2)(CH_3)$) - *Polymerisation **TS***	0	2	0.809	-4455.217415	-4454.455760	-4454.581315	-4454.578208
	[ABP]ClTi$^{III}OC(OCH_3)C(CH_3)_2CH_2C(CH_3)C(OCH_3)OTi^{IV}$[ABP]Cl - *Ti(III)-PMMA-Ti(IV)*	0	2	0.759	-4455.268673	-4454.502712	-4454.624413	-4454.621305
	The species involved in the bimetallic group transfer polymerisation mechanism.							

	Formula	C	M	S(S+1)	E	H	G	G, 1 M
Complexes in Scheme 3.12	$[^{N,O,O}ABP]ClTi^{IV}(OC(OCH_3)C(CH_3)_2)$ - *T(IV)-enolate + arm dissociation*	0	1	0.000	-2227.881903	-2227.497421	-2227.578238	-2227.575130
	$[^{N,O,O}ABP]ClTi^{IV}(OC(OCH_3)C(CH_3)_2)$ $(OC(OCH_3)C(CH_2)(CH_3))$ - *Ti(IV)-enolate + MMA with carbonyl coordination*	0	1	0.000	-2573.226476	-2572.707658	-2572.802790	-2572.799682
	$[^{N,O,O}ABP]ClTi^{IV}(OC(OCH_3)C(CH_3)_2)$ $(OC(OCH_3)C(CH_2)(CH_3))$ - *Polymerisation* ***TS***	0	1	0.000	-2573.214135	-2572.696019	-2572.787752	-2572.784644
	$[^{N,O,O}ABP]ClTi^{IV}(OC(OCH_3)C(CH_3)CH_2C(CH_3)_2COOCH_3)$ - *Ti(IV)-(enolate+MMA) + arm dissociation*	0	1	0.000	-2573.250298	-2572.729660	-2572.820720	-2572.817612
	$[^{N,N,O,O}ABP]ClTi^{IV}(OC(OCH_3)C(CH_3)CH_2C(CH_3)_2COOCH_3)$ - *Ti(IV)-(enolate+MMA)*	0	1	0.000	-2573.272045	-2572.750313	-2572.841487	-2572.838379
	The species involved in the monometallic group transfer polymerisation mechanism with the simplified ligand framework.							

	Formula	C	M	S(S+1)	E	H	G	G, 1 M
Complexes in Scheme 3.13	[^{N,N,O,O}Me-ABP]ClTi^{IV}(OC(OCH$_3$)C(CH$_3$)$_2$) - ***Ti2****(IV)*-*enolate*	0	1	0.000	-2770.304687	-2769.645572	-2769.749184	-2769.746076
	[^{N,O,O}Me-ABP]ClTi^{IV}(OC(OCH$_3$)C(CH$_3$)$_2$) - ***Ti2****(IV)*-*enolate + arm dissociation*	0	1	0.000	-2770.273165	-2769.614837	-2769.720630	-2769.717522
	[^{N,O,O}Me-ABP]ClTi^{IV}(OC(OCH$_3$)C(CH$_3$)$_2$) (OC(OCH$_3$)C(CH$_2$)(CH$_3$)) - *Polymerisation* ***TS***	0	1	0.000	-3115.598971	-3114.805532	-3114.923316	-3114.920209
	The key species involved in the monometallic group transfer polymerisation mechanism with the methyl-substituted ligand framework.							
Complexes in Scheme 3.14	[^{N,N,O,O}tBu-ABP]ClTi^{IV}(OC(OCH$_3$)C(CH$_3$)$_2$) - ***Ti1****(IV)*-*enolate*	0	1	0.000	-2770.227503	-2769.199303	-2769.324577	-2769.321470
	[^{N,O,O}tBu-ABP]ClTi^{IV}(OC(OCH$_3$)C(CH$_3$)$_2$) - ***Ti1****(IV)*-*enolate + arm dissociation*	0	1	0.000	-2770.199988	-2769.173635	-2769.304489	-2769.301382
	The key species involved in the monometallic group transfer polymerisation mechanism with the *tert*-butyl-substituted ligand framework.							

5.7 References

1 K. Min, H. Gao, J. A. Yoon, W. Wu, T. Kowalewski and K. Matyjaszewski, *Macromolecules*, 2009, **42**, 1597–1603.

2 E. Penzel and N. Goetz, *Die Angew. Makromol. Chemie*, 1990, **178**, 191–200.

3 A. B. Dwyer, P. Chambon, A. Town, T. He, A. Owen and S. P. Rannard, *Polym. Chem.*, 2014, **5**, 3608–3616.

4 S. Grcev, P. Schoenmakers and P. Iedema, *Polymer (Guildf).*, 2004, **45**, 39–48.

5 D. F. Evans, *J. Chem. Soc.*, 1959, 2003–2005.

6 O. V. Dolomanov, L. J. Bourhis, R. J. Gildea, J. A. K. Howard and H. Puschmann, *J. Appl. Crystallogr.*, 2009, **42**, 339–341.

7 G. M. Sheldrick, *Acta Crystallogr. Sect. C Struct. Chem.*, 2015, **71**, 3–8.

8 G. M. Sheldrick, *Acta Crystallogr. Sect. A Found. Crystallogr.*, 2008, **64**, 112–122.

9 V. Kumar, A. Kalita and B. Mondal, *Dalt. Trans.*, 2013, **42**, 16264–16267.

10 E. Y. Tshuva, I. Goldberg, M. Kol and Z. Goldschmidt, *Inorg. Chem.*, 2001, **40**, 4263–4270.

11 S. Groysman, I. Goldberg, M. Kol, E. Genizi and Z. Goldschmidt, *Organometallics*, 2004, **23**, 1880–1890.

12 M. M. Olmstead, P. P. Power and S. C. Shoner, *Inorg. Chem.*, 1991, **30**, 2547–2551.

13 N. A. Jones, S. T. Liddle, C. Wilson and P. L. Arnold, *Organometallics*, 2007, **26**, 755–757.

14 S. Barroso, J. Cui, J. M. Carretas, A. Cruz, I. C. Santos, M. T. Duarte, J. P. Telo, N. Marques and A. M. Martins, *Organometallics*, 2009, **28**, 3449–3458.

15 Repeated elemental analysis of this sample consistently gave lower than expected C, H, N compositions. This is most likely to be due to oxidative decomposition of the (air-sensitive) sample either during transit or analytical sample preparation (or both).

16 A. L. Johnson, M. G. Davidson and M. F. Mahon, *Dalt. Trans.*, 2007, 5405.

17 S. Groysman, I. Goldberg, Z. Goldschmidt and M. Kol, *Inorg. Chem.*, 2005, **44**, 5073–5080.

18 M. J. Frisch, G. W. Trucks, H. B. Schlegel, G. E. Scuseria, M. A. Robb, J. R. Cheeseman, G. Scalmani, V. Barone, B. Mennucci, G. A. Petersson, H. Nakatsuji, M. Caricato, X. Li, H. P. Hratchian, A. F. Izmaylov, J. Bloino, G. Zheng, J. L. Sonnenberg, M. Hada, M. Ehara, K. Toyota, R. Fukuda, J. Hasegawa, M. Ishida, T. Nakajima, Y. Honda, O. Kitao, H. Nakai, T. Vreven, J. A. Montgomery, J. E. Peralta, F. Ogliaro, M. Bearpark, J. J. Heyd, E. Brothers, K. N. Kudin, V. N. Staroverov, R. Kobayashi, J. Normand, K. Raghavachari, A. Rendell, J. C. Burant, S. S. Iyengar, J. Tomasi, M. Cossi, N. Rega, J. M. Millam, M. Klene, J. E. Knox, J. B. Cross, V. Bakken, C. Adamo, J. Jaramillo, R. Gomperts, R. E. Stratmann, O. Yazyev, A. J. Austin, R. Cammi, C. Pomelli, J. W. Ochterski, R. L. Martin, K. Morokuma, V. G. Zakrzewski, G. A. Voth, P. Salvador, J. J. Dannenberg, S. Dapprich, A. D. Daniels, Farkas O., J. B. Foresman, J. V. Ortiz, J. Cioslowski and D. J. Fox, *Gaussian 09, Revis. E.01, Gaussian, Inc.*, 2013.

19 V. S. Bryantsev, M. S. Diallo and W. A. Goddard III, *J. Phys. Chem. B*, 2008, **112**, 9709–9719.